AWARD NUMBER: # **W81XWH-10-1-0876**

TITLE: **Molecular Signatures and Diagnostic Biomarkers of Cumulative Blast-Graded Mild TBI**

PRINCIPAL INVESTIGATOR: **Stanislav Svetlov, M.D Ph.D.**

RECIPIENT: **Banyan Biomarkers, Inc.**
Alachua, FL 32615

REPORT DATE: **December 2014**

TYPE OF REPORT: **Final**

PREPARED FOR: U.S. Army Medical Research and Materiel Command
Fort Detrick, Maryland 21702-5012

REPORT DOCUMENTATION PAGE

Form Approved
OMB No. 0704-0188

1. REPORT DATE	2. REPORT TYPE	3. DATES COVERED
December 2014	Final	15Sep2010-14Sep2014

4. TITLE AND SUBTITLE
Molecular Signatures and Diagnostic Biomarkers of Cumulative, Blast-Graded Mild TBI

5a. CONTRACT NUMBER

5b. GRANT NUMBER
W81XWH-10-1-0876

5c. PROGRAM ELEMENT NUMBER

6. AUTHOR(S)
Ronald Hayes, PhD , Olena Glushakova, MS

E-Mail:rhayes@banyanbio.com; oglushakova@banyanbio.com

5d. PROJECT NUMBER

5e. TASK NUMBER

5f. WORK UNIT NUMBER

7. PERFORMING ORGANIZATION NAME(S) AND ADDRESS(ES)

Banyan Biomarkers, Inc.

Alachua, Fl 32615

8. PERFORMING ORGANIZATION REPORT NUMBER

9. SPONSORING / MONITORING AGENCY NAME(S) AND ADDRESS(ES)

U.S. Army Medical Research and Materiel Command
Fort Detrick, Maryland 21702-5012

10. SPONSOR/MONITOR'S ACRONYM(S)

11. SPONSOR/MONITOR'S REPORT NUMBER(S)

12. DISTRIBUTION / AVAILABILITY STATEMENT

Approved for Public Release; Distribution Unlimited

13. SUPPLEMENTARY NOTES

14. ABSTRACT
During grant the period, the PI established and standardized blast load characteristics produced by mild through severe TBI and defined 'composite' and primary blast parameters and brain injury signatures in these two blast modalities. Neuro-glial injury was evaluated by silver staining. GFAP and CNPase up-regulation in brain tissue was assessed by immunohistochemistry. The levels of biomarkers in biofluids were assessed by ELISA, antibody microarrays, and Western Blot. Single and repeated blast increased levels of selected biomarkers in a time dependent manner. Multiple blasts significantly augmented increased levels of GFAP, UCH-L1, CNPase, NSE, IL-1, IL-10, sICAM, L- and E-selectins, NSE and NRP-2, but not Orexin A, as compared to a single blast. In contrast, a low magnitude blast produced no significant effects on the levels of these biomarkers. We found and characterized new signatures of blast injuries: thrombin activity measured by calibrated activated thrombography (CAT), linked to microcirculation disorders following blast exposures. In addition, we developed, characterized and validated a portable cumulative blast detection device using novel MEMS chip technology (FIT).

15. SUBJECT TERMS: Multiple blast exposures; brain injury; 'composite' blast; primary blast; Cumulative Blast and Impulse Exposure Sensing Package, (CBI-ESP); GFAP; CNPase; NSE, Orexin A; Neuropilin-2 (NRP-2), sICAM, thrombin biomarkers

16. SECURITY CLASSIFICATION OF:			17. LIMITATION OF ABSTRACT	18. NUMBER OF PAGES	19a. NAME OF RESPONSIBLE PERSON
a. REPORT	b. ABSTRACT	c. THIS PAGE			USAMRMC
Unclassified	Unclassified	Unclassified	Unclassified	162	19b. TELEPHONE NUMBER *(include area code)*

Table of Contents

1. **INTRODUCTION:** Narrative that briefly (one paragraph) describes the subject, purpose and scope of the research.

Objectives of the entire project are: (i) Develop an experimental framework for reproducing multiple blast wave exposures and recording multiple blasts in an animal model using a prototype sensor device, (ii) define cumulative blast load upon multiple blast exposures and distinguish pathophysiological mechanisms of mild TBI to formulate blast load injury scale, (iii) identify and validate novel biochemical markers of single and multiple blast exposures and formulate blast load injury scale.

2. **KEYWORDS:** Provide a brief list of keywords (limit to 20 words).

Multiple blast exposures; brain injury; 'composite' blast; primary blast; Cumulative Blast and Impulse Exposure Sensing Package (CBI-ESP); GFAP; CNPase; NSE, Orexin A; Neuropilin-2 (NRP-2), sICAM, thrombin, biomarkers, Blood brain barrier (BBB).

3. **OVERALL PROJECT SUMMARY**

The project was performed at Banyan Biomarkers from 2010 to 2014. The report was created based on the annual reports provided by PI (Dr. Svetlov) who was not longer employed by Banyan since September 2014. In June, 2014 the responsibility for this project was taken over by Dr. Hayes, Director of Banyan Laboratories, Founder and President of Banyan Biomarkers, and Ms. Glushakova, Principal Scientist at Banyan Biomarkers.

First year 2011:

In year 1, we determined blast load characteristics producing mild through severe TBI and defined 'composite' and primary blast parameters. Schlieren optics technique was used to visualize blast wave interaction with experimental animal. The pathological effects of primary blast OP exposure of controlled duration, peak pressure and transmitted impulse were compared with brain injury by a severe blast load accompanied with strong head acceleration. We assessed and partially characterized brain injury signatures when primary blast wave hits frontal head with open or covered body vs. composite blast: neuro-glial injury evaluated by silver staining, and GFAP/CNPase and NSE. Biomarkers of neuro-glial injury GFAP, CNPase and NSE were accumulated in circulation in a particular time-dependent fashion. We developed a v1.1 of sensor package for detecting/recording a cumulative blast exposure, and begin to characterize mechanisms and biomarkers of brain injury in response to multiple mild/moderate blast exposures.

SOW1. **Establish blast load characteristics producing mild through severe TBI upon total body exposure compared to head-directed, body protected blast. Define a preliminary blast exposure, brain injury graded scale. (Months 1-18, Banyan Biomarkers; Florida Institute of Technology, FIT)**

Task 1a. IACUC has been approved through Univ. of Florida and DoD ACURO office (completed).
Task 1b. Determine and standardize blast parameters (peak overpressure, duration, and impulse power) on the surface of rats at various orientations to the blast wave **(Months 1-6, completed)**.
At this point, calibration of blast parameters has been accomplished on rat head at several distances and angles related to shock tube nozzle reflecting head/body orientation blast to front of blast wave. The realistic pictures and graphical presentation of set-ups is given below in Fig. 1:

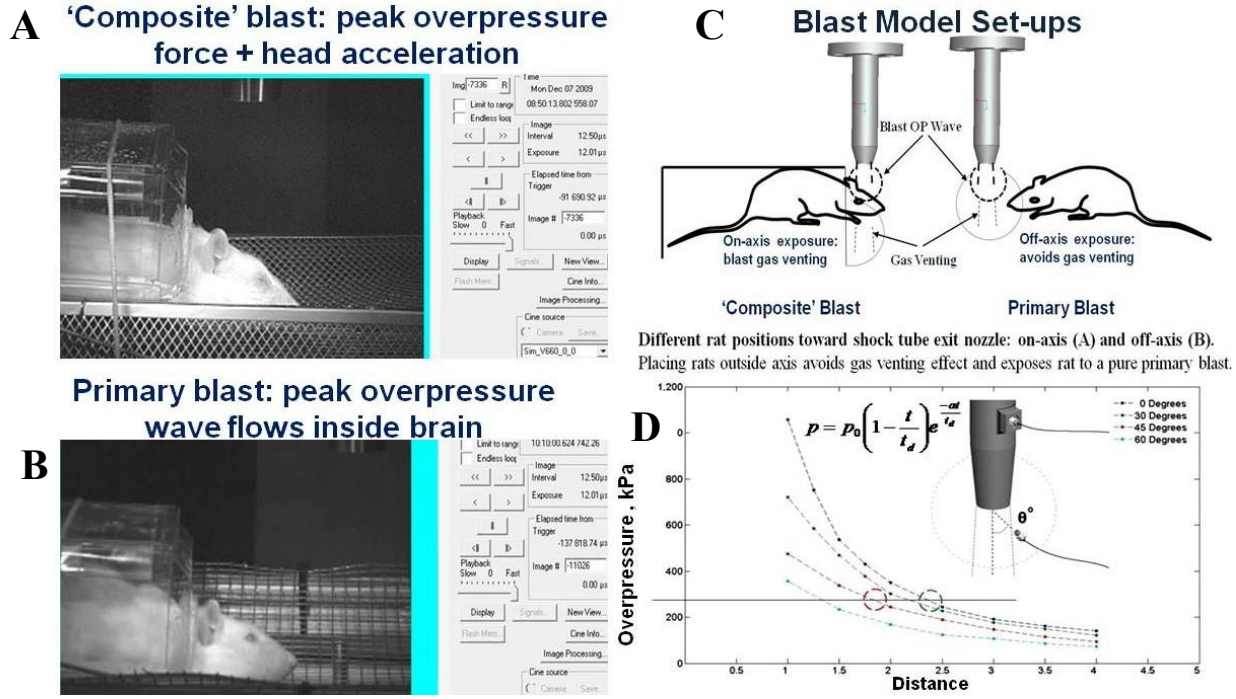

Fig.1. Two general experimental set-ups for rat's exposure to shock tube-generated blast waves. A: on-axis of shock tube nozzle position: peak overpressure + venting gas produce head acceleration 'Composite blast'; B: off-axis position: blast wave peak overpressure only hitting rats; C graphic representation of two different set-ups; and D: Calibration of pressure on rat head depending on the angle and distance from the nozzle of shock tube.

An empirical expression for the pressure decay with time at a fixed distance is shown in Table 1, characterized by a decay parameter, α [Kinney, Gilbert & Graham, Kenneth (1985). Explosive Shocks in Air, 2nd Sub edition. Springer], Table 1.

Level 1 –moderate/severe, everything at angle 0 is severe.
Level 2a-moderate
Level 2b-mild/moderate
Level 3 –mild

	Angle Nozzle/ Head	Distance		Peak Over-pressure (psi/kPa)	Positive Phase Duration (μs)	Impulse/ Area Unit (kPa-msec)
		D	cm			
	0º	2	5.08	52.6/361	NA	NA
	0°	4	10.16	20.3/140	NA	NA
Level 1	30º	2.5	6.35	33.9/234	113.8	10.6
	30°	4	10.16	17.7/122	138.0	8.37
Level 2a	45°	2	5.08	35.2/243	53.1	6.46
Level 2b	45°	4	10.16	13.8/95	85.3	4.04
	60°	2	5.08	24.5/169	32.9	2.76
Level 3	60°	4	10.16	10.6/73	60.3	2.20

Table 1. Standardized blast parameters (peak overpressure, duration, and impulse power) on the surface of rats at various orientations to the blast wave

To justify the positions of rats relative to the tube nozzle allowing to expose to composite blast (on-axis) or primary blast (off axis), we used Schlieren optics to visualize blast front and venting gas interaction with the rat head (Fig. 2)

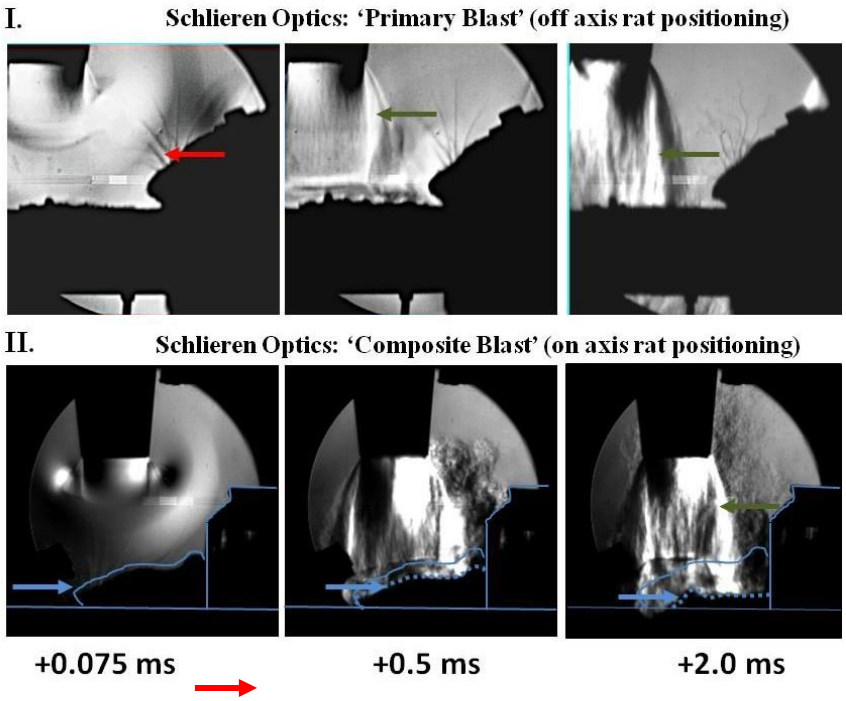

Fig 2. Visualization of blast wave interaction with head ON-AXIS (composite blast) and OFF-AXIS (primary blast) using SCHLIEREN SYSTEM

Red arrows indicate formation, traveling and interaction of blast wave with rat head. Accomplished within ~0.1 ms Green arrows show gas venting jet hitting rat head after blast passed through. Persists for milliseconds. Blue arrows depict rat head hyperacceleration/deformation.

Task 2: Assess brain injury signatures when blast wave hits whole body, including head, vs. local, head-directed blast wave exposure (Months 2-18, in progress, ~75 % completed).

Silver staining of neurodegeneration level in rat brain after different blast exposures.

Rats were subjected to (i) 'composite' head-directed severe blast exposure (52 psi/10 msec total) on axis (body protected) accompanied by strong head movement; (ii) off-axis (30' degree) exposure to the blast of same shock tube settings resulted in 33.9 psi peak overpressure at the middle of frontal head **(Fig. 3 C)** lasted for 113 microseconds; and (iii) controlled cortical impact (CCI) of 2.0 mm depth.

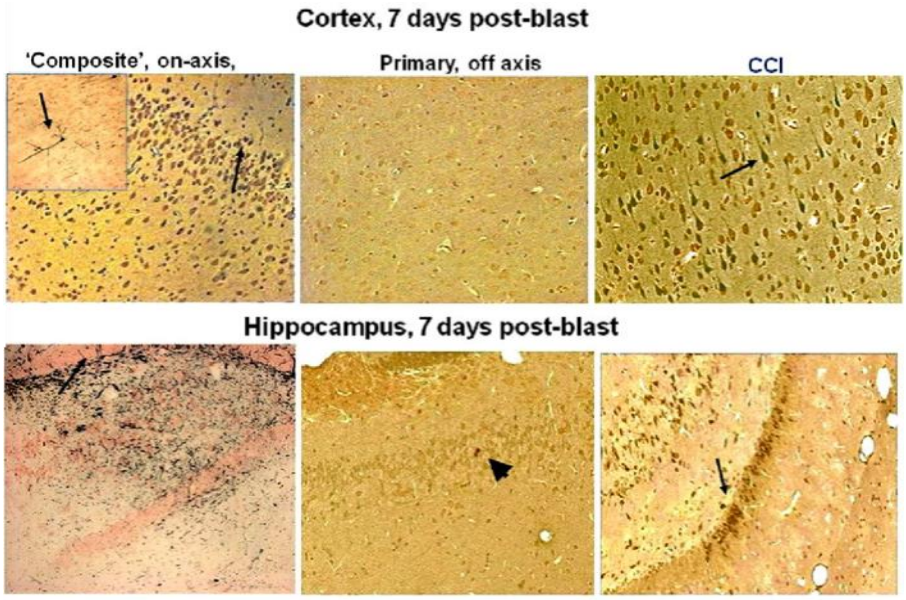

Fig. 3 Silver staining in coronal sections of midbrain (mesencephalon). Positive silver accumulation accumulation is indicated by arrows. Inset (cortex composite) shows degenerated neuron. Arrowhead in hippocampus after primary blast points on possible silver accumulation in the cell.

As can be seen in **Fig. 3,** on-axis blast produces silver accumulation at 7 day post-blast, particularly in hippocampus (indicated by arrows). CCI also results in positive staining in ipsilateral cortex and hippocampus. In contrast, there was a rare occurrence of silver accumulation observed in cortex or hippocampus after exposure to primary blast (arrowhead).

T o asses if markers of neuronal injury are released into circulation, we assayed serum levels of neuron-specific enolase (NSE) and UCH-L1 after different blast exposures. Rats were exposed to on-axis single composite blast of 52 psi, 10 msec total duration of positive phase + venting gas. Serum NSE **(Fig. 4A)** and UCH-L1 **(Fig. 4B)** were measured using SW ELISA Kits.

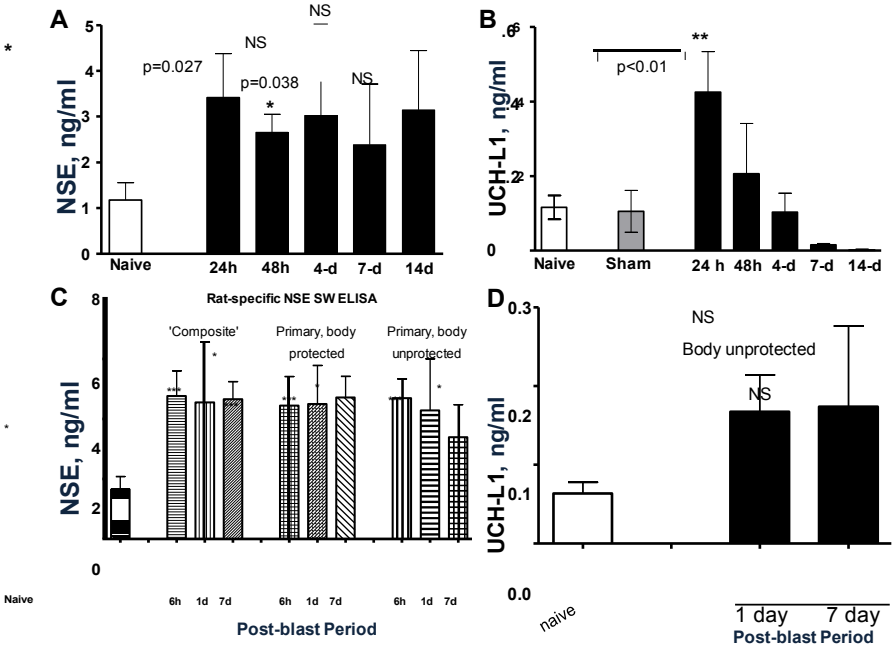

Fig. 4 NSE and UCH-L1 accumulation in blood after different types of blast exposure. A, B: serum NSE and UCH-L1 after on-axis 'Composite blast'; C, D: serum NSE and UCH-L1 after off-axis primary blast; Mean + SEM are shown of at least 3 rats per point from each group performed in duplicate. Unpaired t-test was employed to analyze statistical significance of values. *p<0.05, ** p<0.01; ***, p<0.005

The same settings of shock tube were used to challenge rats to off-axis primary blast (30^{o} degree from nozzle) with PO 33.9 psi, duration of113 µsec registered at the head with body covered or unprotected as indicated. NSE was significantly elevated in serum within first 24-48 hours after composite blast **(Fig. 4A)**, and the increase trend persisted up to 14 day although was not statistically significant (n=4 rats in each group). In this set of experiments, NSE SW ELISA Kit (Alpha Diagnostics), not rat-specific was employed.

In the subsequent sets of experiments **(Fig. 4C)**, we used NSE SW ELISA Kit from Life Sciences Advanced Technologies designed to detect specifically rat NSE. As can be seen in **Fig. 4A**, remarkable accumulation of NSE was detected in serum within 6 hours following exposure to either 'composite' or primary blast. Serum UCH-L1 elevated at 24 hours after 'composite' blast followed by a rapid decline **(Fig. 4B)**. Increases in serum UCH-L1 were not statistically significant after a single primary blast exposure (n=4), although an elevation trend could be detected **(Fig. 4B)**.

Gliosis and up-regulation of astrocyte and oligodendrocyte markers after different blast exposures.

I. Time-dependent GFAP **(Fig. 5)** and CNPase **(Fig. 6)** expression in rat brain was studied after severe composite on-axis blast (52.6 psi/~10 msec) accompanied by strong head acceleration and off-axis moderate/severe primary blast (33.9psi/113.8 μsec positive phase) with minor head acceleration.

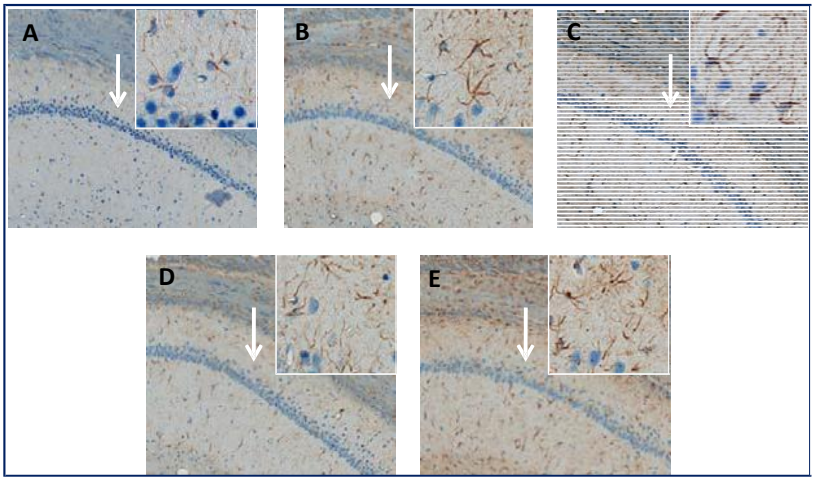

Figure 5. Expression of GFAP in Hippocampus (CA1 region) of OBI injured rats.
A, control naïve, B on axis 1 day, C, on axis 7 days, D, off axis 1 day and E on axis 7 days. Low magnification 5 x and high magnification 20x CA1 regions boxed in top of panels are shown.

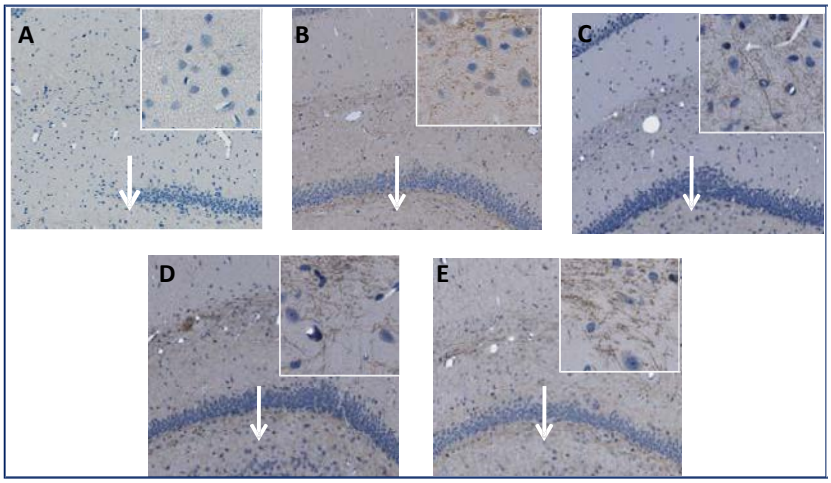

Figure 6. Expression of CNPse in Hippocampus (DG region) of OBI injured rats.
A, control naïve, B on axis 1 day, C, on axis 7 days, D, off axis 1 day and E off axis 7 days. Low magnification 5 x and high magnification 20x CA1 regions boxed in top of panels are shown.

Next, we determined levels of GFAP and CNPase in circulation.

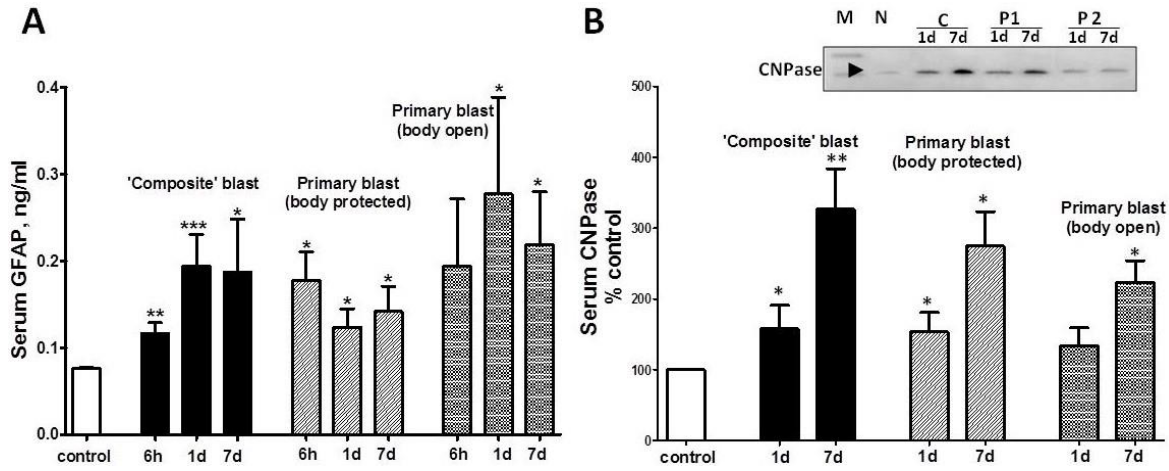

Fig. 7. GFAP and CNPase levels in blood after different blast exposures. A: serum GFAP after different types of blast; B: semi-quantitative serum CNPase by western blot densitometry after different blasts. Inset: representative western blot. t-test with Welch correction was done. (*-p<0.05), **-p<0.01; ***-p<0.005 Mean ± SEM of values from 3 to 5 rats per point is shown.

To examine systemic responses after blast, we examined several critical molecules of inflammatory and microvascular responses including Interleukins 1 and 10, CX3CL1 fractalkine and cell adhesion integrin alpha/beta, soluble ICAM (sICAM), E- and L-selectins. Serum IL-1, IL-10 (Fig. 8A, B), fractalkine and Integrin α/β (Fig. 8 C, D), a complement receptor composed of CD11c and CD18, was determined by semi quantitative antibody array (Quantibody, Ray Biotech). SICAM and L-selectin were determined by rat-specific ELISA assays (Fig. 9, Antibody on-line).

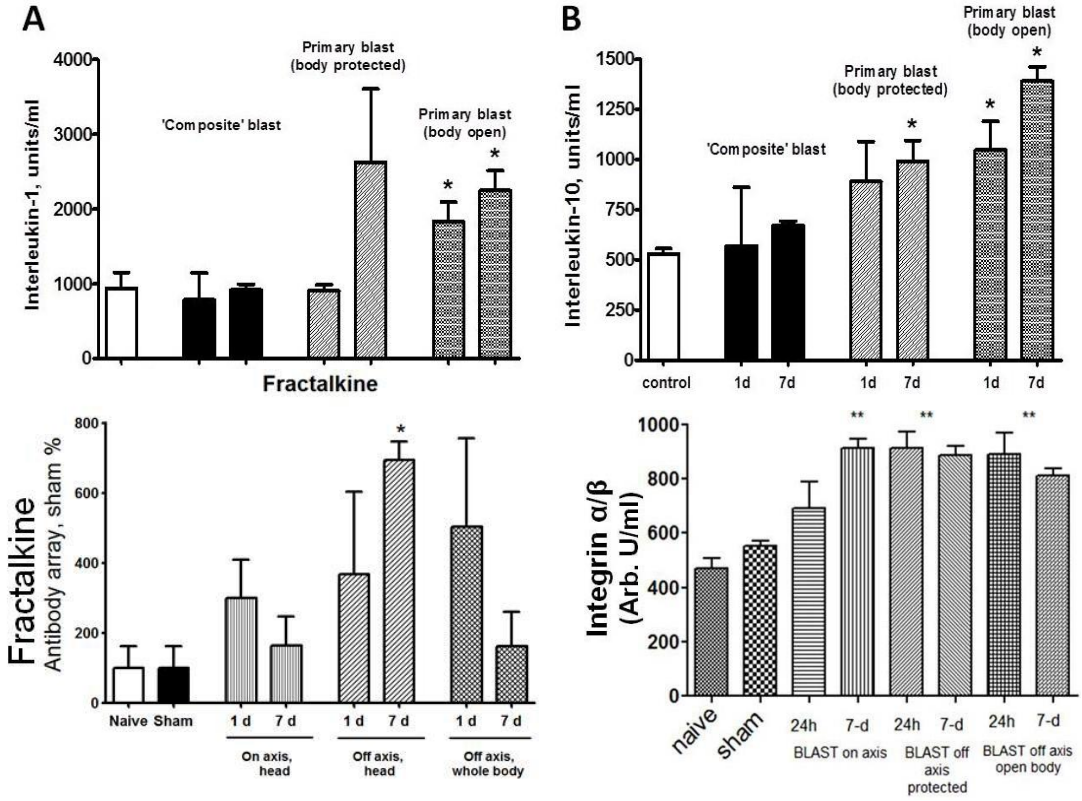

Fig. 8. Serum levels of Interleukins, fractalkine and integrin alpha/beta measured by quantibody array. t-test was done. (*-p<0.05), **-p<0.01; ***-p<0.005 Mean ± SEM of values from 4 rats per point is shown.

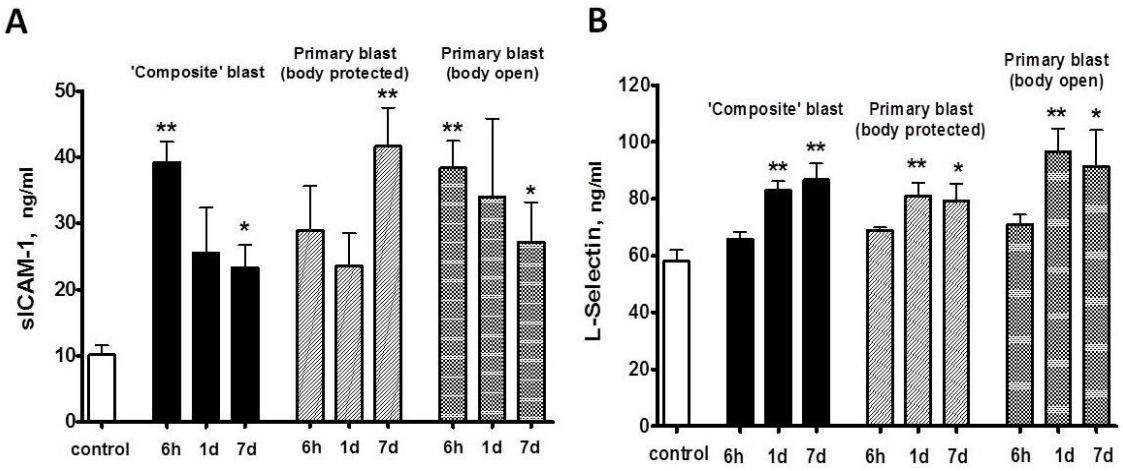

Fig.9A. sICAM-1 accumulation in serum after blast (ELISA). Serum was collected from overpressure-exposed rats at different shock tube set-ups. Fig.9B. L-Selectin accumulation in serum after blast (ELISA). Serum was collected from overpressure-exposed rats at different shock tube set-ups. Data are Mean+SEM of at least 4 rats, each assay performed in triplicate. *=p<0.05 and **-p<0.01 vs. naive according unpaired t-test analysis.

Soluble intercellular adhesion molecules play a role in cell-to-cell communications in various vascular responses to stressors,including shear stress and blast wave. L-selectin are adhesion molecules which characterize the activation of vascular component of inflammation and interaction of circulatory cells with endothelial component of blood-brain-barrier (BBB). Rats were subjected to off-axis head + total body blast: 33.9psi, 113 msec, 10.6 kPa-msec with body armored or uncovered. Blood was collected and cytokines were assayed in serum using SW ELISA Kits.

The most prominent activation of vascular components of blast responses occurs when peak overpressure interacts with the frontal part of head without significant acceleration: "flowing blast insight the brain" (blast off-axis open body).

Finally for this task, we determined serum levels of Neuropilin-2 (NRP-2) reflecting neuroregeneratory ability of CNS in combination with NGF-beta, which was analyzed in previous project.

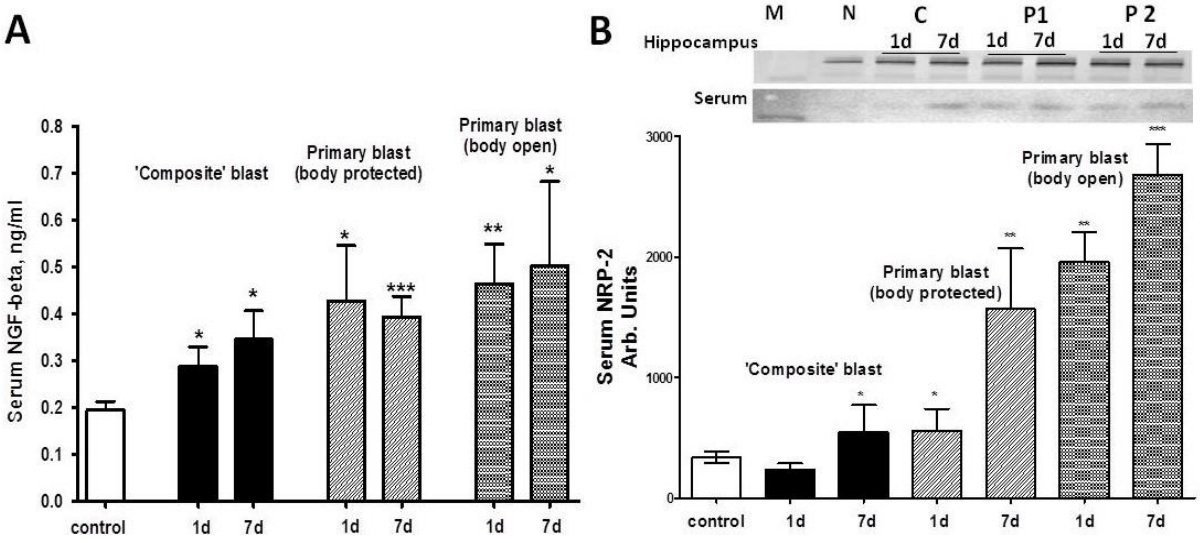

Fig.10A. β-NGF accumulation in serum after blast (ELISA). Serum was collected from overpressure-exposed rats at different shock tube set-ups. 10 B. Levels of soluble Neuropilin-2 in Rat Serum (Western blot and quantitative protein array, Western blot with Abs from Cell Signaling t-test was done. (*-p<0.05), **-p<0.01; ***-p<0.005 Mean ± SEM of values from 4 rats per point is shown.

SOW 2: Develop a cumulative blast detecting/recording module, and characterize pathophysiology of mTBI in response to multiple blast exposures. Define cumulative blast load upon multiple blast exposures and distinguish pathophysiological mechanisms of mild TBI to formulate blast load injury scale. (**Months 2-24, Banyan Biomarkers**; **FIT, in progress ~60% completed**)

Task 3: Characterize and validate a portable cumulative blast detection device using novel MEMS chip technology **(FIT)**. Assess detection of multiple blast exposures at different 3-D rat orientations to blast wave, and compare cumulative effects in rats using our existing modular system and portable device. (**Months 2-18, ~ 75 % completed) Please see Appendices for complete technical information**

Cumulative Blast and Impulse (CBI) Exposure Sensing Package (ESP)- CBI-ESP

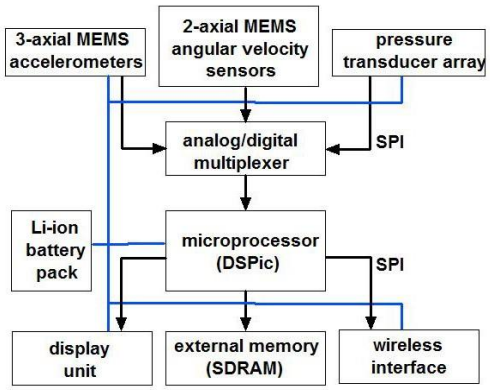

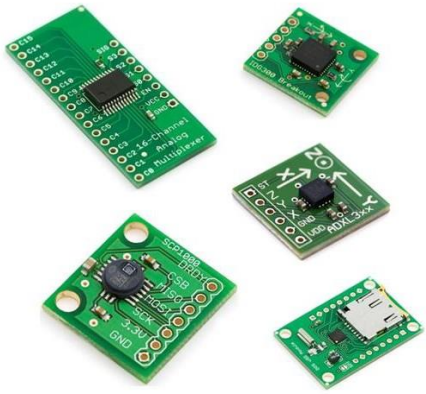

A. CBI-ESP Layout:

- **CBI-ESP: based on ultra-light MEMS-IC sensor arrays embedded on protective gear**
- **Accelerometers and gyros to measure exposure to impulse and angular acceleration**
- **Array of pressure sensors to measure peak pressure and exposure to blast waves**
- **RISC-based microprocessor for A/D conversion, signal interfacing, data recording and storage, display and real-time communication**

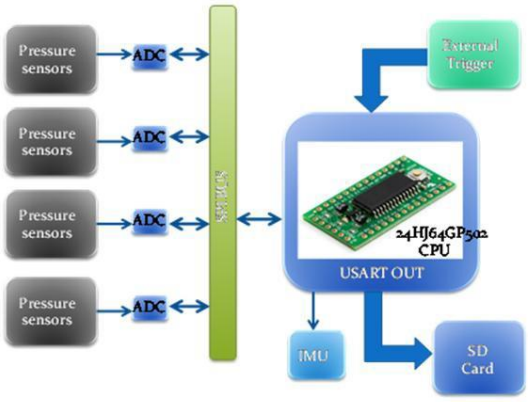

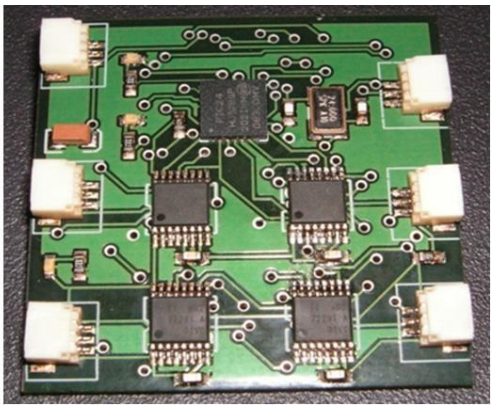

B. CBI-ESP Main Board:

- **16-bit, 80 MHz, 40 MIPS RISC-based processor (PIC24HXX)**
- **Four independent simultaneous 12-bit A/D converters (ADS7229**
- **Max. rate: 1.1 Msample/sec, connected to SPI bus for simultaneous acquisition of pressure readings and calibrated against PBC blast sensors**
- **Analog pressure transducers – Max. pressure = 44 psi**
- **Four pressure sensors in any desired location within test specimen**
- **Data streamed to micro SD card or RAM buffer**

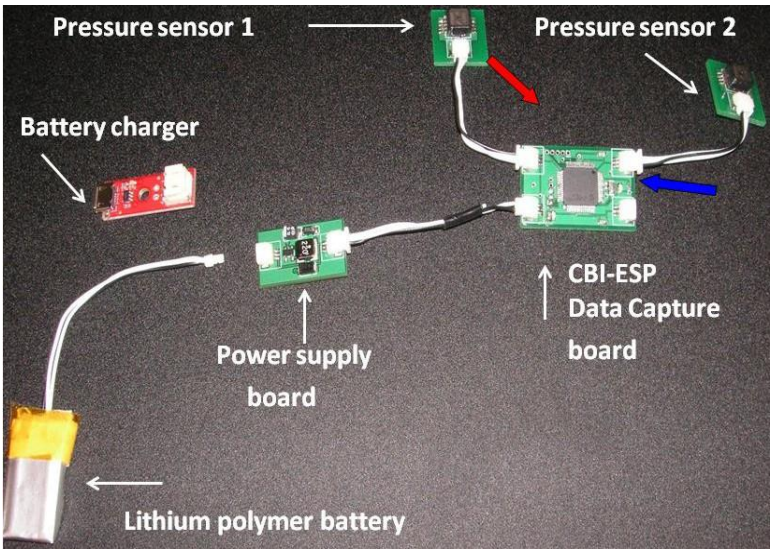

Red arrow: Connector for firmware upgrade
Blue arrow: connector for inertial measurement board

CBI-ESP: Version 1.1

Animal Testing General Setup for Single and Cumulative Exposures:

Diaphragm	External sensor R=2 in @ 45 deg from shock tube exit – (psi)
0.003 + 4 layer of tape	35 .12
0.004 + 4 layer of tape	43.53
0.005 + 4 layer of tape	54.74

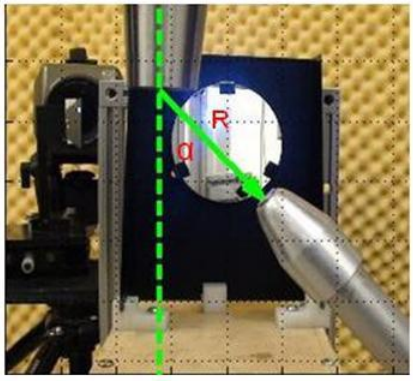

Raptured diaphragm with taping

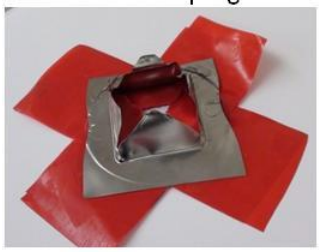

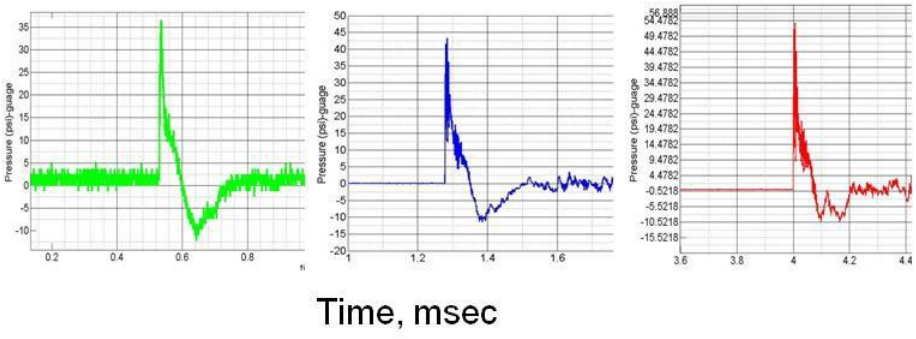

Fig. 11 Peak overpressure values in modified Banyan's shock tube for three different diaphragm configurations. Several model experiments were conducted with external 'pencil' PCB to capture and record a peak overpressure at 45 degree from shock tube nozzle.

In parallel, we performed blast exposures of lightly anesthetized rats with attached v1.1 CBI-ESP:

Fig. 12 Layout of CBI-ESP portable sensor package on a rodent for blast pressure testing.

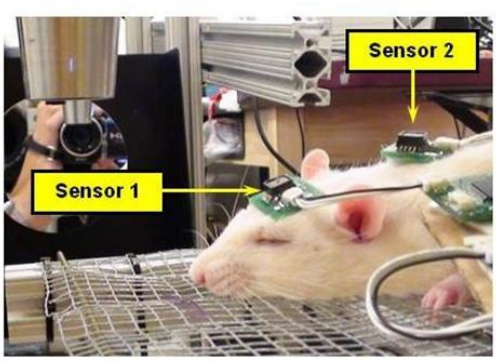

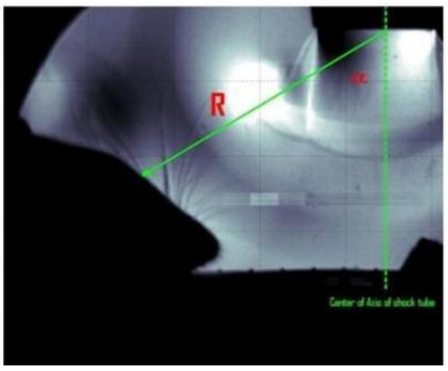

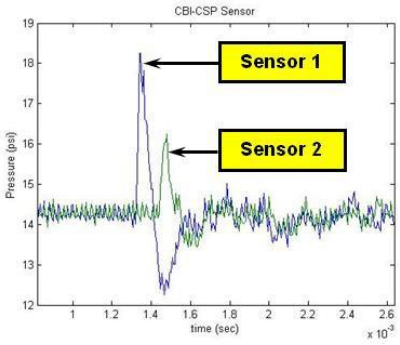

	Mach number	Details	R	α	Sensor 1 (CSB-CSP) -Absolute	Sensor 1 Impulse (psi-msec)	Sensor 2 (CSB-CSP)-Absolute	Sensor 2 Impulse (psi-msec)
rat1	2.16	1 BLASTEXPOSURE FULL BODY	2.22	59.91	18.66	0.1308	16.46	0.0503
Rat1	2.06	2nd BLAST EXPOSURE FULL BODY, 28 min from 1st blast	2.13	47.33	20.94	0.1773	16.77	0.0412
rat3	2.13	3rd BLAST EXPOSURE FULL BODY, 24 min from 2nd blast	2.31	52.32	20.55	0.1677	16.77	0.0502

Fig. 13. Actual anesthetized rat testing the actual v1.1 CBI-ESP. Please note the differences in peak overpressure detected by sensor 1 and 2 and detected by pencil PCB in Figure 11. The likely reason is that the electronic card in portable device is not up to date and upgrading require a significant additional funds.

Task 4: Assess brain injury characteristics upon exposure to repeated low level blast; determine cumulative blast load-injury correlations **(Months 4-24, ~20 % completed)** .

Rat-specific GFAP assay has been in development in Banyan. In addition, we employed rat-specific NSE from Antibody on-line. Using these sensitive and specific assay Kits, we measured GFAP and NSE levels in separate group of rats subjected to a single and repeated blast exposure.

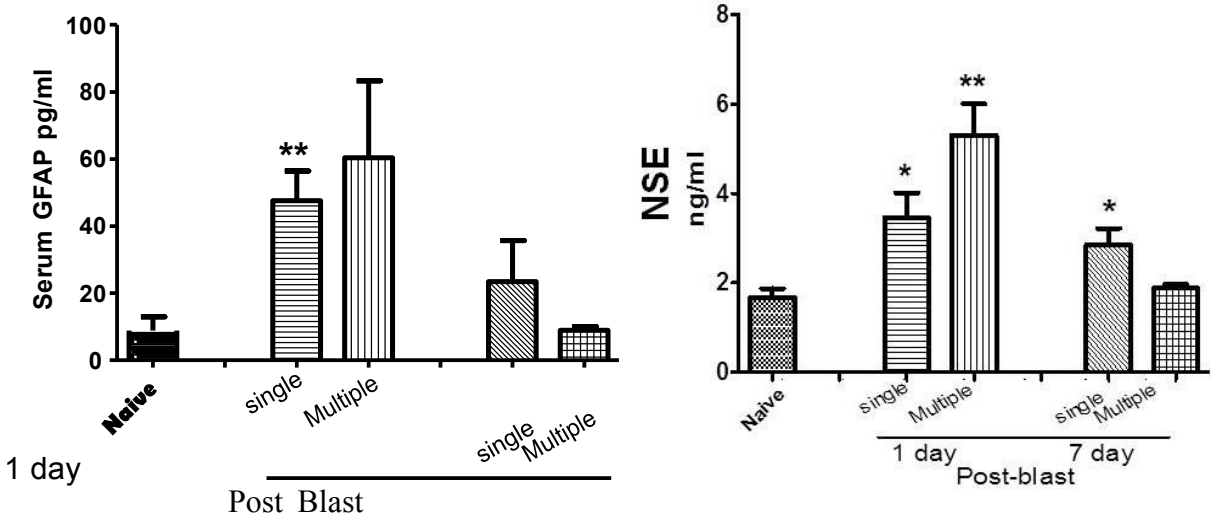

Fig. 14 Serum levels of GFAP and NSE after single and multiple primary blasts measured by rat-specific SW ELISA kits (Banyan and Antibody on line). Rats exposed to a primary blast (PO-53 psi total, 75 µsec duration) Multiple: 3 times with 45 min to 1 hour recovery period. *-p<0.05; **-p<0.01

Only 3 rats in every group have been processed and serum samples measured. The experiments are under way to reproduce these data in a larger group and standardize the conditions of blast-post-blast care.

Second year 2012:

The objectives of year 2 of the project has been (i) complete characterization severe/moderate TBI upon primary blast (peak overpressure) exposure compared to composite blast, (ii) continue developing a cumulative blast detecting/recording module, and (iii) characterizing biomarkers of TBI in response to multiple vs. single blast exposures. Multiple blasts significantly augmented increased levels of GFAP, UCH-L1, NSE and NRP-2, but not Orexin A, vs. single 1 day post- blast, while at 7 days the cumulative effects of multiple blasts were much lower, if any. On the other hand, serum CNPase after multiple blasts was significantly augmented vs. single blast both at 1 day and 7 days post exposure. The improved prototype of cumulative blast sensor and signal conditioning circuit were tested at Banyan Biomarkers on 19 October 2012.

In the body section, I present novel data and progress related to multiple blast biomarker responses. Recent issues pertinent to the development of cumulative blast sensor have been also briefly discussed. Detailed explanation and solutions of a sensor have been presented in FIT appendix. In addition, comparing biomarkers of moderate 'composite'blast TBI , accompanied with head

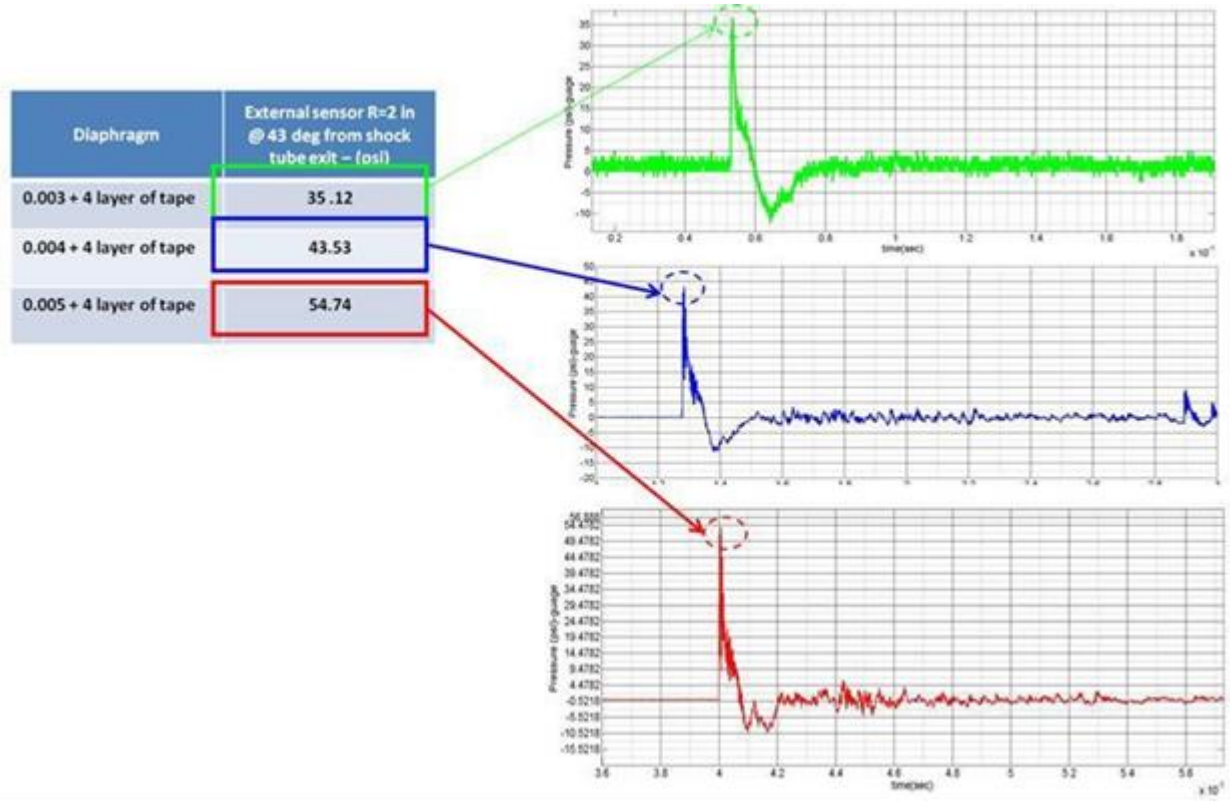

acceleration with primary blast, in which peak overpressure 'flows the head through a rostral part of the brain w/o significant head acceleration', is presented in detail in published paper in Appendix.

SOW 2: Develop a cumulative blast detecting/recording module, and characterize pathophysiology of mTBI in response to multiple blast exposures. Define cumulative blast load upon multiple blast exposures and distinguish pathophysiological mechanisms of mild TBI to formulate blast load injury scale. (Months 2-24)

Task 3: Characterize and validate a portable cumulative blast detection device using novel MEMS chip technology (FIT). Assess detection of multiple blast exposures at different 3-D rat orientations to blast wave, and compare cumulative effects in rats using our existing modular system and portable device. (Months 2-18, in progress).

1. Maximum peak overpressure achieve with Banyan's current 1-inch shock tube. Banyan's 1-inch shock tube can reach peak overpressure up to nearly 55 psi.
This has been consistently recorded and documented. We demonstrated that the use of successively thicker diaphragms, in combination with layers of tape used as sealant, provided increased peak overpressures as expected and shown in the table and plots above. Peak overpressure events last one to a few microseconds in near ideal blast waves (i.e., when the

effect of venting gas is almost completely eliminated). Advanced PXI-based data acquisition modules from FIT, at sample rates up to 50 Msamples/sec, were used to establish that to accurately capture peak overpressure events at sampling rate of at least 2.5 Msamples/second is needed.

The plots shown in previous page were sampled at 2.5 Msamples/sec (non-multiplexed) using a PXI-6132 14Bit, 2.5 MSample/sec/channel, simultaneous sampling multifunction data acquisition board. For the same reasons, it was also discovered during September session, that the currently existing data acquisition board on use at Banyan (DAQcard 6062E) sampling four multiplexed pressure sensors at 90 kSamples/sec, has a high chance of missing the peak overpressure event, and therefore fails recording the correct value of the peak overpressure.

1. Preliminary testing from blast events using the CBI-CSP (Cummulative blast injury sensing package) have been performed at Banyan using two sensors and one data capture board, as shown in the figures below:

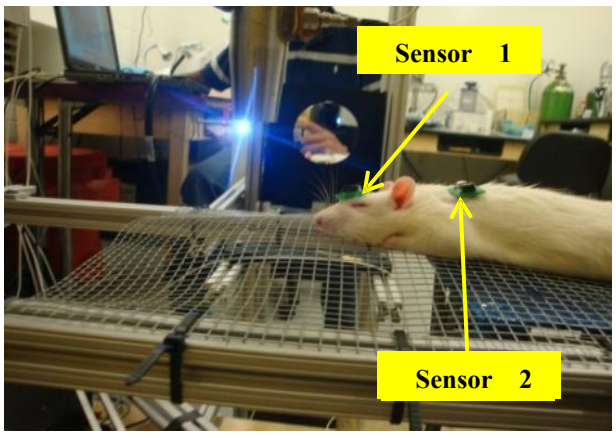

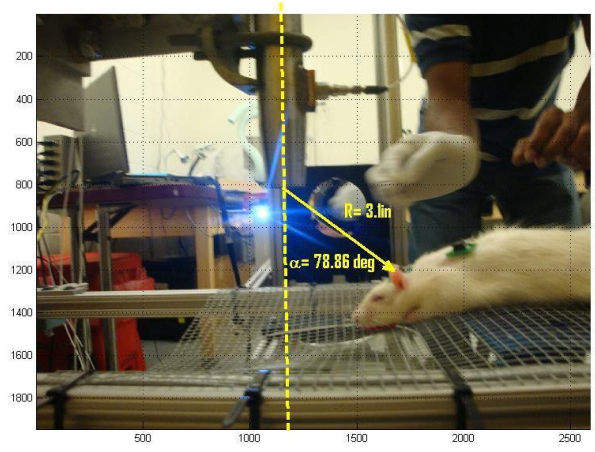

Test #	Sensor 1 (psi) peak Overpressure(psi)	Sensor 2 (psi) peak Overpressure(psi)	Location from exit of shock tube	Time
Test 1	19.15	17.15	R=3.13 in Angle =78.86 deg	
Test 2	18.24	16.25	R=3.19 in Angle=68.50deg	5 mins after Test 1
Test 3	20.28	16.19	R= 3.02 in A Angle=68.25 deg	20 mins after Test 2

Table 1 – Low pressure tests using CBI-CSP device. Diaphragm thickness = 0.003 inch, no tape. The data in table 1 shows results recorded in the SD memory card attached to the CBI-CSP data capture board in three successive tests, for sensor locations 1 and 2, at "low pressure" (0.003 inch diaphragm with no sealant tape). More detailed results from all testing conducted that day at Banyan using the CBI-CSP device were included and discussed in the corresponding quarterly report (Table 2).

Specimen Number	Test Name	Mach number	Details	R	α	Sensor 1 (CSB-CSP)	Sensor 2 (CSB-CSP)
Specimen 1	rat1	2.12	SINGLE BLAST , HEAD EXPOSURE	2.01	46.33	NA	NA
Specimen 2	rat2	2.061	SINGLE BLAST , HEAD EXPOSURE	2.18	48.79	NA	NA
Specimen 3	rat3	2.03	SINGLE BLAST, FULL BODY EXPOSURE	2.20	55.19	NA	NA
Specimen 4	rat4	2.09	SINGLE BLAST, FULL BODY EXPOSURE	2.47	47.62	NA	NA
Specimen 5	rat5	2.16	SINGLE BLAST, FULL BODY EXPOSURE	2.08	49.44	NA	NA
Specimen 6	rat6	2.13	SINGLE BLAST, FULL BODY EXPOSURE	2.26	47.12	NA	NA
Specimen 7	rat7	2.17	1 BLAST EXPOSURE FULL BODY	2.11	46.15	NA	NA
	rat9	2.05	2nd BLAST EXPOSURE FULL BODY, 25 min from 1st blast	2.25	54.76	18.69	15.96
	rat11	2.09	3rd BLAST EXPOSURE FULL BODY, 28 min from 2nd blast	2.51	53.58	19.53	16.72
Specimen 8	rat8	2.16	1 BLASTEXPOSURE FULL BODY	2.22	59.91	18.66	16.46
	rat10	2.06	2nd BLAST EXPOSURE FULL BODY, 28 min from 1st blast	2.13	47.33	20.94	16.77
	rat12	2.13	3rd BLAST EXPOSURE FULL BODY, 24 min from 2nd blast	2.31	52.32	20.55	16.77
Specimen 9	rat13	2.17	1 BLAST EXPOSURE, FULL BODY	2.47	52.66	19.42	16.93
	rat15	2.04	2nd BLAST EXPOSURE FULL BODY, 15 min from 1st blast	2.01	58.43	18.16	15.96
	rat17	2.16	3rd BLAST EXPOSURE FULL BODY,18 min from 2nd blast	2.20	42.22	23.52	17.48
Specimen 10	rat14	2.14	1 BLAST EXPOSURE, FULL BODY	2.40	49.90	NA	NA
	rat16	2.24	2nd BLAST EXPOSURE FULL BODY, 20 min from 1st blast	2.20	46.22	22.99	17.19
	rat18	2.11	3rd BLAST EXPOSURE FULL BODY, 15 min from 2nd blast	2.10	43.18	22.75	17.24

Table 2. Summary table of high pressure testing using the CBI-CSP device on 01-July-11. Diaphragm thickness was 0.005 inch + 4 Layers of Tape

As shown in Page 1 of this document, a 0.003 inch diaphragm with no sealant tape should have produced an overpressure event with peak pressure near or above 30 psi at a location (R and □) as shown in Figures 1-2 in the previous page. Instead, the CBI-CSP consistently recorded peak pressures near 20 psi.

There are two possible reasons for that and solutions which are described in detail in FIT Appendices.

Briefly:

1. The maximum sampling rate of the analog to digital converter available on the CBI-CSP device at the time of these tests was 150 kSamples/sec/channel. While this is more than 50% better than the maximum sampling rate available on the DAQCard 6062E currently deployed at Banyan, it is still 17 times slower than the 2.5 Msamples/sec/channel that was later found adequate to accurately detect the peak overpressure values. Version 1 of the CBI-CSP device was designed before we had an accurate numerical and experimental assessment of the sampling rate required to accurately capture the peak overpressure event. Version 1 is the first version designed and released within our currently ongoing development contract, and as such it was deployed as a preliminary prototype for assessment and future improvement.

2. The type of pressure sensing device on board Version 1 of the CBI-CSP package is the calibrated MPXH6300A Integrated Silicon Pressure Sensor for absolute pressure, with on-chip signal conditioning and temperature compensation, from Freescale Corporation (http://www.freescale.com). The principle of operation of this sensor is shown below:

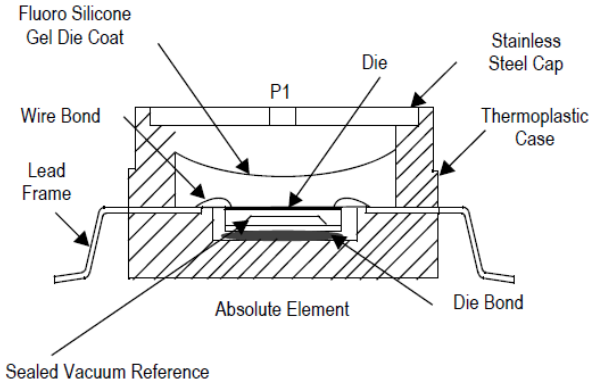

The type of sensing technology for pressure sensors to be used in the CBI-CSP device is highly limited due to size and weight restrictions of the application, in particular if the device must be small enough to be used in rodents. Under such restrictions, the use of piezoelectric pressure transducers is prohibitive in terms of weight and size due to their need of signal conditioning and the typical size and shape of piezoelectric piezo transducers.

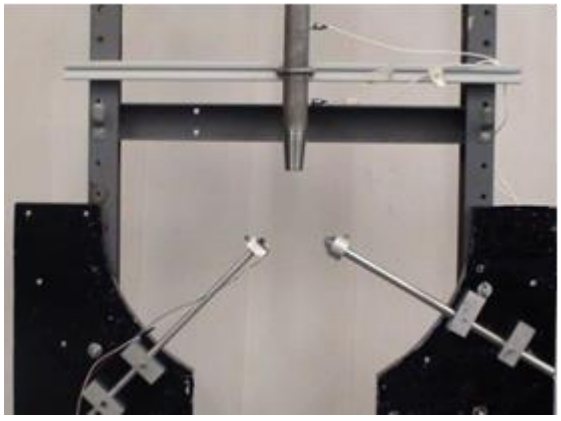

Task 4: Assess brain injury characteristics upon exposure to repeated low level blast; determine cumulative blast load-injury correlations.

Next round of testing in rats was performed with the sensors calibrated using The test rig shown in Figure 7 below will be used during the next quaternary period to test the performance of both the proposed sensing

elements and signal conditioner circuit with blast events created on the 1 inch shock tube at Florida Tech. The critical performance metric for both sensing elements and circuit prototype is the capacity to capture the correct peak overpressure value and time domain shape of the blast event, as compared to those measured using a laboratory-grade reference system. Figure 7. Experimental Test set up to compare pressure traces using the CBI-CSP pressure sensor and signal conditioner (left) versus a reference laboratory sensor (PCB pressure sensor Model Y102A) (right)

That provided the signal intensity and shape similar to the previous Banyan experimental series, resulting in effective Peak Overpressure 50-53 psi for 75 □sec.

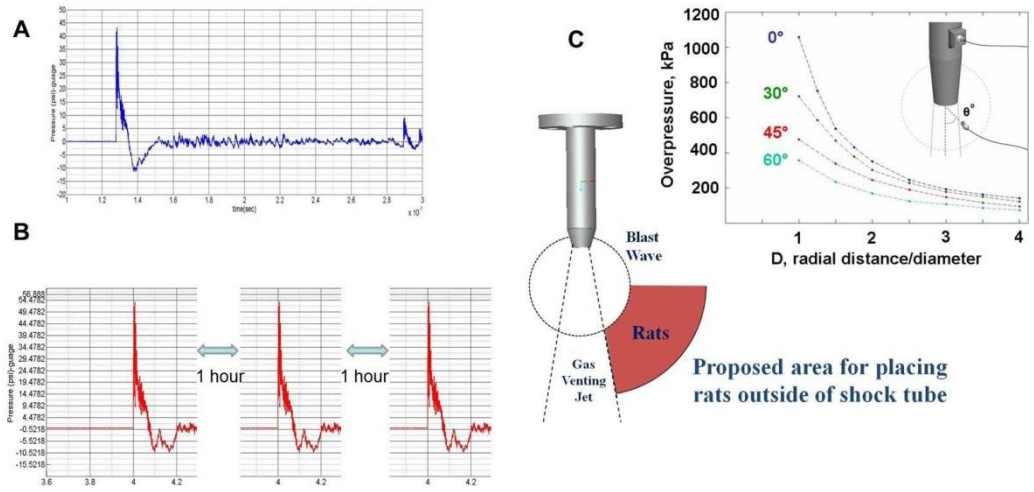

Representative overpressure traces during single (A) and multiple (B) blast exposures; (C) Blast wave overpressure as a function of radial distance and angle.

I. Neural-Glial TBI Markers released in Blood after Single/Multiple Blast:

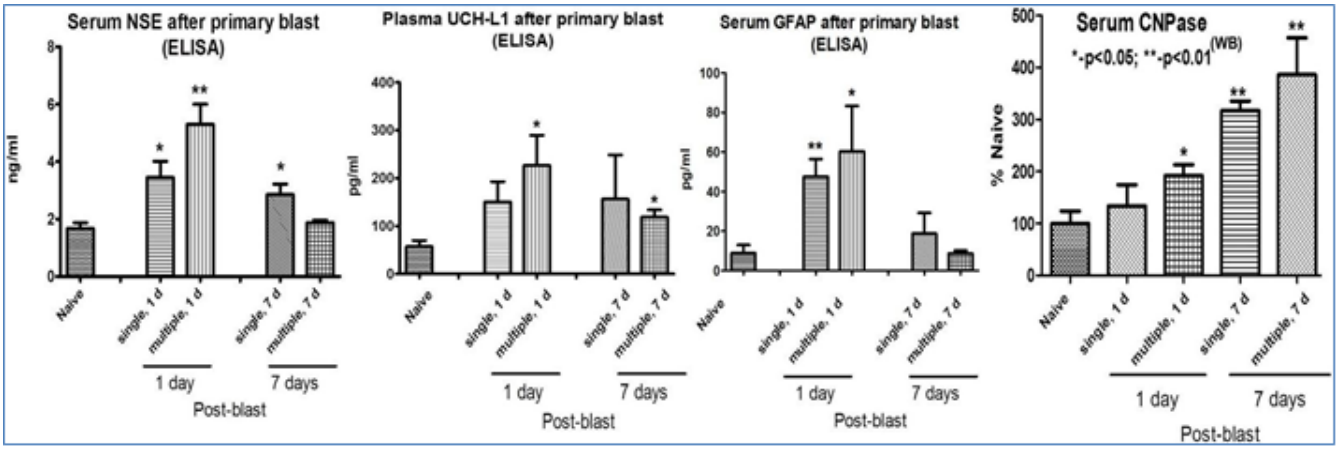

Rats were subjected to a primary blast of 50-53 psi kPa overpressure and total duration of 75 μsec at the frontal part of the rat's skull. Portable cumulative blast sensors were placed on the head front and rat spine. Multiple blasts were performed as a series of 3 exposures, with a 45 min to 1 hr recovery between each blast. High speed imaging revealed a low degree of acceleration at rat position "off-axis" toward external shock tube. Multiple

blasts significantly augmented increased levels of GFAP, UCH-L1 and NSE vs single blast at 1 day post blast. No augmentation was found at 7 day post-blast. On the other
hand, serum CNPase after multiple blasts was significantly augmented vs. single blast both at 1 day and 7 days post exposure. At least 4 rats were examined in each group. *-p<0.05; **-p<0.01.

II. Neuroendocrine, inflammatory and growth factor blast TBI Markers

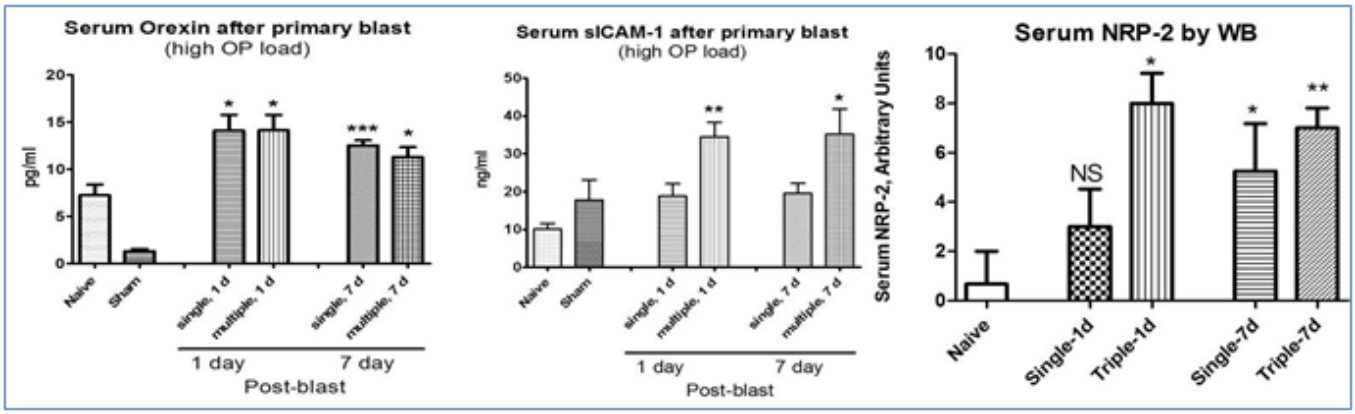

The conditions of rat exposures were as shown above for neuro-glial markers. Although Orexin A was dramatically elevated at day 1 and 7 post-blast, no differences in multiple blast responses vs. single were found. In contrast, both sICAM and NRP-2 serum levels after multiple blasts were higher than after single at day 1 and 7 post-blast. At least 4 rats were examined in each group. *-p<0.05; **-p<0.01

Finally, we compared Blood Brain Barrier (BBB) permeability following single and multiple blasts.

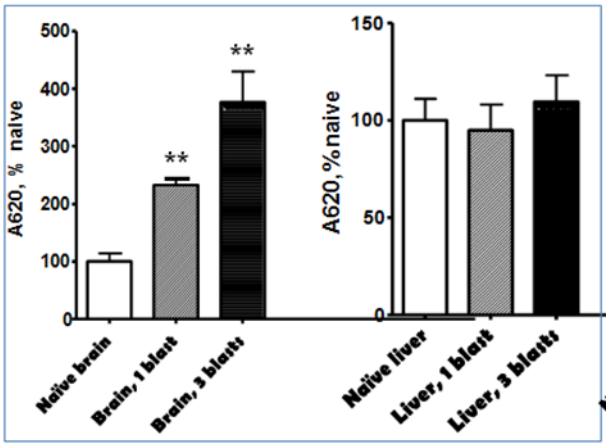

BBB Permeability after Blast |

A 2% solution of Evans Blue Dye in PBS (4 mL/kg of body weight) was injected i.p. and the stain was allowed to circulate for 3 hours. At 4 hrs after first blast the anesthetized animals were intracardially perfused with PBS. Brain and liver samples were then isolated and weighed, homogenized in 2 ml 50% trichloroacetic acid per gram tissue and centrifuged. The absorbance of the extracted dye in supernatant at 620 nm was used to quantify the relative tissue content of EBD.

As can be seen, blast exposure induces Evans Blue Dye accumulation in brain but not in the liver. Moreover, multiple blast further augmented the Dye accumulation suggesting that BBB has a tendency and ability to reopen after repeated blast exposures.

Third Year 2013. Objectives of the project are: (i) Develop an experimental framework for reproducing multiple blast wave exposures and recording multiple blasts in an animal model using a

prototype sensor device, (ii) define cumulative blast load upon multiple blast exposures and distinguish biomarkers of mild through severe TBI, (iii) identify and characterize biochemical markers of multiple vs. single blast exposures, and formulate blast load injury scale.

In year 1, we determined blast load characteristics producing mild through severe TBI and defined 'composite' and primary blast parameters. Schlieren optics was used to visualize blast wave interaction with experimental animal. The pathological effects of primary blast overpressure were compared with brain injury via 'composite' blast accompanied by strong head acceleration. We assessed neuro-glial injury evaluated by silver staining, and GFAP/CNPase and NSE. Biomarkers of neuro-glial injury GFAP, CNPase and NSE were accumulated in circulation in a particular time-dependent fashion. Sensor package for detecting/recording a cumulative blast exposure was designed and version 1.1 of sensor was produced. **In year 2** of the project we nearly accomplished characterization severe to moderate TBI upon primary blast (peak overpressure) vs. composite blast, (ii) continued developing a cumulative blast detecting/recording module, and (iii) began characterization of biomarkers of TBI in response to multiple vs. single blast exposures. We characterized several systemic/inflammatory, neuroendocrine and growth factor signatures and revealed their relationships and diagnostic value (L-selectin, sICAM, Orexin A, neuropilin-2). Compared to single exposure, multiple blasts augmented increases of GFAP, UCH-L1, NSE and NRP-2, but not Orexin A, at day 1 post-blast, while at 7 days the cumulative effects were much lower, if any. The improved prototype of cumulative blast sensor and signal conditioning circuit were tested at Banyan Biomarkers on 19 October 2012. **In year 3**, improved prototype (final version) of cumulative blast sensor and signal conditioning circuit has been produced and tested at Banyan Biomarkers November/December, 2013 and January/February 2013. We were capable of capturing at least 3 consecutive blasts and integrate a cumulative load. Also, we continued to fully characterize brain injury and biomarkers after repeated primary blast exposure adding and characterizing novel molecular signatures such as metalloproteinases and thrombin generation biomarkers. We found that in contrast to GFAP/UCH-L1, NSE and NRP-2, serum CNPase and sICAM after multiple blasts was significantly augmented vs. single blast both at 1 day and 7 days post exposure.

Third year 2013

In the body section, I present general outline of fully functional v2 of the cumulative blast sensor. The detail pertaining to the sensor are provided in Manual, see Appendix. Also, I present new data on Thrombin biomarker signatures of a single moderate primary blast vs. 'composite' blast. In addition, comparing biomarkers of single and multiple blast exposure, is presented which include sICM as inflammatory signature and CNPase (in depth analysis).

A version 2 of cumulative blast sensor package has been developed and preliminary tested at Banyan Biomarkers using an improved shock tube.

The system is composed of the following components:

1. The data acquisition board (DAQ board)
2. The sensor board
3. Power source (Lithium polymer rechargeable battery)

Figure 1: Complete cumulative injury-energy sensing package (CBI-ESP), final delivery

Figure 2 Real size of CBI-ESP sensor and DAQ board

To verify functionality and accuracy of the CBI-ESP v2 system, a comparison between data from the CBI-ESP v2.0 and a standard off- the-shelf high speed blast pressure sensor (PCB-Piezotronics) was conducted using a National Instruments PXI-8331 high speed data acquisition card for data collection.

Both sensors were placed outside the venting cone of the shock tube as shown in Figure 3, (a) and (b). In this configuration, both sensors are expected to read approximately the same pressure event at similar phase, although some minor differences are expected due to reflections from the experimental setup.

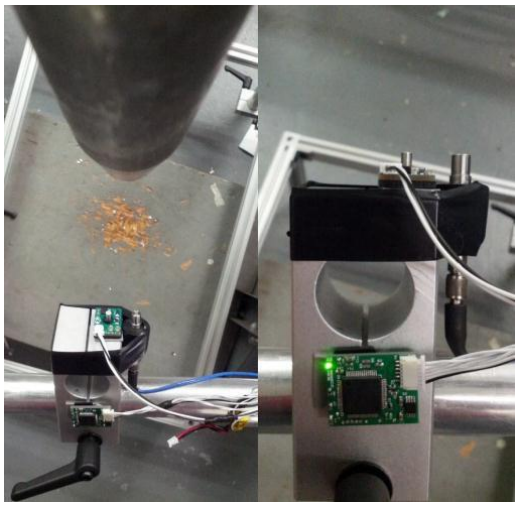

Figure 3 (a): Location of the CBI-ESP sensor board (right) relative to the witness sensor (PCB Piezotronics)

The test was conducted with 1000 psi driver pressure and a driven/driver ratio of 15, using a 0.002 in thick stainless steel shim. The results are shown in **Figure 4.** The standard system was sampled using NI-LabView at 10 Megasamples/sec, and the CBI-ESP v2.0 operated at its native sampling rate of 1 Megasamples/sec.

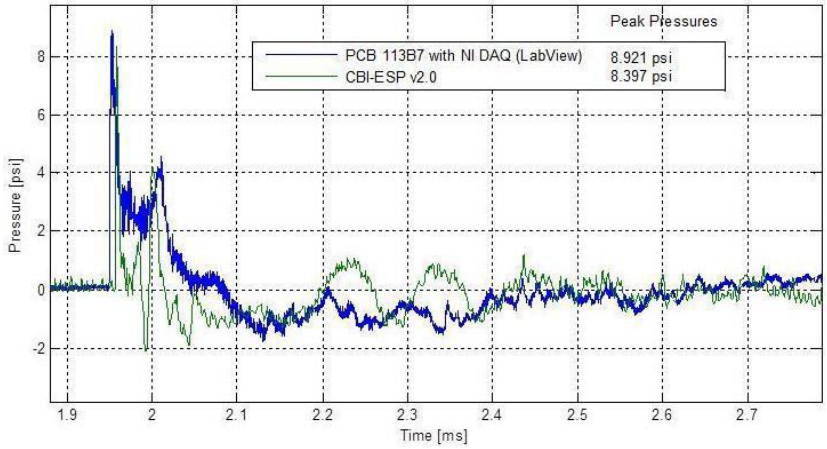

Figure 4 Calibration and validation. Standard blast measurement system (PCB Piezotronics pressure transducer with NI-LabView) compared to the same blast event captured using the CBI-ESP v2.0.

The difference between traces and secondary peak is attributed to slight differences in sensor placement and overpressure wave reflections from two sensors.

Using this package, we performed the series of experiments using repeated blast exposures in rats. We subjected rats combined blast exposure, the first being blast 'on axis' accompanied by head acceleration and two subsequent, with 1 h interval, primary blast OP exposure with negligible or no head acceleration according to the following Table1 .

Table 1 Setup and description of repeated blasts.

Blast OBI rats 11-28-2012_12-05-2012> Protocol #:201004486>
Requisition #13054

	ID #	SSB	Received Date	Birth Date	Sex	Treatment	Treatment Date	# Animals	Comments
4	380, 381	SD	11/27/12	09/29/12	Male	Single blast	11/28/12	2; sOBI	Single on-axis blast (#380:)
5	382, 383	SD	11/27/12	09/29/12	Male	Single blast	11/28/12	2; sOBI	Single on-axis blast (#382:)
6	384, 385	SD	11/27/12	09/29/12	Male	Single blast	11/28/12	2; sOBI	Single on-axis blast (#384:)
8	386, 387	SD	11/27/12	09/29/12	Male	Multiple blast	11/29/12	2; mOBI	Single on-axis blast followed by two more off-axis blasts with ~1 h pauses.
9	388, 389	SD	11/27/12	09/29/12	Male	Multiple blast	11/29/12	2; mOBI	Single on-axis blast followed by two more off-axis blasts with ~1 h pauses.
0	390, 391	SD	11/27/12	09/29/12	Male	Multiple blast	11/29/12	2; mOBI	Single on-axis blast followed by two more off-axis blasts with ~1 h pauses.
1	392, 393	SD	11/27/12	09/29/12	Male	No treatment	NA	2, naive	Naïve control
2	394, 395	SD	11/27/12	09/29/12	Male	No treatment	NA	2, naive	Naïve control
3	396, 397	SD	11/27/12	09/29/12	Male	No treatment	NA	2, naive	Naïve control
4	398, 399	SD	11/27/12	09/29/12	Male	Sham treatment	12/05/12	2, sham	Sham control; ~130 dB noise exposure
5	400, 401	SD	11/27/12	09/29/12	Male	Sham treatment	12/05/12	2, sham	Sham control; ~130 dB noise exposure
6	402, 403	SD	11/27/12	09/29/12	Male	Sham treatment	12/05/12	2, sham	Sham control; ~130 dB noise exposure
8	NA	SD	11/27/12	09/29/12	Male	NA	NA	1	Was used in mOBI series to replace #386

Serum and brain tissue was collected and is being analyzed. Cumulative blast load data are being assessed using MatLab software. The ID numbers for blast-exposed animals are as printed on the labels for 1.5 ml serum collection tubes: 6 sOBI animals (IDs: 380-385); 6 mOBI animals (IDs: 386-391); 6 naïve animals (IDs: 392-397); 6 sham animals (IDs: 398-403).

Task 5 through task 7 of **Specific aim 3** are in progress and are slightly modified. Specifically, we omitted measurement of MBP and focused on studies of CNPase as better marker of myelination disorders and NSE as marker of neuronal injury, which reflects also non-CNS involvement, e.g. platelet activation.

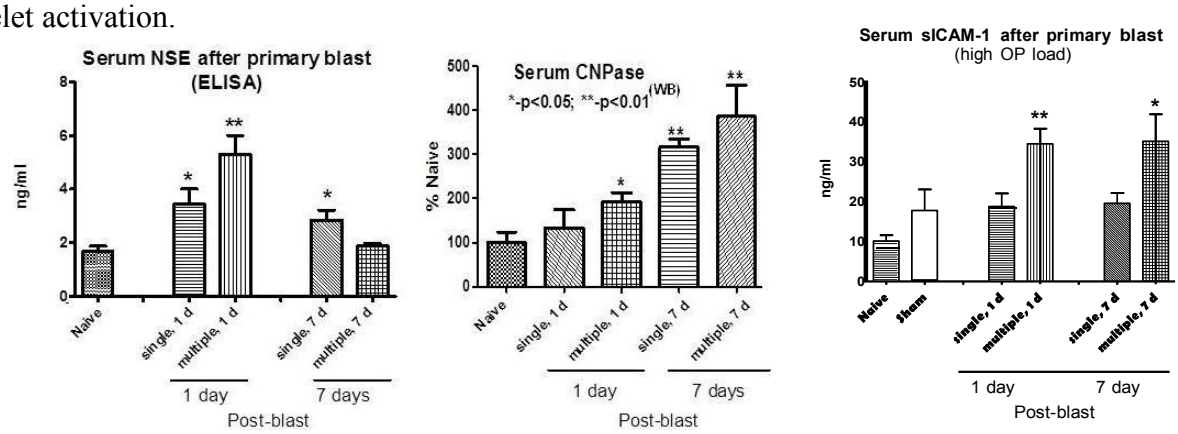

Figure 5 NSE, sICAM and CNpase after single and multiple primary blast

The time-course of NSE, sICAM and CNPase was characterized after single and repeated moderate primary blasts. Biomarker levels rose significantly as a rapid response at day one post- blast, with the CNPase and NSEs after repeated blast exposures elevating further over single

blast. The appearance of characteristic proteins in circulation may reflect deterioration of the BBB and can be used for assessment of injury accumulation. However, triple consecutive blast exposures did not produce a further elevation in biomarkers at 7 days post exposure compared to a single blast. At this time point, their increased levels depend on the cell-specific origin of biomarkers and that stage of injury, rather than reflecting a cumulative blast load.

Task 8 is ~90 % complete. Neuropiline-2 and NGF-beta have been identified and are being investigated as chronic biomarkers after multiple blast reflecting neurorepair. They were reported previously and currently we collect more samples to increase sample size.

According to task 8 of Specific aim 4, we identify thrombin biomarkers as additional critical components of blast brain injury and employed Calibrated Automated Thrombography for assays.
The combined data on thrombin activity at different time-points and blast setups are presented in the Table 2.

Table 2. Indices of Thrombin Activity after Exposure to a Primary/Composite Blast Wave Load.

Primary Blast	CAT parameter	Baseline	6 hr post-blast	1 day post-blast	7 days post-blast
	TG max (nM)	121.0 ± 38.0	513.0 ± 44.0*	212.0 ± 68.0*	255.0 ± 49.0*
	t (Peak) (min)	4.8 ±0.19	8.0 ± 0.24*	7.0 ± 0.12*	5.0 ± 0.11*
	t (Start) (min)	1.1 ± 0.07	1.0 ± 0.08*	1.0 ± 0.09*	1.0 ± 0.07*
	t (Mean) (min)	6.4 ± 0.17	5.4 ± 0.18*	4.5 ± 0.15*	4.0 ± 0.13*
Composite Blast	CAT parameter	Baseline	6 hr post-blast	1 day post-blast	7 days post-blast
	TG max (nM)	120.1 ± 7.2	540.0 ± 26.1*	450.0 ± 23.3*	250.0 ± 11.1*
	t (Peak) (min)	5.0 ±0.14	8.0 ± 0.13*	7.0 ± 0.13*	5.0 ± 0.10
	t (Start) (min)	1.2 ± 0.08	1.0 ± 0.07*	1.0 ± 0.06*	1.0 ± 0.06*
	t (Mean) (min)	6.4 ± 0.12	5.5 ± 0.13*	4.5 ± 0.11*	4.0 ± 0.10*

* P value <0.05 vs. naïve samples.

All indices of TG were remarkably affected in all blast exposed rats compared to naïve animals. However, in 'composite' blast exposed animals, TGmax peaked at 6 hr (~4.5-fold vs. control), sustained at 1 day (~3.8-fold increase), and declined to a 2-fold increase over control levels at day 7 post-blast. In rats subjected to primary blast, TGmax also rose to ~4.2-fold of control values at 6 hours, dropped to ~1.7-fold of control levels at 1 d post-blast, and then exhibited a secondary increase in 2-fold of control values at day 7 post-blast (Fig. 2 A).

Other TG indices did not differ significantly between two types of blast exposure. After either 'composite' or primary blast loads the t -Peak times significantly increased compared to control

values while corresponding t-Mean values decreased at both blast setups. The representative overlapped TG tracings after a primary blast wave load are illustrated in Figure 6 B.

The cumulative analysis of the data suggests strong time-dependent stimulation of overall thrombin production by blast exposure.

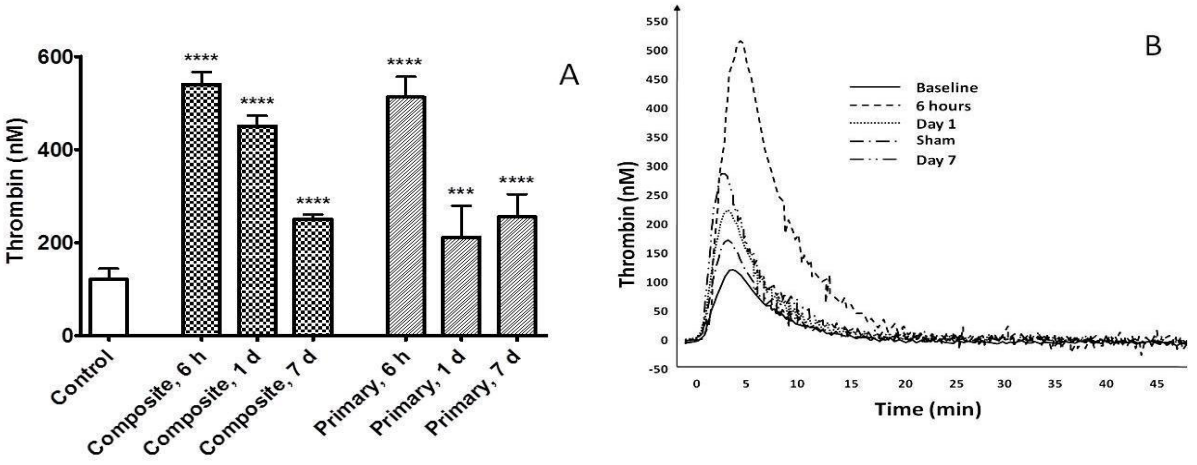

Figure 6 Plasma levels of Thrombin after blast. Concentrations of Thrombin were assessed in rat plasma by CAT technology (A). Representative thrombography tracings after primary blast exposure (B). Data shown are Mean+SEM of at least three independent experiments. *-p<0.001; ****-p<0.0001 vs. control samples**

Concentrations of matrix metalloproteinases MMP-2 (D), MMP-8 (E) and MMP-13 (F) were assessed in rat serum by antibody arrays and ELISA. Please see Materials and Methods for details.

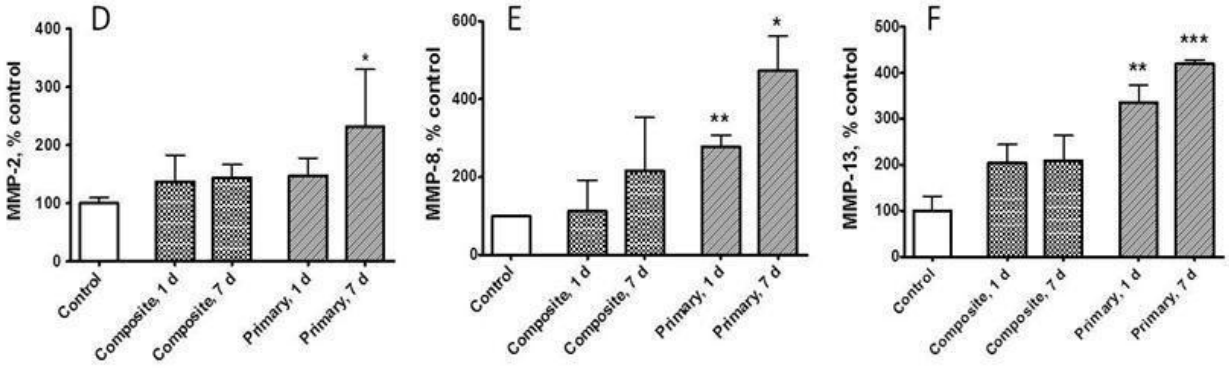

Figure 7 Levels of Matrix metalloproteinases MMP-2 (D), MMP-8 (E) and MMP-13 (F) in serum of rats subjected to moderate primary blast.

Blood was collected from OP-exposed rats at different shock tube set-ups. Data shown are Mean±SEM of at least three independent experiments. *-p<0.05; **-p<0.005; ***-p<0.001 vs. control samples.

In conjunction with vascular/microcirculation biomarkers sICAM and integrin-α/β, this indicates the importance of general inflammatory reactions in response to blast exposure and transition to tissues inflammation.

We assessed Neuroendocrine dysfunctions after single and repeated blast exposure in addition to Orexin A reported previously. Combined data are shown in the table below and detailed in the published paper attached in the appendix:

Table 3. **Catecholamine biosynthetic enzymes and NPY protein in the adrenal medulla of control and overpressure blast injury animals**

Protein	Control (n=4)	OBI (n=4)
TH	100 ± 2%	120 ± 7%*
DβH	100 ± 4%	125 ± 9%*
NPY	100 ± 9%	191 ± 20%*

Values are mean ± SE of 4 rats/group expressed as percentage of control. The level of the averaged control for each protein is arbitrarily set to 100 with SE adjusted proportionally with remaining groups normalized to the level in control. *Significantly increased versus Control; P=0.022 (TH), P=0.031 (DβH), P=0.006 (NPY). TH = tyrosine hydroxylase, DβH = dopamine
β-hydroxylase, NPY = neuropeptide Y.

Fourth Year (2013-2014)

Task 3: Characterize and validate a portable cumulative blast detection device using novel MEMS chip technology (FIT). Assess detection of multiple blast exposures at different 3-D rat orientations to blast wave, and compare cumulative effects in rats using our existing modular system and portable device. We compared with PCB Piezotronics pressure transducer with NI-LabView and determined reproducibility of the sensor. Thus this task has been 100% accomplished, which was technically difficult and challenging task.

Task 4: Assess brain injury characteristics upon exposure to repeated low level blast; determine cumulative blast load-injury correlations. Task 4 experiments in rats were continued using portable sensor and stationary PCB system. Rats were assessed for survival following x3 times cumulative blast at different blast magnitude exposure see table 1 below.

Table 1. **Cumulative overpressure exposures and rat survival.**

Diphargm sickness (in)	Driver overpressure (psi)	Sensor distance (in)	Overpressure rat Skull (45 deg)	Rat #/Exposure #	Survival 24 h/14d
0.002	750	5	24.8	2/3	2/2
0.002	750	7.5	20.1	3/3	3/3
0.002	750	10	16.9	4/3	4/3
0.002	750	15	7.4	3/3	3/3

All rats assessed but 1 survived for 14 days post blasts, which is consistent with the previous data and is anticipated. The tracings of overpressure captured by our sensor was coincident with external PCB standard. Task 4 experiments in rats were continued using portable sensor and stationary PCB system. Rats were assessed for survival following x3 times cumulative blast at different blast magnitude exposure see table 2 below.

Table 2. **Cumulative overpressure exposures and biomarker levels at day 14 .**

Sensor distance (in)	OP rat skull (45^{o})	Blast Exposure #,	GFAP 1 exp/3 exp	UCHL1 1 exp/3 exp	CNPase 1 exp/3 exp
5	24.8	1/3	26.4/31.9 *	105.2/127.5 **	276/294 ***
7.5	20.1	1/3	22.4/27.1 *	94/100.4 *	235/289 ***
10	16.9	1/4	19.5/25.5 *	ND	190/235 **
15	7.4	1/4	-ND-	ND	ND

- not significant vs sham; **- p<0.05, and *-p<0.01**
Rat number in each group ranged 4-7. Mean, pg/ml for GFAP and UCHL1 and AU in % control for CNPase .

Task 4 experiments in rats were nearly completed using stationary PCB system. Rats were assessed for survival following x3 times cumulative blast at different blast magnitude exposure see table 3 below.

Experiments were continued to complete 3. **Single/repeated overpressure exposures and biomarker levels at day 1 (GFAP, UCH-L1) and day1/day7 and 14 (CNPase, NRP-2).**

Distance in/angle	OP rat skull	Blast #	GFAP 1 exp/3 exp	UCHL1 1 exp/3 exp	CNPase 1 exp/3 exp 14d		NRP-2 1exp/3exp 14 d	
5/30°	50-52 (high)-old settings-	1/3, n=4	47.57*/60.38 ** §	150.7*/206.8** §	131*/191** 297/294*** §	261.9/ 382.1 §	167*/322 ** ¶ 375/458*	
5/45°	35 (old set) moderate /24.8	1/3, n=3,4 or 5	36.4*/ 41.9* Averaged with 20.1:	105.2/127.5 *	140*/ 179* 230/289	299.8/ 376.2	130/139* 201/299**	
7.5	20.1		ND	-	-		-	
10	16.9		ND	ND	ND			

***- not significant vs sham; **- p<0.05, and ***-p<0.01; multiple vs single: §- not significant; ¶- significant**

Rat number in each group ranged 3-5. Mean, pg/ml for GFAP and UCHL1 and Arbitrary Units (AU) in % control for CNPase and NRP-2. All rats assessed but 1 survived for 14 days post blasts, which is consistent with the previous data and is anticipated. The tracings of overpressure captured by our sensor was coincident with external PCB standard.

The time-course of CNPase was characterized after single and repeated moderate primary blasts. Biomarker levels rose as a rapid response at day one post-blast, with the CNPase levels were not significant after a single moderate blast and augmented sharply after repeated blast exposures elevating further over single blast. The appearance of CNPase in circulation may reflect deterioration of the BBB and can be used for assessment of injury accumulation. The serum CNPase persisted for a months after exposures, both single and repeated. Triple consecutive blast exposures did not produce further significant elevation in biomarker during 7-30 days post exposure compared to a single blast, the trend to further increase however can be seen at the graph. At this time point, their increased levels depend on the cell-specific origin of biomarkers and that stage of injury, rather than reflecting a cumulative blast load. We are currently extending further the sample size of low to moderate blast exposures at a single and triple load.

Experiments were continued to complete ***Task 5 through task 8*** of Specific aim 3 with emphasis on validation of CNPase as better marker of myelination disorders in chronic phase of post blast TBI. We increased significantly the sample size and extended time post blast to 30 days. Given lifespan of rats as 3-4 years maximum, this roughly corresponds to > than a year in primates. In a previous report, we demonstrated a time course of CNPase and NRP up to 30 days at moderate PO of ~35 psi for 53 µsec, impulse 6.46 kPa-s; Multiple: 3 times with 45 min to 1 hour recovery period. During this period we performed series of experiments and analyzed data at blast magnitude indicated in table. The magnitude of 24.8 psi corresponds to a 35 psi tested previously.

Task 5 through task 7 of Specific aim 3 with emphasis on validation of CNPase as better marker of myelination disorders in chronic phase of post blast TBI. We increased significantly the sample size and extended time post blast to 30 days. Given lifespan of rats as 3-4 years maximum, this roughly corresponds to > than a year in primates **(Fig. 1).**

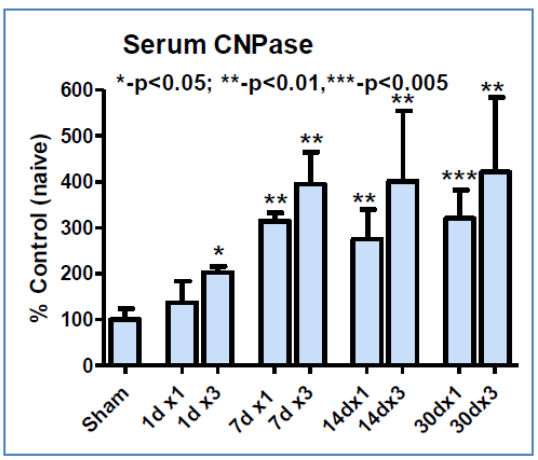

Figure 1. Serum CNpase levels after single and multiple primary blast, n=4 in 1 day and 30 days post blast and n=5 in 7 and 14 days post exposure. Each point represents also 2 independent measurements.

The time-course of CNPase was characterized after single and repeated moderate primary blasts. Biomarker levels rose as a rapid response at day one post-blast, with the CNPase levels were not significant after a single moderate blast and augmented sharply after repeated blast exposures elevating further over single blast. The appearance of CNPase in circulation may reflect deterioration of the BBB and can be used for assessment of injury accumulation. The serum CNPase persisted for a months after exposures, both single and repeated. Triple consecutive blast exposures did not produce further significant elevation in biomarker during 7-30 days post exposure compared to a single blast, the trend to further increase however can be seen at the graph **(Fig. 1)**. At this time point, their increased levels depend on the cell-specific origin of biomarkers and that stage of injury, rather than reflecting a cumulative blast load.

Task 8 Neuropiline-2 and NGF-beta have been identified and are being investigated as chronic biomarkers after multiple blast reflecting neurorepair. We have increased a sample size and extended analysis time to 30 day post blast **(Fig. 2**).

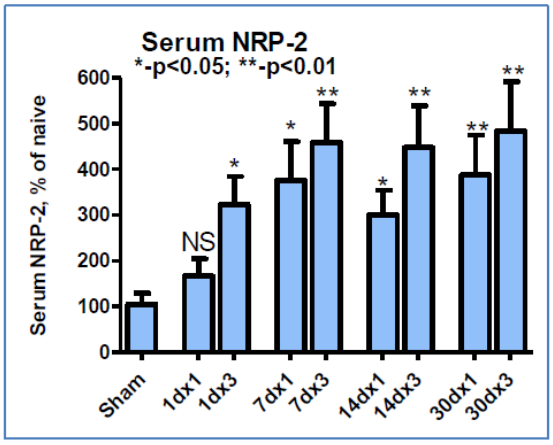

Figure 2. Serum NRP-2 levels after single and multiple primary blast, similar to CNPase, n=4 in 1 day and 30 days post blast and n=5 in 7 and 14 days post exposure. Each point represents also 2 independent measurements.

According to task 8 of Specific aim 4, we identified several additional critical components of blast brain injury. Specifically, in previous report, we showed increased matrix metalloproteinases MMP-2, MMP-8 and MMP-13 in rat serum by antibody arrays and ELISA. Blood was collected from OP-exposed rats at different shock tube set-ups. In this report we also show increased levels of metalloproteinase inhibitors and several other components:

1 d and 7d on are post 'composite' blasts 1 and 7 days, while 1d and 7 d off are post primary blast exposures

Positive Control Normalization without Background															
	sham	sham	sham	1d on	1d on	1d on	7d on	7d on	7d on	1d off	1d off	1 d off	7d off	7d off	7d off
POSITIVE	28,302	28,302	28,302	28,302	28,302	28,302	28,302	28,302	28,302	28,302	28,302	28,302	28,302	28,302	28,302
CD106	842	749	917	324	666	1,174	667	626	662	2,058	1,049	1,291	1,680	2,352	1,111
CINC-3	1	24	1	36	23	28	23	1	51	67	69	27	90	60	8
MCP-1	697	626	640	323	251	1,095	787	701	760	2,271	1,000	1,298	1,400	2,204	1,719
MIP-2	423	584	638	312	741	1,108	662	660	890	1,376	893	748	1,177	1,209	701
TIMP-1	25	76	14	53	41	62	52	26	53	78	110	81	97	32	25
TIMP-2	1,047	1,135	1,140	774	864	1,972	1,622	1,379	1,542	2,324	1,506	1,784	2,002	2,888	1,473
TIMP-3	94	150	34	138	72	160	101	162	117	162	144	147	176	206	146
Internal control	1,553	1,401	1,470	1,661	1,406	2,839	3,584	3,152	2,975	2,229	2,292	2,617	2,644	3,316	2,880

day 1 and 7. The quantitative analysis of these components is under way and will be presented in the next report.

Finally, we performed immunohistochemistry of CNPase and GFAP at 14 day post primary blast exposure to assess accumulation of CNPase in cortex and hippocampus. The cortex data are shown in Fig. 3

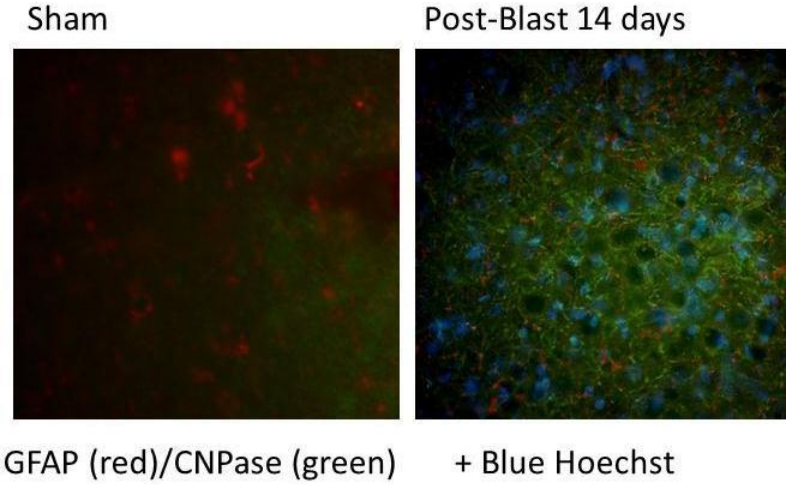

Figure 3. Cortex immunostaining with GFAP (red) and CNPase (green) 14 day post primary blast (20.1 psi, three times). Overlays show co-localization (sparce). The blue is nuclear staining with Hoechst.

All rats assessed but 1 survived for 14 days post blasts, which is consistent with the previous data and is anticipated. The tracings of overpressure captured by our sensor was coincident with external PCB standard.

The time-course of CNPase was characterized after single and repeated moderate primary blasts. Biomarker levels rose as a rapid response at day one post-blast, with the CNPase levels were not significant after a single moderate blast and augmented sharply after repeated blast exposures elevating further over single blast. The appearance of CNPase in circulation may reflect deterioration of the BBB and can be used for assessment of injury accumulation. The serum CNPase persisted for a months after exposures, both single and repeated. Triple consecutive blast exposures did not produce further significant elevation in biomarker during 7-30 days post exposure compared to a single blast, the trend to further increase however can be seen at the graph. At this time point, their increased levels depend on the cell-specific origin of biomarkers and that stage of injury, rather than reflecting a cumulative blast load. We are currently extending further the sample size of low to moderate blast exposures at a single and triple load.

According to task 8 of Specific aim 4, we identified several additional critical components of blast brain injury. Specifically, in previous report, we showed increased matrix metalloproteinases MMP-2, MMP-8 and

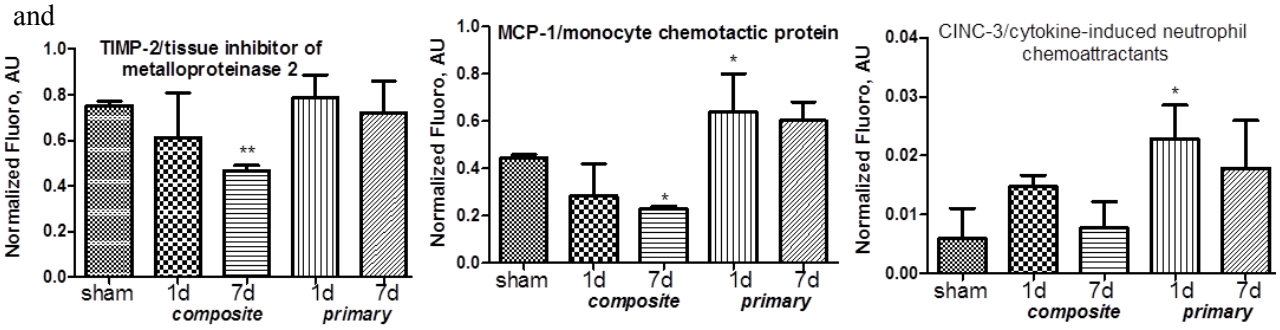

*p<0.05 vs sham

MMP-13 in rat serum by antibody arrays and ELISA. Blood was collected from OP-exposed rats at different shock tube set-ups. We also presented serum levels of metalloproteinase inhibitors, MCP-1/monocyte chemotactic protein, CD106/VCAM-1, and CINC-3/cytokine-induced neutrophil chemoattractant. 1 d and 7d on are post 'composite' blasts 1 and 7 days, while 1d and 7 d off are post primary blast exposures day 1 and 7. The quantitative analysis of these components is shown below in graphs

As can be seen, levels of TIMP-2 and MCP-1 decreased following composite blast at 7d, while MCP-1 and CINC-3 increased at day 1 after primary blast. These data further support importance of systemic inflammatory response after blast, likely at microcirculatory level.

According to task 8 of Specific aim 4, we identified several additional critical components of blast brain injury. Blood was collected from OP-exposed rats at diff erent shock tube set-ups. Specifically, in previous report, we showed increased matrix metalloproteinases MMP-2, MMP-8 and MMP-13 in rat serum by antibody arrays and ELISA. We also presented serum levels of metalloproteinase inhibitors TIMP-2, MCP-1/monocyte chemotactic protein, and CINC-3/cytokine-induced neutrophil chemoattractant. TIMP-2 and MCP-1 decreased following composite blast at 7d, while MCP-1 and CINC-3 increased at day 1 after primary blast. The quantitative analysis of CD106/VCAM-1 and macrophage- inhibitory protein MIP-2 is shown below in graphs.

As can be seen, levels of VCAM/CD106 reactive protein decreased significantly in serum after blast accompanied by head acceleration, but not primary blast. These data further support importance of systemic inflammatory response after blast, likely at microcirculatory level.

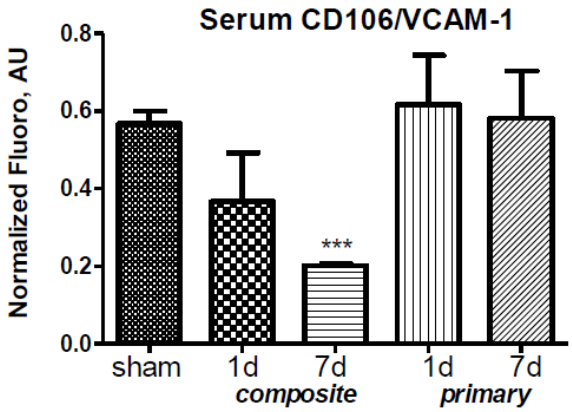

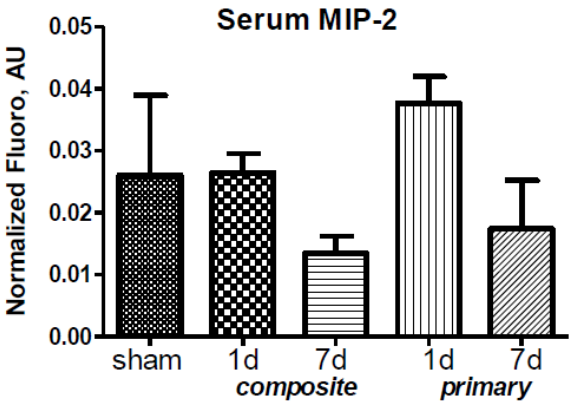

*-p<0.05 vs sham

According to sp. aim 4, we performed assays of miRNAs as potential novel biomarkers of blast TBI. The data are summarized below. We are currently performing a pathophysiology and correlation analysis.

			Control		24 hours Post-Blast		
	Probe_ID	MicroRNA_Accession	Mean	STD	Mean	STD	Control vs Blast_24h: t-test
	rno-miR-341	MIMAT0000587	5.109	0.009	4.439	0.066	0.0001
	rno-miR-133b	**MIMAT0003126**	3.235	0.155	**3.857**	0.091	0.0039
	rno-miR-335	MIMAT0000575	2.876	0.174	2.112	0.228	0.0100
	rno-miR-543*	**MIMAT0003175**	3.515	0.152	**3.041**	0.128	0.0145
	rno-miR-431	MIMAT0001626	3.815	0.152	3.426	0.095	0.0198
	rno-miR-340-3	MIMAT0000585	2.889	0.084	3.118	0.066	0.0208
	rno-miR-342-5	MIMAT0004652	2.294	0.125	2.005	0.064	0.0235
	rno-miR-495	MIMAT0005320	3.968	0.202	3.564	0.062	0.0296
	rno-miR-99b	MIMAT0000821	5.754	0.122	6.004	0.059	0.0331
	rno-miR-7b	MIMAT0000780	3.544	0.542	2.374	0.375	0.0371
	rno-miR-532-5	MIMAT0005322	2.144	0.093	1.641	0.273	0.0391
	rno-miR-369-5	MIMAT0003206	6.631	0.127	6.278	0.159	0.0398
	rno-miR-127	MIMAT0000833	8.053	0.113	7.855	0.040	0.0463
	rno-miR-873	MIMAT0005339	3.174	0.165	2.673	0.280	0.0558
	rno-miR-300-3	MIMAT0000902	6.393	0.103	5.980	0.249	0.0568
	rno-miR-7a	MIMAT0000606	6.867	0.725	5.169	0.841	0.0571
	rno-miR-410	MIMAT0005311	7.078	0.218	6.448	0.353	0.0582
	rno-miR-376a	MIMAT0003198	4.227	0.212	3.866	0.124	0.0640
			Control		7 days Post-Blast		
	Probe_ID	MicroRNA_Accession	Mean	STD	Mean	STD	Control vs Blast-7 days: t-test
	rno-miR-411	MIMAT0005312	2.740	0.098	2.422	0.112	0.0209
	rno-let-7e	MIMAT0000777	9.637	0.035	9.351	0.150	0.0323
	rno-miR-31	MIMAT0000810	2.522	0.249	3.410	0.419	0.0345
	rno-miR-98	MIMAT0000819	5.023	0.133	4.569	0.256	0.0526
	rno-miR-133b	**MIMAT0003126**	3.235	0.155	**3.746**	0.286	0.0528
	rno-miR-664	MIMAT0003382	3.706	0.114	3.957	0.132	0.0672
	rno-miR-543*	**MIMAT0003175**	3.515	0.152	**3.280**	0.068	0.0704
	rno-miR-150	MIMAT0000853	5.765	0.168	6.285	0.338	0.0753
	rno-miR-221	MIMAT0000890	3.963	0.311	3.512	0.112	0.0771

Probe ID	Precursor Accession	MicroRNA Sequence	Fold change 1 day	Fold change 7 days	Main Biological Processes
rno-miR-34a	MI0000877	UGGCAGUGUCUUAGCUGGUUGU	1.78	1.43	Cell differentiation; Wound repair; Mitogenic signaling
rno-miR-31	MI0000872	AGGCAAGAUGCUGGCAUAGCUG	1.72	1.85	Wound repare; Cell cycle regulation; Cell differentiation
rno-miR-206	MI0000948	UGGAAUGUAAGGAAGUGUGUGG	1.71	1.50	DNA damage response; Cell differentiation; Cell cycle
rno-miR-34c	MI0000876	AGGCAGUGUAGUUAGCUGAUUGC	-1.51	-1.38	Estrogen signaling; Mitogenic signaling; Cell cycle regulation
rno-miR-410	MI0006143	AAUAUAACACAGAUGGCCUGU	-1.55	-1.29	Cell differentiation; Vasodilation; Diuresis
rno-miR-137	MI0000910	UUAUUGCUUAAGAAUACGCGUAG	-1.60	-1.54	Cell differentiation; Wound repair; Neurotransmission
rno-miR-7a	MI0000641	UGGAAGACUAGUGAUUUUGUUGU	-3.24	-2.46	Inflammatory response; Wound repair; Immune

Table 1. Representative miRNA changes following mild blast TBI in rat model.

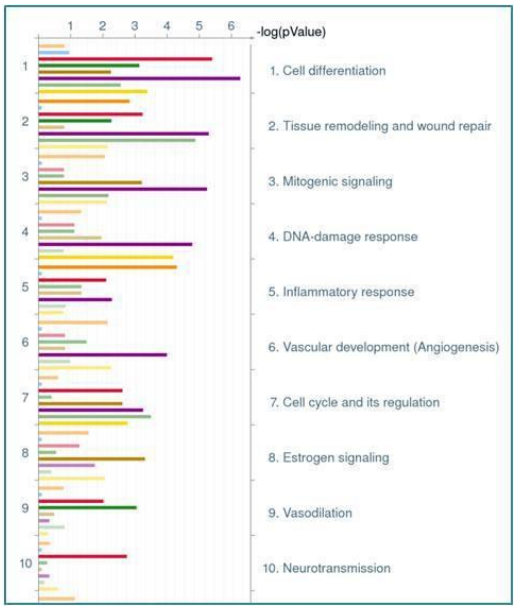

Figure 1. GeneGo Map folder - collection of pathway maps, grouped hierarchically into folders according to main biological processes. Different colored bars represent miRNAs changing >1.5 fold after blast TBI; p-value reflects the significance of association.

The analytical work is in final stage to create a biomarker pathways, including several miRNas found so far, and link to current protein biomarkers including CNPase and NRP-2.

In summary,work in the next period will complete analysis of CNPase and NRP-2 of brain injury in rats subjected to low level of blast exposure at 16.9 psi for three times .

The following workflow is set for on-going experiments.

Diaphragm Thickness 0.002 in Driver Overpressure-750:

Distance Overpressure @ target @ 450 (psi)

10 ~16.8

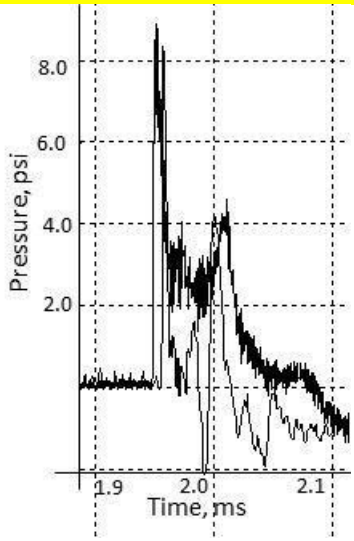

Diaphragm Thickness 0.005 in Driver Overpressure-750: Need to verify:

10 17.8

Experimental Table for current set of repeated blast exposures
3 exposures with 1h interval

Endpoints	Sham 24h/14d/30d	24 h post-blast	14 days post-blast	30 days post-blast
#	2rats-day 1 /2rats-day2 /2rats-day3	6 rats	6 rats	6 rats

Detailed timeline for blast experiment: to assign rat ID #404-430 (the last rat examined was 403). Provided rats arrive Monday or Tuesday, Jun 10-11.

30 days post-blast endpoint:

Rat ID\Date	***Tue, Jun 17***	***Wed, Jul 16*:** **Sample collection**	***Wed, Jun 18***	***Thu, Jul 17*** **Sample collection**	***Thu, Jun 19***	***Fri, Jul 18*** **Sample collection**
#404, 405-sham, #406-411-blast	2 rats at 16.2 psi 3 times with 45 min interval (#406, 407); 1 sham (#404)	Anesthesia, Blood collection	2 rats at 16.2 psi 3 times with 45 min interval (#408, 409); 1 sham (#405)	Anesthesia, Blood collection	2 rats at 16.2 psi 3 times with 45 min interval (#410, 411)	Anesthesia, Blood collection

14 days post-blast endpoint:

Rat ID\Date	***Wed, Jun 25***	***Wed, Jul 9:*** **Sample collection**	***Thu, Jun 26***	***Thu, Jul 10*** **Sample collection**	***Fri, Jun 27***	***Fri, Jul 11*** **Sample collection**
#412, 413-sham, #414-419-blast	2 rats at 16.2 psi 3 times with 45 min interval (#414, 415); 1 sham (#412)	Anesthesia, Blood collection	2 rats at 16.2 psi 3 times with 45 min interval (#416, 417); 1 sham (#413)	Anesthesia, Blood collection	2 rats at 16.2 psi 3 times with 45 min interval (#418, 419)	Anesthesia, Blood collection

24 h post-blast endpoint:

Rat ID\Date	***Mon, Jun 30***	***Tue, Jul 01:*** **Sample collection**	***Wed, Jul 2***	***Thu, Jul 3*** **Sample collection**	***Mon, Jul 7***	***Tue, Jul 8*** **Sample collection**
#420, 421-sham, #422-427-blast	2 rats at 16.2 psi 3 times with 45 min interval (#422, 423); 1 sham (#420)	Anesthesia, Blood collection	2 rats at 16.2 psi 3 times with 45 min interval (#424, 425); 1 sham (#421)	Anesthesia, Blood collection	2 rats at 16.2 psi 3 times with 45 min interval (#426, 427)	Anesthesia, Blood collection

IACUC renewal was approved on 5/19/14 and the *in vivo* experiments were performed according to the plan detailed in aforementioned table.

The parameters of OBI presented in the table below:

Diaphragm Thickness -in	Driver Overpressure - psi	External Sensor Distance (in)	Overpressure @ target (@ 45 deg)-psi
0.002	750	10	16.2 (50-60 usec)

The following ELSIA results were obtained:

- **Rat sICAM-1/CD54**

sICAM-1/CD54 levels in CSF and Serum were determined using sICAM-1/CD54 ELISA kit (R&D, Cat#RIC100). This assay kit allows quantitatively determine the levels of sICAM-1/CD54 in CSF and serum. The results did not show any significant up-regulation of sICAM-1/CD54 in the CSF and serum following repetitive level of blast exposure at 16.9 psi (Figure 1).

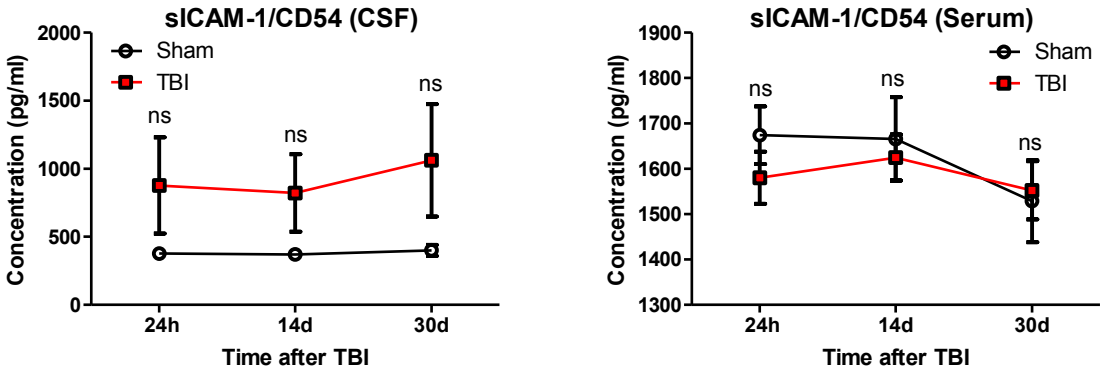

Figure 1. Effect of repetitive blast exposure on the levels of sICAM-1/CD54 in CSF and serum. The graphs represent ELISA results showing temporal profile of the levels of sICAM-1/CD54 in CSF (**A**) and serum (**B**) following repetitive blast exposure (16.9 psi for three times). "ns" denotes not significantly different between values from sham and TBI groups at corresponding time points obtained from two-way ANOVA followed by Bonferroni's multiple comparison test (n=2 for sham groups and n=6 for TBI groups at each time point).

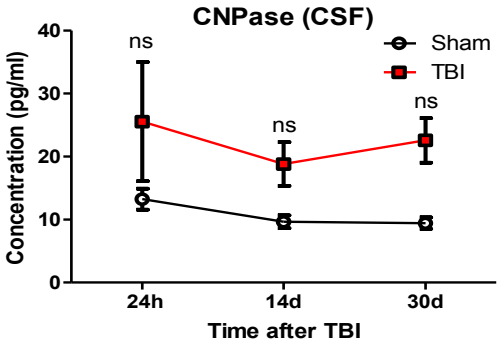

Figure 2. Effect of repetitive blast exposure on the levels of CNPase in CSF. The graphs represent ELISA results showing temporal profile of the levels of CNPase in CSF following repetitive blast exposure (16.9 psi for three times). "ns" denotes not significantly different between values from sham and TBI groups at corresponding time points obtained from two-way ANOVA followed by Bonferroni's multiple comparison test (n=2 for sham groups and n=6 for TBI groups at each time point).

Rat CNPase

CNPase levels in CSF were determined using CNPase ELISA kit (EIAab, Cat#E15033r). This assay kit allows quantitatively determinine the levels of CNPase in serum. The results did not show any significant up-regulation of CNPase in the CSF and serum following repetitive level of blast exposure at 16.9 psi (Figure 2).

- **Rat Orexin**

Orexin level in in CSF was determined using Orexin ELISA kit (ordered through Antibody online, Cat#MBS700368). According to manufacture instruction, this assay kit allowed to quantitatively determine levels of Orexin in serum. The results did not show any significant up-regulation of Orexin in the CSF and serum following repetitive level of blast exposure at 16.9psi (Figure3).

- **Rat Neuropilin2**

Rat Neuropilin2 levels in CSF and serum were determined using Neuropilin2 ELISA kit (Cat# ABIN819129, ordered through Antibodies online). According to manufacture instruction, this assay kit allowed to quantitatively determine levels of rat Neuropilin2 in biofluids. The results did not show any significant up-regulation of Neuropilin2 in the CSF and serum following repetitive level of blast exposure at 16.9 psi (Figure 4).

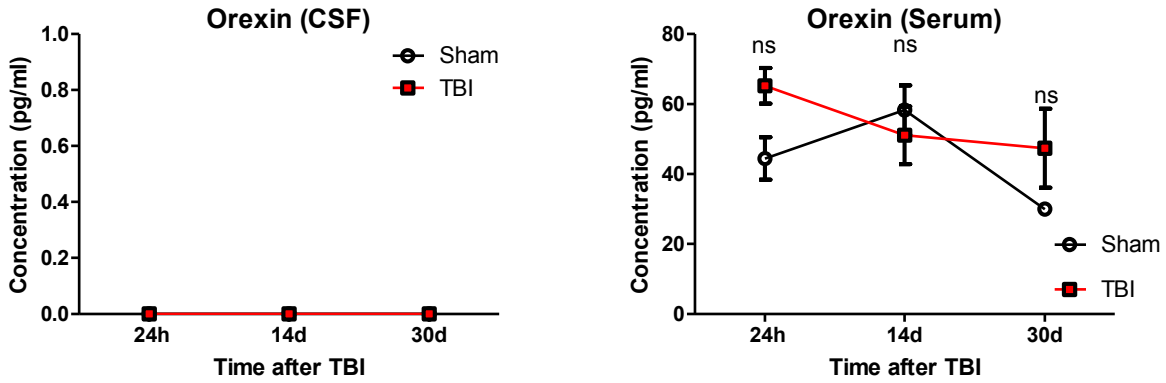

Figure 3. Effect of repetitive blast exposure on the levels of Orexin in CSF and serum. The graphs represent ELISA results showing temporal profile of the levels of Orexin in CSF (**A**) and serum (**B**) following repetitive blast exposure (16.9 psi for three times). "ns" denotes not significantly different between values from sham and TBI groups at corresponding time points obtained from two-way ANOVA followed by Bonferroni's multiple comparison test (n=2 for sham groups and n=6 for TBI groups at each time point).

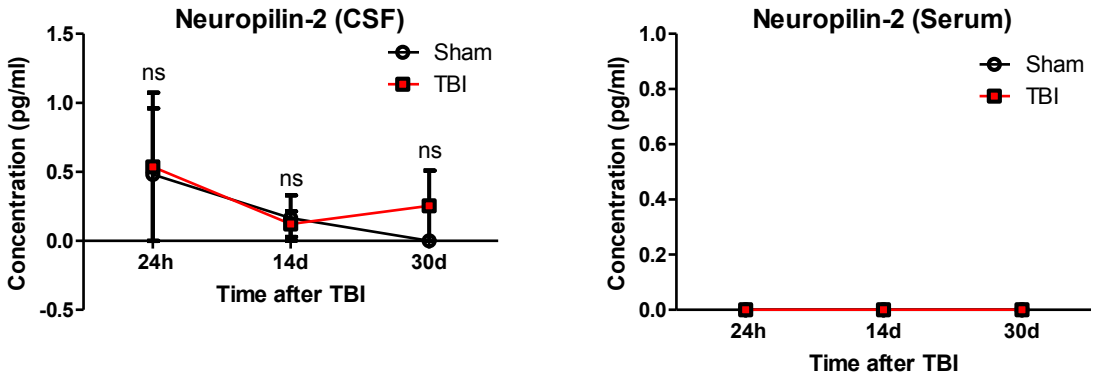

Figure 4. Effect of repetitive blast exposure on the levels of sICAM-1/CD54 in CSF and serum. The graphs represent ELISA results showing temporal profile of the levels of sICAM-1/CD54 in CSF (**A**) and serum (**B**) following repetitive blast exposure (16.9 psi for three times). "ns" denotes not significantly different between values from sham and TBI groups at corresponding time points obtained from two-way ANOVA followed by Bonferroni's multiple comparison test (n=2 for sham groups and n=6 for TBI groups at each time point).

Western Blots results

- **Rat Neuropilin2**

Rat Neuropilin2 levels in CSF were determined using Western Blot (Figure 5).

The Western Blot results did not show any significant up-regulation of Neuropilin2 in theCSF and serum following repetitive level of blast exposure at 16.9 psi (Figure 6).

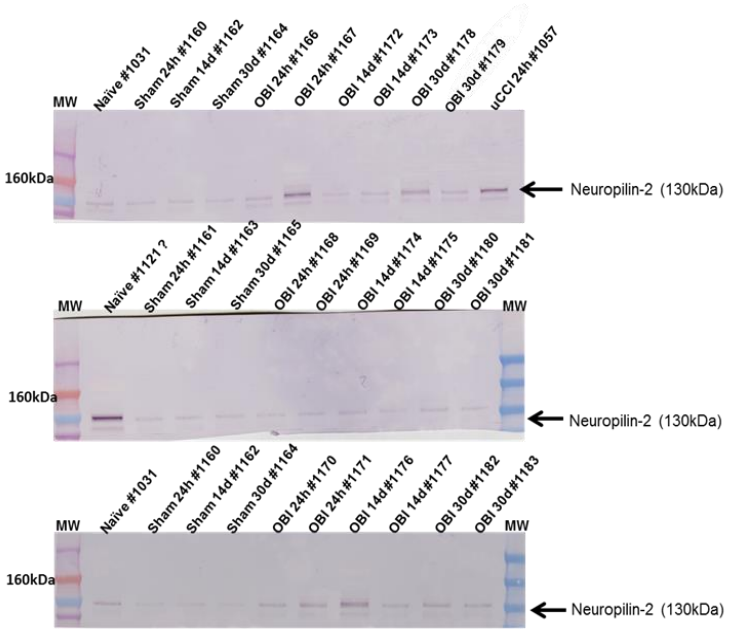

Figure 5. Western Blot for Neuropilin2 in the CSF of sham- and TBI-injured rats.

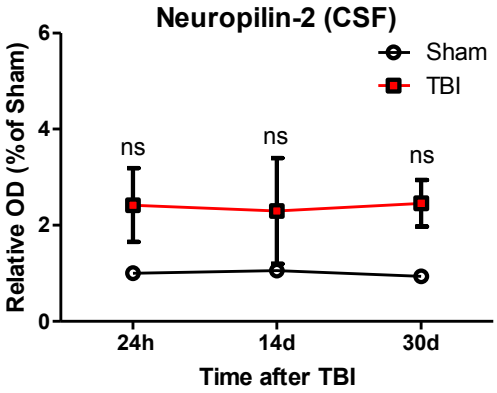

Figure 6. Effect of repetitive blast exposure on the levels of rat Neuropilin2 in CSF. The graphs represent Western Blot results showing temporal profile of the levels of CNPase in CSF following repetitive blast exposure (16.9 psi for three times). "ns" denotes not significantly different between values from sham and TBI groups at corresponding time points obtained from two-way ANOVA followed by Bonferroni's multiple comparison test (n=2 for sham groups and n=6 for TBI groups at each time point).

- **MAP2**

Additionally MAP2 levels in CSF were determined using Western Blot (Figure 7).
The Western Blot results did not show significant up-regulation of MAP2 in rat CSF following repetitive OBI (low level) Figure 8.

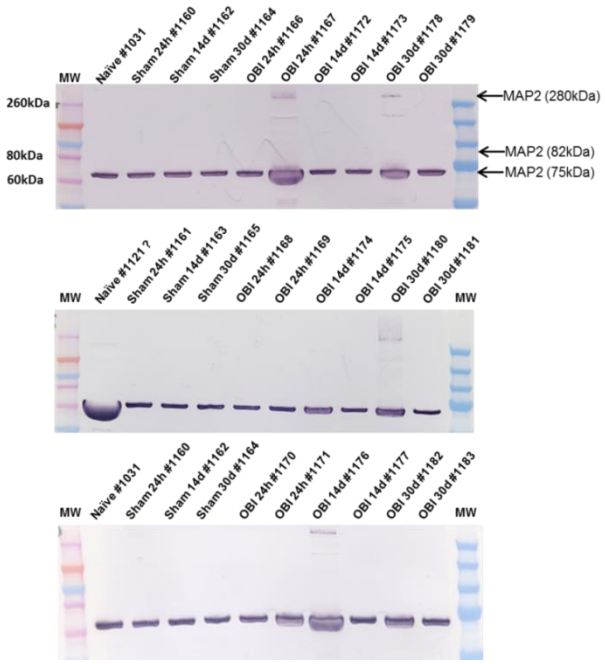

Figure 7. Western Blot for MAP2 in the CSF of sham- and TBI-injured rats.

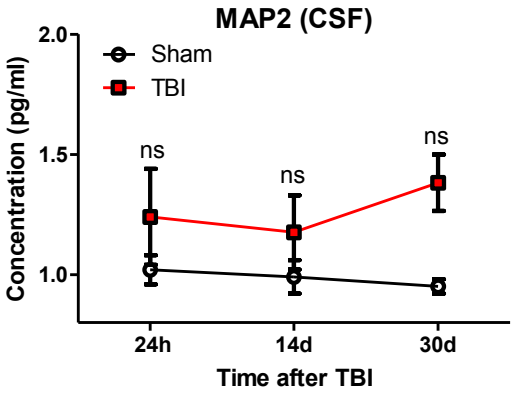

Figure 8. Effect of repetitive blast exposure on the levels of rat MAP in CSF. The graphs represent Western Blot results showing temporal profile of the levels of CNPase in CSF following repetitive blast exposure (16.9 psi for three times). "ns" denotes not significantly different between values from sham and TBI groups at corresponding time points obtained from two-way ANOVA followed by Bonferroni's multiple comparison test (n=2 for sham groups and n=6 for TBI groups at each time point).

In summary, the data obtained from ELISA and semi-quantitative Western Blot analyses indicate that repetitive blast exposure using 16.9 psi magnitude performed 3 times each 45 min had no significant effect on the CSF and serum levels of CNPase, Orexin, Neuropilin2 and MAP as compared with sham at corresponding time points. In some cases the levels of the selected biomarkers in animals exposed to blast were markedly higher than those in the corresponding sham groups, though, still not significantly different possibly due to small sample size (n=2) requested for sham groups in these experiments.

4. KEY RESEARCH ACCOMPLISHMENTS:

Year 1: An accurate model of blast exposure in rats, reproducing generally 2 variants of blast exposure: primary and 'composite', has been validated. The precise calibration of the angle, distance and corresponding OP magnitude, duration and impulse has been achieved and tabulated.

- Comparison of moderate 'Primary' and 'Composite' blast responses revealed the differences in pathogenic pathways and biomarker patterns. While both type of exposures were characterized by prominent gliosis. Composite blast on the head (accompanied by head acceleration) produces slightly higher level of neuronal injury evidenced by silver staining.

- GFAP, NSE and CNPase have been demonstrated to be sensitive and specific biomarkers in serum of rats subjected toboth moderate composite and primary blast. However, the pattern of release in circulation has shown to be different.

- The serum level of UCH-L1 was not increased upon single moderate primary blast exposure indicating that neuron body injury was not prominent at that level of single primary blast.

- Systemic, vascular, neuroinflammatory and neuroendocrine responses are essential components in responses to blast:

    - When rats were exposed to peak OP through frontal region of the head w/o head accelleration, the levels of IL-1, IL-10, Selectins and chemokine Fractalkine response was slightly higher than compared to head-directed exposure of a same magnitude: body protection decreased biomarkers release in circulation.

- NGF-beta and Neuropilin-2 have been shown to significantly elevate in serum after blast, may have neurotrophic functions and be a marker of adaptive responses/neurorepair after blast induced TBI.

- Version 1 of Cumulative Blast and Impulse (CBI) Exposure Sensing Package (ESP) has been developed and is being tested.

- Preliminary data on biomarker panel utility in single vs. multiple blast have been obtained. However, initial experiments show that responses to repeated primary moderate/severe blast may be more complex than simple additive effects of triple blast exposures. Studies are under way to elucidate the underlying mechanisms.

Year2

- Further detailed comparison of moderate 'Primary' and 'Composite' blast responses revealed the differences in pathogenic pathways and biomarker patterns. While both type of exposures were characterized by strong gliosis, 'composite' blast on the head (accompanied by head acceleration) produces significantly higher neuronal injury.

- Systemic, vascular, neuroinflammatory and neuroendocrine responses are essential components in responses to blast:
- Orexin A, sICAM and Neuropilin-2 (NRP-2) appear to be the most prominent biomarkers
- The FIT prototype sensor and signal conditioning circuit have been designed, built and successfully tested. The proposed prototype has demonstrated enough response speed to accurately record the peak overpressure of the blast event as compared to the benchmark PCB sensor.
- Different biomarkers exhibited significantly different response to a single vs. multiple blast:

- Although Orexin A was dramatically elevated at day 1 and 7 post-blast, no differences in multiple blast responses vs. single were found. In contrast, both sICAM and NRP-2 serum levels after multiple blasts were higher than after single at day 1 and 7 post-blast.

- Multiple blasts significantly augmented increased levels of GFAP, UCH- L1 and NSE vs single blast at 1 day post blast. No augmentation was found at 7 day post-blast. On the other hand, serum CNPase after multiple blasts was significantly augmented vs. single blast both at 1 day and 7 days post exposure.

- Multiple blast further augmented the Dye accumulation suggesting that

BBB has a tendency and ability to reopen after repeated blast exposures**.**

Year3

- The final sensor prototype version 2.0 and signal conditioning circuit have been produced and successfully tested. The proposed prototype has shown the response speed to accurately record the peak overpressure of the blast event as compared to the benchmark PCB sensor.

- A comprehensive evaluation has been done to characterize mild through severe blast TBI and differences revealed between moderate 'Primary' vs 'Composite' blast responses in pathogenic pathways and biomarker responses. While both type of exposures were characterized by strong gliosis, 'composite' blast on the head (accompanied by head acceleration) produces significantly higher neuronal injury.

- We have shown that systemic, vascular, neuroinflammatory and neuroendocrine responses are essential components in responses to blast in general and primary OP exposure in particular:

    - Orexin A, sICAM and Neuropilin-2 (NRP-2) have been confirmed as the most prominent biomarker candidates having subacute and chronic diagnostic utility

    - We demonstrate increases in tissue metalloproteinases MMP-2 (D), MMP-8 (E) and MMP-13 (F) after primary blast further supporting systemic responses to blast exposure. This was co-incident with increases in integrin- -α/β,

- Orexin A was dramatically elevated at day 1 and 7 post-blast, no differences in multiple blast responses vs. single were found. In contrast, both sICAM and NRP-2 serum levels after multiple blasts were higher than after single at day 1 and 7 post-blast.

- Multiple blasts significantly augmented increased levels of GFAP, UCH-L1 and NSE vs single blast at 1 day post blast. No augmentation was found at 7 day post-blast. On the other hand, serum CNPase, sICAM and NRP-2 after multiple blasts were significantly augmented vs. single blast both at 1 day and 7 days post exposure.

- Multiple blast further augmented the Dye accumulation suggesting that BBB has a tendency and ability to reopen after repeated blast exposures.

- Novel thrombin-generated biomarkers of blast exposure linking microcirculatory, inflammatory and coagulation disorders have been assessed and their importance in pathogenesis has been demonstrated.

- A substantial activation of catecholamine biosynthetic enzymes and Neuropeptide Y has been shown supporting a profound neuroendocrine responses after blast exposures.

Year 4

- Characterized and validated a portable cumulative blast detection device using novel MEMS chip technology (FIT) has been completed. We compared with PCB Piezotronics pressure transducer with NI-LabView and determined reproducibility of the sensor. Thus this task has been 100% accomplished, which was technically difficult and challenging task.
- Assessed brain injury characteristics upon exposure to repeated low level blast; determined cumulative blast load-injury and correlations were completed.

- Neuropiline-2 and NGF-beta were identified and investigated as chronic biomarkers after multiple blast reflecting neurorepair.

- According to task 8 of Specific aim 4, we identified several additional critical components of blast brain injury. Specifically, in previous report, we showed increased matrix metalloproteinases MMP-2, MMP-8 and MMP-13 in rat serum by antibody arrays and ELISA.

5. CONCLUSION

In the first year of the project, we generally validated the models of 'composite' blast exposure accompanied by head acceleration vs primary blast load, where peak overpressure 'flows the head through a rostral part of the brain' w/o significant head acceleration. Schlieren optics was used to visualize blast wave interaction with experimental animal. Blast peak overpressure, duration, and impulse on the surface of rats at various orientations to the blast wave were determined and standardized. We began characterizing molecular signatures of blast brain injury and outlines several categories of signatures: neuroglial, microvascular, systemic & neuroinflammation, and neuroendocrine changes.

During the second year, we continued comparing blast load characteristics producing mild through severe TBI of 'composite' with primary blast. Also, we initially characterized brain injury and biomarkers after repeated blast exposure by ELISA, antibody microarrays, and Western blot. Rats were subjected to blast of different magnitude, including primary blast of 50-53 psi kPa overpressure, 75 μsec at the frontal part of the rat's skull. We measured blood accumulation of GFAP and CNPase, neuronal UCH-L1 and NSE, neuroendocrine peptide Orexin A, and Neuropilin-2 at different times post-blast. We demonstrated the importance of the orientation of head/body to blast wave for the response and biomarker accumulation. While both type of exposures were characterized by strong gliosis, 'composite' blast on the head (accompanied by head acceleration) produces significantly higher neuronal injury. We also revealed several systemic and microcirculatory inflammation biomarkers such as L-selectin and s-ICAM involved in molecular mechanisms of blast-induced injury. The FIT prototype sensor (version 1) to capture multiple blast exposures was designed, built and successfully tested. We performed preliminary calibration and evaluation of sensor in rats after multiple blasts as a series of 3 exposures, with a 45 min to 1 hr recovery between each blast. Repeated blasts augmented increased levels of GFAP, UCH-L1 and NSE vs single blast at 1 day post blast. No augmentation was found at 7 day post-blast. On the other hand, serum CNPase after multiple blasts was significantly augmented vs. single blast both at 1 day and 7 days post exposure.

In year 3, we completed a comprehensive evaluation of mild through severe blast TBI and differences revealed between moderate 'Primary' vs 'Composite' blast responses in pathogenic pathways and biomarker responses. While both type of exposures were characterized by strong gliosis, 'composite' blast on the head (accompanied by head acceleration) produces significantly higher neuronal injury. The final version of improved prototype (final version) of cumulative blast sensor and signal conditioning circuit has been produced and tested at Banyan Biomarkers November/December, 2013 and January/February 2013. We were capable of capturing at least 3 consecutive blasts and integrate a cumulative load. Serum CNPase and sICAM after multiple blasts was significantly augmented vs. single blast both at 1 day and 7 days post exposure. In contrast, repeated blasts cumulated the increase of GFAP, UCH-L1, NSE and NRP-2, but not Orexin A at day 1 only, while at 7 days the cumulative effects were much lower. Novel thrombin-generated biomarkers of blast exposure linking microcirculatory, inflammatory and coagulation disorders have been assessed and their importance in pathogenesis has been demonstrated. A strong correlation has been shown with integrin α/β. A substantial activation of catecholamine biosynthetic enzymes and Neuropeptide Y has been shown supporting a profound neuroendocrine responses after blast.

In year 4th, we completed characterization and validation of a portable cumulative blast detection device using novel MEMS chip technology (FIT). Assessed detection of multiple blast

exposures at different 3-D rat orientations to blast wave, and compared cumulative effects in rats using our existing modular system and portable device. We compared with PCB Piezotronics pressure transducer with NI-LabView and determined reproducibility of the sensor.
Assessed brain injury characteristics upon exposure to repeated low level blast, determined cumulative blast load-injury correlations and validated our biomarker of chronic brain injury NRP-2 and CNPase (CTE) up to 30 days post-blast.

6. PUBLICATIONS:

1. Svetlov, S.I., V. Prima, D.R. Kirk, H. Gutierrez, K.C. Curley, R.L. Hayes, and K.K. Wang, Morphologic and biochemical characterization of brain injury in a model of controlled blast overpressure exposure. J Trauma, 2010. 69(4): p. 795-804.

2. Svetlov, S.I., V. Prima, O. Glushakova, A. Svetlov, D.R. Kirk, H. Gutierrez, V.L. Serebruany, K.C. Curley, K.K. Wang, and R.L. Hayes, Neuro-glial and systemic mechanisms of pathological responses in rat models of primary blast overpressure compared to "composite" blast. Front Neurol, 2012. 3: p. 15.

3. Prima, V., V.L. Serebruany, A. Svetlov, R.L. Hayes, and S.I. Svetlov, Impact of moderate blast exposures on thrombin biomarkers assessed by calibrated automated thrombography in rats. J Neurotrauma, 2013. 30(22): p. 1881-7.

4. Tumer, N., S. Svetlov, M. Whidden, N. Kirichenko, V. Prima, B. Erdos, A. Sherman, F. Kobeissy, R. Yezierski, P.J. Scarpace, C. Vierck, and K.K. Wang, Overpressure blast-wave induced brain injury elevates oxidative stress in the hypothalamus and catecholamine biosynthesis in the rat adrenal medulla. Neurosci Lett, 2013. 544: p. 62-7.

5. Kobeissy, F., S. Mondello, N. Tumer, H.Z. Toklu, M.A. Whidden, N. Kirichenko, Z. Zhang, V. Prima, W. Yassin, J. Anagli, N. Chandra, S. Svetlov, and K.K. Wang, Assessing neuro-systemic & behavioral components in the pathophysiology of blast-related brain injury. Front Neurol, 2013. 4: p. 186.

6. Adams, S., J.A. Condrey, H.W. Tsai, S.I. Svetlov, and P.W. Davenport, Respiratory responses following blast-induced traumatic brain injury in rats. Respir Physiol Neurobiol, 2014. 204: p. 112-9.

7. REPORTABLE OUTCOMES:

Year 1

1. The paper entitled "**Morphologic and biochemical characterization of brain injury in a model of controlled blast overpressure impact**" by **Svetlov SI,** Prima V, Kirk DR, Gutierrez H, Curley KC, Hayes RL, Wang KK. has been published in J Trauma. 2010 October;69(4):795-804. **see Appendices**

2. Oral presentation at National Neurotrauma Society Meeting in Fort Lauderdale NNS- July, 2011: **DIVERSE MECHANISMS OF BLAST INDUCED NEUROTRAUMA IN RAT MODELS** - Objectives:
1) Demonstrate different effects of shock wave components on rat head mobility upon blast exposure. 2) Reveal importance of animal position toward shock/blast impulse for pathological responses. 3) Establish systemic, vascular, neuroendocrine and glia-neuron responses after blast exposure in rats.

3. In Progress Review (IPR), pre-ATACCC-2011 DoD oral presentation and progress report on current project, August 2011, Fort Lauderdale

4. Abstract and poster entitled 'Establishing Biomarker/Brain Injury Metrics in Rat Models of Cumulative Blast Overpressure" by V. Prima1, O. Glushakova1, A. Svetlov1, D. R. Kirk2 , H. M. Gutierrez2, K. C. Curley3, R. L. Hayes1, K. W. Wang1, ***S. I. Svetlov***1was presented at Advanced Technology Applications for Combat Casualty Care (ATACCC) August, 2011 Ft. Lauderdale, **see Appendices**

5. Presentation and published paper entitled "**Neuro-glial and systemic mechanisms of athological responses to primary blast overpressure (OP) compared to 'composite' blast accompanied by head acceleration in rats" by Stanislav Svetlov**, Victor Prima, Daniel Kirk, Hector Gutierrez, Kenneth Curley, Ronald Hayes, Kevin Wang was presented at NATO Conference 'A Survey of Blast Injury across the Full Landscape of Military Science, October 2011, Halifax. Proceeding of NATO conference HFN-207 **see Appendices**

Year 2

1. The paper invited for special topic Blast-induced Neurotrauma and entitled "Neuro-glial and systemic mechanisms of pathological responses in rat models of primary blast overpressure compared to "composite" blast." by Svetlov SI, Prima V, Glushakova O, Svetlov A, Kirk DR, Gutierrez H, Serebruany VL, Curley KC, Wang KK, Hayes RL. Has been published in Frontiers in Neurol. 2012;3:15. Epub 2012 Feb 9.see Appendices

2. Abstract and poster entitled 'MULTIPLE BLAST EXPOSURES ALTERS NEUROGLIAL, NEUROENDOCRINE AND GROWTH FACTOR BIOMARKERS TO BLAST LOAD IN RATS" by Prima V1 , Scharf D1, Gutierrez H2, Kirk DR2 Svetlov A1, Curley KC3, Hayes RL1, Svetlov SI was presented at Advanced Technology Applications for Combat Casualty Care (ATACCC)/ The Military Health System
Research Symposium (MHSRS) August, 2012 Ft. Lauderdale, see Appendices

3. Presentation and published paper entitled “Neuro-glial and systemic mechanisms of pathological responses to primary blast overpressure (OP) compared to ‘composite’ blast accompanied by head acceleration in rats” by Stanislav Svetlov, Victor Prima, Daniel Kirk, Hector Gutierrez, Kenneth Curley, Ronald Hayes, Kevin Wang was presented at NATO Conference 'A Survey of Blast Injury across the Full Landscape of Military Science, October 2011, Halifax. Proceeding of NATO conference HFN-207 see Appendices

Year 3

1. A previous paper for special topic Blast-induced Neurotrauma “Neuro-glial and systemic mechanisms of pathological responses in rat models of primary blast overpressure compared to "composite" blast.” by Svetlov SI, Prima V, Glushakova O, Svetlov A, Kirk DR, Gutierrez H, Serebruany VL, Curley KC, Wang KK, Hayes RL. has been published in Frontiers in Neurol. 2012; 3:15,

This paper has been already cited by Zou e t al. in Primary blast injury-induced lesions in the retina of adult rats;J Neuroinflammation. 2013; 10: 79. doi: 10.1186/1742-2094-10-79 and by Mac Donald et al. in Cerebellar White Matter Abnormalities following Primary Blast Injury in US Military Personnel PLoS One. 2013; 8(2): Published online 2013 February 7. doi: 10.1371/journal.pone.0055823

2. A paper has been published: Prima V, Serebruany VL, Svetlov A, Hayes RL and Svetlov SI Impact of Moderate Blast Exposures on Thrombin Biomarkers Assessed by Calibrated Automated Thrombography in Rats J Neurotrauma. 2013 Oct 4. [Epub ahead of print] PMID: 23805797 see Appendices

3. A paper has been published: Tümer, Svetlov SI, Whiddenh M, Kirichenko N, Prima V, Erdos B, Sherman A, Kobeissy F, Yezierski R, Scarpace PJ, Vierck C and Wang K.W. Overpressure blast-wave induced brain injury elevates oxidative stress in the hypothalamus and catecholamine biosynthesis in the rat adrenal medulla. Neuroscience Lett. 2013 Jun 7;544:62-7, see Appendices

4. A review has been in press : Kobeissy F, Mondello S, Tumer N, Toklu HZ, Whidden MA, Kirichenko N, Zhang Z, Prima V, Yassin V, Svetlov SI, Wang KKW Assessing Neuro-Systemic & Behavioral Components in the Pathophysiology of Blast-Related Brain Injury. Frontiers in Neurotrauma, 2013 (in press). see Appendices

5. Adams S, Condrey JA, Tsai HW, Prima V, Svetlov SI, Sumners C, and Davenport PW. Anxiety Produced in Rats by Over-Pressurization Blast Injury International Society for the Advancement of Respiratory Pyschophysiology held in Leuven, Belgium, September 22-26, 2012. see Appendices

Year 4

1. A review “Assessing Neuro-Systemic & Behavioral Components in the Pathophysiology of Blast-Related Brain Injury. Frontiers in Neurotrauma”, Kobeissy F, Mondello S, Tumer N, Toklu HZ, Whidden, A, Kirichenko N, Zhang Z, Prima V, Yassin V, Svetlov SI, Wang KKW has been published in Frontiers in Neurotrauma, 2013, see Appendices

2. A paper by Adams, S., J.A. Condrey, H.W. Tsai, S.I. Svetlov, and P.W. Davenport, “Respiratory responses following blast-induced traumatic brain injury in rats.” has been published in Respir Physiol Neurobiol, 2014 see Appendices.

8. REFERENCES:

Prima V, Serebruany V, Svetlov A, Hayes RL, Svetlov S. Impact of moderate blast exposures on thrombin biomarkers assessed by Calibrated Automated Thrombography (CAT) in rats. J Neurotrauma. 2013 Jun 27. [Epub ahead of print]

Tümer, Svetlov SI, Whiddenh M, Kirichenko N, Prima V, Erdos B, Sherman A, Kobeissy F, Yezierski R, Scarpace PJ, Vierck C and Wang K.W. Overpressure blast-wave induced brain injury elevates oxidative stress in the hypothalamus and catecholamine biosynthesis in the rat adrenal medulla. Neuroscience Lett. 2013 Jun 7;544:62-7

Svetlov SI, Prima V, Kirk DR, Gutierrez H, Curley KC, Hayes RL, Wang KK. Morphologic and Biochemical Characterization of Brain Injury in a Model of Controlled Blast Overpressure Exposure. J Trauma. 2010 Oct;69(4):795-804

Svetlov SI, Prima V, Kirk DR, Gutierrez H, Curley KC, Hayes RL, Wang KKW. Neuro-glial and systemic mechanisms of pathological responses to primary blast overpressure (OP) compared to 'composite' blast accompanied by head acceleration in rats. In: Proceeding of NATO conference 'A Survey of Blast Injury across the Full Landscape of Military Science, 2011.

Stuhmiller JH, Ho KH, Vander Vorst MJ, et al. A model of blast overpressure injury to the lung. J Biomech 1996;29:227-234.

Jaffin JH, McKinney L, Kinney RC, et al. A laboratory model for studying blast overpressure injury. J Trauma 1987;27:349-356.

Atkinson JP, Faure JM, Kirk DR, et al. Generation and Analysis of Blast Waves from a Compressed

Air-Driven Shock Tube. The American Institute of Aeronautics and Astronautics (AIAA) Journal 2010;In press.

Guy RJ, Kirkman E, Watkins PE, et al. Physiologic responses to primary blast. J Trauma 1998;45:983-987.

Cooper PW. Explosives Engineering. Wiley-VCH; 1996.

Saljo A, Bao F, Haglid KG, et al. Blast exposure causes redistribution of phosphorylated neurofilament subunits in neurons of the adult rat brain. J Neurotrauma 2000;17:719-726.

Elsayed NM. Toxicology of blast overpressure. Toxicology 1997;121:1-15.

Stuhmiller JH. Biological response to blast overpressure: a summary of modeling. Toxicology 1997;121:91-103.

Svetlov SI, Larner SF, Kirk DR, et al. Biomarkers of Blast-Induced Neurotrauma: Profiling Molecular and Cellular Mechanisms of Blast Brain Injury. J Neurotrauma 2009, 26:1-9

de Olmos JS, Beltramino CA, de Olmos de Lorenzo S. Use of an amino-cupric-silver technique for the detection of early and semiacute neuronal degeneration caused by neurotoxicants, hypoxia, and physical trauma. Neurotoxicol Teratol 1994;16:545-561.

Switzer RC, 3rd. Application of silver degeneration stains for neurotoxicity testing. Toxicol Pathol 2000;28:70-83.

Kupina, N.C., Nath, R., Bernath, E.E., Inoue, J., Mitsuyoshi, A., Yuen, P.W., Wang, K.K., and Hall, 16 E.D. (2001). The novel calpain inhibitor SJA6017 improves functional outcome after delayed administration in a mouse model of diffuse brain injury. J Neurotrauma 18, 1229-1240.

Galea, E., P. Dupouey and D. L. Feinstein (1995). "Glial fibrillary acidic protein mRNA isotypes: expression in vitro and in vivo." J Neurosci Res 41(4): 452-461.

Urrea C, Castellanos DA, Sagen J, et al. Widespread cellular proliferation and focal neurogenesis after traumatic brain injury in the rat. Restor Neurol Neurosci 2007;25:65-76.

Nylen K, Ost M, Csajbok LZ, et al. Increased serum-GFAP in patients with severe traumatic brain injury is related to outcome. J Neurol Sci 2006;240:85-91.

Kaur, C., J. Singh, M. K. Lim, B. L. Ng and E. A. Ling (1997a). "Macrophages/microglia as 'sensors' of injury in the pineal gland of rats following a non-penetrative blast." Neurosci Res 27(4): 317-322.

9. Appendices

Experimental Framework for Cumulative Blast Detection and Data Acquisition for Assessment of Blast-Related Injury in Animal Studies

Progress Report No. 4

Hector Gutierrez and Daniel Kirk

Department of Mechanical and Aerospace Engineering
Florida Institute of Technology
Melbourne FL 32901

June 27th , 2011

Part 1. Development of Synchronous High Speed Imaging and Data Acquisition interface for blast Experiments in the Labview Platform

Two new Labview programs for data acquisition in the Banyan shock tube were developed, tested and delivered during this period of performance.

The first set was based on Banyan's currently existing DAQ System (DAQCard 6062E), and implements synchronization of the DAQ system with the high speed camera using an analog pulse once a threshold in a pressure sensor is reached. The user interface and diagram windows are shown below.
The program controls the firing solenoid via a digital output and provides synchronized acquisition from the pressure sensors with the trigger pulse that starts the high speed image acquisition.

The program was delivered and tested successfully at Banyan on 31 May 2011.

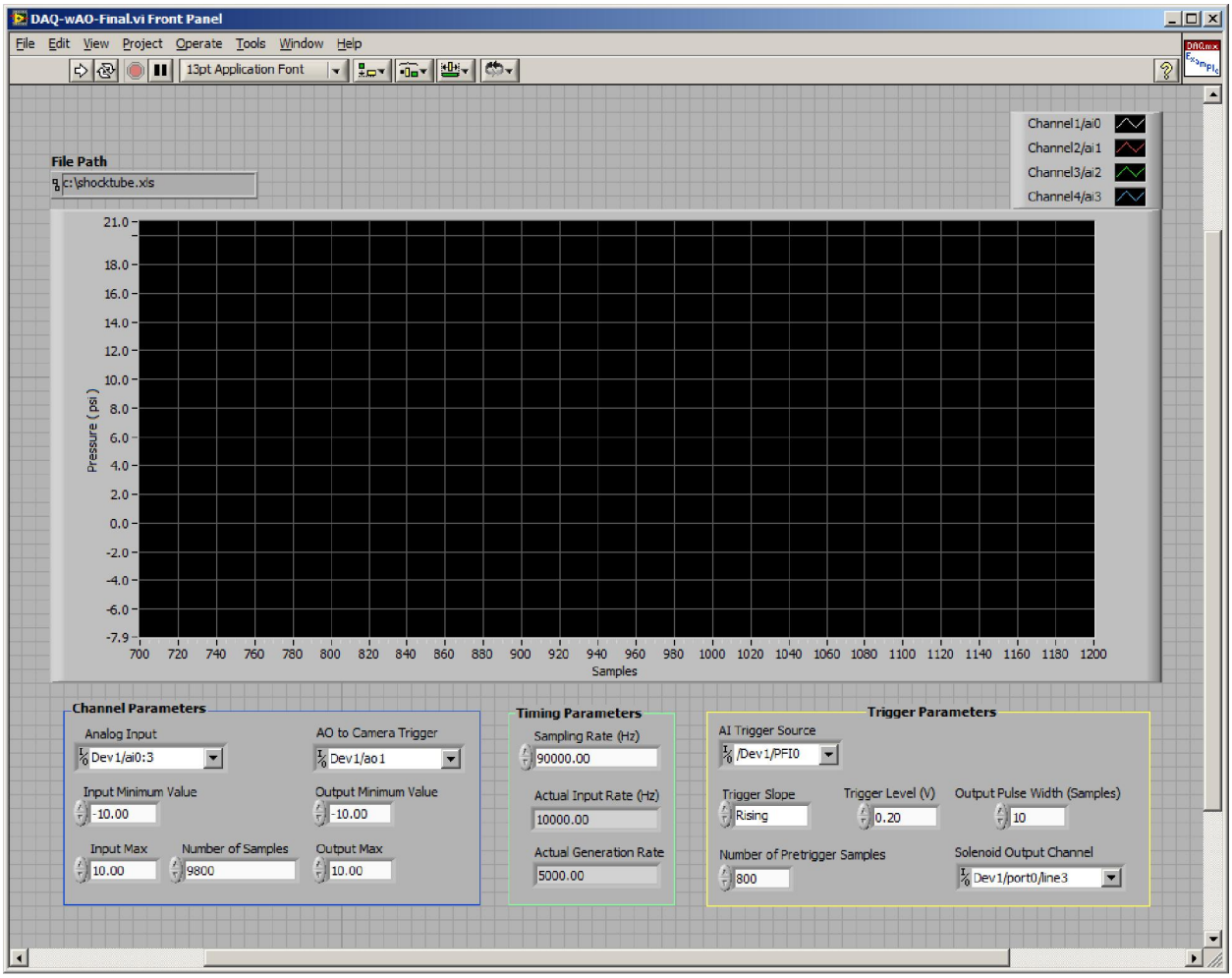

Figure 1. Data acquisition program for Banyan's DAQCard 6062E System – User Interface

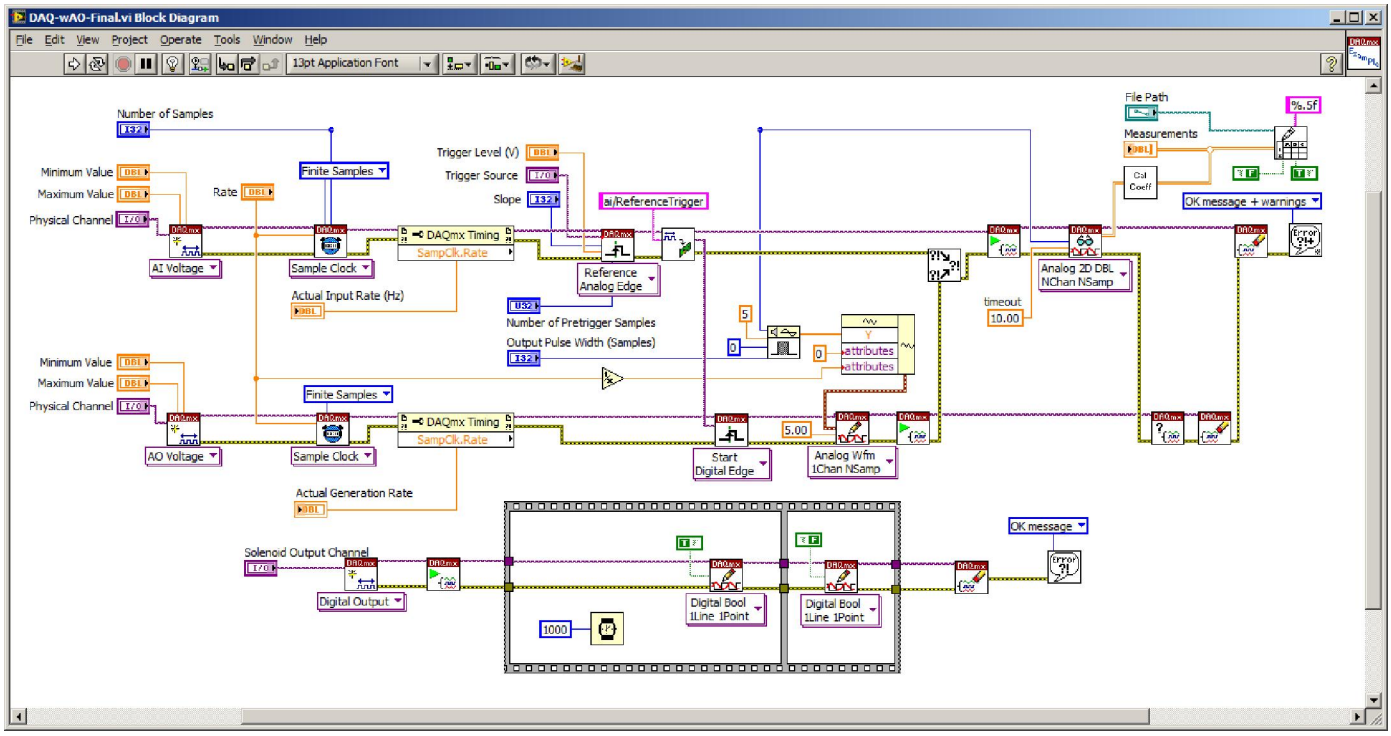

Figure 2. Data acquisition program for Banyan's DAQCard 6062E System – Diagram Window

Comparisons with data acquired at higher sampling rates at FIT's Fluid Dynamics Laboratory suggest that the current DAQ system at Banyan based on the DAQCard 6062E system does not provide fast enough sampling rate in multiple pressure sensors to properly detect and measure the peak overpressure. This is shown in Figure 3, where the peak overpressure is correctly detected and measured when sampled at 20 Msamples/sec. Successive traces at higher decimations (i.e., skipping an integer number of points between samples) show that the value and location of the peak can by incorrectly measured if the sampling rate is not high enough.

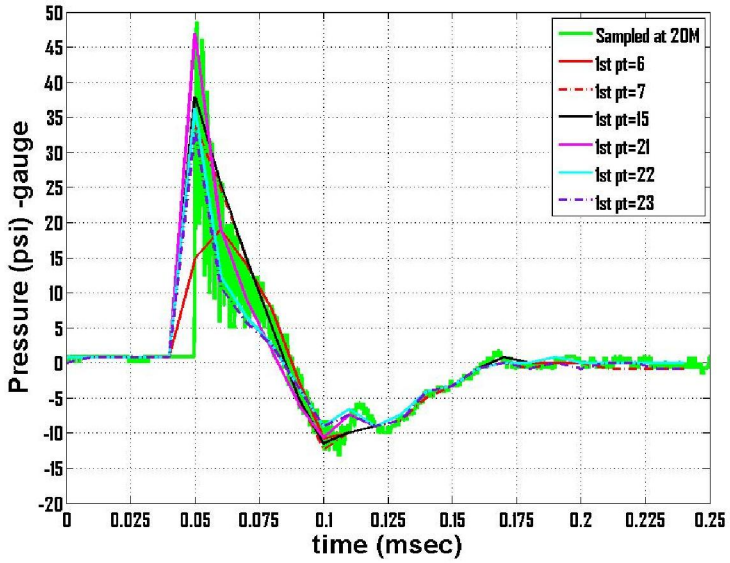

Figure 3. Effect of low sampling rates in the detection and measurement of peak overpressure in blast pressure traces.

This finding prompted the need to use a different DAQ system for future tests at Banyan at higher pressures. A new DAQ system was implemented using a PXI-1003 chassis and a PXI-6132 14-Bit, 2.5 MSamples/sec/channel simultaneous sampling data acquisition system. This system does not have analog outputs and therefore uses a counter/timer pulse to synchronize the high speed camera to the analog data acquisition. A new data acquisition program was developed to control firing the solenoid via a digital output and provide synchronized acquisition from the pressure sensors and high speed camera with the trigger pulse generated by a counter/timer. The user interface and corresponding diagram are shown in Figure 4 and 5.

The program was delivered and tested successfully at Banyan on 27 June 2011 along with the portable data acquisition electronics.

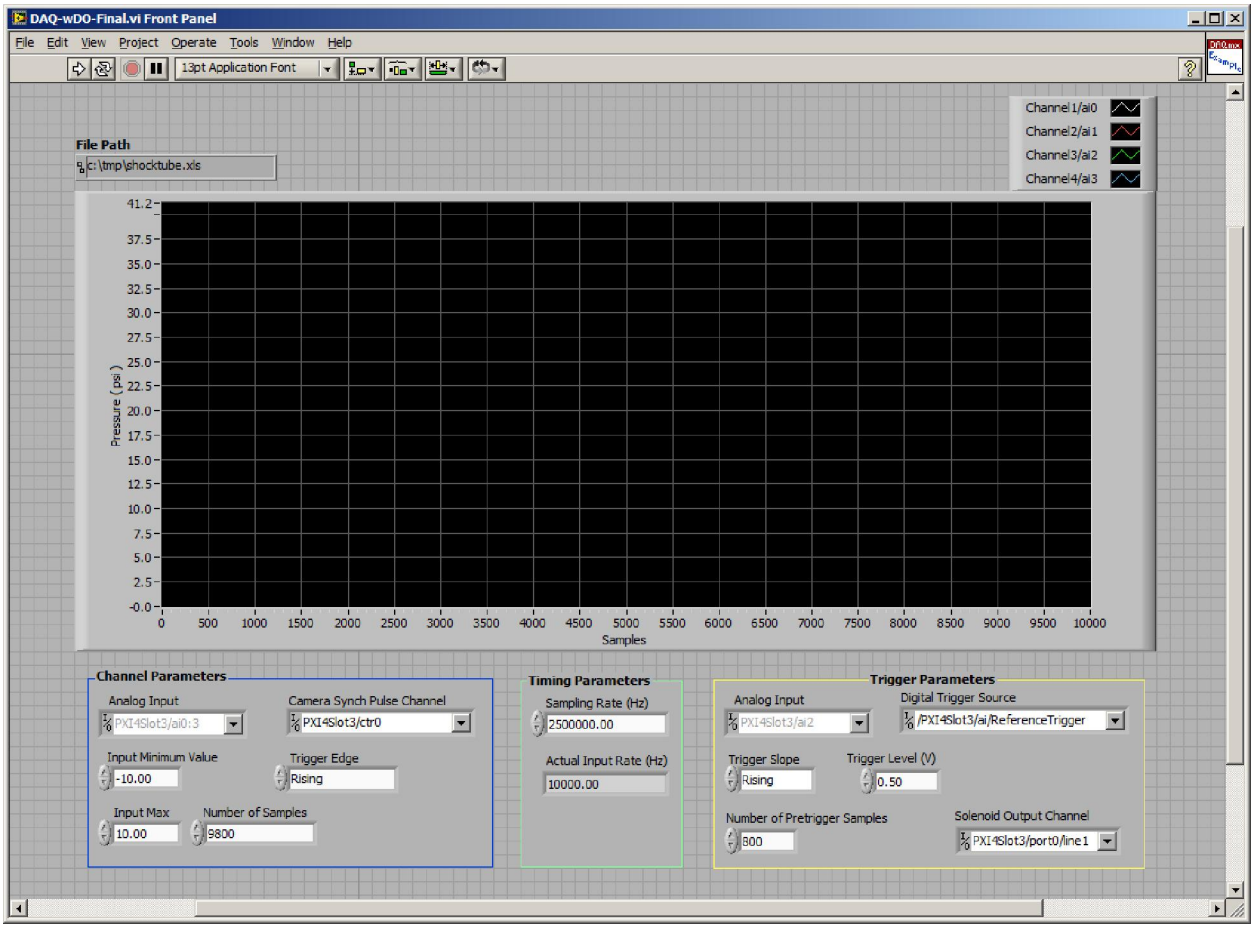

Figure 4. Data acquisition program the PXI-1003 System with the PXI 6132 card – User Interface

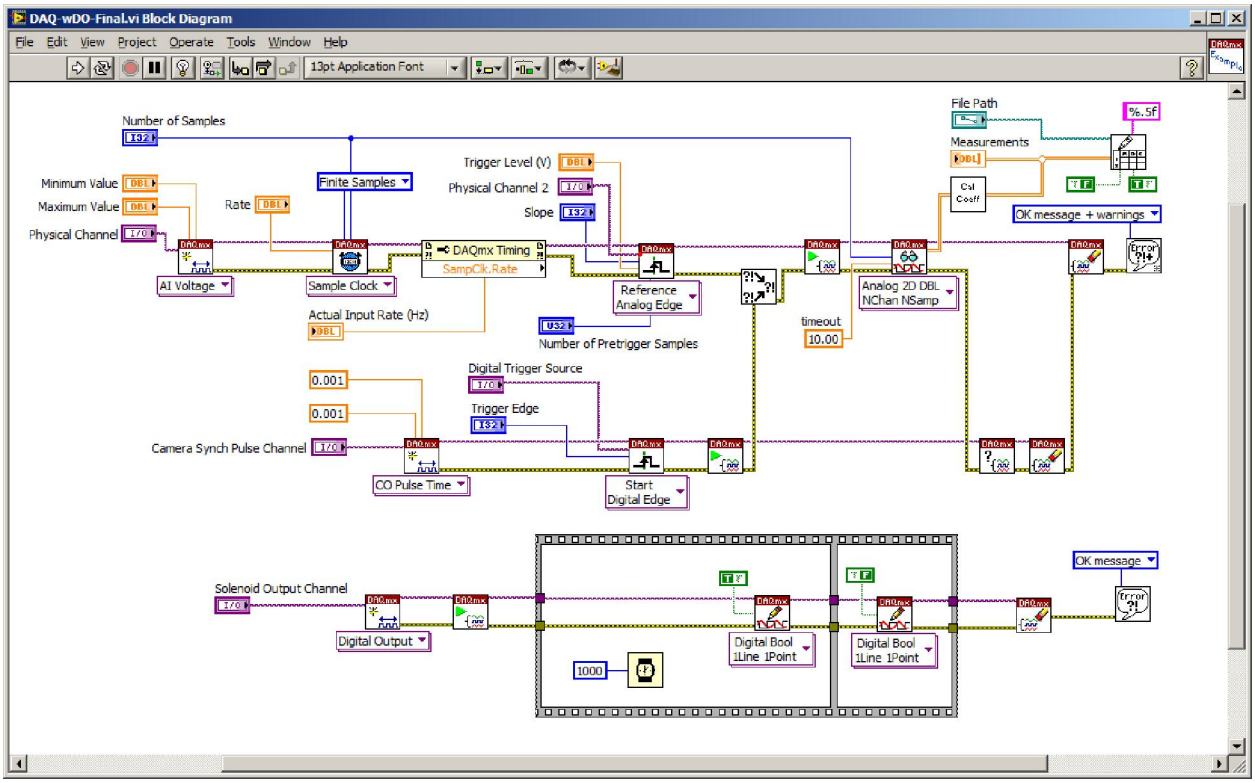

Figure 5. Data acquisition program the PXI-1003 System with the PXI 6132 card – Diagram Window

Part 3. Development and Testing of Schlieren Optics for High Speed Image Acquisition of Blast Events.

During this period of performance, the FIT team developed, tested and delivered a experimental rig for Schlieren optics for high speed image acquisition of blast events as needed in support of Banyan's testing in live rodents. The system is based in the Phantom V7.3 high speed camera from Vision Research, Inc. Synchronized video from these tests, both at Florida Tech and Banyan, allowed to clearly establish the effect of the venting gas on the target when shooting the shock tube on-axis, as can be seen in the video clips attached to this report as separate files (Figure 67)

The integrated high speed data acquisition and high speed imaging system was delivered and tested and Banyan on 01 July, 2011. A detailed report of the results is included in Appendix 2 (Banyan Tests-01-July-2011). This includes detailed descriptions of the tests carried out, and comparisons between data collected using the PXI-based high speed data acquisition system, and the portable CBI-CSP package.

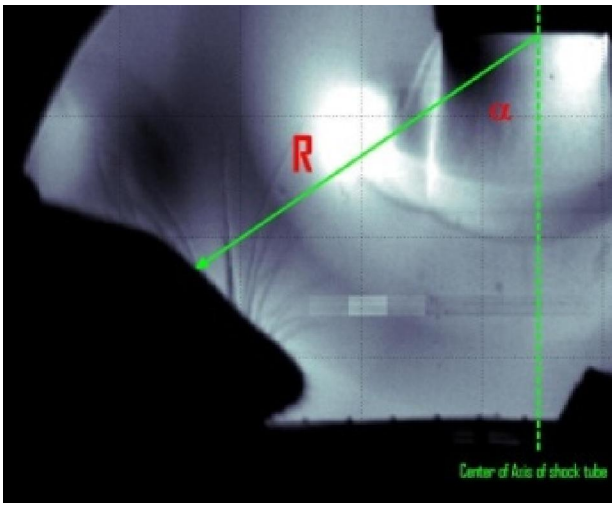

Figure 6. Interaction of a blast pressure wave with an off-axis live target

Part 4. Cumulative Blast and Impulse (CBI) Exposure Sensing Package (ESP)

Overview. A novel, portable, instrumentation and data acquisition platform was developed and delivered to Banyan, enabling:

(i) Simultaneous acquisition of pressure, acceleration and rate of rotation at multiple points within the specimen on an unconstrained live target

(ii) Data recording of cumulative blast sensor data to solid-state memory, and

(iii) Untethered operation.

These objectives are achieved by a microprocessor-based data acquisition and storage device that incorporates state-of-the-art miniature sensors, solid-state memory and compact rechargeable lightweight batteries, being therefore small enough to be attached to a test specimen such as a rodent without need of external wiring. The first version of the system is shown in Figure 6.

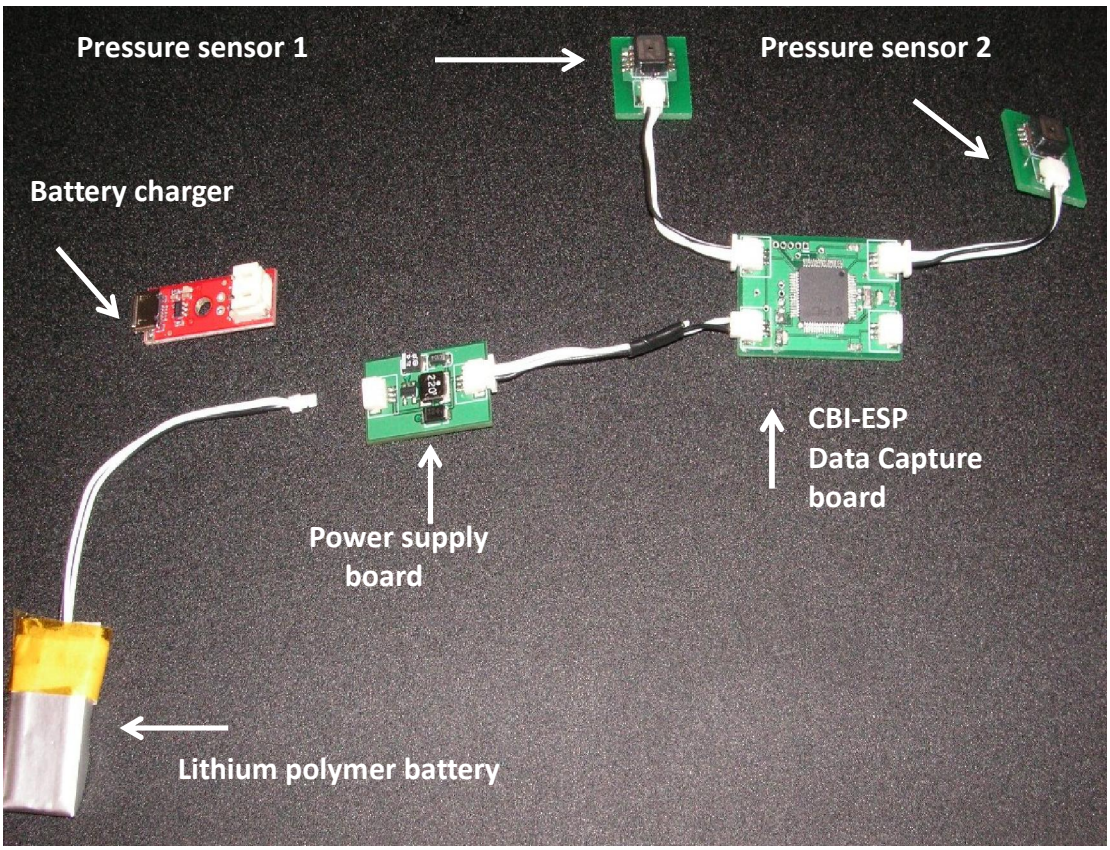

Figure 7. Cumulative Blast and Impulse - Exposure Sensing Package (CBI-ESP) – Version 1.0

Hardware Setup

The sensor and data acquisition package consists of:

1. Main sensor board, including:

- 16-bit, 80 MHz, 40 MIPS RISC-based processor (PIC24HXX)
- Two built-in independent simultaneous 12-bit A/D converters. Max. rate: 150 ksample/sec.

- Analog pressure transducers – Max. pressure = 44 psi
- Two pressure sensors that can be placed in any desired location within the test specimen
- Data streamed to micro SD card on the back of the board

2. Inertial measurement board, including:

- 16-bit, 80 MHz, 40 MIPS RISC-based processor (PIC24HXX)
- One Tri-axial analog accelerometer (ADXL335): +/- 3 g, 300 mV/g, 4.0x4.0x1.5 mm
- One Tri-axial analog gyroscopic angular rate sensor (LYPR540AH): 0 to 1600 degrees/sec, 0.8 mV/deg/sec, 4.4x7.5x1.1 mm
- One Tri-axial digital compass (HMC5843): 7 mGauss/bit, 12-bit ADC, I2C interface, 4.0x4.0x1.3 mm
- Data streamed to micro SD card

3. Power supply board, to interface to Lithium-polymer battery

4. Pressure transducer boards. This setup allows the user to place pressure sensors in any desired pattern or desired location within the test specimen.

The main board is preprogrammed to acquire a set number of samples at a fixed sampling rate (800 msec at 150 kSamples/sec). The use of independent analog to digital converters enables simultaneous data acquisition of both pressure sensors placed on the test specimen. After sampling, the data is stored to the external SD card in a raw format to reduce data collection overhead and allow high speed sampling. Once the board has completed acquiring the desired number of samples, the file is read back and converted to a tab delimited text file. Such format can be easily read and post processed using Matlab or any other data processing software.

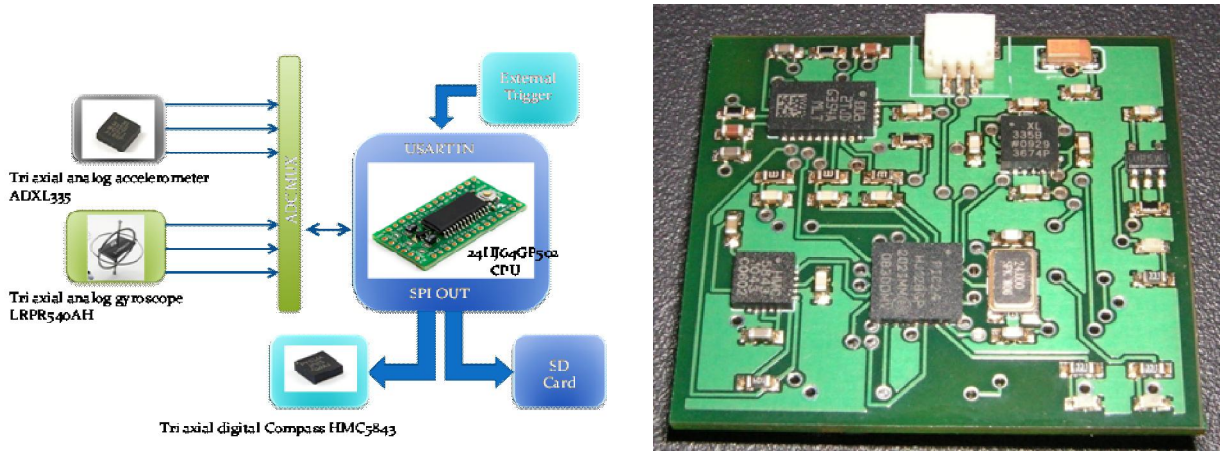

Figure 8. Inertial Measurement Board. The IMU board is connected to the Main board by a trigger and power lines

The inertial measurement board (IMU) is a standalone unit that includes a tri-axial analog accelerometer, tri-axial analog gyroscopic sensor, and tri-axial digital compass. Operation of the IMU board is controlled by its own CPU, externally triggered by the Main board. This design allows uninterrupted IMU data streaming, which can be logged to its own SD memory card. The Slave board

uses the PIC24HJ's built-in ADC module, multiplexed to both the tri-axial accelerometer as well as the tri-axial gyro (6 analog input channels). Figure 8 shows the block diagram and Revision 1 of the IMU board.

Once the IMU (Slave) board is triggered by the Main board, it collects data from all its analog sensors at a set sampling rate, and appends them to a text file created on the SD card when the trigger pulse is received for the first time. The board can also be turned off by the same trigger used to activate it. In addition to the accelerometers and gyroscopic sensors, the IMU board also contains a three axis digital compass. This compass is used to correct gyro drift during post processing. This compass uses a digital SPI interface and the data is also logged to the end of the file. A similar data collection sequence as the one described above is used to enable faster sampling rates.

During this period of performance the IMU board was subject to preliminary testing, and version 1.0 of the firmware was developed and tested to reconstruct the spatial trajectory of a free-flying target propelled by an off-axis blast wave as shown in Figure 9.

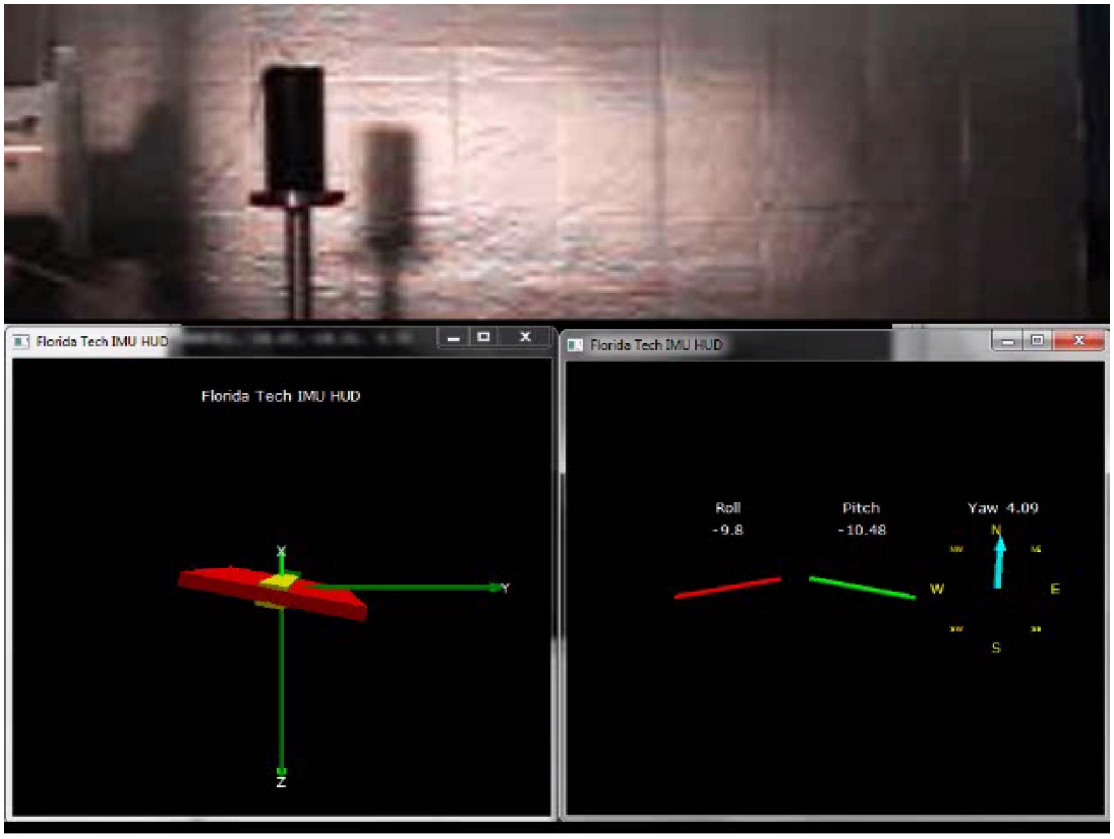

Figure 9. Testing of the portable IMU board attached to a free-flying target propelled by an off-axis pressure blast. The lower panes demonstrate the use of the 9-DOF IMU data to reconstruct the trajectory of the free moving target.

Operation

The portable data acquisition device is connected as follows;

- Main board connected via ribbon cable (middle connector of main board, right side, to power supply board (output side)

- Power supply board: output side connected to main board, input side connected to Li-Po battery
- Two pressure transducer boards are to be connected with ribbon cables to each of the corner connectors on the main board
- Inertial measurement board (Figure 8) is connected to main board via ribbon cable (middle connector of main, left side, Figure 7). Connection of the inertial measurement board is optional. The system can operate with only the main board and pressure transducer boards.

Operation starts when the power cable to the battery is connected to the input side of the power supply board. In Revision 1, the main board CPU acquires constantly data on a circular buffer. After a blast event is detected (when a threshold is reached in the pressure sensors) the blast event (0.8 sec of data at 150 kSample/sec) is recorded to SD memory. The content of the buffer frame immediately prior to the blast event is also saved to SD memory to store the start of the event. The IMU board starts acquisition at lower rate (100 samples/sec) when triggered by the main board, and stops when the trigger goes low again. IMU data is then stored to the corresponding SD card. Examples of placement of the pressure boards, main board and IMU board on a rodent are shown in Figure 10.

Several tests can be conducted within the life of the battery (30 to 40 min). After disconnecting the battery, extract both SD cards and save files to computer hard drive. Battery requires 1-hour of charging (multiple batteries can be used to avoid delays).

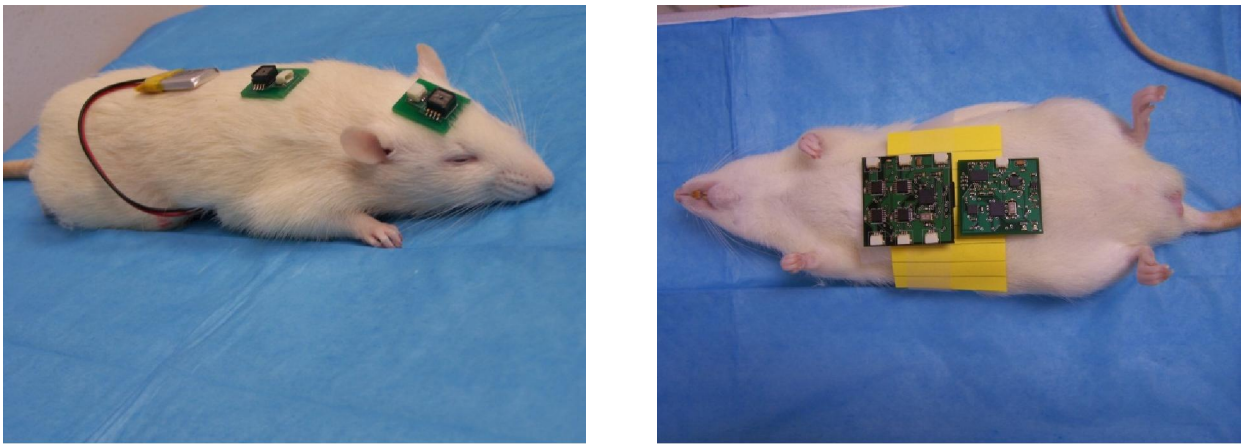

Figure 10. Layout of CBI-ESP portable sensor package on a rodent for blast pressure testing

Part 4. Evaluation and modifications of driver and driven section in Banyan's shock tube facility.

To achieve substantial injury with off-axis blast exposure (i.e., pure blast exposure with minimal or no exposure to venting gases), substantially higher pressures are required in the driver section of a shock tube. Bayan's shock tube design was revised and the shock tube modified to be able to achieve up to 50 psi with off-axis exposure to pressure waves up to 2 inches from the end of the driven section.
Results shown in Figure 11 (sampled with PXI-1003 simultaneous 4-channel system) show that peak overpressure in excess of 50 psi can be achieved in Banyan's shock tube with no exposure to venting effects.

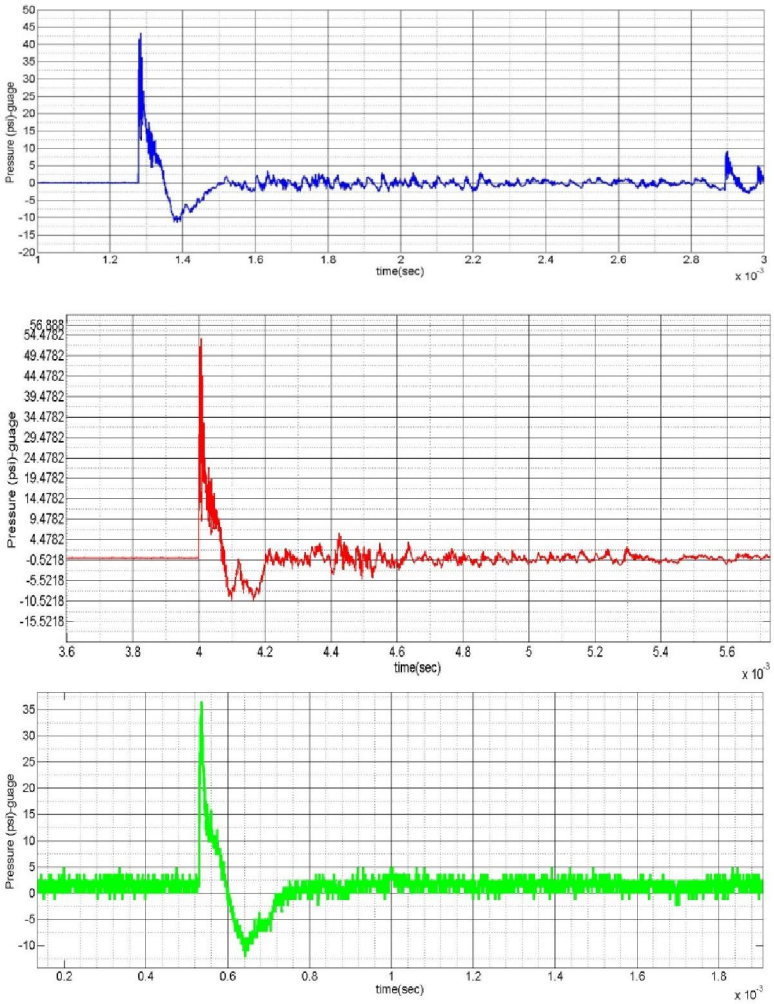

Diaphragm	External sensor R=2 in @ 43 deg from shock tube exit – (psi)
0.003 + 4 layer of tape	35.12
0.004 + 4 layer of tape	43.53
0.005 + 4 layer of tape	54.74

Figure 11. Peak overpressure values in modified Banyan's shock tube for three different diaphragm configurations

Summary

In this performance period, the following activities were conducted:

- Programming for data acquisition and synchronization with high speed camera using DAQCard 6062E
- Programming for data acquisition and synchronization with high speed camera using PXI-1003 and PXI-6132
- Development and testing of optical system for Schlieren high speed video of blast events.
- Testing of live targets using the CBI-ESP portable sensor package.
- Reconstruction of 3D trajectory of free flying target subject to off-axis blast pressure wave using portable 9-DOF inertial measurement module.
- Evaluation and modifications of driver and driven section in Banyan's shock tube facility to achieve higher pressures (up to 50 psi) for off-axis blast exposure testing with no venting effects.

Experimental Framework for Cumulative Blast Detection and Data Acquisition for Assessment of Blast-Related Injury in Animal Studies

Year 2, Progress Report No. 3 (Revised)

Hector Gutierrez and Daniel Kirk

Department of Mechanical and Aerospace Engineering

Florida Institute of Technology

Melbourne FL 32901

April 16, 2012 / October 21, 2012

Experimental Framework for Cumulative Blast Detection and Data Acquisition for Assessment of Blast-Related Injury in Animal Studies

Year 2 – Report 3 (Revised).

Introduction.

The experiences gained during Year 1 of this project pointed in the direction of two critical aspects of the instrumentation, data acquisition and data logging technology. First, a sensing device with response time below 1 microsecond must be used to properly capture the peak overpressure, since it's believed that one of the mechanisms of injury is related to the exact value of peak overpressure. Second, the data acquisition and data logging electronics have to be fast enough to properly capture a sub-microsecond event, which is very challenging considering that the size of the devices is ideally in the order of one inch square (to be usable in rodent testing).

To capture a blast event where the peak overpressure lasts only 1~3 microseconds, a sensor with frequency response in excess of 1 MHz is needed. Candidate technologies must be compact enough such that both the sensing element and the conditioning electronics can fit on a printed circuit board of approx. 1 inch square in area. A candidate sensor element based on a piezo disc has been used to develop a dedicated sensor for the CBI-ESP sensor package.

This report describes the development and testing of a new piezo-based portable high-speed blast sensor, and presents its results in monitoring blast exposure on a rodent.

Piezo electric sensors

Piezoelectric transducers can be used in conjunction with board-level signal conditioning to develop a very compact micro transducer with frequency response comparable to that of the fastest pressure transducers currently available. Piezo materials generate an electrical charge that is proportional to the pressure applied. If a reciprocating force is applied, an ac voltage is seen across the terminals of the device. Piezoelectric sensors are not suited for static or dc applications because the electrical charge produced decays with time due to the internal impedance of the sensor and the input impedance of the signal conditioning circuits. However, they are well suited for dynamic or ac applications.

Signal Conditioning for piezo-electric sensors

Key items to consider when designing a piezo signal conditioner are:

- Frequency of operation
- Signal amplitude
- Input impedance
- Mode of operation

The high impedance of the sensor requires an amplifier with high-input impedance. JFET or CMOS input op amps, like the TLV2771, are natural choices. Two circuit approaches were tested for signal conditioning. Figure 1 shows a voltage mode amplifier circuit, which was selected as the best choice. Voltage mode amplification is used when the amplifier is very close to the sensor, charge mode amplification is used when the amplifier is remote to the sensor.

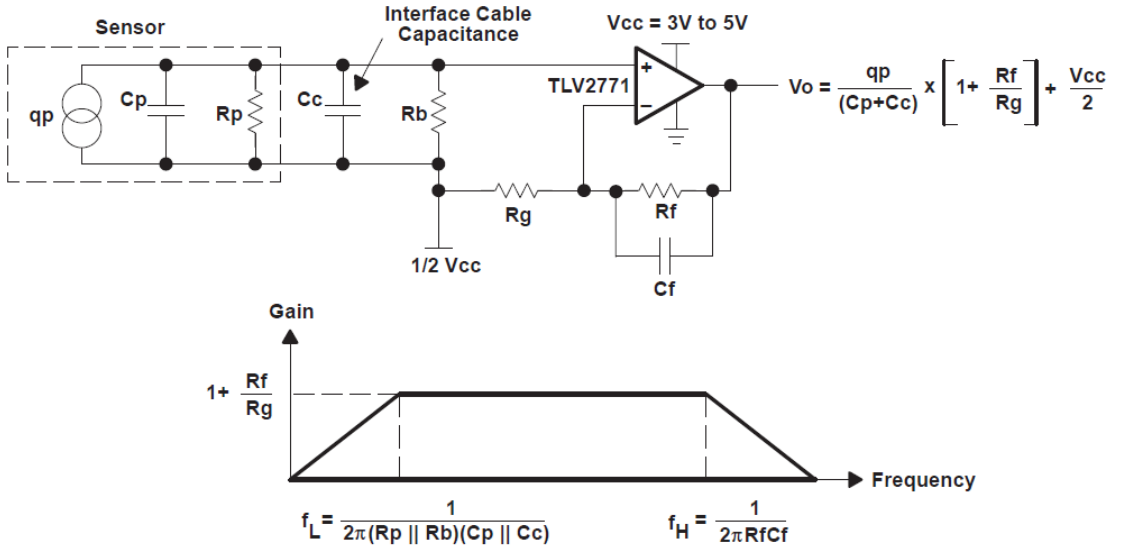

Figure 1. Voltage mode signal conditioner for a piezoelectric sensing element

In a voltage mode amplifier, the output depends on the amount of capacitance seen by the sensor. In the charge mode amplifier the charge injected into the negative input is balanced by charging the feedback capacitor Cf.

Usually it is difficult to get enough sensitivity and bandwidth using a single gain stage. Therefore it is usually necessary to amplify signal in two successive stages. If both the first and second stages are inverting amplifiers, so polarity (phase) of the signal is corrected. A high pass filter before the input of second stage Op-Amp is placed to eliminate the DC offset generated by the first stage Op-Amp. A low pass filter is placed to attenuate the peak sensitivity at the resonant frequency. In an application that requires a wide flat sensitivity band, it may be difficult to get enough attenuation by a low order low pass filter and cascaded filters can be used, at the expense of additional phase delay.

The work in the last quaternary period has been focused on prototyping, debugging and bench testing several circuit topologies to find one that meets all the requirements of the CBI-ESP application. The approaches previously discussed have been combined to implement a conditioning circuit that has the required performance for the CBI-ESP high-speed portable sensor package. During the prototype stage the signal conditioning circuits were tested using bench top signal generators, prior to final testing with blast events. The proposed signal conditioner circuits have been tested with three types of waveforms:

- Sinusoidal waveforms at 1 kHz, 10 kHz, 100 kHz, 1 MHz
- Triangular waveforms at 1 kHz, 10 kHz, 100 kHz, 1 MHz
- Pulse waveforms at 10 kHz, 100 kHz, 400 kHz

Results from these tests are shown in Figures 2, 3, 4, 5, 6 and 7. The current prototype performs very well with a flat gain response (x16) up to 400 kHz; the gain rolls of to x12 at 1 MHz. It is estimated that to properly capture (with no scale distortion) the peak overpressure of a blast event, the circuit needs a flat gain response in excess of 1.2 MHz, which has been achieved with the current prototype.

Another development task during the last period of performance has been to identify and procure sensor candidates for the CBI-ESP device. The sensor candidates have to meet the size and frequency response requirements of the CBI-ESP: they have to be flat, able to be surface mounted on a 1 inch x 1 inch printed circuit board, and have frequency response in excess of 1 Mhz. The following sensors that meet all these requirements have been identified and purchased:

- Piezoelectric disks, from Steiner and Martins, Inc.
  Four different piezoelectric sensing elements have been procured: 1.7 MHz (15 x 1.2 mm), 3.4 MHz (12 x 0.6 mm), 3.5 MHz (9 x 0.5 mm) and 5 MHz (10 x 0.4 mm).

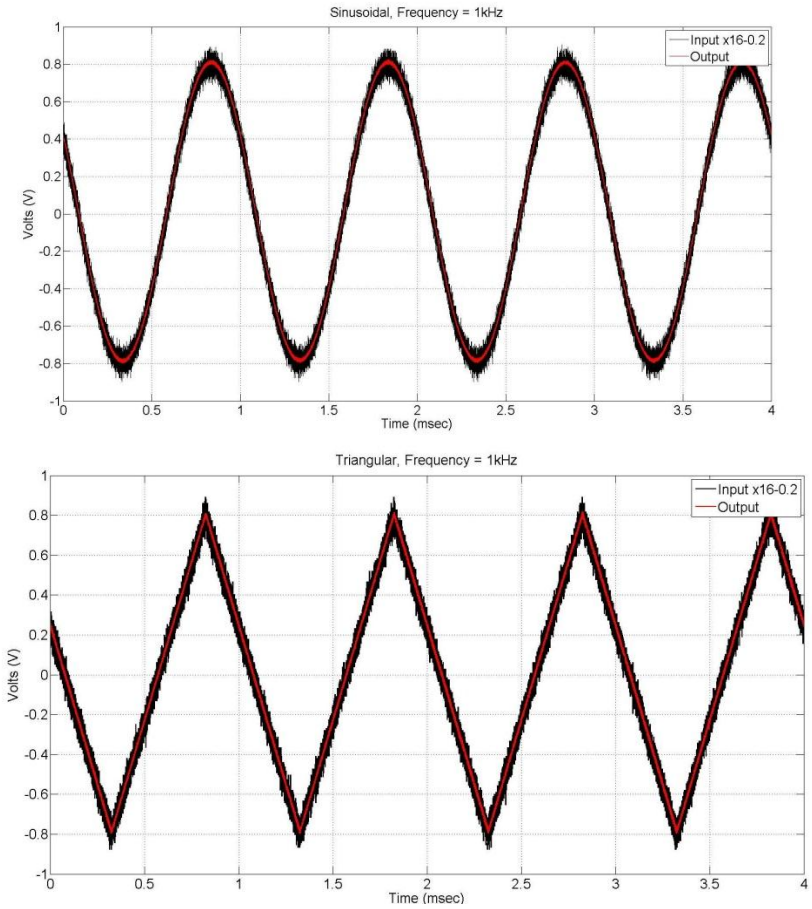

Figure 2. Response of the CBI-ESP signal conditioner circuit prototype to sine waves and triangular waveforms at 1 kHz.

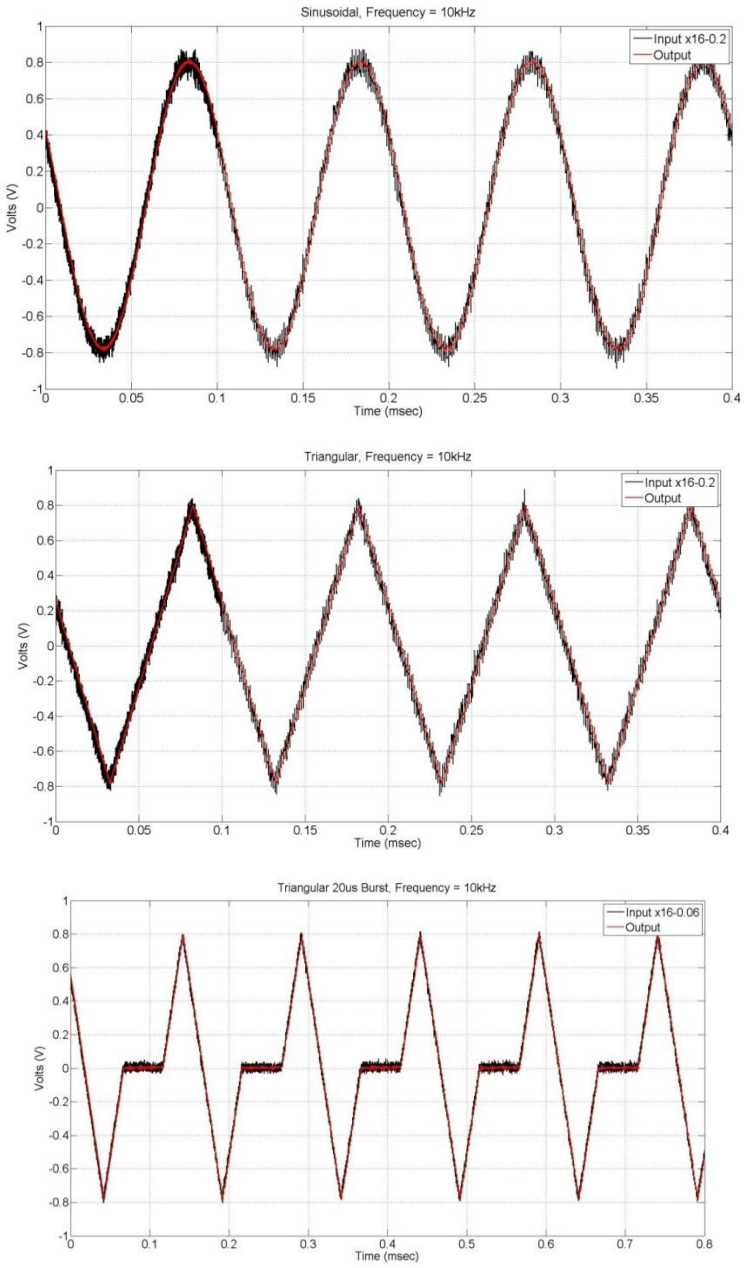

Figure 3. Response of the CBI-ESP signal conditioner circuit prototype to sine waves, triangular waveforms and pulse waveforms at 10 kHz.

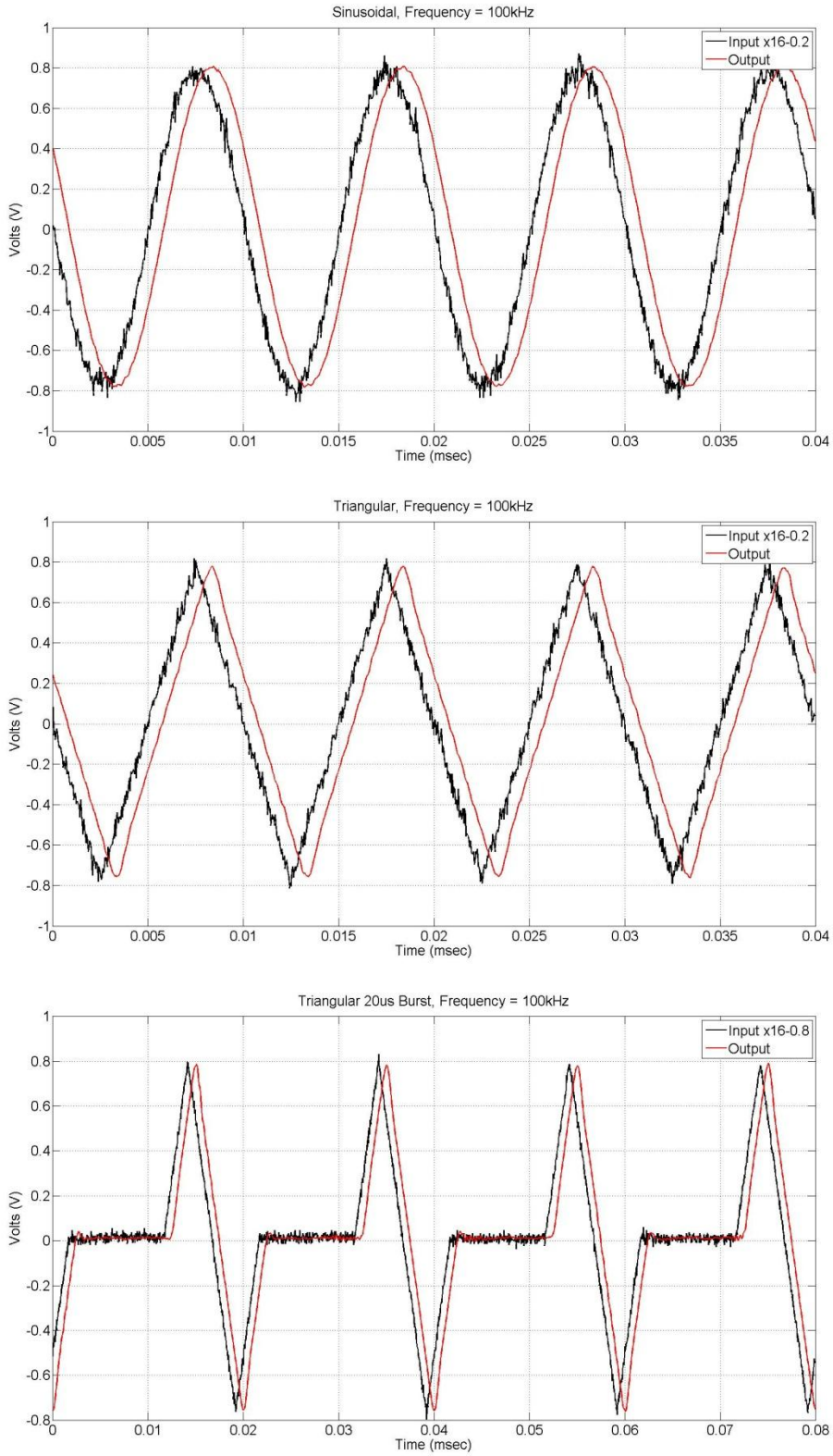

Figure 4. Response of the CBI-ESP signal conditioner circuit prototype to sine waves, triangular waveforms and pulse waveforms at 100 kHz.

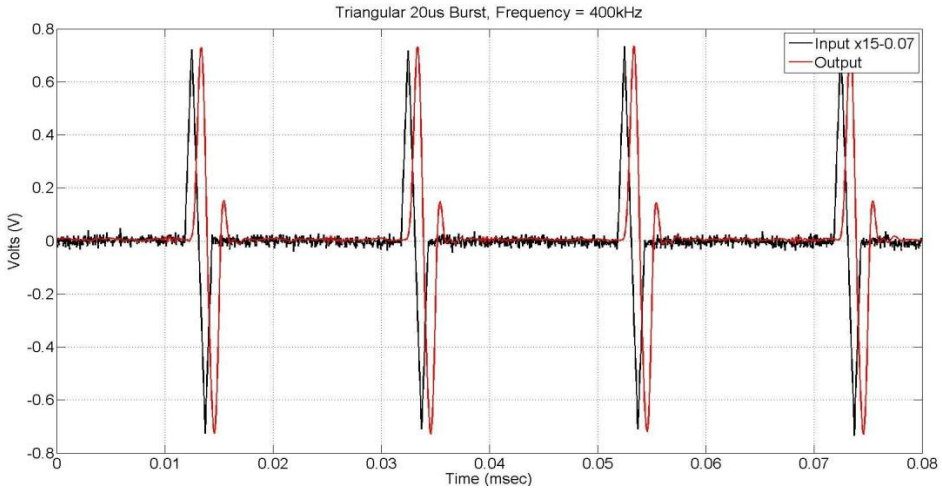

Figure 5. Response of the CBI-ESP signal conditioner circuit prototype to pulse waveforms at 400 kHz.

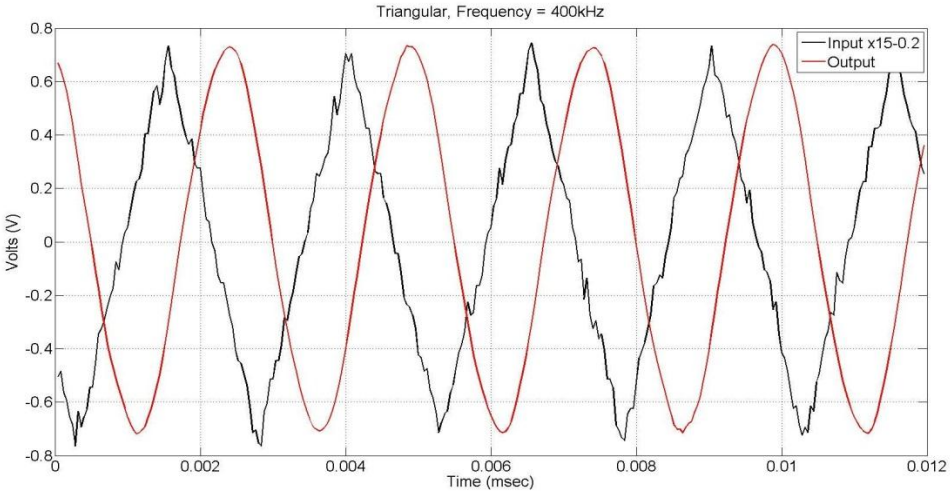

Figure 6. Response of the CBI-ESP signal conditioner prototype to triangular waveforms at 400 kHz.

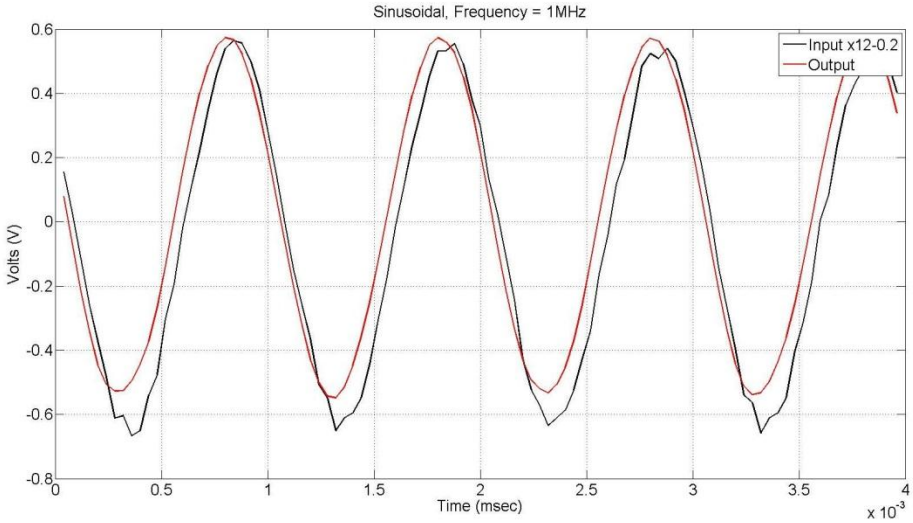

Figure 7. Response of the CBI-ESP signal conditioner prototype to sinusoidal waveforms at 1 MHz.

Tests at Banyan Biomarkers

The prototype sensor and signal conditioning circuit were tested at Banyan Biomarkers on 19 October 2012. The sensor and conditioning circuits were tested as follows:

- Both the FIT prototype and PCB benchmark sensor in parallel configuration (Figure 8). Eight tests were conducted at different radial distances from the opening of the shock tube to characterize sensitivity of the FIT prototype at different peak pressures (Figure 12).
- FIT prototype on toy rat in triangular configuration to verify approximate peak pressure level on test specimen prior to the live test (Figure 9)
- FIT prototype and PCB benchmark sensor in triangular configuration, to deliver repeated blast exposure to laboratory animal (three tests, 30 min apart). (Figure 10).

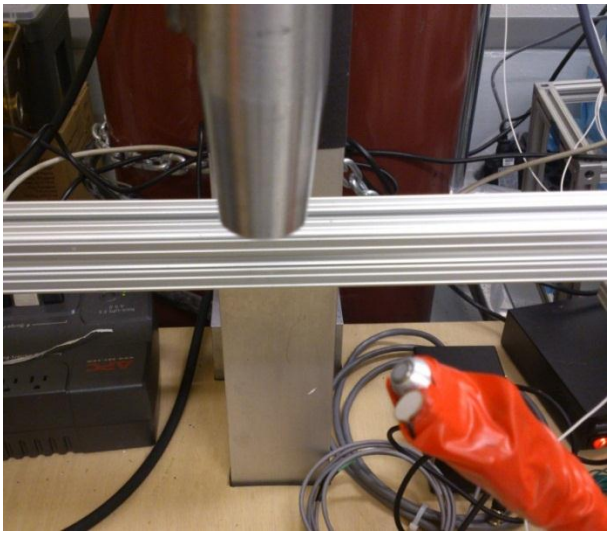

Figure 8. Parallel configuration, PCB sensor (up) and FIT prototype (down)

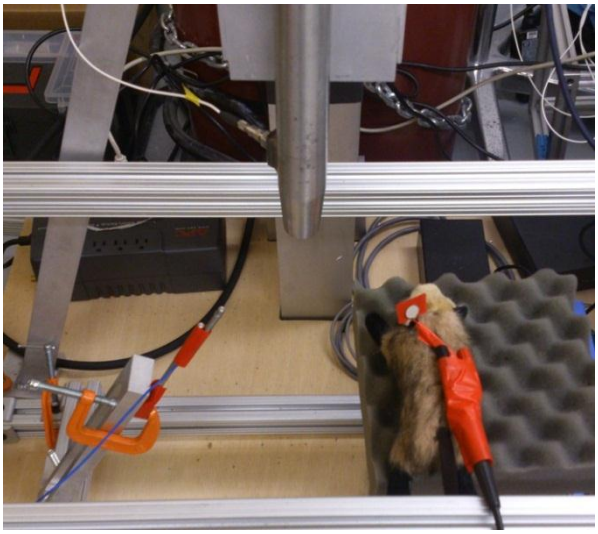

Figure 9. Triangular configuration to verify peak overpressure on target location prior to animal tests

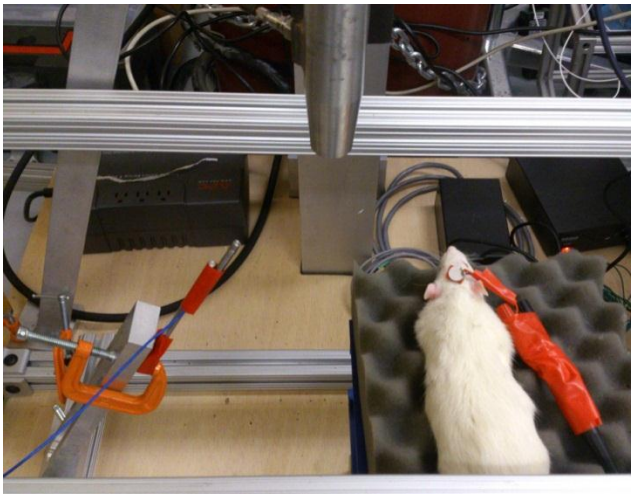

Figure 10. Triangular configuration for animal testing including both PCB benchmark sensor (left) and FIT sensor prototype (right, on animal's head)

Results

The prototype sensor and signal conditioning circuit demonstrated fast enough response to accurately detect the peak overpressure as compared to the benchmark PCB sensor. The results are shown in Figure 11, 12 and 13. All tests were conducted at a sampling rate of 10 Msamples/sec/channel using a PXI data acquisition chassis from National Instruments.

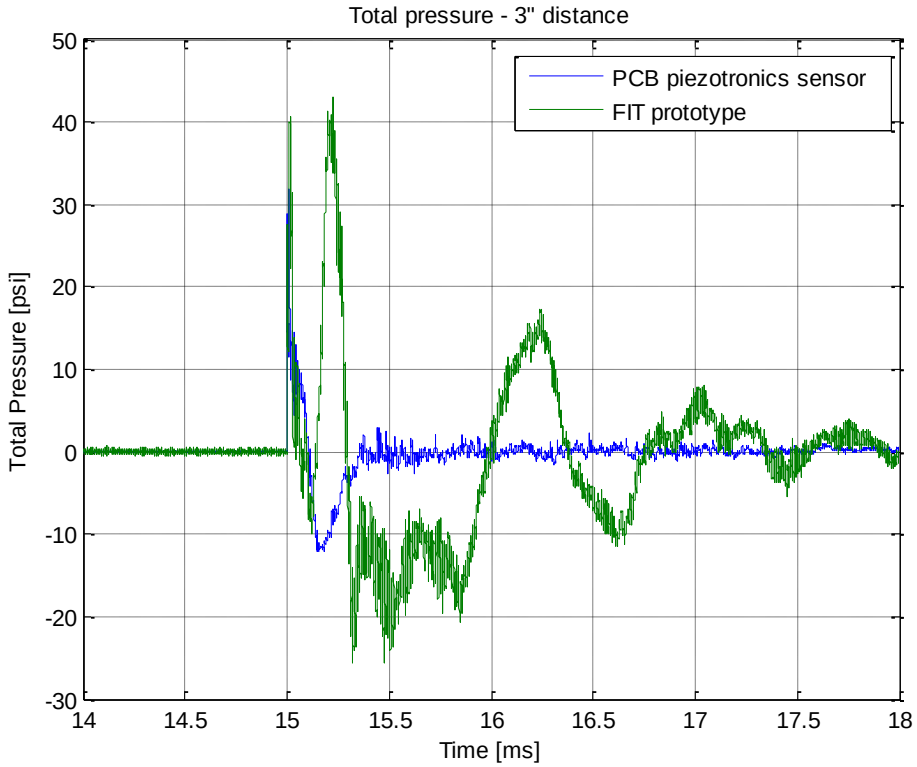

Figure 11. Typical pressure trace of the FIT prototype compared to the PCB benchmark sensor

Figure 11 shows a typical pressure trace obtained with the FIT prototype sensor and signal conditioner (green trace) compared to the PCB benchmark sensor (blue trace). The plot shows that both sensors can capture the peak overpressure event at the same time and with the same intensity (as converted from volts to psi).

Both the PCB pressure sensor and the FIT prototype suffer from resonant ringing at a frequency that depends on both the material and construction of the sensor. This is typical of all piezoelectric-based sensing systems, and can be compensated by off-line data post processing assuming that the signal was sampled at high enough frequency to avoid aliasing. In our case, the piezo resonances are at 200 kHZ (for the FIT prototype) and 250 kHz (for the PCB sensor), which considering our sampling rate of 10 Msamples/sec/channel provide ample margin for accurate off-line digital filtering.

The ringing frequency was measured in both the PCB and FIT sensors and found to be constant for all testing conditions, as shown in Figure 12. This confirms that the ringing frequency is characteristic of the sensor material and geometry and is not affected by the test conditions.

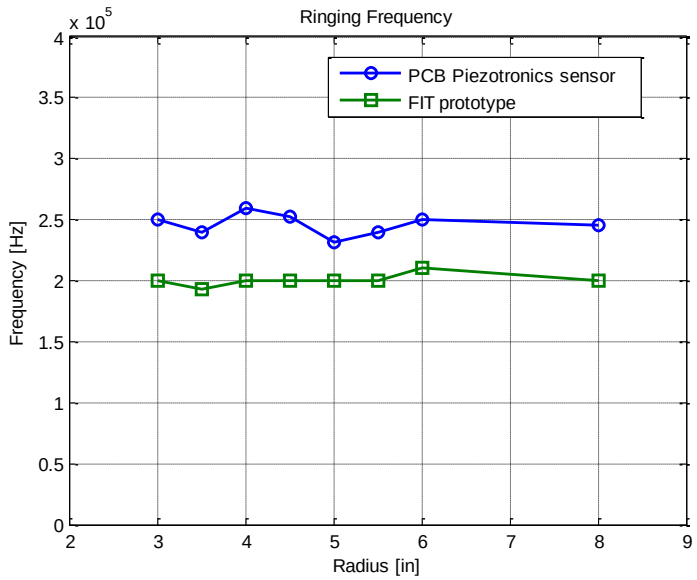

Figure 12. Measured resonant frequency of both sensor systems for different distances to the shock tube opening

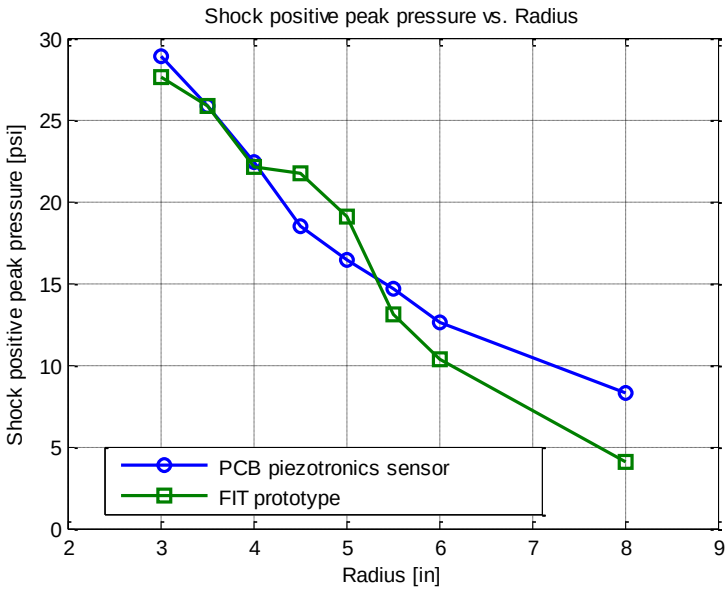

Figure 13. Positive peak pressure (psi) of both sensor systems for different distances to the shock tube opening

Figure 13 shows the correlation between positive peak pressure and distances to the shock tube opening for both the PCB and FIT sensor systems. This shows that the FIT system is capable of measuring the peak overpressure of the blast event. These test will be repeated on an improved test rig to further demonstrate the performance of the FIT sensor system under more geometrically accurate placing.

Conclusion.

The FIT prototype sensor and signal conditioning circuit have been designed, built and successfully tested. The proposed prototype has demonstrated enough response speed to accurately record the peak overpressure of the blast event as compared to the benchmark PCB sensor. Further tests on an improved test rig will help to further demonstrate the performance of the FIT sensor using a better method to accurately place both sensors in the field of the blast relative to each other and to the blast axis.

Ringing has been detected on both the PCB and FIT sensors, as expected on any piezo electric devices operating under blast conditions. The ringing frequency is constant for a given sensor and depends only on its material properties and geometric configuration. Therefore, the ringing frequency can be corrected by off-line filtering assuming the data has been collected at fast enough rate (~ 10 times faster than the piezo resonance is a safe rule of thumb).

The captured waveform on the FIT prototype shows a second positive phase that seems indicative of a reflection of the incoming pressure wave front. This might be due to the specific characteristics of the geometric layout used in these tests. Accurate placement of both pressure sensors in an improved test rig will help clarify the reason for this apparent reflected second peak in pressure.

The last component missing in the proposed CBI-ESP device (cumulative blast and impulse electronic sensing package) is a new data logger capable to provide sampling rate up to 1 MHz in a package no larger than 1 inch square. This is the focus of the next performance period of this subcontract.

APPENDICES

EXPERIMENTAL FRAMEWORK FOR CUMULATIVE BLAST DETECTION AND DATA ACQUISITION FOR ASSESSMENT OF BLAST-RELATED INJURY IN ANIMAL STUDIES

Cumulative Blast and Impulse Exposure Sensor Package (CBI-ESP)

Version 2.0 rev B

USER MANUAL

Hector Gutierrez and Daniel Kirk

Department of Mechanical and Aerospace Engineering

Florida Institute of Technology

Melbourne FL 32901

Jan 3rd , 2013

1 Operating Instructions

The Cumulative Blast and Impulse Exposure Sensor Package (CBI-ESP) is a miniaturized sensor package designed to measure multiple blast events and record cumulative blast exposure data to an external SD card. The data is stored as text files of pressure versus time. The CBI-CSP data acquisition board can accommodate up to two sensor boards, and is programmed to acquire both channels for a fixed time when a pre-programmed trigger pressure value is reached.

1.1 Handling and setup

Like most electronics, the main pressure board is sensitive to static electricity. Always store the main board inside the supplied static protection bag. The sensor board and DAQ board are connected to each other by a miniature wiring harnesses. These harnesses are very delicate and should be handled with care. Do not pull from the wires when trying to disconnect any pin headers. Instead, please pull *from the edge of the white plastic header connectors*, which have a rim to pull using your fingernails.

The system is composed of the following components:

1. The data acquisition board (DAQ board)
2. The sensor board
3. Power source (Lithium polymer rechargeable battery)

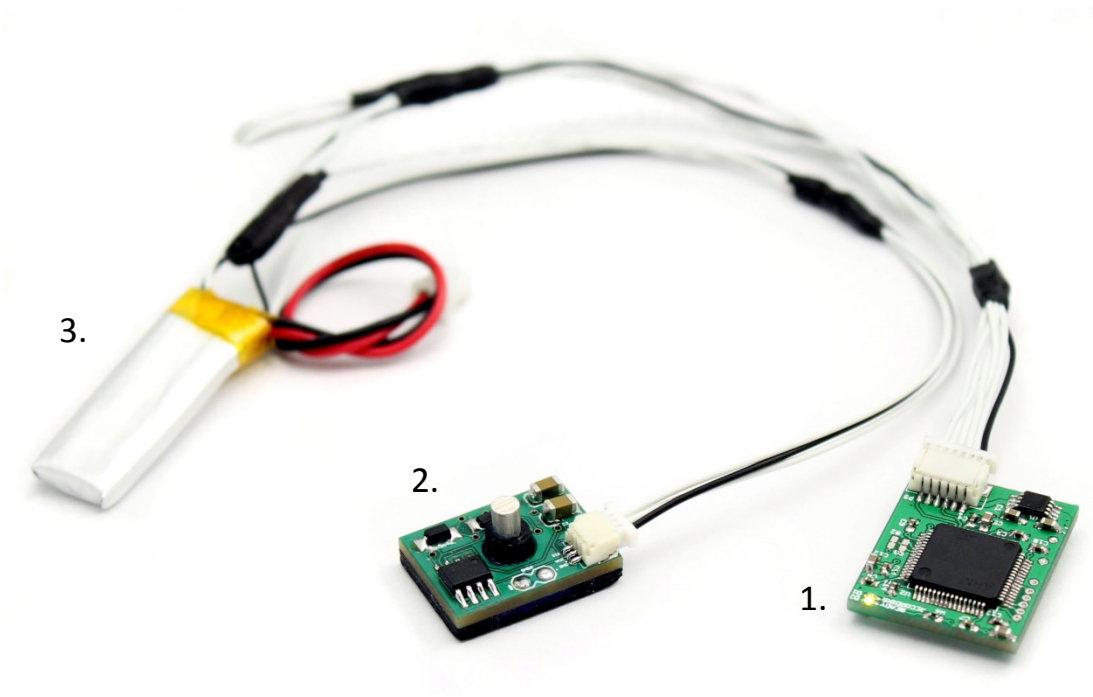

Figure 1: Complete system

1.2 Powering up

1. Insert a micro SD card formatted in FAT16 format, with the required configuration file in it (see Section 2.2.2) into the card holder located in the underside of the DAQ board. Simply push the card in and the socket will click.

2. Connect the DAQ board to the sensor board
3. Wait a few seconds to allow stabilization of the sensor
4. Connect the battery to the DAQ board. After connecting the battery you should see a steady green light in the DAQ board, which indicates that power is adequate and the board is operational, waiting to trigger. If the light is not steady green, refer to 2.2.1. If a pre-trigger occurs, wait until the data is fully written into the SD card and observe its behavior: the RED LED must flash shortly and GREEN LED must turn steady on. If the pre-triggering keeps occurring, check the value of the trigger (Section 2.2.2)

1.3 Data Conversion

Data is stored as raw text by the analog to digital conversion device. Each pressure value is stored as an integer between 0 and 4096. To convert the data to pressure, the bias value V_{bias} has to be known. The conversion to pressure is given by:

$$P = \left(V_{sample} - V_{bias}\right) * \frac{3300}{4096} * \frac{1}{S}$$

Where:

P: measured pressure, in psi

V_{sample}: raw sample (integer 0..4096)

V_{bias}: bias value: integer value corresponding to the atmospheric pressure before the blast event occurs. A good estimate can be obtained from averaging the first 500 microseconds of data (500 samples).

S: Sensitivity of the sensor in mV/psi

2 System Description

2.1 Calibration and System Validation

To verify functionality and accuracy of the CBI-ESP v2 system, a comparison between data from the CBI-ESP v2.0 and a standard off-the-shelf high speed blast pressure sensor (PCB-Piezotronics) was conducted using a National Instruments PXI-8331 high speed data acquisition card for data collection. Both sensors were placed outside the venting cone of the shock tube as shown in Figure 3, (a) and (b). In this configuration, both sensors are expected to read approximately the same pressure event at similar phase, although some minor differences are expected due to reflections from the experimental setup.

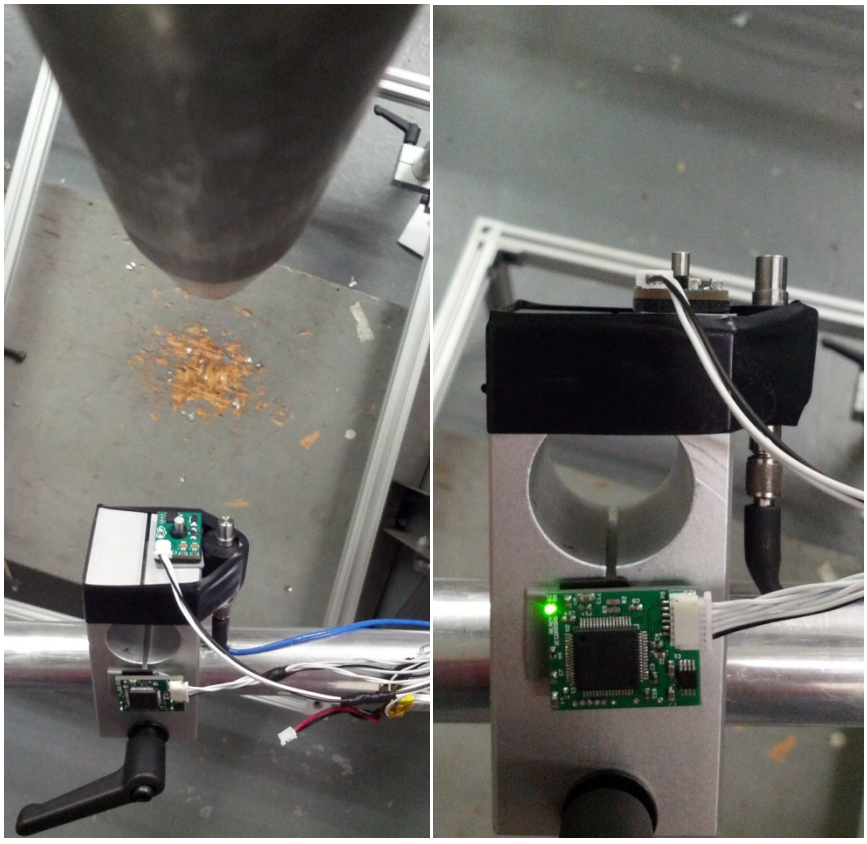

Figure 3 (a): Location of the CBI-ESP sensor board (right) relative to the witness sensor (PCB Piezotronics)

The test was conducted with 1000 psi driver pressure and a driven/driver ratio of 15, using a 0.002 in thick stainless steel shim. The results are shown in Figure 4, showing almost identical peak pressures and very similar pressure traces. None of the signals were filtered. The standard system was sampled using NI-LabView at 10 Megasamples/sec, and the CBI-ESP v2.0 operated at its native sampling rate of 1 Megasamples/sec. The difference between traces is attributed to slight differences in sensor placement.

Figure 3 (b): Location of the pressure sensors relative to the shock tube axis:

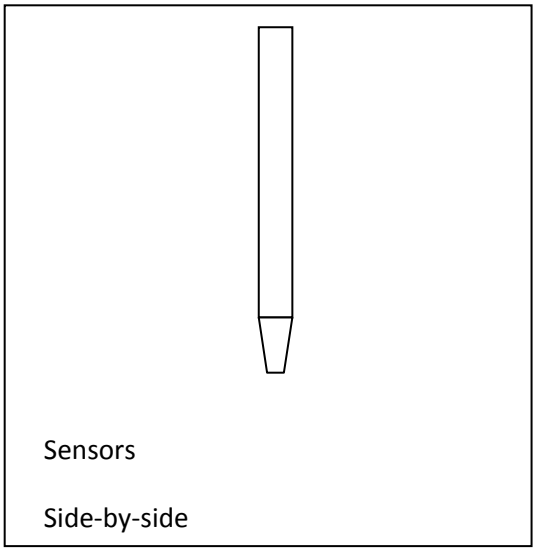

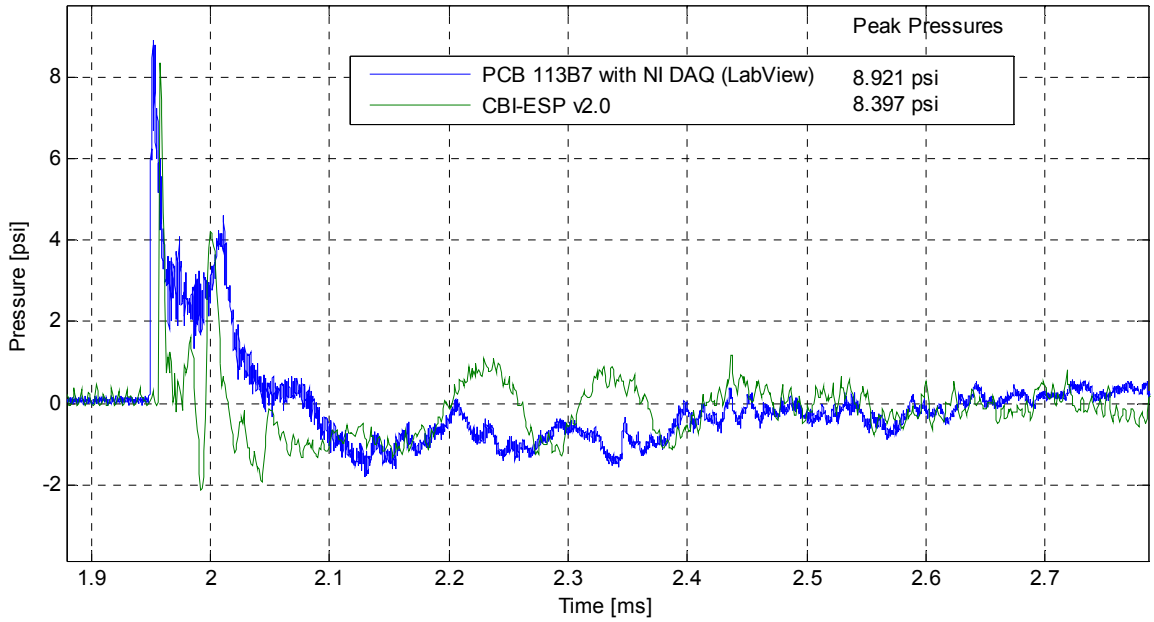

Figure 4: Calibration and validation. Standard blast measurement system (PCB Piezotronics pressure transducer with NI-LabView) compared to the same blast event captured using the CBI-ESP v2.0.

2.2 Data Acquisition Board

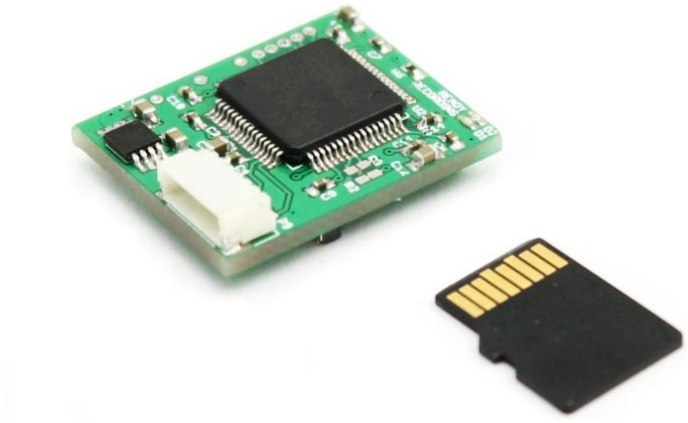

Figure 5: CBI-ESP v2 Data Acquisition Board

The CBI-ESP DAQ board is programmed to collect samples at 1 mega samples/sec from 2 channels simultaneously during up to 20 milliseconds, triggered when either channel goes over a specified programmable trigger value. It stores the data as a text file in a micro SD card, showing two columns: first for channel A, second for channel B. No timestamps are included since the sample rate is fixed. Each data set includes 1000 samples (1 millisecond) of pre-trigger data.

IMPORTANT: When using only one sensor channel, SHORT the UNUSED CHANNEL. DO NOT LEAVE the second channel FLOATING OR IT MAY CAUSE false trigger conditions.

The data acquisition board has a status LED, a 6 pin connector and an SD card slot in its underside.

2.2.1 Status LED

RED LED will flash when:

- No micro-SD card is detected - 250ms period
- Configuration file is missing - 125ms period
- Error creating data file - 50ms period
- After data has been written to the SD card and device is getting ready to collect data again, it will light up once for 250ms.

GREEN LED will be:

- Steady ON, when the board powers up and no error conditions are found. The DAQ board is ready and waiting for trigger.
- Flashing: after a trigger condition occurs, the GREEN LED will flash until it is done writing the pressure event to the micro-SD card, which takes between 30 to 50 seconds depending on the amount of data recorded.

2.2.2 SD Card

The SD card is formatted in the FAT format and needs to have a file called config.txt containing two values separated by a space (4 characters SPACE 2 characters). The first value consists of four digits that represent the trigger level (an integer between 0000 to 4096) that can be changed by the user. When the board detects a value (in either channel) higher than the trigger level indicated in the config.txt file, data acquisition starts.

The second value are two digits that represent the time, in milliseconds, that data collection will last. The possible range is 01 to 20.

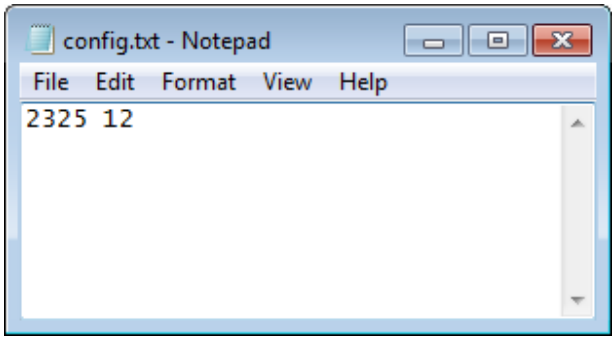

Figure 6: Default values of config.txt file

The collected pressure data will be stored in a separate file called DATA####.txt, where #### is a number between 0000 and 9999. File names for different events are consecutive (DATA0000.txt, DATA0001.txt, DATA0002.txt, and so on). No timestamp can be set to these files since there is no clock present on the board for simplicity.

The data corresponding to the pressure event is stored as text in two columns, space separated, as integers between 0 and 4096 to be converted to psi as described in Section 1.3

The Analog-to-Digital conversion is done in 12-bit resolution, with "0" representing ground, and 4096 representing 3.3V. Thus, the smallest resolution of the DAQ board is 805.7 μV/count.

To convert integer values to voltage, multiply the stored integers by the resolution (3.3 divided by 4096).

2.2.3 Pinout – DAQ Board connector

The pins of the DAQ connector header are shown below:

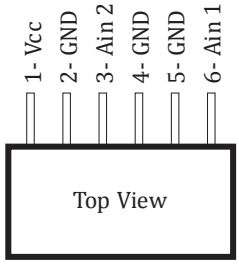

Figure 7: Pin out of the DAQ connector header - Top View

2.3 Sensor Board

Figure 8: Sensor Board

The sensor board boosts the supply voltage (min 2.7V, max 5.5V) to 24V, and limits the current to 4.5mA to feed a Piezotronics 132A31 ICP sensor. It then scales the sensor output voltage to the usable range of the data acquisition board through a gain of 0.2206

The sensor board has the following electrical characteristics:

- Measurement range: zero to 50psi
- Sensitivity: 31 mV/psi ± 1%
- Voltage bias at atmospheric pressure: typically ~1. 8V [1]

For all other electrical characteristics, please refer to the corresponding manufacturer documentation (PCB Piezotronics, 132A31 ICP sensor).

2.3.1 Sensor Board Pinout

The connection pins in the sensor board are as follows:

- Pin 1 GND: Ground
- Pin 2 VCC: Voltage supply (min 2.7V, max 5.5V)
- Pin 3 Vout: Voltage output (0 to 3.3V) [2]

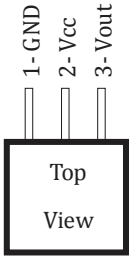

Figure 9: Sensor Board pin out - Top View

[1] Recommended practice: average first 500 pre-trigger samples to obtain accurate voltage bias.
[2] Signal ground is the same as power (battery) ground

Establishing Biomarker/Brain Injury Metrics in Rat Models of Cumulative Blast Overpressure

V. Prima[1], O. Glushakova[1], A. Svetlov[1], D. R. Kirk[2], H. M. Gutierrez[2], K. C. Curley[3], R. L. Hayes[1], K. W. Wang[1], S. I. Svetlov[1]

[1]Center of Innovative Research, Banyan Biomarkers; [2]Florida Institute of Technology; [3]US Army Medical Research and Material Command

Rationale

A lack of assessment criteria and devices indicating the risk from low level multiple blast loads, especially mild traumatic brain injury (mTBI) is of a special concern for the health care of soldiers performing multiple tours of duty in Iraq and Afghanistan. This study was aimed to establish a valid animal model in search of correlations between exposure to cumulative blast events and injury types/severity.

Our previous studies characterized positional interaction of animal body with blast wave in a rat model of overpressure-induced TBI. Here, we compared the effects of a single or multiple body/head exposures to a moderate primary overpressure with TBI by a severe composite ("on-axis") blast. Assessment of cumulative blast TBI responses in live animals was done using multiple controlled blast loads on rat's head and total body at different timing schedules.

Comprehensive evaluation in live animals of cumulative blast injury will be used to develop multiple Blast-mTBI scale using biomarker/brain injury metrics.

Methodology

Existing experimental setups for studies of blast effects in small animals have significant flaws in their design impeding precise modeling of primary blast injury. Here, we compared the effects of primary blast exposure of controlled duration, peak pressure and impulse with brain injury by a severe blast load accompanied with strong head acceleration. We studied critical components of pathological pathways as potential markers of blast responses. Brain, blood and CSF samples were examined via ELISA, antibody microarrays, immunohistochemistry and Western blot following blast exposure of different magnitude and multiplicity. The high speed imaging with Schlieren optics demonstrated animal head acceleration/jolting depending on the experimental setup.

Summary

- Controlled blast loads were employed to examine the spatial effects of animal body interaction with a primary blast peak OP wave compared to "composite" shock wave including also a venting gas jet. Multiple blasts were used to assess the risks from low level multiple TBI accumulation.
- The high speed imaging revealed strong head acceleration/jolting resulting from the "composite" shock wave hitting rat head ("on-axis" setup). On the contrary, placing rats outside shock tube axis exposed rats to a peak overpressure only (primary blast event), allowing close mimicking of explosive blast TBI.
- Nerve growth factor beta-NGF , neuronal VEGF/semaphorin receptor Neuropilin-2, adipose derived hormone Resistin and inflammation-related cytokins IL-1 and IL-10 were significantly elevated in blood within the first week post-blast.
- Neuropeptide hormone Orexin A content showed drastic raise in blood at 24 h after blast targeting total body, followed by gradual decline. On the contrary, blast targeting only head caused gradual raise of Orexin through 30 d post exposure.
- GFAP and CNPase, markers of astroglia and oligodendroglia, accumulated substantially in hippocampus, cortex and CSF 24 h after blast and persisted for 30 days post-blast.
- For all putative biomarkers the detected levels raised substantially at all the setups studied. However, the most significant and persistent changes in serum levels were observed when the total animal body was subjected to a primary blast wave compared to setups where only animal head was hit either by a composite blast or by a primary peak OP. For the brain-specific biomarkers studied cumulative effects of multiple blasts were observed at the earlier time points (1 day).

Modeling Primary, 'Composite' and Multiple Blast Exposures

Variable Length Driver: adjustment of over-pressure and shock wave duration. No reported blast wave simulators have this unique feature

Adjustable blade cutter: change of diaphragm materials and vary range of operational pressures

Variable length driven: turning a normal shock wave into a blast wave prior to exit

Interchangeable holders allow for variable animal positioning relative to a blast wave front

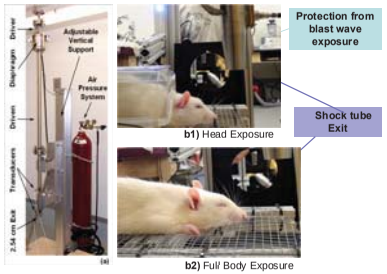

Fig. 1. a) General Shock Wave Generator setup. b) Animal positioning for the off-axis primary blast wave. b1) Head exposure. b2) Full Body exposure.

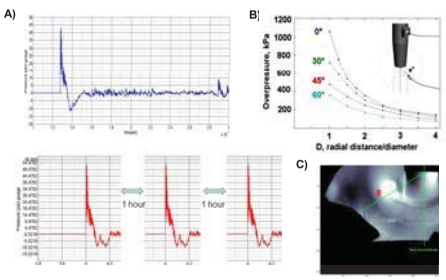

Fig. 2. A) Representative overpressure traces during single and multiple blast exposures; B) Blast wave overpressure as a function of radial distance and angle. C) Schlieren image of rat and off-axis shock wave.

TBI Biomarkers following Primary vs. 'Composite' Blast

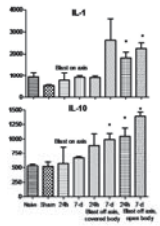

Fig.3. Interleukin-1 and Interleukin-10 accumulation in serum after blast (u/l)

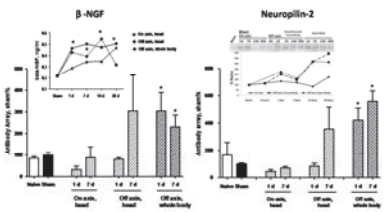

Fig.4. Antibody arrays for serum β-NGF and NRP-2 (insets: β-NGF ELISA and NRP-2 Western blot)

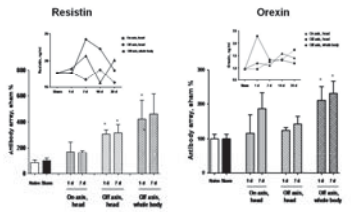

Fig.5. Resistin and Orexin accumulation in rat serum after blast (inset - ELISA)

TBI Biomarkers following Single vs. Multiple (x3) Blasts

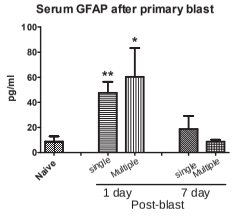

Fig.6. GFAP accumulation in serum after blast (ELISA)

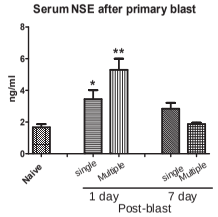

Fig.7. NSE accumulation in serum after blast (ELISA)

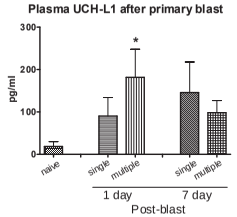

Fig.8. Expression of UCH-L1 in plasma after blast (ELISA)

High-Speed Blast Imaging

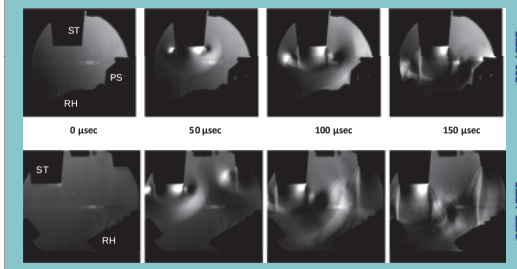

Fig. 4. Shock wave interaction with target revealed by high speed imaging with Schlieren optics (ST-shock tube, RH-rat head, PS-protective shield). On-axis vs. off-axis exposure.

TBI Biomarkers analysis by IHC

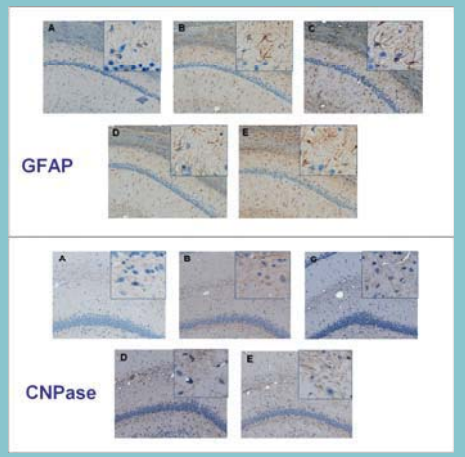

Figure 11. Expression of GFAP and CNPase in Hippocampus (CA1 region) of overpressure-injured rats.
A) control naive; B) on-axis 1 day; C) on-axis 7 days; D) off-axis 1 day and E) on-axis 7 days.
Magnifications 5 x and 20x of CA1 region are shown.

Supported by grants N14-06-1-1029, W81XWH-8-1-0376 and W81XWH-07-01-0701 from Department of Defense.

Anxiety Produced in Rats by Over-Pressurization Blast Injury

Sherry Adams[1], Jillian A. Condrey[1], Hsiu-Wen Tsai[1], Victor Prima [2], **Stanislav I. Svetlov [2, 3]** Colin Sumners[3] and Paul W. Davenport[1]

[1]Department of Physiological Sciences, University of Florida, Gainesville, FL 32610,
[2]Banyan Laboratories, Inc, Alachua, FL, USA and
[3]Department of Physiology and Functional Genomics, University of Florida, Gainesville, FL, USA

ABSTRACT

Traumatic brain injury (TBI) occurs in individuals exposed to direct force trauma and close proximity explosions. Blast TBI is an injury that is the result of an explosion generating an over-pressurization blast (OB) wave in close proximity to the individual producing closed-head brain injury. Individuals experiencing Blast TBI have behavioral (post-traumatic stress disorder, PTSD), respiratory (apnea) and cardiovascular changes directly correlated with the blast-induced TBI. There is also a correlation between a history of TBI and PTSD. PTSD symptoms include anxiety and fear. An OB injury rat model was used in this study to test the hypothesis that anxiety/fear can be induced in rats following exposure to a moderate to severe OB. The elevated-plus maze (EPM) test was used before and after OB to assess anxiety. Rats underwent EPM testing 4-5 days prior to the OB. The animals were anesthetized and the OB brain injury produced by a compressed air-driven shock tube directed at the dorsal surface of the head of the rat with an average peak overpressure of 90 psi at the shock-tube resulting in a 52 psi at head with a total duration of 10 msec of blast exposure. The body was protected from the pressure wave by a plexiglass cover. Three days following the OB, the rats were retested on EPM. Animals spent 60.9% of time in closed arm pre-OB and 89.9% of time in closed arm post-OB ($p < 0.05$). Animals spent 30.9% of time in the center pre-OB and 0.10% of time post-OB ($p < 0.05$). Animals spent significantly shorter time in open arm post-OB ($p < 0.05$). There were no significant differences in these EPM parameters for control animals. These results would suggest that rodents exposed to a moderate to severe blast wave have heightened anxiety/fear possibly associated with blast-induced TBI.

INTRODUCTION

Mild traumatic brain injury affects nearly two million people yearly at an estimated annual cost of $76.5 billion in the United States (Brain Injury Association of America). The leading cause of TBI are motor-vehicle crashes, falls and sporting accidents, violence and firearms in the civilian population. Whereas military personnel suffer the majority of TBIs from blast injuries caused by improvised explosive devices (IEDs) (Brain Injury Association of America). TBI causes behavioral as well as physiological changes. Depression following TBI is highly variable and ranges from 6% to 77% of TBI patients (Morton and Wehman 1995). Male rats exposed to repetitive blasts experienced PTSD symptoms including increased anxiety (Elder, et al., 2012). An impact acceleration model of TBI demonstrated long-term increase in stress and anxiety in rats consistent with depression (Fromm, et al., 2004).

Experimental blast injury induces a traumatic brain injury by directing a jet of pressurized air at the skull. This pressurized air sends an impulse wave throughout the brain and brainstem causing shearing and stressing of the tissue and potentially disrupting neuronal connections. Concussion models have shown excitotoxicity that affect the hippocampus and other brain areas controlling affective behavior following a TBI. Our animals are exposed to an over-pressurization blast injury (OBI) used to model blast TBI. Diaphragm EMG activity was used to determine the effect of OBI on breathing pattern and the elevated plus maze (EPM) was used to test fear and anxiety.

HYPOTHESES

1. We hypothesized that OBI would induce an initial apnea followed by variable and decreased ventilation.
2. We hypothesized in conscious rats exposed to OBI there would be increased fear/anxiety.

METHODS

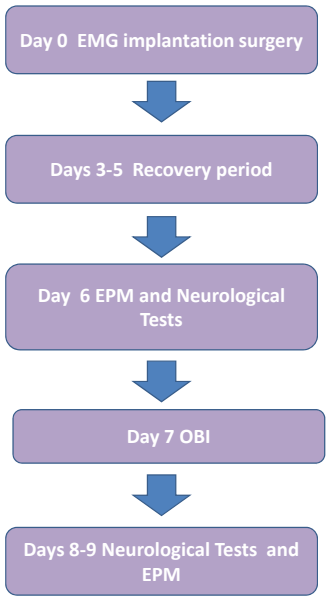

Animal Model
•Adult male Sprague Dawley rats (n=27) weighing between 250 to 310 grams were anesthetized using Isoflurane.
•Diaphragm EMG electrodes were implanted. The animals were allowed to recover and Dia EMG activity recorded pre-OBI to ascertain a reliable EMG signal.
•Animals were transported to laboratory where the OBI was induced.
• Animals were anesthetized with Isoflurane. OB brain injury was produced by a compressed air-driven shock tube directed at the dorsal surface of the head of the rat near Bregma. The pressure wave was delivered with an average peak overpressure of 90 psi at the shock-tube resulting in a 52 psi at head with a total duration of 10 msec of blast exposure. The body was protected from the pressure wave by a plexiglass cover.
•Diaphragm EMG was recorded in the anesthetized rat 5 minutes prior, during and 5 minutes post-OBI using PowerLab and LabChart software. The EMG was integrated with a 50 msec moving time average.

Behavioral Testing
Conscious animals received behavioral tests prior and after OBI.
EPM: The animal was placed in the center of an EPM. Rat position and movement were recorded to determine the time spent in open, closed and middle sections.
Proprioception and Vibrasse: A rod was used to elicit a withdrawal response by tapping the skin in the external oblique area (left and right) and brushing caudal to cranial through the vibrasse. The withdrawal response was scored on a 1-3 scale: 1=no response, 2=response one side and 3=response both sides

Statistical Analysis
•A paired t-test between groups was used to determine significance in pre- and post-blast measurements as well as irregular breathing and psi levels.
•A one-way repeated measure analysis of variance with Shapiro Wilk normality test between groups was used to determine significance in apneic and irregular ventilton periods.
•The significance criterion for all analyses was set at p<0.05.

RESULTS

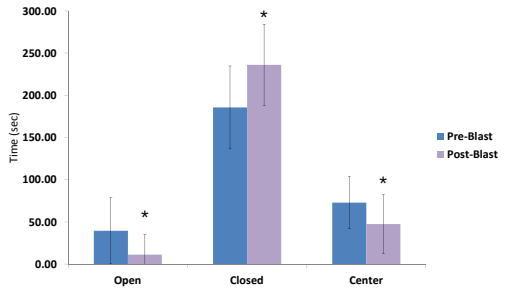

Figure 1. Elevated Plus Maze. The animals were tested pre- and post-blast. They spent less time in both the open and center sections of the elevated plus maze and more time in the closed section. All sections reached statistical significance (*$p < 0.05$).

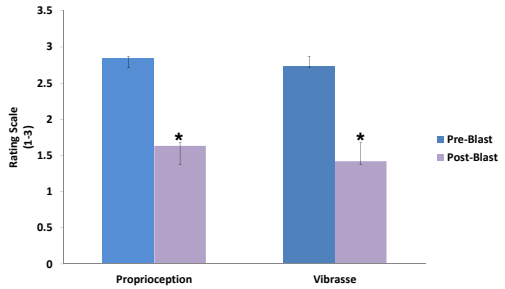

Figure 2. Neurological Testing. Proprioception and vibrasse withdrawal responses significantly decreased 24 hours post-blast. *($p < 0.05$).

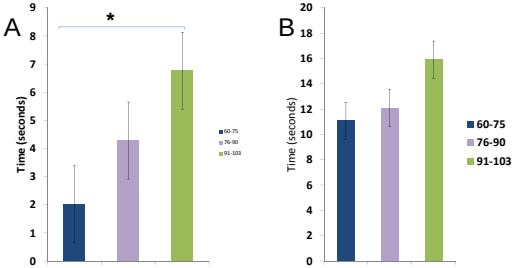

Figure 3. A. OBI Pressure and Apneic Period. Between 60-75 psi and 91-103 psi statistical significance was seen for apneic period (sec). No significance was seen between 76-90 psi and either 60-75 psi or 91-103 psi. * $p < 0.05$). **B. OBI Pressure and Irregular Breathing Period.** Irregular breathing is defined as augmented or attenuated inspiratory efforts until return to a post-blast baseline breathing pattern. No significance was seen in groups. *($p < 0.05$).

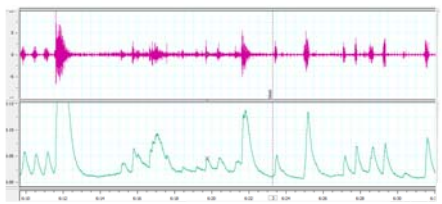

Figure 5. Animal 5, psi 102.6. Irregular breathing pattern following OBI apnea. Panel A: Raw dEMG signal. Panel B: Integrated dEMG signal.

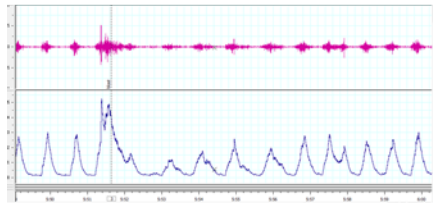

Figure 6. Animal 19, psi 69.9. Irregular breathing pattern following OBI apnea. Panel A: Raw dEMG signal. Panel B: Integrated dEMG signal.

CONCLUSIONS

- OBI induced apnea and irregular ventilation during pressure exposure in anesthetized rats.
- The apneic periods were significantly longer in the 91-103 psi group when compared to the 60-75 psi group. This is consistent with animal studies that show increased apneic period in higher severity brain injuries.
- The apneic period was not significantly different between 76-90 psi group and either 60-75 psi or 91-103 psi groups suggesting a threshold for OBI related apnea.
- Apnea is different as a function of psi but the duration of disordered breathing was similar in all animals.
- The blast injury resulted in a decrease in time spent in the open arms of the EMP consistent with OBI induced increase in fear/anxiety response.
- The OBI resulted in decreased somatosensory function evidenced by decreased sensation to proprioception and vibrasse stimuli as a result of brain injury.

REFERENCES

Brain Injury Association of America. http://www.biausa.org/.

Elder, G. A., N. P. Dorr, et al. (2012). "Blast Exposure Induces Post-Traumatic Stress Disorder-Related Traits in a Rat Model of Mild Traumatic Brain Injury." J Neurotrauma.

Fromm, L., D. L. Heath, et al. (2004). "Magnesium attenuates post-traumatic depression/anxiety following diffuse traumatic brain injury in rats." J Am Coll Nutr **23**(5): 529S-533S.

MULTIPLE BLAST EXPOSURES ALTERS NEURO-GLIAL, NEUROENDOCRINE AND GROWTH FACTOR BIOMARKERS TO BLAST LOAD IN RATS

Prima V[1] , Scharf D[1], Gutierrez H[2], Kirk DR[2] Svetlov A[1], Curley KC[3], Hayes RL[1], Svetlov SI[1]

[1]Banyan Biomarkers; [2]Florida Institute of Technology; [3]US Army Medical Research and Material Command

Abstract

PROBLEM/CHALLENGE: Blast-induced neurotrauma is frequently accompanied by blood–brain barrier (BBB) disruption, which permits the release of brain-specific proteins into circulation and facilitates exchange of neuromediators. While repeated blast exposures is a common hazard for war zone personnel and civilian populations, the cumulative effects of multiple blasts on brain injury biomarkers have not been investigated.

PURPOSE: Evaluate the potential cumulative effects of blast load by comparing the responses after multiple blast exposures to a single overpressure event, inducing brain injury in rats.

DESIGN: Rats were subjected to a primary blast of 365 kPa overpressure and total duration of 75 μsec at the frontal part of the rat's skull. Portable cumulative blast sensors were placed on the head front and rat spine. Multiple blasts were performed as a series of 3 exposures, with a 45 min to 1 hr recovery period between each blast. High speed imaging revealed a negligible degree of acceleration at rat position "off-axis" toward external shock tube, thus confirming primary blast kinematics.

METHODS: Assessment of previously characterized and potential novel TBI biomarkers was done by ELISA, antibody microarrays, and Western blot. We measured blood accumulation of glial markers (GFAP and CNPase), neuronal markers (UCH-L1 and NSE), neuroendocrine peptide Orexin A, and Neuropilin-2 (receptor for VEGF and semaphorins) at 1 day and 7 days post-blast.

RESULTS: Remarkable elevation of all proteins studied was observed at 1 day after either single or multiple exposures to blast. Of note, multiple blasts significantly increased blood levels of GFAP, UCH-L1, NSE and NRP-2, but not Orexin A, vs. single blast exposure 1 day post-blast, while at 7 days the cumulative effects of multiple blasts were much lower, if any, compared to a single blast. On the other hand, serum CNPase after multiple blasts was significantly elevated compared to single blast both at 1 day and 7 days post exposure.

Summary: The time-course of several serum biomarkers of neurotrauma was characterized after single and repeated moderate primary blasts. Biomarker levels rose significantly as a rapid response at day one post-blast, with the CNPase, NSE, UCH-L1, and NRP-2 levels after repeated blast exposures elevating further over single blast. The appearance of characteristic proteins in circulation may reflect deterioration of the BBB and can be used for assessment of injury accumulation. However, triple consecutive blast exposures did not produce a further elevation in biomarkers at 7 days post exposure compared to a single blast. At this time point, their increased levels depend on the cell-specific origin of biomarkers and that stage of injury, rather than reflecting a cumulative blast load.

Conclusions

- Controlled repeated blast loads in a shock tube animal model were employed to characterize the accumulation of serum biomarkers of neuro-glial injury.
- The high speed imaging revealed that placing rats outside shock tube axis exposed rats to a peak overpressure only (primary blast event), allowing close mimicking of explosive blast TBI and avoiding strong head acceleration/jolting due to the compressed air jet .
- Blood levels rose significantly for GFAP, CNPase, NSE, UCH-L1, Orexin , sICAM and NRP-2. Aas a rapid response at day one post-blast, after repeated blast exposures elevating further over single blast.
- Only for CNPase and sICAM the corresponding systemic levels continued to significantly increase at 7 days post-blast over the 1 day post-blast values.
- For all putative brain-specific biomarkers the serum levels raised substantially at 1 day after multiple blasts however accumulation was not linearly proportional to the number of blasts.
- The above phenomenon was observed also for the leakage of albumin-EBD complex in the reverse direction from circulation to the brain tissue.

Modeling Multiple Blast Exposures

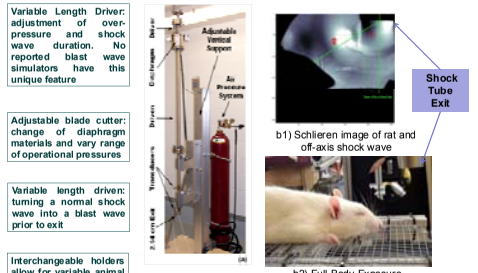

a) Shock Wave Generator setup. b) Animal positioning for the off-axis primary blast. b1) Schlieren imaging. b2) Blast exposure.

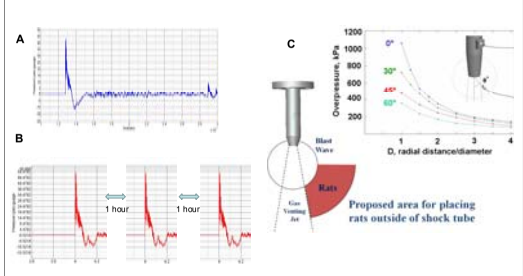

Representative overpressure traces during single (A) and multiple (B) blast exposures; (C) Blast wave overpressure as a function of radial distance and angle.

Neural-Glial TBI Markers released in Blood after Single/Multiple Blast

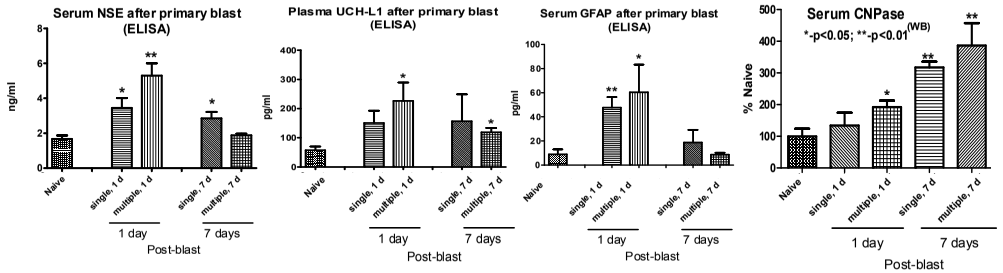

Neuroendocrine, inflammatory and growth factor TBI Markers

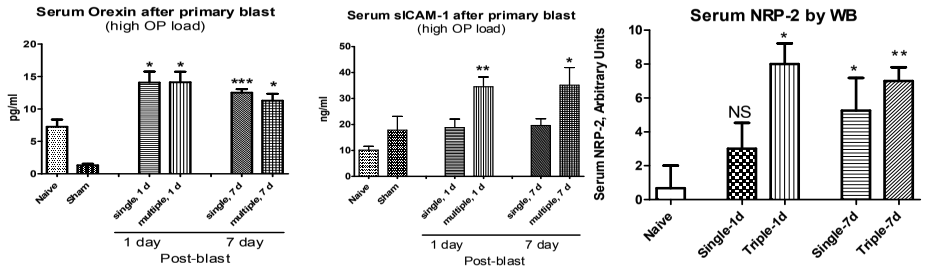

High-Speed Blast Imaging

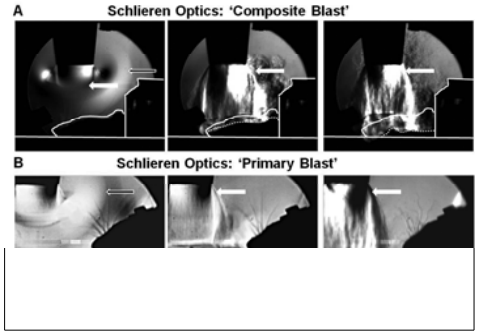

Comparison of blast wave interaction with head On-axis ('Composite' Blast) vs. Off-axis (Primary Blast)

High-speed recording with Schlieren Optics: A) 'Composite Blast'; B) 'Primary Blast'. Black arrows indicate formation and interaction of blast wave with rat head (accomplished within ~0.1 ms). White arrows show gas venting jet hitting rat head after blast wave passed through (persists for milliseconds). The solid contour line in panel A outlines the shape of animal head at time point 0; the dotted line- current shape.

BBB Permeability after Blast

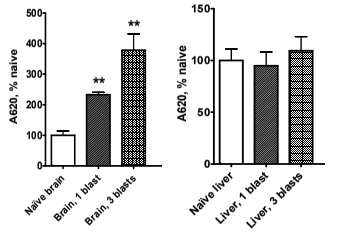

A 2% solution of Evans Blue Dye in PBS (4 mL/kg of body weight) was injected i.p. and the stain was allowed to circulate for 3 hours. At 4 hrs after first blast the anesthetized animals were intracardially perfused with PBS. Brain and liver samples were then isolated and weighed, homogenized in 2 ml 50% trichloroacetic acid per gram tissue and centrifuged. The absorbance of the extracted dye in supernatant at 620 nm was used to quantify the relative tissue content of EBD.

Download this poster

Supported by grants N14-06-1-1029, W81XWH-8-1-0376 and W81XWH-07-01-0701 from Department of Defense.

Neuro-glial and systemic mechanisms of pathological responses to primary blast overpressure (OP) compared to 'composite' blast accompanied by head acceleration in rats.

Stanislav I. Svetlov[1], Victor Prima[1], Daniel R. Kirk[2], Hector Gutierrez[2], Kenneth C. Curley[3], Ronald L Hayes[1], Kevin K.W. Wang[1]

[1]Center of Innovative Research, Banyan Biomarkers Inc., 12085 Research Drive, Alachua, FL 32615, USA

[2]Mechanical & Aerospace Engineering, Florida Institute of Technology, Melbourne FL 32901, USA

[3]U.S. Army Medical Research and Materiel Command, Fort Detrick, Frederick, MD, USA

ssvetlov@banyanbio.com

Energy distribution in modern technosphera, and particularly the 21st century warfare, has led to a significant increase of human exposure to blast overpressure (OP) impulses. Blast forces, even of low magnitude, are believed to produce minor but sustained neurological deficits, and when repeated, can lead to neuro-somatic damage and neurodegeneration. Most prominent changes may occur at the level of intercellular circuits that involve neurons, glia, vascular cells and neural progenitors.

Reproducible models of military-relevant blast injury, including generators which precisely control parameters of the blast wave have been developed and examined. Our studies demonstrated the importance of positional orientation of head and whole body toward blast wave in animal models. Here, we compare the effects of body/head exposure to a moderate primary overpressure (OP) with brain injury produced by a severe blast accompanied by strong head acceleration.

The high speed imaging demonstrated the interaction of blast wave with animal head/body and revealed a negligible degree of acceleration at rat positioning 'off-axis' toward shock tube (primary blast) compared to 'on-axis' experimental setup accompanied by strong head/cervical acceleration. We examined brain expression of glial and neural markers including GFAP and revealed strong glyosis accompanied by a time-dependent proliferation of activated astrocyte and oligodendrocyte lineages after exposures to primary and 'composite' blast. GFAP and neuronal markers UCH-L1 and NSE were also detectable in plasma/serum after blast exposures. Serum levels of IL-1 and IL-10 were significantly elevated, predominantly after primary blast exposure reflecting systemic body responses. Brain up-regulation of cell adhesion molecules L- and E-selectins, nerve growth factor beta-NGF and neuronal receptor Neuropilin-2 was also detected.

A specific dynamics of corresponding biomarkers in serum was established and characterized. For major pathway's signatures and biomarkers, the detected levels raised at all the setups studied. However, the most significant and persistent changes in neuro-glial markers were found after composite blast, while primary blast instigated prominent systemic/vascular reactions, particularly when the total animal body was subjected to blast wave.

In conclusion, several crucial pathogenic components of neural and systemic responses were raised in a time-dependent and setup-dependent fashion. We suggest that the mechanisms underlying blast brain injuries, particularly mild and moderate, may be triggered by systemic, cerebrovascular and neuro-glia responses as consecutive but overlapping events.

INTRODUCTION

Medical, Social and Military Importance. The nature of warfare in the 21st century has led to a significant increase in primary blast or over-pressurization component of body injury which manifests as a complex of neuro-somatic damage, including traumatic brain injury (TBI), and often accompanied by posttraumatic stress syndrome (PTSD). Blast-related coalition fatalities, including IED, RPG, and rocket attacks, outnumber conventional fatalities during the last several years in Iraq and Afghanistan (**Fig. 1,** http://www.icasualties.org/). Moreover, for every blast-related fatality, many more soldiers suffer multiple, non-lethal blast exposures. This often leads to mild traumatic brain injury (mTBI), which is rarely recognized in a timely manner and has become a signature injury of the Iraq and Afghanistan conflicts (1-3).

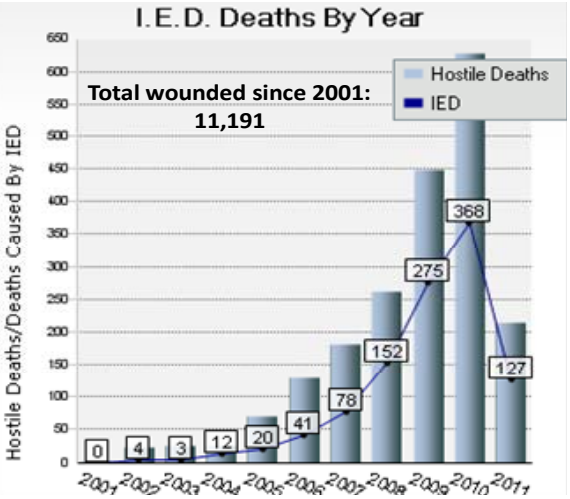

Fig. 1: Blast-related fatalities during OIF/OEF

Blast forces, particularly those that are repeated and low magnitude, are believed to produce minor but sustained disorders when neural damage cannot be detected or diagnosed by existing methods. Symptoms of mild or moderate blast brain injury often do not manifest themselves until sometime after the injury has occurred (4-6) and go undiagnosed and untreated because emergency medical attention is directed towards more visible injuries such as penetrating flesh wounds (7-9). However, even mild and moderate brain injuries can produce significant deficits and when repeated can lead to sustained neuro-somatic damage and neurodegeneration (4). Although exposure to repeated low level blasts is a common feature of war zones personnel/civilian population (OEF/OIF), the cumulative effect of multiple blasts on brain injury has not been investigated.

Data from our laboratories (10, 11) and others suggest that the mechanisms underlying such 'minor' injuries appear to be distinct from those imposed by mechanical impact or acceleration. Thus, identifying pathogenic mechanisms and biochemical markers of blast brain injury is vital to the development of diagnostics for mTBI through severe TBI. Validation of diagnostics and grading brain injury depending on the cumulative blast load will provide a dose-injury scale for personnel monitoring on the battlefield using portable blast "dosimeter" and/or a point of care diagnostic device.

Methodology and Results

Experimental Models for Studies of Blast Injury. Exposures to blast waves have the potential to inflict multi-system, including neurotrauma, as well as life threatening injuries to many personnel simultaneously (see (4) for review). It is generally accepted that primary blast injuries are generated as the over-pressurization wave propagates through the body causing damage at gas-fluid interfaces (12). The types of injuries inflicted include pulmonary barotraumas, tympanic membrane ruptures and middle ear damage, abdominal hemorrhage and perforation, rupture of the eye balls, and concussions (13).

A number of investigations have employed compressed air-driven shock tubes and nitrogen-driven blast wave generators for blast exposures of various animals (e.g. rats, mice, rabbits) to address mechanisms of injury (14-20). Small animals are placed in orthopedic stockinet slings, and large animals in open mesh Nylon TM slings, and subjected to blast exposure at varying distances and body orientations with or without a supportive/reflective plate behind the animal.

Our shock tube was designed and built to model a freely expanding blast wave as generated by a typical explosion **(see 11 for details)**. Blast injury modeling framework is shown in **Fig. 2.** Modular design allows for the flexibility to perform various types of tests: design is lightweight while maintaining necessary strength and stiffness. Data were acquired with PCB dynamic blast pressure transducers and LabView 8.2. Images were captured at 30 fps (frames per second) resolution. National Instruments 500,000 samples/sec data acquisition card were used to acquire data on multiple channels. Following the diaphragm rupture, the driver gas sets up a series of pressure waves in the low pressure driven section that coalesces to form the incident shockwave. In our shock tube, the burst pressure of the diaphragm separating the driver and driven sections do not change. Repeatability of diaphragm burst pressure was accomplished through the use of a cutter assembly directly in front of the diaphragm. Preliminary tests were conducted without animal specimens to optimize the peak overpressure (OP) and exposure time to accurately reproduce blast events: driver pressure and volume, diaphragm material, and shock tube exit geometry. Both static and dynamic (total) pressure was measured using piezoelectric blast pressure sensors/transducers positioned at the target. The shockwave recorded by blast pressure transducers in the driven section and at the target showed three distinct events: (i) peak overpressure, (ii) gas venting jet and (iii) negative pressure phase. Peak overpressure, positive phase duration, and impulse are the key parameters that correlate with injury and likelihood of fatality in animals and humans, for various orientations of the specimen relative to the blast wave (15, 16, 21-24). After the pressure history is recorded and the sensors removed, the animal can be carefully positioned at the same location and the test repeated, since it has been previously demonstrated that the proposed shock tube design has excellent repeatability characteristics.

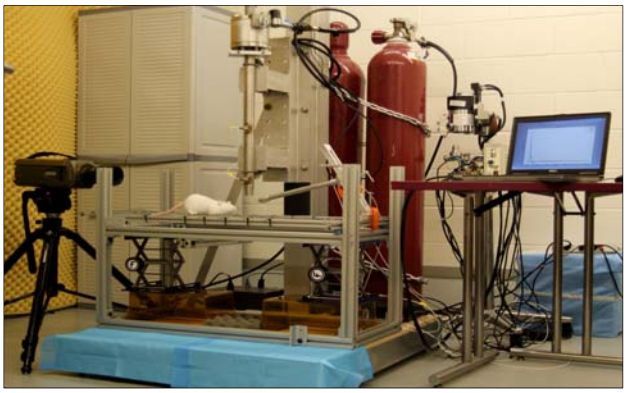

Fig.2 Overview of shock tube and experimental blast model facility at Banyan Biomarkers, Inc.

However, because of inconsistent designs among blast generators used in the different studies, the data on brain injury mechanisms and putative biomarkers have been difficult to analyze and compare. The main problem is that following blast peak overpressure, shock tubes immediately produce 'venting gas jet', substantially contaminating the blast wave **(Fig. 3).** Due to the complex nature of the blast event, the brain injury is a result of a combined impact of the "composite" blast including all 3 major phases of a shockwave shown in **Fig. 3 A and B**. Gas venting jet, albeit lower in magnitude than peak overpressure, lasts the longest, and represents the bulk of blast impulse and possibly produces the most devastating impact. We demonstrated previously a strong downward head acceleration following the passage of peak overpressure which lasts ~36 µsec (11). However, cranial deformation was more severe during the gas venting phase, lasting up to ~5-6 msec (Fig. 3A). These findings points to a potential flaw in several previous studies

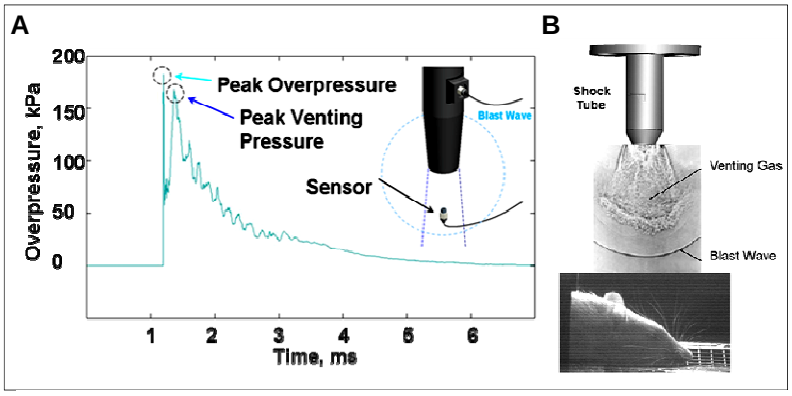

Fig. 3 Components of shock tube-generated shock wave. A: Peak overpressure and venting gas measured by PCB dynamic pressure sensors, and B: Rat head positioning relative to shock tube and visualization of shock wave using Schlieren optics

described in the literature: animal specimens are usually placed along the axis of the shock wave generator. In such location, the venting gas jet creates a much larger impulse (energy transfer) in the specimen than the peak overpressure itself. This effect can be virtually eliminated by placing rats off-axis from the venting jet in a way that the main effect acting on the specimen is the peak overpressure event.

Normal explosions produce blast winds that follow behind the incident shock. This effect is mimicked by shock tubes as the wave spherically expands. However, gas venting impulse is hard to control and it is probably not associated with the physics of primary blast event. A novel solution to address this problem is to place the target at an off-axis angle to avoid the venting altogether **(Fig. 4).**

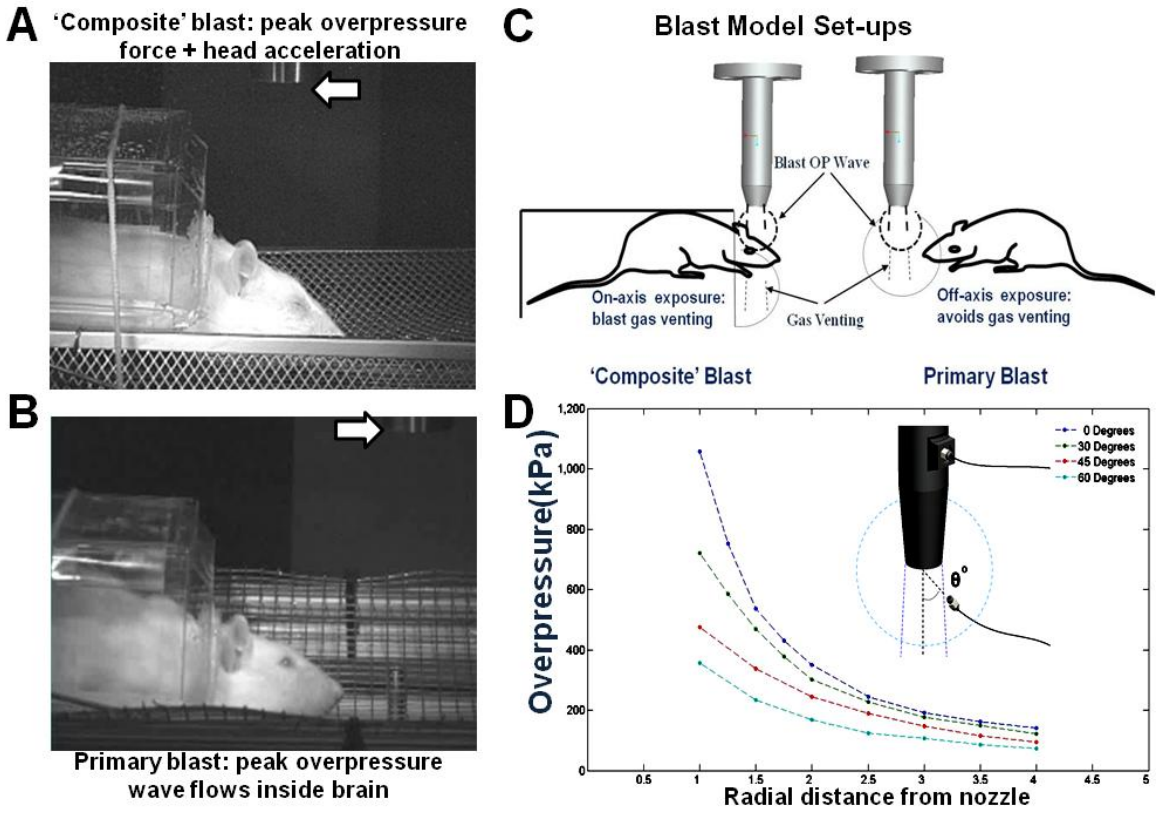

Fig. 4 Two general experimental set-ups for rat's exposure to shock tube-generated blast waves. A: on-axis of shock tube nozzle position: peak overpressure + venting gas produce head acceleration 'Composite blast'; B: off-axis position: blast wave peak overpressure only hitting rats; C graphic representation of two different set-ups; and D: Calibration of pressure on rat head depending on the angle and distance from the nozzle of shock tube.

The changing local speed of sound behind the wave causes the duration to increase with distance. For example, the 45° data shows duration increases from 53.1 to 85.3μs as the distance increases from 2D to 4D. By varying pressure settings, driven and driver lengths, and specimen location, independent control of blast overpressure, duration, and impulses may be achieved. Two different set-ups is shown in **Fig. 4.** We exposed rats to blast wave of a precisely controlled magnitude, duration and impulse at the surface of rat at various orientations of head to the blast wave with open or armored body: on axis and off-axis.

Molecular Components/Biomarkers of Blast-Induced Injury in Rats.

General hypothesis is that blast-induced brain injury is triggered and mediated by systemic, cerebrovascular, neuroinflammatory, neuroendocrine and neuro-glial responses as consecutive but overlapping events. Based on our previous global and targeted proteomic data, the following molecular components and injury biomarkers were assessed. Systemic/vascular responses: interleukin-1 and interleukin-10 (IL-1, IL-10), soluble intercellular adhesion molecule-1 (sICAM-1), L- and E-selectins. Glyosis was assessed by astrocytic marker GFAP and oligodendrocyte marker CNPase in both brain tissue and as biomarkers in serum. Neuronal injury was evaluated using brain tissue silver staining and serum levels of ubiquitin-C-terminal hydrolase UCH-L1 and Neuron-specific enolase (NSE). Neuroregenerative processes were evaluated by measuring brain tissue and serum levels of neuropilin-2 (NRP-2), receptor for VEGF and semaphorins.

Methods and Experimental Procedures. Neuroinjury and neurodegeneration was evaluated in the perfused and fixed brains using silver staining procedures at Neuroscience Associates (Knoxville, TN) utilizing the deOlmos Amino Cupric Silver Stain (http://www.neuroscienceassociates.com/Stains/silver_degen.htm). In addition, silver staining Kit from FD NeuroTechnologies was used where indicated (Ellicott City, MD). GFAP and CNPase immunohistochemistry was performed using mouse mAbs (Cell Singaling) and visualized using DAB Vector Labs Kit. Serum content of IL-1, IL-10, Integrin α/β, L- and E-selectins, Fractalkine, and Neuropilin-2 were measured using rat Quantibody array (Ray Biotech, GA USA). Also, sICAM and L-selectin were quantified independently using SW ELISA Kits. In addition, Neuropilin-2 and CNPase levels in serum and expression in brain was analyzed by Western blot with corresponding antibodies (Cell Signaling, Abcam) and bands were calculated using ImageJ software. Amounts of GFAP and UCH-L1 in serum were determined using SW ELISA Kits developed at Banyan Biomarkers, Inc., and NSE was assayed by rat-specific SW ELISA (Life Sciences Advanced Technologies, Saint Petersburg, FL).

Silver staining of neurodegeneration level in rat brain after different blast exposures. Rats were subjected to (i) 'composite' head-directed severe blast exposure (52 psi/10 msec total) on axis (body protected) accompanied by strong head movement; (ii) off-axis (30' degree) exposure to the blast of same shock tube settings resulted in 33.9 psi peak overpressure at the middle of frontal head **(Fig. 4 C)** lasted for 113 microseconds; and (iii) controlled cortical impact (CCI) of 2.0 mm depth.

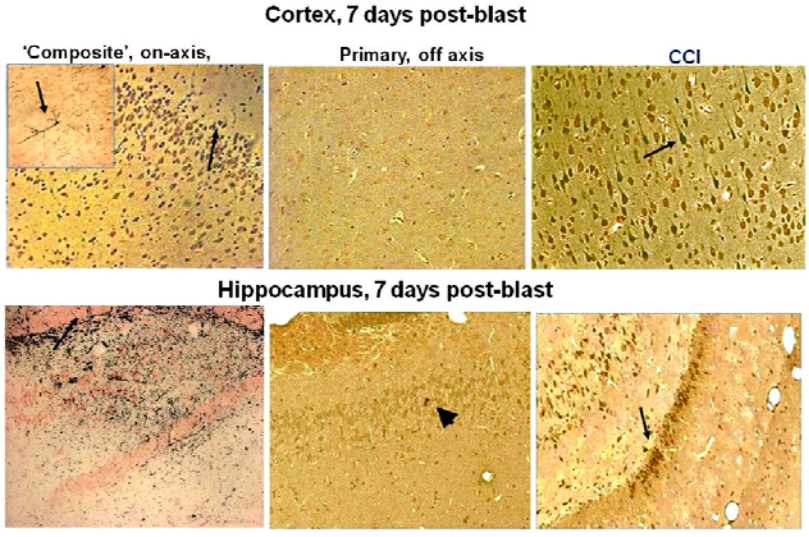

Fig. 5 Silver staining in coronal sections of midbrain (mesencephalon). Positive silver accumulation accumulation is indicated by arrows. Inset (cortex composite) shows degenerated neuron. Arrowhead in hippocampus after primary blast points on possible silver accumulation in the cell.

As can be seen in **Fig. 5,** on-axis blast produces significant silver accumulation at 7 day post-blast, particularly in hippocampus (indicated by arrows). CCI also results in positive staining in ipsilateral cortex and hippocampus. In contrast, there was a rare occurrence of silver accumulation observed in cortex or hippocampus after exposure to primary blast (arrowhead).

Serum levels of NSE and UCH-L1 as biomarkers of neuronal injury after different blast exposures. Rats were exposed to on-axis single composite blast of 52 psi, 10 msec total duration of positive phase + venting gas. Serum NSE **(Fig. 6A)** and UCH-L1 **(Fig. 6B)** were measured using SW ELISA Kits.

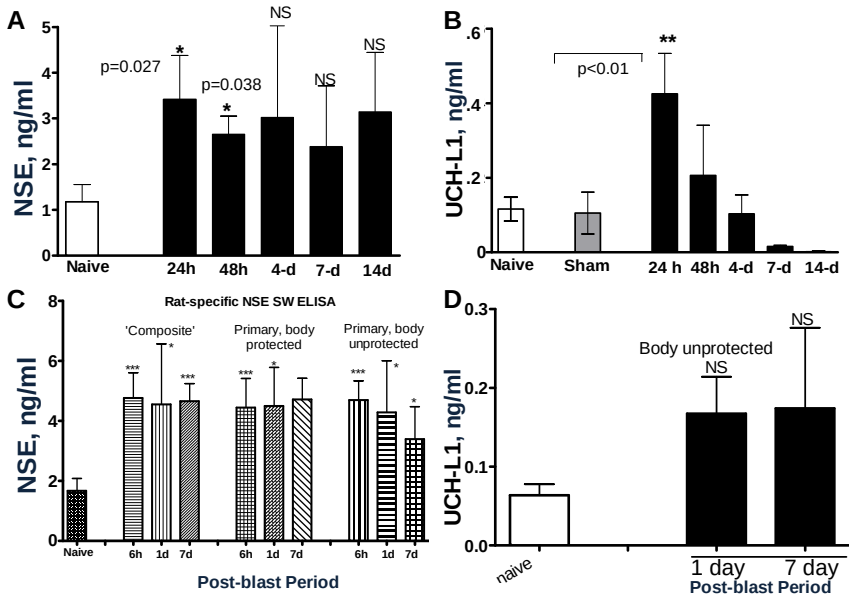

Fig. 6 NSE and UCH-L1 accumulation in blood after different types of blast exposure. A, B: serum NSE and UCH-L1 after on-axis 'Composite blast'; C, D: serum NSE and UCH-L1 after off-axis primary blast; Mean + SEM are shown of at least 3 rats per point from each group performed in duplicate. Unpaired t-test was employed to analyze statistical significance of values. *p<0.05, ** p<0.01; ***, p<0.005

The same settings of shock tube were used to challenge rats to off-axis primary blast (30^{o} degree from nozzle) with PO 33.9 psi, duration of 113 µsec registered at the head with body covered or unprotected as indicated.

NSE was significantly elevated in serum within first 24-48 hours after composite blast **(Fig. 6A)**, and the increase trend persisted up to 14 day although was not statistically significant (n=4 rats in each group). In this set of experiments, NSE SW ELISA Kit (Alpha Diagnostics), which was not specifically designed for rat NSE, was employed. In the subsequent sets of experiments **(Fig. 6C)**, we used NSE SW ELISA Kit from Life Sciences Advanced Technologies designed to detect specifically rat NSE. As can be seen in **Fig. 6A**, remarkable accumulation of NSE was detected in serum within 6 hours following exposure to either 'composite' or primary blast. NSE increase sustained up-to 14 days post-blast interval. Serum UCH-L1 elevated at 24 hours after 'composite' blast followed by a rapid decline **(Fig. 6B)**. Increases in serum UCH-L1 were not statistically significant after a single primary blast exposure (n=4), although an elevation trend could be detected **(Fig. 6B)**. Studies of NSE and UCH-L1 as serum biomarkers after multiple blast exposures of various magnitude are under way.

Serum levels of GFAP as marker of glyosis (astrocytes). GFAP was increased within 24 hours after composite blast and rapidly returned to baseline at 4-14 days **(Fig. 7A)**. While there was a significant increase of GFAP after primary blast at body protected and open (partially), the magnitude of increase was lower than after composite blast. In contrast, the GFAP increases lasted for 7 days following primary but not composite blast exposures **(Fig. 7 A, B)**.

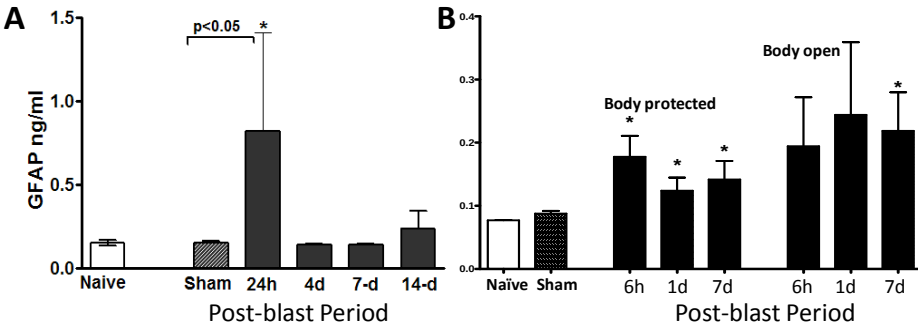

Fig. 7. GFAP levels in blood after different blast exposures. A: serum GFAP after on-axis 'Composite blast'; B: serum GFAP after off-axis primary blast; On axis: Unpaired t-test was employed to analyze statistical significance of values. (*-p<0.05; **-p<0.01). Off axis: t-test with Welch correction was done. (*-p<0.05), Mean + SEM of values from 3 to 5 rats per point is shown.

Cytokine/Chemokine responses after blast exposures. We hypothesized that systemic and neuroinflammmation together with impaired vascular reaction in the brain, result in enhancement of endothelial permeability/leakage, infiltration of macrophages from circulation and activation of brain-resident microglia cells:

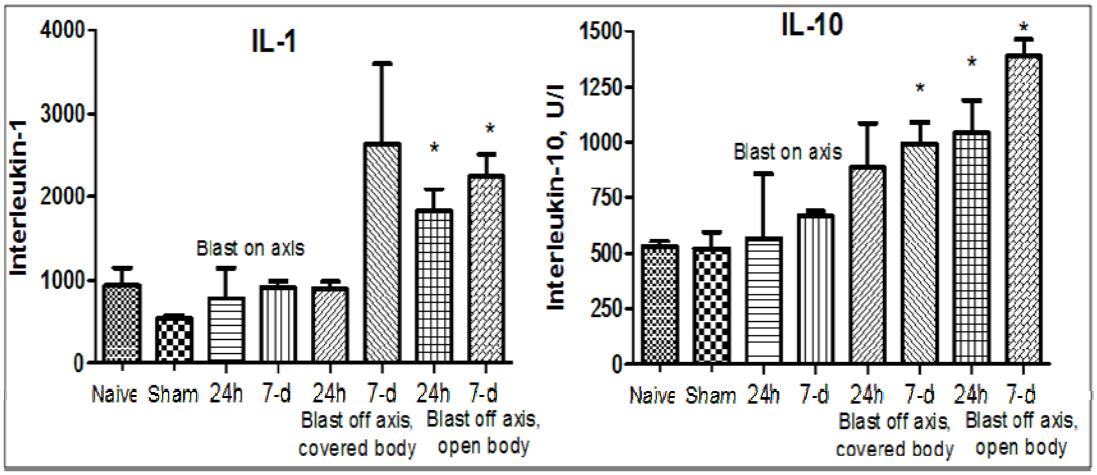

Fig. 8. Serum IL-1 and IL-10 at different times post-blast on- and off-axis. Note: the most prominent response occurs when OP wave 'flows inside the brain'- off axis frontal exposure with open body. *=p<0.05 vs. naïve/sham was considered as statistically significant according to unpaired t-test, NS-Not significant

As can be seen in **Fig. 8,** both pro-inflammatory (IL-1) and counteracting anti-inflammatory molecules (IL-10) accumulate in circulation at 24 hour after open body exposure to frontal (off-axis) blast.

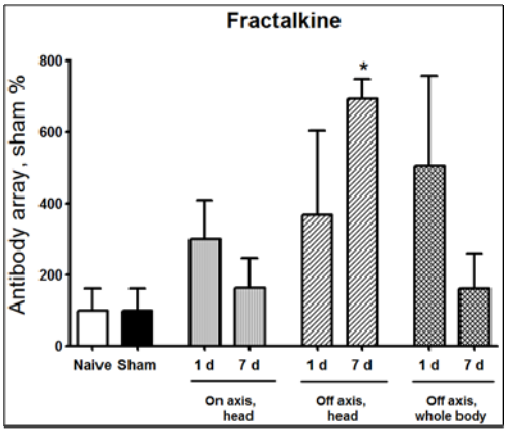

These results are in agreement with data obtained using non-blast TBI models (25). Moreover, CX3CL1 chemokine Fractalkine was also significantly elevated after different types of blast further suggesting systemic component in response to blast **(Fig. 9)** consistent with reports on the level of this chemokine in patients with TBI and in mouse model of closed head injury (26).

Fig. 9 . Levels of Fractalkine after different types of blast. *p<0.05, t-test, NS-not significant

Vascular responses and dysregulation of cell adhesion molecules. E-selectin and L-selectin as bridges connecting vascular-endothelial-neural tissue disturbances.

E-selectin and L-selectin are adhesion molecules which characterize the activation of vascular component of inflammation and interaction of circulatory cells with endothelial component of blood-brain-barrier (BBB) (27).

As can be seen in **Fig. 10**, the most prominent activation of vascular components of blast responses occurs when peak overpressure interacts with the frontal part of head without significant acceleration: "flowing blast insight the brain" (blast off-axis open body).

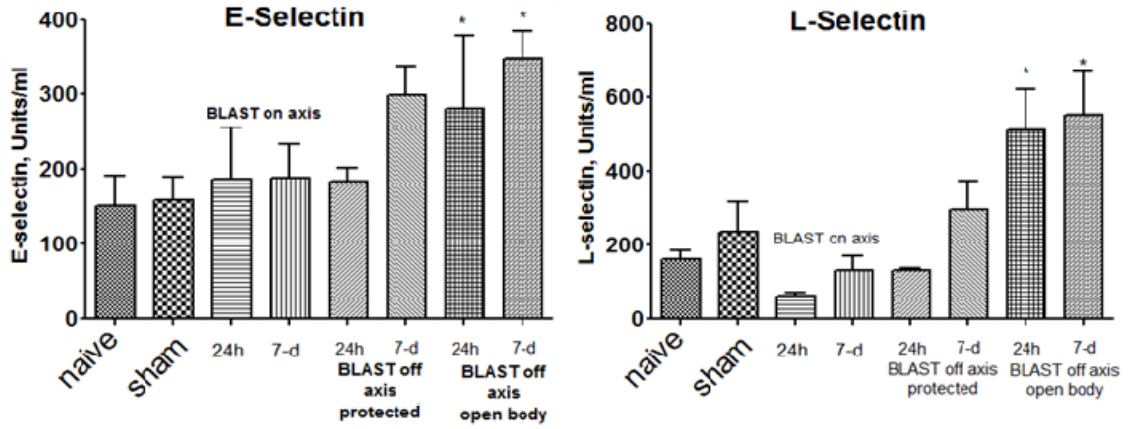

Fig. 10 Levels of L-selectin and E-selectin in serum after different types of blast exposure. Rats were subjected to off-axis head + total body blast: 33.9psi, 113 msec, 10.6 kPa-sec with body armored or uncovered. Blood was collected and cytokines were assayed in serum using RayBiotech L-arrays and expressed in arbitrary Units/ml. Data are Mean+SEM of 3 independent experiments (rats), each assay performed in triplicate. *=p<0.05 vs. sham (noise exposed rats) according unpaired t-test analysis. NS- Not significant.

Using targeted approach, we identified additional component of neurotrophic response to blast exposure. Serum levels of Nerve Growth Factor beta (beta-NGF) was assessed using SW ELISA and Neuropilin-2 (NRP-2) by antibody array (Ray Biotech) after blast exposure at different set-up. The results are presented in **Fig. 11A and B** below.

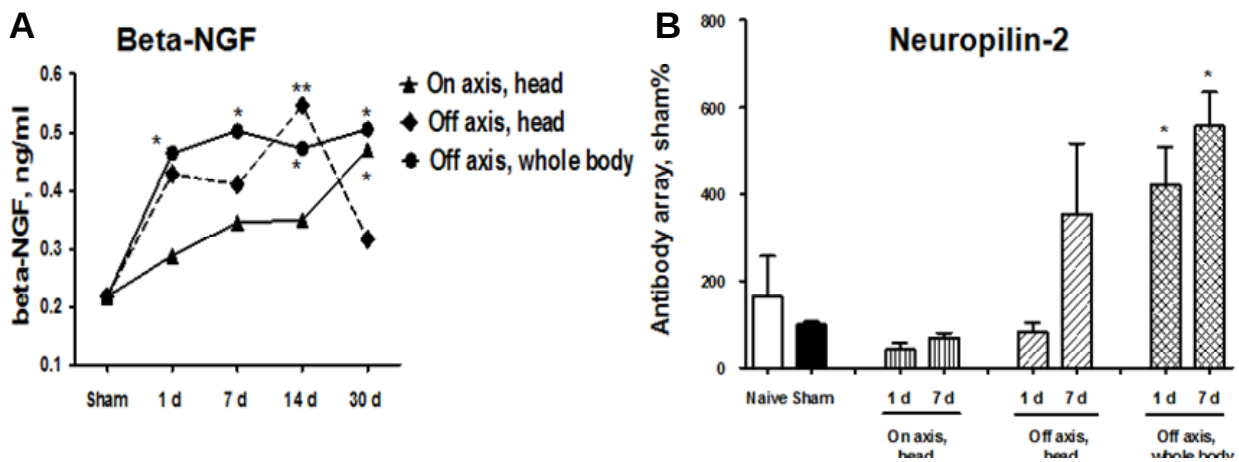

Fig. 11. Time-course of serum beta-NGF (A) and NRP-2 (B) following on-axis vs. off axis positions (primary blast overpressure only). Data point represents Mean values of 3 rat samples from each group and time points. *-p<0.05 and **-p<0.01 vs. sham group according to unpaired t-test with Welch correction.

Beta-NGF has been suggested to play a neurotrophic role in several neurodegenerative diseases (*39-41*). Our data indicate that NGF may also have neuroprotective functions and be involved in adaptive responses/neurorepair after blast induced TBI. As can be seen, exposure of whole body to primary overpressure blast instigated a rapid and sustained accumulation of beta-NGF in serum. Neuropilin-2 is receptor for VEGF and semaphorins, a large family of secreted and transmembrane signaling proteins that

regulate axonal guidance in the developing CNS (*42-44*). Our preliminary data **(Fig. 11B**) suggest that predominantly primary blast activates neuroregeneration and that NRP-2 may be involved in this process. Studies are under way to determine diagnostic and/or prognostic roles for NRP-2 in multiple low level blast as well as mechanisms of blast stimulation of neural injury/repair.

In summary, the most profound and persistent changes in serum levels of NSE/UCH-L1, GFAP were observed upon composite blast. However, prominent systemic and persistent glial up-regulation was observed after primary blast particularly when the total animal body was subjected to blast exposures. We suggest that the mechanisms underlying blast brain injuries, particularly mild and moderate, may be triggered by systemic, cerebrovascular and neuro-glia responses as consecutive but overlapping events. More in detail investigation is required to delineate primary blast injury from peak overpressure and distinguish from 'composite' blast. The pathophysiological signatures of mild/moderate blast, particularly cumulative effects of multiple exposures remain to be elucidated.

References.

1. Jones, E., Fear, N.T., and Wessely, S. 2007. Shell shock and mild traumatic brain injury: a historical review. *Am J Psychiatry* 164:1641-1645.
2. Terrio, H., Brenner, L.A., Ivins, B.J., Cho, J.M., Helmick, K., Schwab, K., Scally, K., Bretthauer, R., and Warden, D. 2009. Traumatic brain injury screening: preliminary findings in a US Army Brigade Combat Team. *J Head Trauma Rehabil* 24:14-23.
3. Warden, D. 2006. Military TBI during the Iraq and Afghanistan wars. *J Head Trauma Rehabil* 21:398-402.
4. Cernak, I., and Noble-Haeusslein, L.J. 2009. Traumatic brain injury: an overview of pathobiology with emphasis on military populations. *J Cereb Blood Flow Metab*.
5. Cernak, I., Savic, J., Ignjatovic, D., and Jevtic, M. 1999. Blast injury from explosive munitions. *J Trauma* 47:96-103; discussion 103-104.
6. Yilmaz, S., and Pekdemir, M. 2007. An unusual primary blast injury Traumatic brain injury due to primary blast injury. *Am J Emerg Med* 25:97-98.
7. Belanger, H.G., Scott, S.G., Scholten, J., Curtiss, G., and Vanderploeg, R.D. 2005. Utility of mechanism-of-injury-based assessment and treatment: Blast Injury Program case illustration. *J Rehabil Res Dev* 42:403-412.
8. Nelson, T.J., Wall, D.B., Stedje-Larsen, E.T., Clark, R.T., Chambers, L.W., and Bohman, H.R. 2006. Predictors of mortality in close proximity blast injuries during Operation Iraqi Freedom. *J Am Coll Surg* 202:418-422.
9. Wolf, S.J., Bebarta, V.S., Bonnett, C.J., Pons, P.T., and Cantrill, S.V. 2009. Blast injuries. *Lancet* 374:405-415.
10. Svetlov, S.I., Larner, S.F., Kirk, D.R., Atkinson, J., Hayes, R.L., and Wang, K.K. 2009. Biomarkers of blast-induced neurotrauma: profiling molecular and cellular mechanisms of blast brain injury. *J Neurotrauma* 26:913-921.
11. Svetlov, S.I., Prima, V., Kirk, D.R., Gutierrez, H., Curley, K.C., Hayes, R.L., and Wang, K.K.W. 2009. Morphologic and biochemical characterization of brain injury in a model of controlled blast overpressure exposure. *Journal of Trauma* 2010, 69(4) 795-804.

Neuro-glial and systemic mechanisms of pathological responses to primary blast overpressure (OP) compared to 'composite' blast accompanied by head acceleration in rats.

Stanislav I. Svetlov[1], Victor Prima[1], Daniel R. Kirk[2], Hector Gutierrez[2], Kenneth C. Curley[3], Ronald L Hayes[1], Kevin K.W. Wang[1]

[1]Center of Innovative Research, Banyan Biomarkers Inc., 12085 Research Drive, Alachua, FL 32615, USA

[2]Mechanical & Aerospace Engineering, Florida Institute of Technology, Melbourne FL 32901, USA

[3]U.S. Army Medical Research and Materiel Command, Fort Detrick, Frederick, MD, USA

ssvetlov@banyanbio.com

Energy distribution in modern technosphera, and particularly the 21st century warfare, has led to a significant increase of human exposure to blast overpressure (OP) impulses. Blast forces, even of low magnitude, are believed to produce minor but sustained neurological deficits, and when repeated, can lead to neuro-somatic damage and neurodegeneration. Most prominent changes may occur at the level of intercellular circuits that involve neurons, glia, vascular cells and neural progenitors.

Reproducible models of military-relevant blast injury, including generators which precisely control parameters of the blast wave have been developed and examined. Our studies demonstrated the importance of positional orientation of head and whole body toward blast wave in animal models. Here, we compare the effects of body/head exposure to a moderate primary overpressure (OP) with brain injury produced by a severe blast accompanied by strong head acceleration.

The high speed imaging demonstrated the interaction of blast wave with animal head/body and revealed a negligible degree of acceleration at rat positioning 'off-axis' toward shock tube (primary blast) compared to 'on-axis' experimental setup accompanied by strong head/cervical acceleration. We examined brain expression of glial and neural markers including GFAP and revealed strong glyosis accompanied by a time-dependent proliferation of activated astrocyte and oligodendrocyte lineages after exposures to primary and 'composite' blast. GFAP and neuronal markers UCH-L1 and NSE were also detectable in plasma/serum after blast exposures. Serum levels of IL-1 and IL-10 were significantly elevated, predominantly after primary blast exposure reflecting systemic body responses. Brain up-regulation of cell adhesion molecules L- and E-selectins, nerve growth factor beta-NGF and neuronal receptor Neuropilin-2 was also detected.

A specific dynamics of corresponding biomarkers in serum was established and characterized. For major pathway's signatures and biomarkers, the detected levels raised at all the setups studied. However, the most significant and persistent changes in neuro-glial markers were found after composite blast, while primary blast instigated prominent systemic/vascular reactions, particularly when the total animal body was subjected to blast wave.

In conclusion, several crucial pathogenic components of neural and systemic responses were raised in a time-dependent and setup-dependent fashion. We suggest that the mechanisms underlying blast brain injuries, particularly mild and moderate, may be triggered by systemic, cerebrovascular and neuro-glia responses as consecutive but overlapping events.

INTRODUCTION

Medical, Social and Military Importance. The nature of warfare in the 21st century has led to a significant increase in primary blast or over-pressurization component of body injury which manifests as a complex of neuro-somatic damage, including traumatic brain injury (TBI), and often accompanied by posttraumatic stress syndrome (PTSD). Blast-related coalition fatalities, including IED, RPG, and rocket attacks, outnumber conventional fatalities during the last several years in Iraq and Afghanistan (**Fig. 1,** http://www.icasualties.org/). Moreover, for every blast-related fatality, many more soldiers suffer multiple, non-lethal blast exposures. This often leads to mild traumatic brain injury (mTBI), which is rarely recognized in a timely manner and has become a signature injury of the Iraq and Afghanistan conflicts (1-3).

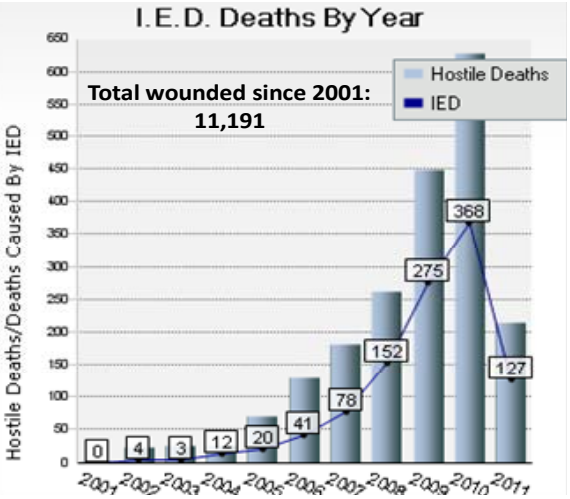

Fig. 1: Blast-related fatalities during OIF/OEF

Blast forces, particularly those that are repeated and low magnitude, are believed to produce minor but sustained disorders when neural damage cannot be detected or diagnosed by existing methods. Symptoms of mild or moderate blast brain injury often do not manifest themselves until sometime after the injury has occurred (4-6) and go undiagnosed and untreated because emergency medical attention is directed towards more visible injuries such as penetrating flesh wounds (7-9). However, even mild and moderate brain injuries can produce significant deficits and when repeated can lead to sustained neuro-somatic damage and neurodegeneration (4). Although exposure to repeated low level blasts is a common feature of war zones personnel/civilian population (OEF/OIF), the cumulative effect of multiple blasts on brain injury has not been investigated.

Data from our laboratories (10, 11) and others suggest that the mechanisms underlying such 'minor' injuries appear to be distinct from those imposed by mechanical impact or acceleration. Thus, identifying pathogenic mechanisms and biochemical markers of blast brain injury is vital to the development of diagnostics for mTBI through severe TBI. Validation of diagnostics and grading brain injury depending on the cumulative blast load will provide a dose-injury scale for personnel monitoring on the battlefield using portable blast "dosimeter" and/or a point of care diagnostic device.

Methodology and Results

Experimental Models for Studies of Blast Injury. Exposures to blast waves have the potential to inflict multi-system, including neurotrauma, as well as life threatening injuries to many personnel simultaneously (see (4) for review). It is generally accepted that primary blast injuries are generated as the over-pressurization wave propagates through the body causing damage at gas-fluid interfaces (12). The types of injuries inflicted include pulmonary barotraumas, tympanic membrane ruptures and middle ear damage, abdominal hemorrhage and perforation, rupture of the eye balls, and concussions (13).

A number of investigations have employed compressed air-driven shock tubes and nitrogen-driven blast wave generators for blast exposures of various animals (e.g. rats, mice, rabbits) to address mechanisms of injury (14-20). Small animals are placed in orthopedic stockinet slings, and large animals in open mesh Nylon TM slings, and subjected to blast exposure at varying distances and body orientations with or without a supportive/reflective plate behind the animal.

Our shock tube was designed and built to model a freely expanding blast wave as generated by a typical explosion **(see 11 for details)**. Blast injury modeling framework is shown in **Fig. 2.** Modular design allows for the flexibility to perform various types of tests: design is lightweight while maintaining necessary strength and stiffness. Data were acquired with PCB dynamic blast pressure transducers and LabView 8.2. Images were captured at 30 fps (frames per second) resolution. National Instruments 500,000 samples/sec data acquisition card were used to acquire data on multiple channels. Following the diaphragm rupture, the driver gas sets up a series of pressure waves in the low pressure driven section that coalesces to form the incident shockwave. In our shock tube, the burst pressure of the diaphragm separating the driver and driven sections do not change. Repeatability of diaphragm burst pressure was accomplished through the use of a cutter assembly directly in front of the diaphragm. Preliminary tests were conducted without animal specimens to optimize the peak overpressure (OP) and exposure time to accurately reproduce blast events: driver pressure and volume, diaphragm material, and shock tube exit geometry. Both static and dynamic (total) pressure was measured using piezoelectric blast pressure sensors/transducers positioned at the target. The shockwave recorded by blast pressure transducers in the driven section and at the target showed three distinct events: (i) peak overpressure, (ii) gas venting jet and (iii) negative pressure phase. Peak overpressure, positive phase duration, and impulse are the key parameters that correlate with injury and likelihood of fatality in animals and humans, for various orientations of the specimen relative to the blast wave (15, 16, 21-24). After the pressure history is recorded and the sensors removed, the animal can be carefully positioned at the same location and the test repeated, since it has been previously demonstrated that the proposed shock tube design has excellent repeatability characteristics.

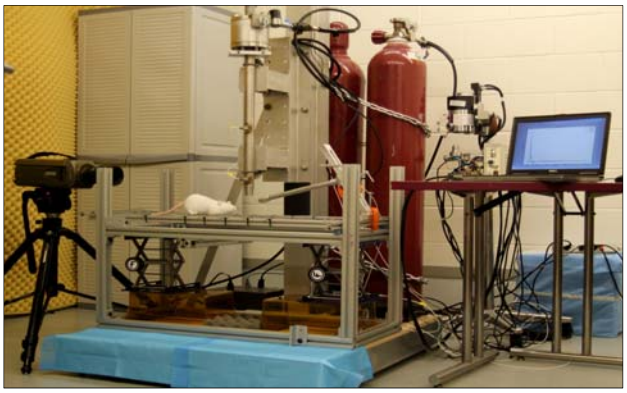

Fig.2 Overview of shock tube and experimental blast model facility at Banyan Biomarkers, Inc.

However, because of inconsistent designs among blast generators used in the different studies, the data on brain injury mechanisms and putative biomarkers have been difficult to analyze and compare. The main problem is that following blast peak overpressure, shock tubes immediately produce 'venting gas jet', substantially contaminating the blast wave **(Fig. 3).** Due to the complex nature of the blast event, the brain injury is a result of a combined impact of the "composite" blast including all 3 major phases of a shockwave shown in **Fig. 3 A and B**. Gas venting jet, albeit lower in magnitude than peak overpressure, lasts the longest, and represents the bulk of blast impulse and possibly produces the most devastating impact. We demonstrated previously a strong downward head acceleration following the passage of peak overpressure which lasts ~36 µsec (11). However, cranial deformation was more severe during the gas venting phase, lasting up to ~5-6 msec (Fig. 3A). These findings points to a potential flaw in several previous studies

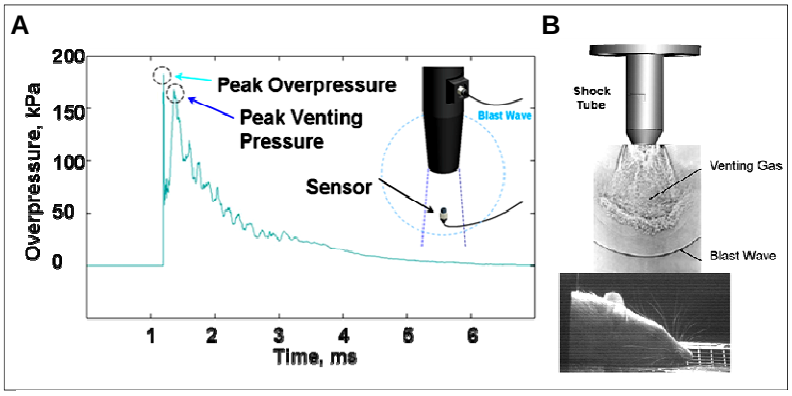

Fig. 3 Components of shock tube-generated shock wave. A: Peak overpressure and venting gas measured by PCB dynamic pressure sensors, and B: Rat head positioning relative to shock tube and visualization of shock wave using Schlieren optics

Serum levels of NSE and UCH-L1 as biomarkers of neuronal injury after different blast exposures. Rats were exposed to on-axis single composite blast of 52 psi, 10 msec total duration of positive phase + venting gas. Serum NSE **(Fig. 6A)** and UCH-L1 **(Fig. 6B)** were measured using SW ELISA Kits.

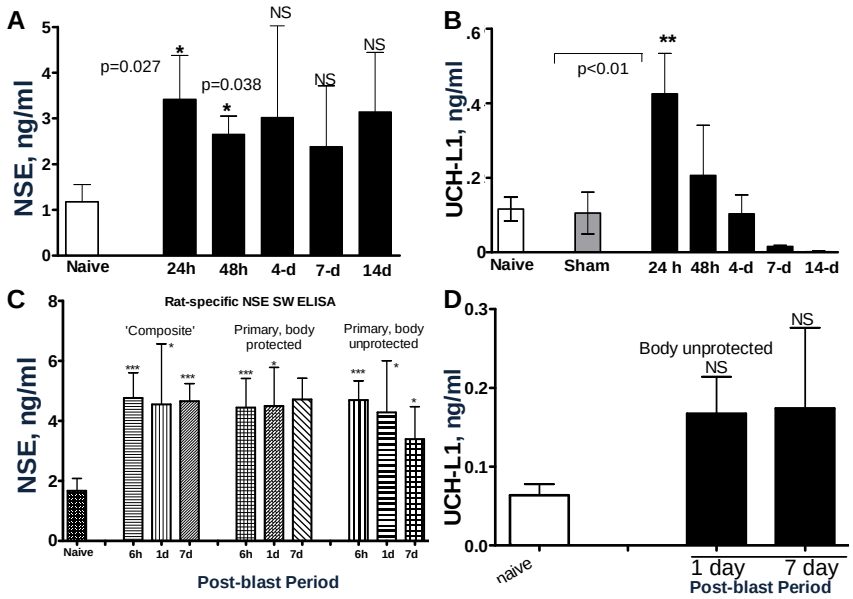

Fig. 6 NSE and UCH-L1 accumulation in blood after different types of blast exposure. A, B: serum NSE and UCH-L1 after on-axis 'Composite blast'; C, D: serum NSE and UCH-L1 after off-axis primary blast; Mean + SEM are shown of at least 3 rats per point from each group performed in duplicate. Unpaired t-test was employed to analyze statistical significance of values. *p<0.05, ** p<0.01; ***, p<0.005

The same settings of shock tube were used to challenge rats to off-axis primary blast (30^{o} degree from nozzle) with PO 33.9 psi, duration of 113 µsec registered at the head with body covered or unprotected as indicated.

NSE was significantly elevated in serum within first 24-48 hours after composite blast **(Fig. 6A)**, and the increase trend persisted up to 14 day although was not statistically significant (n=4 rats in each group). In this set of experiments, NSE SW ELISA Kit (Alpha Diagnostics), which was not specifically designed for rat NSE, was employed. In the subsequent sets of experiments **(Fig. 6C)**, we used NSE SW ELISA Kit from Life Sciences Advanced Technologies designed to detect specifically rat NSE. As can be seen in **Fig. 6A**, remarkable accumulation of NSE was detected in serum within 6 hours following exposure to either 'composite' or primary blast. NSE increase sustained up-to 14 days post-blast interval. Serum UCH-L1 elevated at 24 hours after 'composite' blast followed by a rapid decline **(Fig. 6B)**. Increases in serum UCH-L1 were not statistically significant after a single primary blast exposure (n=4), although an elevation trend could be detected **(Fig. 6B)**. Studies of NSE and UCH-L1 as serum biomarkers after multiple blast exposures of various magnitude are under way.

Serum levels of GFAP as marker of glyosis (astrocytes). GFAP was increased within 24 hours after composite blast and rapidly returned to baseline at 4-14 days **(Fig. 7A)**. While there was a significant increase of GFAP after primary blast at body protected and open (partially), the magnitude of increase was lower than after composite blast. In contrast, the GFAP increases lasted for 7 days following primary but not composite blast exposures **(Fig. 7 A, B)**.

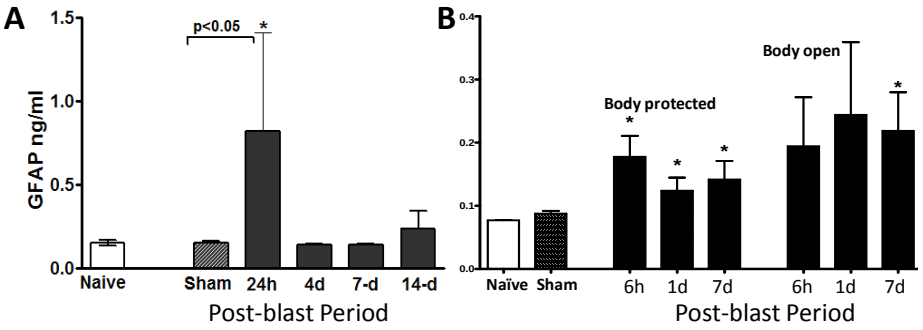

Fig. 7. GFAP levels in blood after different blast exposures. A: serum GFAP after on-axis 'Composite blast'; B: serum GFAP after off-axis primary blast; On axis: Unpaired t-test was employed to analyze statistical significance of values. (*-p<0.05; **-p<0.01). Off axis: t-test with Welch correction was done. (*-p<0.05), Mean + SEM of values from 3 to 5 rats per point is shown.

Cytokine/Chemokine responses after blast exposures. We hypothesized that systemic and neuroinflammmation together with impaired vascular reaction in the brain, result in enhancement of endothelial permeability/leakage, infiltration of macrophages from circulation and activation of brain-resident microglia cells:

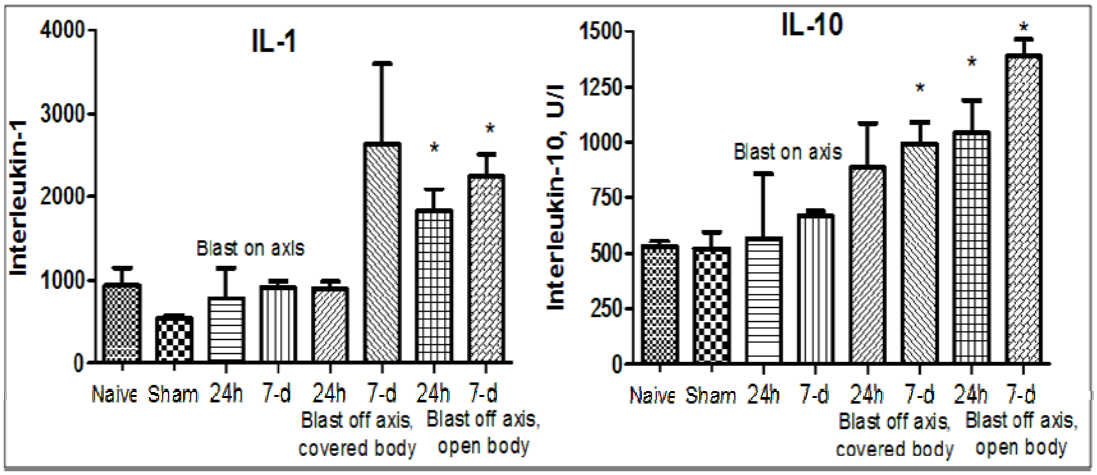

Fig. 8. Serum IL-1 and IL-10 at different times post-blast on- and off-axis. Note: the most prominent response occurs when OP wave 'flows inside the brain'- off axis frontal exposure with open body. *=p<0.05 vs. naïve/sham was considered as statistically significant according to unpaired t-test, NS-Not significant

As can be seen in **Fig. 8,** both pro-inflammatory (IL-1) and counteracting anti-inflammatory molecules (IL-10) accumulate in circulation at 24 hour after open body exposure to frontal (off-axis) blast.

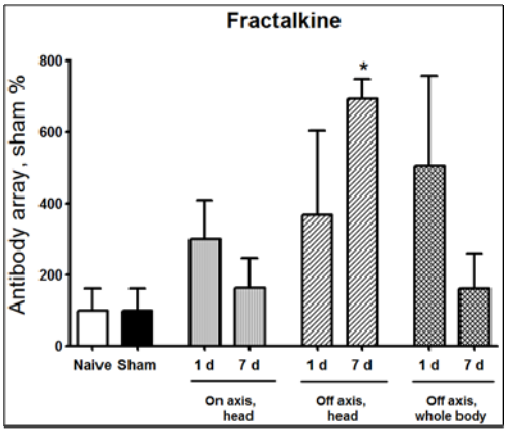

These results are in agreement with data obtained using non-blast TBI models (25). Moreover, CX3CL1 chemokine Fractalkine was also significantly elevated after different types of blast further suggesting systemic component in response to blast **(Fig. 9)** consistent with reports on the level of this chemokine in patients with TBI and in mouse model of closed head injury (26).

Fig. 9 . Levels of Fractalkine after different types of blast. *p<0.05, t-test, NS-not significant

Vascular responses and dysregulation of cell adhesion molecules. E-selectin and L-selectin as bridges connecting vascular-endothelial-neural tissue disturbances.

E-selectin and L-selectin are adhesion molecules which characterize the activation of vascular component of inflammation and interaction of circulatory cells with endothelial component of blood-brain-barrier (BBB) (27).

As can be seen in **Fig. 10**, the most prominent activation of vascular components of blast responses occurs when peak overpressure interacts with the frontal part of head without significant acceleration: "flowing blast insight the brain" (blast off-axis open body).

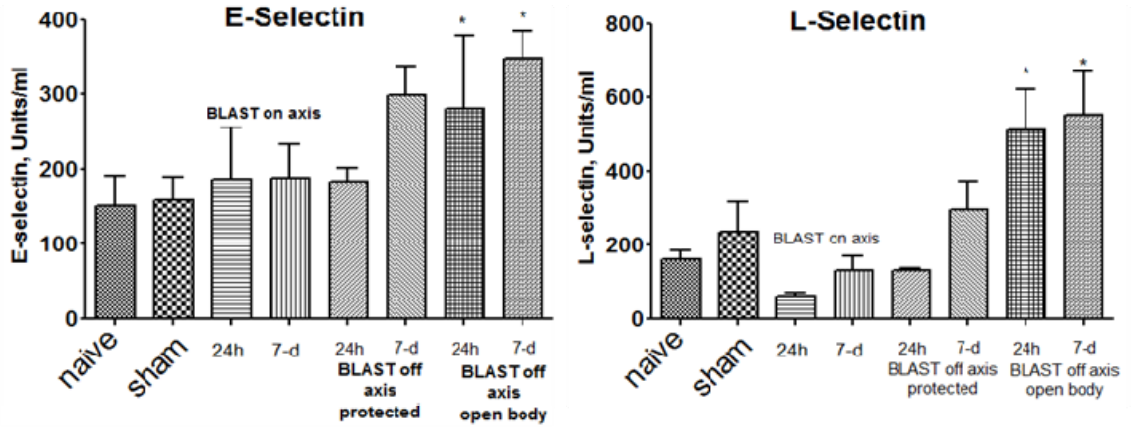

Fig. 10 Levels of L-selectin and E-selectin in serum after different types of blast exposure. Rats were subjected to off-axis head + total body blast: 33.9psi, 113 msec, 10.6 kPa-sec with body armored or uncovered. Blood was collected and cytokines were assayed in serum using RayBiotech L-arrays and expressed in arbitrary Units/ml. Data are Mean+SEM of 3 independent experiments (rats), each assay performed in triplicate. *=p<0.05 vs. sham (noise exposed rats) according unpaired t-test analysis. NS- Not significant.

Using targeted approach, we identified additional component of neurotrophic response to blast exposure. Serum levels of Nerve Growth Factor beta (beta-NGF) was assessed using SW ELISA and Neuropilin-2 (NRP-2) by antibody array (Ray Biotech) after blast exposure at different set-up. The results are presented in **Fig. 11A and B** below.

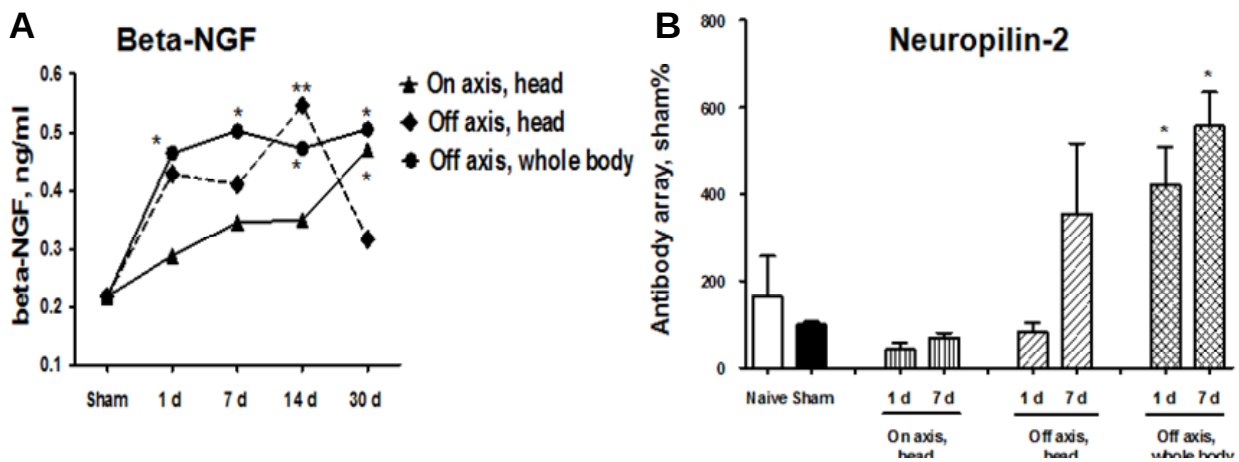

Fig. 11. Time-course of serum beta-NGF (A) and NRP-2 (B) following on-axis vs. off axis positions (primary blast overpressure only). Data point represents Mean values of 3 rat samples from each group and time points. *-p<0.05 and **-p<0.01 vs. sham group according to unpaired t-test with Welch correction.

Beta-NGF has been suggested to play a neurotrophic role in several neurodegenerative diseases (*39-41*). Our data indicate that NGF may also have neuroprotective functions and be involved in adaptive responses/neurorepair after blast induced TBI. As can be seen, exposure of whole body to primary overpressure blast instigated a rapid and sustained accumulation of beta-NGF in serum. Neuropilin-2 is receptor for VEGF and semaphorins, a large family of secreted and transmembrane signaling proteins that

regulate axonal guidance in the developing CNS (*42-44*). Our preliminary data **(Fig. 11B**) suggest that predominantly primary blast activates neuroregeneration and that NRP-2 may be involved in this process. Studies are under way to determine diagnostic and/or prognostic roles for NRP-2 in multiple low level blast as well as mechanisms of blast stimulation of neural injury/repair.

In summary, the most profound and persistent changes in serum levels of NSE/UCH-L1, GFAP were observed upon composite blast. However, prominent systemic and persistent glial up-regulation was observed after primary blast particularly when the total animal body was subjected to blast exposures. We suggest that the mechanisms underlying blast brain injuries, particularly mild and moderate, may be triggered by systemic, cerebrovascular and neuro-glia responses as consecutive but overlapping events. More in detail investigation is required to delineate primary blast injury from peak overpressure and distinguish from 'composite' blast. The pathophysiological signatures of mild/moderate blast, particularly cumulative effects of multiple exposures remain to be elucidated.

References.

1. Jones, E., Fear, N.T., and Wessely, S. 2007. Shell shock and mild traumatic brain injury: a historical review. *Am J Psychiatry* 164:1641-1645.
2. Terrio, H., Brenner, L.A., Ivins, B.J., Cho, J.M., Helmick, K., Schwab, K., Scally, K., Bretthauer, R., and Warden, D. 2009. Traumatic brain injury screening: preliminary findings in a US Army Brigade Combat Team. *J Head Trauma Rehabil* 24:14-23.
3. Warden, D. 2006. Military TBI during the Iraq and Afghanistan wars. *J Head Trauma Rehabil* 21:398-402.
4. Cernak, I., and Noble-Haeusslein, L.J. 2009. Traumatic brain injury: an overview of pathobiology with emphasis on military populations. *J Cereb Blood Flow Metab*.
5. Cernak, I., Savic, J., Ignjatovic, D., and Jevtic, M. 1999. Blast injury from explosive munitions. *J Trauma* 47:96-103; discussion 103-104.
6. Yilmaz, S., and Pekdemir, M. 2007. An unusual primary blast injury Traumatic brain injury due to primary blast injury. *Am J Emerg Med* 25:97-98.
7. Belanger, H.G., Scott, S.G., Scholten, J., Curtiss, G., and Vanderploeg, R.D. 2005. Utility of mechanism-of-injury-based assessment and treatment: Blast Injury Program case illustration. *J Rehabil Res Dev* 42:403-412.
8. Nelson, T.J., Wall, D.B., Stedje-Larsen, E.T., Clark, R.T., Chambers, L.W., and Bohman, H.R. 2006. Predictors of mortality in close proximity blast injuries during Operation Iraqi Freedom. *J Am Coll Surg* 202:418-422.
9. Wolf, S.J., Bebarta, V.S., Bonnett, C.J., Pons, P.T., and Cantrill, S.V. 2009. Blast injuries. *Lancet* 374:405-415.
10. Svetlov, S.I., Larner, S.F., Kirk, D.R., Atkinson, J., Hayes, R.L., and Wang, K.K. 2009. Biomarkers of blast-induced neurotrauma: profiling molecular and cellular mechanisms of blast brain injury. *J Neurotrauma* 26:913-921.
11. Svetlov, S.I., Prima, V., Kirk, D.R., Gutierrez, H., Curley, K.C., Hayes, R.L., and Wang, K.K.W. 2009. Morphologic and biochemical characterization of brain injury in a model of controlled blast overpressure exposure. *Journal of Trauma* 2010, 69(4) 795-804.

12. Born, C.T. 2005. Blast trauma: the fourth weapon of mass destruction. *Scand J Surg* 94:279-285.

13. Wightman, J.M., and Gladish, S.L. 2001. Explosions and blast injuries. *Ann Emerg Med* 37:664-678.

14. Guy, R.J., Glover, M.A., and Cripps, N.P. 1998. The pathophysiology of primary blast injury and its implications for treatment. Part I: The thorax. *J R Nav Med Serv* 84:79-86.

15. Jaffin, J.H., McKinney, L., Kinney, R.C., Cunningham, J.A., Moritz, D.M., Kraimer, J.M., Graeber, G.M., Moe, J.B., Salander, J.M., and Harmon, J.W. 1987. A laboratory model for studying blast overpressure injury. *J Trauma* 27:349-356.

16. Stuhmiller, J.H. 1997. Biological response to blast overpressure: a summary of modeling. *Toxicology* 121:91-103.

17. Stuhmiller, J.H., Ho, K.H., Vander Vorst, M.J., Dodd, K.T., Fitzpatrick, T., and Mayorga, M. 1996. A model of blast overpressure injury to the lung. *J Biomech* 29:227-234.

18. Cernak, I., Wang, Z., Jiang, J., Bian, X., and Savic, J. 2001. Cognitive deficits following blast injury-induced neurotrauma: possible involvement of nitric oxide. *Brain Inj* 15:593-612.

19. Chavko, M., Koller, W.A., Prusaczyk, W.K., and McCarron, R.M. 2007. Measurement of blast wave by a miniature fiber optic pressure transducer in the rat brain. *J Neurosci Methods* 159:277-281.

20. Chavko, M., Prusaczyk, W.K., and McCarron, R.M. 2006. Lung injury and recovery after exposure to blast overpressure. *J Trauma* 61:933-942.

21. Cooper, G.J., and Taylor, D.E. 1989. Biophysics of impact injury to the chest and abdomen. *J R Army Med Corps* 135:58-67.

22. Cooper, P.W. 1996. *Explosives Engineering*: Wiley-VCH.

23. Elsayed, N.M. 1997. Toxicology of blast overpressure. *Toxicology* 121:1-15.

24. Elsayed, N.M., and Gorbunov, N.V. 2007. Pulmonary biochemical and histological alterations after repeated low-level blast overpressure exposures. *Toxicol Sci* 95:289-296.

25. W. D. Dietrich, K. Chatzipanteli, E. Vitarbo, K. Wada, K. Kinoshita, The role of inflammatory processes in the pathophysiology and treatment of brain and spinal cord trauma. Acta Neurochir Suppl 89, 69 (2004).

26. H. Ralay Ranaivo, S. Zunich, N. Choi, J. Hodge, M. Wainwright, Mild stretch-induced injury increases susceptibility to interleukin-1β-induced release of matrix metalloproteinase-9 from astrocytes. J Neurotrauma, 2011 (Jul 6) Epub ahead of print .

27. M. J. Whalen et al., Reduced brain edema after traumatic brain injury in mice deficient in P-selectin and intercellular adhesion molecule-1 J Leukoc Biol 67, 160 (Feb, 2000).

28. P. Calissano, C. Matrone, G. Amadoro, Nerve growth factor as a paradigm of neurotrophins related to Alzheimer's disease. Dev Neurobiol 70, 372 (Apr, 2010).

29. P. Bannerman et al., Peripheral nerve regeneration is delayed in neuropilin 2-deficient mice. J Neurosci Res 86, 3163 (Nov 1, 2008).

30. J. Roffers-Agarwal, L. S. Gammill, Neuropilin receptors guide distinct phases of sensory and motor neuronal segmentation. Development 136, 1879 (Jun, 2009).

12. Born, C.T. 2005. Blast trauma: the fourth weapon of mass destruction. *Scand J Surg* 94:279-285.

13. Wightman, J.M., and Gladish, S.L. 2001. Explosions and blast injuries. *Ann Emerg Med* 37:664-678.

14. Guy, R.J., Glover, M.A., and Cripps, N.P. 1998. The pathophysiology of primary blast injury and its implications for treatment. Part I: The thorax. *J R Nav Med Serv* 84:79-86.

15. Jaffin, J.H., McKinney, L., Kinney, R.C., Cunningham, J.A., Moritz, D.M., Kraimer, J.M., Graeber, G.M., Moe, J.B., Salander, J.M., and Harmon, J.W. 1987. A laboratory model for studying blast overpressure injury. *J Trauma* 27:349-356.

16. Stuhmiller, J.H. 1997. Biological response to blast overpressure: a summary of modeling. *Toxicology* 121:91-103.

17. Stuhmiller, J.H., Ho, K.H., Vander Vorst, M.J., Dodd, K.T., Fitzpatrick, T., and Mayorga, M. 1996. A model of blast overpressure injury to the lung. *J Biomech* 29:227-234.

18. Cernak, I., Wang, Z., Jiang, J., Bian, X., and Savic, J. 2001. Cognitive deficits following blast injury-induced neurotrauma: possible involvement of nitric oxide. *Brain Inj* 15:593-612.

19. Chavko, M., Koller, W.A., Prusaczyk, W.K., and McCarron, R.M. 2007. Measurement of blast wave by a miniature fiber optic pressure transducer in the rat brain. *J Neurosci Methods* 159:277-281.

20. Chavko, M., Prusaczyk, W.K., and McCarron, R.M. 2006. Lung injury and recovery after exposure to blast overpressure. *J Trauma* 61:933-942.

21. Cooper, G.J., and Taylor, D.E. 1989. Biophysics of impact injury to the chest and abdomen. *J R Army Med Corps* 135:58-67.

22. Cooper, P.W. 1996. *Explosives Engineering*: Wiley-VCH.

23. Elsayed, N.M. 1997. Toxicology of blast overpressure. *Toxicology* 121:1-15.

24. Elsayed, N.M., and Gorbunov, N.V. 2007. Pulmonary biochemical and histological alterations after repeated low-level blast overpressure exposures. *Toxicol Sci* 95:289-296.

25. W. D. Dietrich, K. Chatzipanteli, E. Vitarbo, K. Wada, K. Kinoshita, The role of inflammatory processes in the pathophysiology and treatment of brain and spinal cord trauma. Acta Neurochir Suppl 89, 69 (2004).

26. H. Ralay Ranaivo, S. Zunich, N. Choi, J. Hodge, M. Wainwright, Mild stretch-induced injury increases susceptibility to interleukin-1β-induced release of matrix metalloproteinase-9 from astrocytes. J Neurotrauma, 2011 (Jul 6) Epub ahead of print .

27. M. J. Whalen et al., Reduced brain edema after traumatic brain injury in mice deficient in P-selectin and intercellular adhesion molecule-1 J Leukoc Biol 67, 160 (Feb, 2000).

28. P. Calissano, C. Matrone, G. Amadoro, Nerve growth factor as a paradigm of neurotrophins related to Alzheimer's disease. Dev Neurobiol 70, 372 (Apr, 2010).

29. P. Bannerman et al., Peripheral nerve regeneration is delayed in neuropilin 2-deficient mice. J Neurosci Res 86, 3163 (Nov 1, 2008).

30. J. Roffers-Agarwal, L. S. Gammill, Neuropilin receptors guide distinct phases of sensory and motor neuronal segmentation. Development 136, 1879 (Jun, 2009).

Morphologic and Biochemical Characterization of Brain Injury in a Model of Controlled Blast Overpressure Exposure

Stanislav I. Svetlov, MD, PhD, Victor Prima, PhD, Daniel R. Kirk, PhD, Hector Gutierrez, PhD, Kenneth C. Curley, MD, Ronald L. Hayes, PhD, and Kevin K. W. Wang, PhD

Objectives: Existing experimental approaches for studies of blast impact in small animals are insufficient and lacking consistency. Here, we present a comprehensive model, with repeatable blast signatures of controlled duration, peak pressure, and transmitted impulse, accurately reproducing blast impact in laboratory animals.

Materials: Rat survival, brain pathomorphology, and levels of putative biomarkers of brain injury glial fibrillary acid protein (GFAP), neuron-specific enolase, and ubiquitin C-terminal hydrolase (UCH)-L1 were examined in brain, cerebrospinal fluid (CSF), and blood after 10 msec of 358 kPa peak overpressure blast exposure.

Results: The high-speed imaging demonstrated a strong head acceleration/jolting accompanied by typical intracranial hematomas and brain swelling. Microscopic injury was revealed by prominent silver staining in deep brain areas, including the nucleus subthalamicus zone, suggesting both diffused and focal neurodegeneration. GFAP and 2′,3′-cyclic nucleotide 3′-phosphodiesterase (CNPase), markers of astroglia and oligodendroglia, accumulated substantially in the hippocampus 24 hours after blast and persisted for 30 days postblast. However, GFAP content in the blood significantly increased 24 hours after injury, followed by a decline and subsequent accumulation in CSF in a time-dependent fashion. A similar profile is shown for UCH-L1 increase in blood, whereas increased CSF levels of UCH-L1 persisted throughout 14 days after blast and varied significantly in individual rats. Neuron-specific enolase levels in blood were significantly elevated within 24 hours and 48 hours postblast.

Conclusions: The proposed model of controlled nonpenetrating blast in rats demonstrates the critical pathologic and biochemical signatures of blast brain injury that may be triggered by cerebrovascular responses, including blood-brain barrier disruption, glia responses, and neuroglial alterations.

Key Words: Blast, Brain injury, Experimental models, Biomarkers, UCH-L1, GFAP, CNPase.

(*J Trauma.* 2010;69: 795–804)

Submitted for publication May 8, 2009.
Accepted for publication July 23, 2009.

From the Center of Innovative Research (S.I.S., V.P., R.L.H., K.K.W.W.), Banyan Biomarkers, Inc, Alachua, Florida; Department of Mechanical and Aerospace Engineering (D.R.K., H.G.), Florida Institute of Technology, Melbourne, Florida; Departments of Physiological Sciences (S.I.S.) and Psychiatry (K.K.W.W.), University of Florida, Gainesville, Florida; and U.S. Army Medical Research and Materiel Command (MRMC) (K.C.C.), Fort Detrick, Frederick, Maryland.
Supported by Department of Defense grants N14-06-1-1029, W81XWH-8-1-0376, and W81XWH-07-01-0701.
The views expressed herein are those of the authors and do not reflect the official policy or position of the Department of the Army, Department of Defense, or the U.S. government.
Address for reprints: Stanislav I. Svetlov, MD, PhD, Center of Innovative Research, Banyan Biomarkers, Inc, 12085 Research Drive, Alachua, FL 32615; email: ssvetlov@banyanbio.com.

DOI: 10.1097/TA.0b013e3181bbd885

Several decades of medical literature, and particularly recent military operations, provide a number of cases in which brain injuries are likely to have resulted from primary blast forces.[1,2] Thus, identifying pathogenic pathways of primary blast brain injury (BBI) in reproducible experimental models is vital to the development of diagnostic algorithms for mild traumatic brain injury (TBI) through severe TBI, and eventually differentiating mild TBI from posttraumatic stress disorder. A number of experimental animal models, which include rodents and larger animals such as sheep, have been implemented to study the mechanisms of blast wave impacts.[3,4] However, because of inconsistent designs among blast generators used in the different studies, the data on brain injury mechanisms and putative biomarkers have been difficult to analyze and compare.[5–9]

Although there are currently no biomarkers with proven clinical utility for the diagnostics of TBI, whether caused by blast, mechanical trauma, stroke, or other acute brain injuries, research has uncovered several valuable candidates that have shown preclinical and clinical potential.[10] The ones currently generating the most interest include neuron-specific enolase (NSE), glial fibrillary acid protein (GFAP), S-100ß, and myelin basic protein. Although these proteins are still being assessed, they appear to lack either the necessary sensitivity or the brain specificity (except perhaps GFAP) to be used effectively alone.[11,12] However, the combination of these markers can effectively detect conventional TBI and provide outcome predictions.[13,14]

For studies of mechanisms and biomarkers of BBI, we developed and used a model of "composite" blast exposure with controlled parameters of blast wave exposure and brain injury in rats. In this article, we demonstrate that brain damage induced by severe head-directed blast waves is accompanied by time-dependent intracranial hemorrhages and neurodegeneration in deep areas of the brain. This was accompanied by the accumulation of GFAP, NSE, and ubiquitin C-terminal hydrolase (UCH)-L1 in blood and cerebrospinal fluid (CSF) with a characteristic time course suggestive of a rapid blood-brain barrier disruption following blast exposure.

MATERIALS AND METHODS

Shock Tube Design, Construction, and Setup

A compressed air-driven shock tube was used to expose rats to a supra-atmospheric wave of air pressure. A shock tube capable of generating a wide range of controlled blast

waves without the use of explosives was designed, constructed, and tested at both the Florida Institute of Technology and Banyan Biomarkers, Inc. (Fig. 1, A). The tube is separated into two sections, high pressure (driver) and low pressure (driven), separated by a metal diaphragm. The thickness, type of material, driver/driven ratio, and initial driver pressure determine the peak and duration of the overpressure (OP) event. In the presented series of experiments, 0.05-mm thick stainless steel diaphragms were used to generate high-pressure shock waves. The ratio of driver versus driven section lengths was 15 to 1. The driver section was initialized to a pressure of 5,170 kPa and the driven section was left at ambient pressure. The diaphragm rupture initiated by an internal cutter leads to the sudden exposure of a low-pressure air to gas at significantly higher pressure, resulting in the formation of a shock wave. The blast pressure data were acquired using piezoelectric blast pressure transducers and LabView 8.2 software. A National Instruments 1.25 Msamples/sec data acquisition card was used to acquire data from multiple channels. The shock tube was calibrated, so that the peak OP indicated the actual measures (kPa) at the surface of the rat's skull. Images of the rat head during the blast event were captured at 1,000 frames/sec using a high-speed video camera and Schlieren optics.

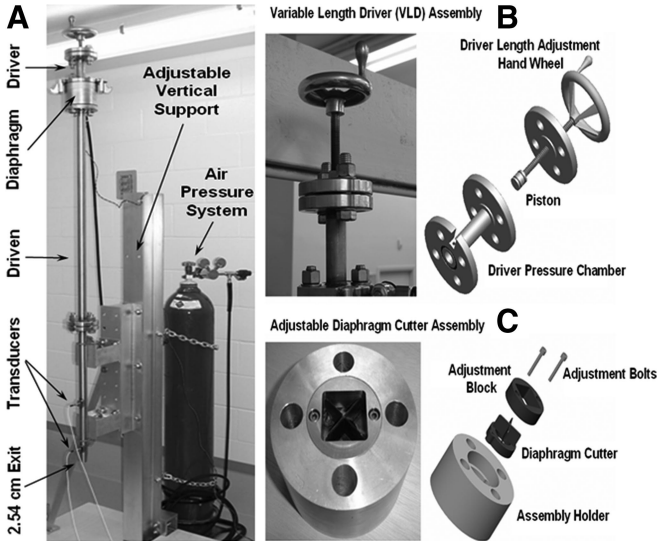

Figure 1. Blast generator setup. Overview of the shock tube (*A*), variable length driver (VLD) assembly (*B*), and adjustable diaphragm cutter unit (*C*), see Materials and Methods section for detail.

Animal Exposure to a Controlled Blast Wave

All rats were anesthetized with isoflurane inhalations described previously in detail. After reaching a deep plane of anesthesia, they were placed into a holder exposing only their head (body-armored setup) at the distance 5 cm from the exit nozzle of the shock tube, which was perpendicular to the middle of the head (Fig. 2). The head laid on a flexible mesh surface composed of a thin steel grating. This diminished the surface reflection of blast waves and decreased the formation of secondary waves that would potentially exacerbate the injury. For pathomorphology and biomarker studies, animals were then subjected to a single blast wave with a mean peak

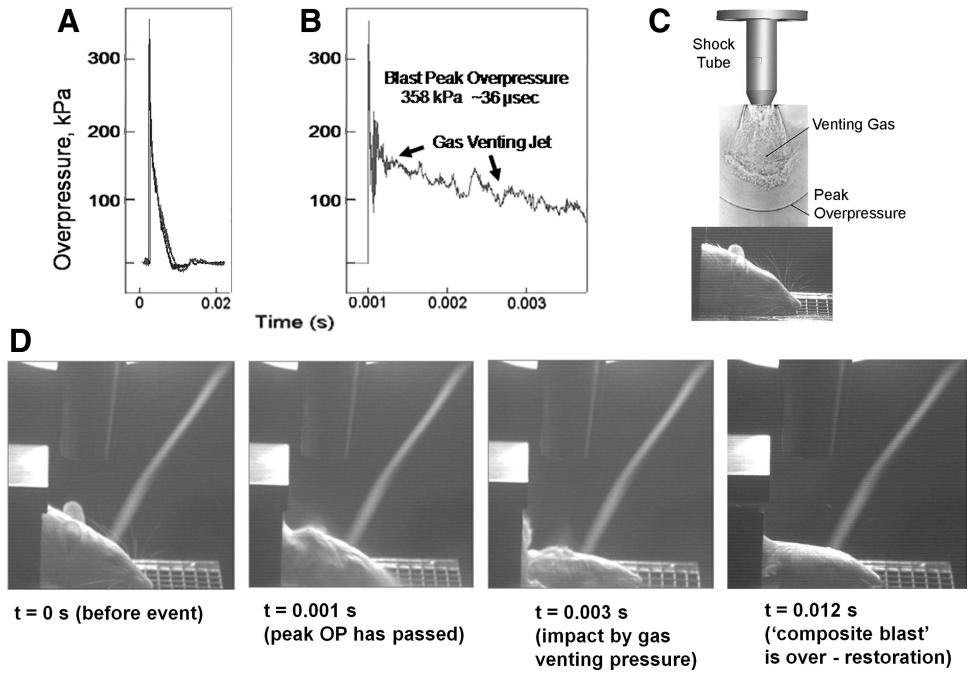

Figure 2. Experimental outline. (*A*) General shape of blast wave hitting an experimental animal showing a presence of negative phase; (*B*) components of shock tube-generated blast wave; (*C*) specimen positioning relative to shock tube, and (*D*) rat head movement and deformation after head-directed, body armored, blast wave exposure of 358 kPa for 10 msec 1,000 Hz high-speed video images using Schlieren optics shown.

TABLE 1. Rat Mortality After Exposure of Total Body and Head (Body Armored) to "Composite Blast"

Peak Overpressure (kPa)	Total Blast Duration (msec)	Mortality
Total exposure (unprotected body)		
110 (n = 3)	2	Survived
170 (n = 2)	4	Lethal
358 (n = 2)	1	Lethal
Head directed (body armored)		
172 (n = 12)	4	All survived
358 (n = 48)	10	All but one survived

Anesthetized rats were placed on a platform in dorsal-up recumbence at different distances from the nozzle. Rats were subjected to blast wave exposures of various magnitude and duration that included exposure to peak overpressure plus gas venting. The magnitude and duration of blast were assessed using data acquired with dynamic blast pressure transducers (see Materials and Methods section for details).

OP of 358 kPa at the head and a total positive-pressure phase duration of ~10 msec (Fig. 2). Because a total blast of 358 kPa magnitude/10 msec duration produced a very strong effect (Fig. 2), although being nonlethal (Table 1), these parameters were chosen for the initial pathomorphology/biomarker assessment presented in this study. For survival studies, body-armored rats were also exposed to head-directed blast of 172 kPa for a total duration of 4 msec. In addition, survival/mortality was investigated in rats exposed to head-directed blast of different magnitude/duration without body protection as shown in Table 1. Two control groups of animals, sham and naïve, underwent the same treatment (anesthesia, handling, and recovery) except they were not exposed to blast. The rats in a sham group were exposed to the noise of a single blast at the 2 m from the shock tube while anesthetized.

Fresh Tissues Collection

At the required time points after blast exposure, animals were killed according to the guidelines approved by the Institutional Animal Care and Use Committee (IACUC) of the University of Florida and tissue samples were collected, snap frozen, and stored at -70°C until further analysis. The rats were anesthetized with 3% to 5% isoflurane in a carrier gas of oxygen using an induction chamber. At the loss of toe pinch reflex, the anesthetic flow was reduced to 1% to 3% and rat was secured in a stereotaxic frame with its head allowed to move freely along the longitudinal axis. A nose cone continued to deliver the anesthetic gases. A dorsal midline incision was made over the cervical vertebrae and occiput. The atlanto-occipital membrane was exposed by blunt dissection. CSF was collected by lowering a 25-gauge needle attached to polyethylene tubing into the cisterna magna. Immediately after CSF collection, the rat was turned over. The chest cavity was opened and 3 mL to 6 mL of blood was withdrawn directly from the heart. After blood collection, the animal was removed from the stereotaxic frame and immediately decapitated (while still under the effects of the anesthesia gases) for fresh brain tissue collection.

Histologic Processing and Staining

Neurodegeneration in injured brains was examined by the de Olmos amino cupric silver histochemical technique developed to study the disintegrative degeneration as previously described in detail.[15,16] At the intended time of sacrifice, rats were deeply anesthetized with sodium pentobarbital (100 mg/kg I.P.) and transcardially perfused with 0.8% NaCl, 0.4% dextrose, 0.8% sucrose, 0.023% $CaCl_2$, and 0.034% sodium cacodylate, followed by a fixative solution containing 4% paraformaldehyde, 4% sucrose, and 1.4% sodium cacodylate. After decapitation, the heads were stored in the perfusion fix for 14 hours, after which the brains were removed, placed in cacodylate storage buffer, and processed for histologic analyses (Neuroscience Associates, Knoxville, TN). Frozen 35-μm-thick coronal sections, taken 420 μm apart between 1.1 mm anterior and 4.4 mm posterior to bregma, were silver stained for neuronal degeneration and counter stained with neutral red. The brain sections were scanned at high resolution.

Western Blot Analysis of Cortex and Hippocampus With GFAP and CNPase

For Western blot analyses, brain tissue samples were homogenized on ice in Western blot buffer as described previously in detail.[17] Samples were subjected to sodium dodecyl sulfate-polyacrylamide gel electrophoresis and electroblotted onto polyvinylidene difluoride membranes. Membranes were blocked in 10 mmol/L Tris, pH 7.5, 100 mmol/L NaCl, and 0.1% Tween-20 containing 5% nonfat dry milk for 60 minutes at room temperature. After overnight incubation with primary antibodies (1:2,000), proteins were detected using a goat anti-rabbit antibody conjugated to alkaline phosphatase (1:10,000–15,000), followed by colorimetric detection system. Bands of interests were normalized for β-actin expression used as a loading control.

GFAP, NSE, and UCH-L1 Enzyme-Linked Immunosorbent Assays

Quantitative detection of UCH-L1 in CSF and plasma was performed using proprietary SW enzyme-linked immunosorbent assay (ELISA) (Banyan Biomarkers, Inc) and recombinant UCH-L1 as standard. For quantification of GFAP and NSE, sandwich ELISA kits from BioVendor (Candler, NC) were used according to the manufacturer's instructions.

Statistics

Statistical analyses were performed using GraphPad Prism 5 software. Values are means ± SEM. Data were evaluated by two-tailed unpaired *t* test and one-way analysis of variance with Dunnett posttest analysis.

RESULTS

Blast Wave Characteristics

To study the injury mechanisms and relevant biomarkers of BBI, the characteristic parameters of the blast waves generated by the shock tube were first considered. The shock tube (Fig. 1) was designed and built to model a freely expanding blast wave as generated by a typical explosion.

Preliminary tests were conducted with no animal specimens to optimize the peak OP and exposure time to accurately reproduce blast events: driver pressure and volume, diaphragm material, and shock tube exit geometry. After the diaphragm rupture, the driver gas sets up a series of pressure waves in the low-pressure driven section that coalesced to form the incident shockwave (Fig. 2, A and B). Both static and dynamic (total) pressures were measured using piezoelectric blast pressure sensors/transducers positioned at the target. The shock wave recorded by blast pressure transducers in the driven section and at the target showed three distinct events: (i) peak OP, (ii) gas venting jet, and (iii) negative-pressure phase. Peak OP, positive phase duration, and impulse appear to be the key parameters that correlate to injury and likelihood of fatality in animals and humans, for various orientations of the specimen relative to the blast wave.[5,18–20] A schematic of a shock tube nozzle and the rat location relative to the shock tube axis, blast OP wave, and gas venting cone is shown in Figure 2, C.

Effect of "Composite Blast" on Rats after Total Body and Head-Directed Exposure

We conducted experiments to compare rat survival upon blast exposure of uncovered versus armored body. The shock tube's nozzle was directed to the rat's head positioned at 5 cm from the opening, along the tube's axis. After exposure of anesthetized rats with unprotected body to blast of 110 kPa (total peak OP) for 2 msec of composite blast wave, all rats remained alive during 24 hours to 48 hours postblast (Table 1). Rats exhibited transitory symptoms of agitation within 15 minutes to 30 minutes after exposure during recovery from anesthesia (data not shown). Further increase of blast OP magnitude to 170 kPa or 358 kPa for total blast duration of 4 msec and 1 msec, respectively, resulted in the increase of rat mortality immediately after blast exposure (Table 1). In contrast, protecting the body significantly increased threshold of mortality, and all rats remained alive after severe blast of 358 kPa peak OP and total duration of ~10 msec (Table 1). Figure 2, D depicts rat head movement and deformation recorded by a high-speed video on this severe head-directed blast wave exposure for 10 msec. Because of the complex nature of the blast event, the brain injury is a result of a combined impact of the "composite" blast including all three major phases of a shock wave shown in Figure 2, A and B. Gas venting jet, albeit lower in magnitude, lasts the longest, represents the bulk of blast impulse and possibly produces the most devastating impact. Figure 2, D demonstrates a strong downward head acceleration after the passage of peak OP that lasts ~36 μsec. However, cranial deformation is more severe during the gas venting phase, lasting up to ~10 msec. Only when the positive-pressure phase is over, the shape of the rat's skull starts to restore. These findings point to a potential flaw in several previous studies described in the literature: animal specimens are usually placed along the axis of the shock wave generator. In such location, the venting gas jet creates a much larger impulse (energy transfer) in the specimen than the peak OP itself. This effect can be virtually eliminated by placing the specimens off-axis from the venting jet in a way that the main effect acting on the specimen is the peak OP event, as will be presented in the Discussion section.

Brain Pathomorphology and Histology

Head acceleration and deformation after severe blast exposure shown in Figure 2 were accompanied by typical focal and massive intracranial hematomas and brain swelling (Fig. 3, B1 and C1). The hemorrhages and hematomas developed within hours after impact and appeared visibly through the undamaged scull at 24 hours to 48 hours after blast exposure (data not shown). The size of hematomas varied significantly in different rats and formed a capsule at 5 days postblast as shown in one the most damaged rat brain after in situ perfusion (Fig. 3, C1). The intracranial blood accumulation partially resolved at day 14 in a majority of rats observed (data not shown). As mentioned earlier, all rats but one remained alive during 14 days of postblast observation. Coronal sections of brains fixed in situ by transcardial perfusion were stained for neurodegeneration using silver impregnation. On microscopic examination, brain sections revealed a prominent silver staining becoming evident in the deep brain areas such as caudal diencephalon, including nucleus subthalamicus zone, at 48 hours postblast (Fig. 3, B2 and C2). The patterns of staining throughout the brain indicate both diffused and focal mild neurodegeneration, predominantly in the deep areas of rostral and caudal diencephalon (Fig. 3, B and C) and mesencephalon (data not shown). Particularly, brain histochemistry indicated a prominent silver accumulation in perivascular spaces and subventricular zones at 48 hours and predominant tissue localization 5 days postblast (Fig. 3, B3 and C3).

Expression of GFAP and CNPase in Brain Cortex and Hippocampus After Blast Impact

There was no significant increase of GFAP in the rat cortex after severe direct blast exposure (Fig. 4, A), in contrast to a significant GFAP accumulation in the hippocampus (Fig. 4, B). It appears to be that GFAP peaked in the hippocampus at 7 days after injury and persisted up to 30 days postblast (Fig. 4, B). In contrast, 2′,3′-cyclic nucleotide 3′-phosphodiesterase (CNPase) accumulated significantly in the cortex between 7 days and 30 days postblast (Fig. 5, A). However, the most prominent, severalfold increase in CNPase expression was found in the hippocampus showing the maximal nearly fourfold increase at 30 days after blast exposure (Fig. 5, B).

We determined quantitatively the amount of GFAP in blood and CSF by commercial sandwich ELISA (SW ELISA) assay. It has been found that increase of GFAP expression in the brain (hippocampus) was accompanied by its rapid and statistically significant accumulation in serum 24 hours after injury followed by a decline thereafter (Fig. 6, A). Although an accumulation of GFAP in CSF was delayed and occurred more gradually, in a time-dependent fashion (Fig. 6, B).

Because GFAP has been considered as a marker of activated astrocytes, the glial activation (gliosis) appears to be a prominent and an early stage feature of blast-induced brain damage.

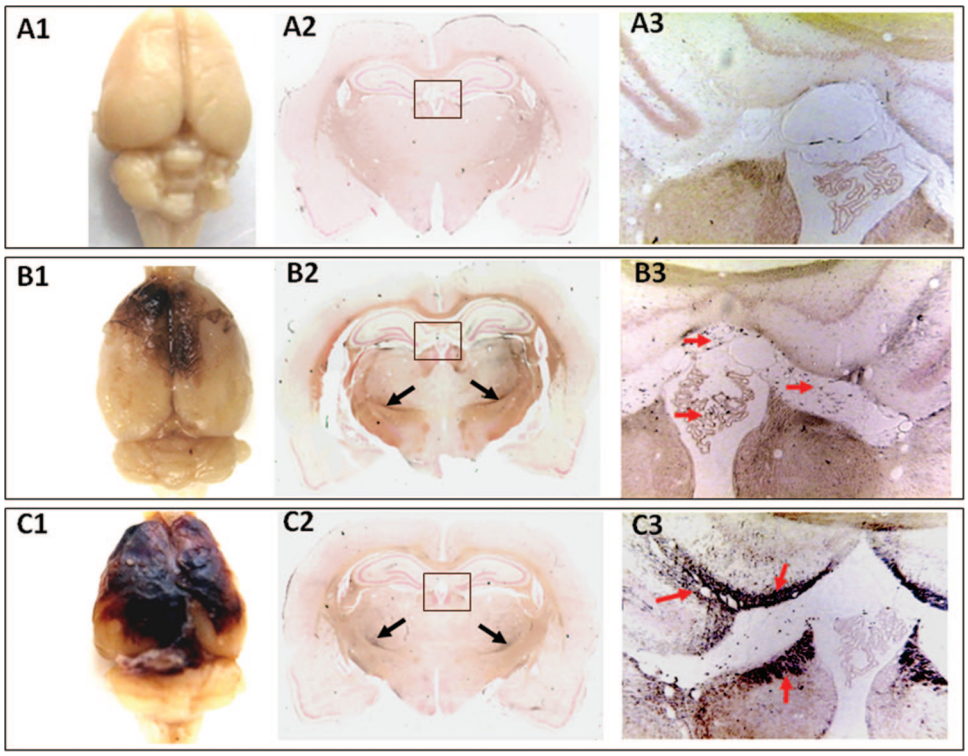

Figure 3. Brain pathomorphology after head-directed exposure to blast wave. Anesthetized rats were subjected to head-directed blast exposure (*B* and *C*) or noise (sham) (*A*). Forty-eight hours after exposures (*A* and *B*) or at 5 days postblast (*C*), brains were perfused in situ, removed, and processed as described in Materials and Methods section in detail. Gross pathology: typical focal intracranial hematomas (*B1* and *C1*) shown from at least three animals at each time point. Histopathology: coronal sections in caudal diencephalon exhibit diffuse and local silver accumulation (*B2* and *C2*). Black arrows indicate strong silver staining in nucleus subthalamicus. Representative microphotographs of whole brains with high-resolution scan (1.5×, *A2–C2*) and corresponding or similar areas at higher magnification (10×) are shown (*A3–C3*). Red arrows point to silver accumulation in perivascular and periventricular tissue zone.

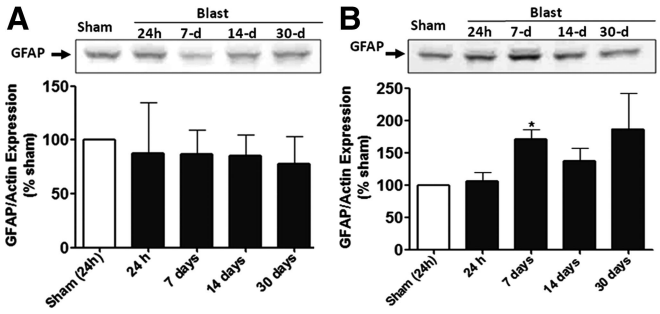

Figure 4. Western blot analysis of GFAP expression in the cortex (*A*) and hippocampus (*B*) of rats with blast-induced nonpenetrating injury. The brains were collected at various times after blast exposure, brain proteins (20 μg) were resolved by SDS-PAGE and immunoblotted with GFAP as described in Materials and Methods section. S, sham (blast noise-treated rats); I, blast wave-exposed rats. Data shown are mean ± SEM of at least three independent experiments. A representative blot out of at least three is shown (*$p < 0.05$).

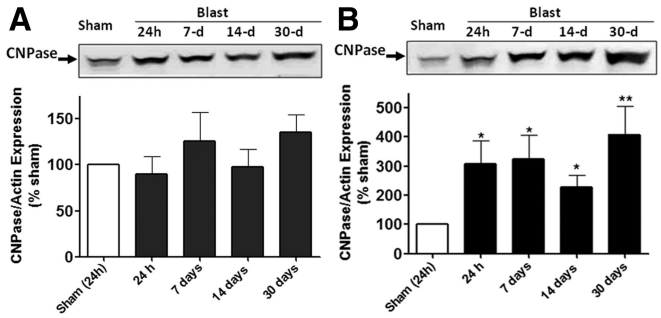

Figure 5. Western blot analysis of CNPase expression in the cortex (*A*) and hippocampus (*B*) of rats with blast-induced nonpenetrating injury. The brains were collected at various times after blast exposure, brain proteins (20 μg) were resolved by SDS-PAGE and immunoblotted with CNPase as described in Materials and Methods section. S, sham (blast noise-treated rats); I, blast wave-exposed rats. Data shown are mean ± SEM of at least three independent experiments. A representative blot out of at least three is shown. (*$p < 0.05$).

NSE and UCH-L1 Accumulation in CSF and Blood After Blast Exposure in Rats

NSE concentrations in serum were determined by commercial SW ELISA assay and were significantly higher at 24 hours and 48 hours postblast period in exposed rats compared with naïve control animals (Fig. 7, B). Although an average of NSE amounts in CSF was substantially high at 24 hours, the difference in CSF levels of NSE

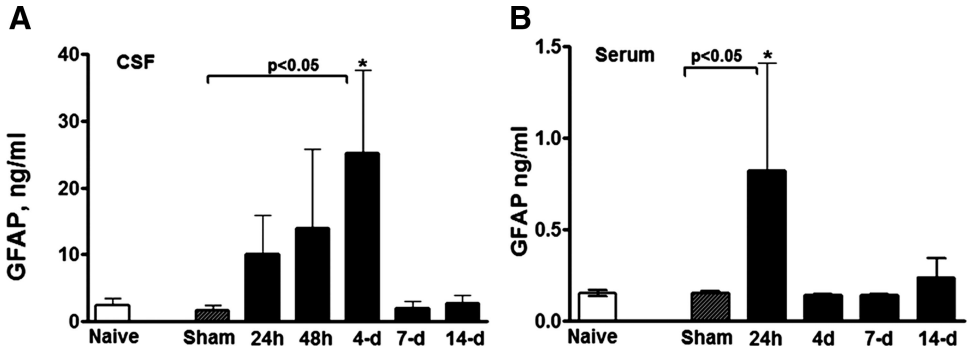

Figure 6. CSF and blood accumulation of GFAP in rats after blast exposure. Rats were subjected to head-directed blast of 358 kPa for total 10 msec. CSF and blood were collected at different times after blast. The levels of GFAP in CSF (*A*) and plasma (*B*) were assayed by SW ELISA as described in Materials and Methods section. Statistical significance was validated using unpaired *t* test and one-way ANOVA with Dunnett posttest analysis. Data shown are mean ± SEM of at least three independent experiments (n = 3–5) (*$p < 0.05$).

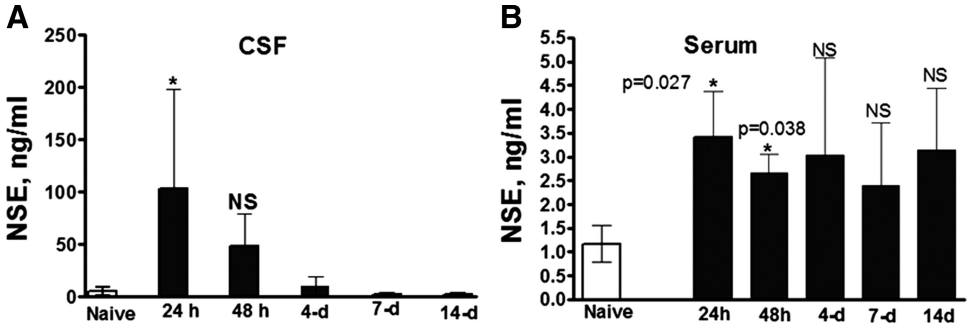

Figure 7. The levels of neurone-specific enolase (NSE) in CSF and blood in rats after blast exposure. Rats were hit by a head-directed blast wave of 358 kPa for total 10 msec. CSF and blood were collected at different times after blast. The levels of NSE in CSF (*A*) and serum (*B*) were assayed by NSE SW ELISA. Unpaired *t* test was used to analyze statistical significance of values. Data shown are mean ± SEM of at least three independent experiments (n = 3–5). (*$p < 0.05$); NS, not significant.

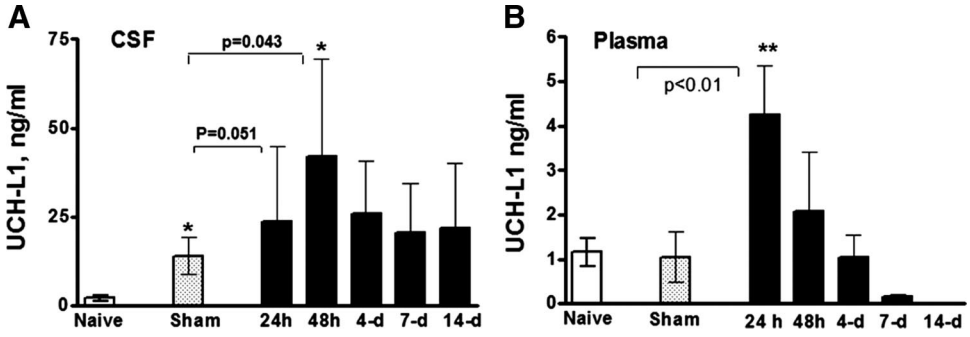

Figure 8. Accumulation of UCH-L1 in CSF and blood in rats after blast exposure. Rats were subjected to a head-directed blast wave of 358 kPa for total 10 msec. CSF and blood were collected at different times postblast. The levels of UCH-L1 in CSF (*A*) and plasma (*B*) were assayed by Banyan UCH-L1 SW ELISA. Unpaired *t* test was used to analyze statistical significance of values. Data shown are mean ± SEM of at least 3 to 10 independent experimental samples of CSF and 4 to 8 experimental samples of plasma (*$p < 0.05$; **$p < 0.01$).

after blast was not statistically significant ($p > 0.05$) and varied remarkably in individual rats that was reflected by the SD values (Fig. 7, A).

To assess UCH-L1 concentration in CSF and blood, we developed validated and used proprietary SW ELISA kit. UCH-L1 rapidly accumulated in blood 24 hours after blast exposure followed by a gradual decline at 14 days postblast recovery period (Fig. 8, B). Average CSF levels of UCH-L1 were slightly increased throughout 14 days after blast exposure and, similarly to NSE and GFAP, varied significantly in individual rats (Fig. 8, A). Both NSE and UCH-L1 have been expressed primarily, but not exclusively, in CNS, localize specifically to the neuronal body and overexpressed during neuronal damage and degeneration.[21–23]

A rapid accumulation of GFAP, NSE, and UCH-L1 in circulation together with a delayed appearance in CSF suggests that cerebrovascular damage, particularly the disruption of blood-brain barrier is a critical and first-response reaction on blast wave exposure.

DISCUSSION

It is still controversial whether primary blast forces directly damage the brain and, if they do, what are the mechanisms mediating the injury[24]? Analysis of mechanisms and development of biomarkers of BBI is complicated by a deficiency of quality experimental studies. Blast generators (shock tubes) are increasingly being used at places such as Walter Reed Army Institute of Research and the Navy Research Laboratory for conducting blast trauma studies on simulated human targets. However, because of inconsistent designs among shock tubes used in the different studies, the data on injury mechanisms, including brain damage, are difficult to analyze and compare if the shock waves used for the experiments are not properly characterized.[5,6,19] A common drawback found in many shock tube blast studies comes from placing the target along the axis of the shock wave generator.[5] This creates exposure to a gas venting jet: after the shock wave passes, the exhaust of the gas used to create the wave substantially alters the pressure and impulse at the target as it vents (Fig. 2, B–D).

The modular design of our shock tube provides the flexibility to perform repeatable blast experiments over a wide range of peak OP, pulse duration, and transferred mechanical energy (impulse), in a relatively lightweight package. A crucial part in using a shock tube for animal blast experiments is reproducibility of the blast events between tests. In our shock tube, the burst pressure of the diaphragm separating the driver and driven sections do not change (Fig. 1). Repeatability of diaphragm burst pressure was accomplished through the use of a cutter assembly directly in front of the diaphragm.[25] Special consideration is also given to properly shaping the exit of the driven section. This is necessary because the structure and flow field of the blast wave at the exit of the tube are influenced by the exit geometry of the driven section. To prevent unnecessary disturbances in the flow field from hindering replication of the proper pressure history at a target, it has been found that the exit of the driven section must be tapered. This allows the blast wave to propagate freely around the end of the driven section without reflecting.

Another important aspect during blast experiments with a shock tube is to ensure proper measurement of the blast event parameters, particularly at the surface of the specimen. To minimize the interaction between the pressure transducer and the target, caused by the alteration in flow pattern in the vicinity of the sensor, the data are first captured at the desired location without any target. After the pressure history is recorded and the sensors removed, the animal can be carefully positioned at the same location and the test repeated because it has been previously demonstrated that the proposed shock tube design has excellent repeatability characteristics.

In the present series of experiments, we placed rats along the shock tube axis (on-axis) and studied the combined effect of blast peak OP and venting gas that creates the impact we call "composite" blast. Although the blast generated in our model is a single blast event, the type of blast load observed resembles the complex effect produced by multiple blasts, such as in a confined space where the blast waves reverberate and overlap, hence the effect of displaced air mass flow on the resultant wave structure and magnitude can be important. It should be noted that in any blast produced in laboratory models, only a particular component of a complex blast experienced on the battlefield is present. We propose that because of the large spherical shape of the blast wave at the exit of the shock tube compared with the confined conical shape of the venting gas (Fig. 2, C), placing a rat outside the gas cone avoids gas venting thus subjecting rats to the effects of a "pure" blast OP. The shock tube was calibrated to achieve desired peak OPs depending on the angle and distance from the tube's nozzle (data not shown). The comparative studies of effects of this pure peak OP component on pathophysiology and biomarkers depending on the magnitude, duration, and number of exposures are under way in our laboratories.

A number of investigations have used compressed air-driven shock tubes and nitrogen-driven blast wave generator[5] for blast exposures of various animals (e.g., rats, mice, and rabbits) to address mechanisms of injury. Small animals are placed in orthopedic stockinette slings and large animals in open mesh nylon TM slings and subjected to blast exposure at varying distances and body orientations with or without a supportive/reflective plate behind the animal (see Ref. 19 for details). A majority of blast injury-related works have been performed using blast exposure of total animal bodies.[3,7,19,26–36] We have learned from reviewing these studies as well as from our own studies that issues of scaling remain a challenge. The blast energy imparted on an animal must be consistently scalable to the blast energy experienced by a service member in the field. Anatomic differences between models are also significant and must be accounted for. In turn, this arena of research would be much advanced if it were easier to obtain actual data on blast exposures along with their pathologic correlates in humans. However, the need for operational security poses a challenge regarding obtaining such data. In the mean time, we recommend collaborating with military medical and explosives experts to ensure that models are appropriate for the questions being addressed.

Our data demonstrate that rat mortality is remarkably higher when the unprotected rat body is exposed to blast, compared with head-directed or body-protected blast impacts of similar magnitude (Table 1). All rats but one subjected to head-directed unprotected body blast survived without visible behavioral signs of abnormality. Generally, these observations are in line with previous extensive studies by Stuhmiller et al. and Stuhmiller performed in rat and sheep.[3,20,37] A significantly lower threshold magnitude of blast that results in immediate rat lethality on exposure of unprotected rats versus head-directed, body-armored impact suggests the importance of systemic reactions that we would like to term "blastogenic

shock." Head-directed strong blast impacts resulted in severe morphologic brain damage including massive and focal hemorrhages (Fig. 3A) but did not lead to significant rat mortality. Moreover, these rats recovered rapidly from the blast exposure and anesthesia and did not show visible signs of behavioral abnormality within 24 hours to 14 days postblast (data not shown). Silver staining, that is, indicative of neurodegeneration,[38] was prominent in various regions of the brain, predominantly in deep areas of the rostral and caudal mesencephalon and diencephalon but not in the cortex (Fig. 3, B). This may suggest that the energy of the blast impulse is transmitted through the skull, induces head acceleration and jolting, and activates responses in deeper structures of the brain, mediated by the cerebral liquid and cisternae system, thus preventing significant injury to the cortex.

In previous studies, using mechanical impact controlled cortical impact (CCI) model of TBI in rats, we have convincingly demonstrated the important role for caspase-3–mediated apoptotic pathways in neuronal injury as well as the calpain-mediated oncosis/necrosis mechanisms.[39–41] We and others found that the signature cleavage products of aII-spectrin spectrin breakdown products (SBDPs) by caspases/calpain accumulated in brain tissue at sites of injury and CSF after brain injury in rats[42–44] and in human CSF after TBI.[17,41] Whether this mechanism operates after blast impact and what are its specific characteristics remain to be investigated.

In a recent study, rats were exposed to a direct single shock wave shot after craniotomy. The high-OP (>10 MPa) shock wave exposure resulted in hemorrhage and a significant increase in terminal deoxynucleotidyl transferase dUTP nick end labeling (TUNEL)-positive neurons with the maximum increase seen at 24 hours after the shock wave application.[45] Low-OP (1 MPa) shock wave exposure resulted in spindle-shaped changes in neurons and elongation of nuclei without marked neuronal injury. The administration of caspase-3 antagonist (Z-VAD-FMK) significantly reduced the number of TUNEL-positive cells observed 24 hours after high-OP shock wave exposure. The authors speculated that the threshold for shock wave-induced brain injury is under 1 MPa, a level that is lower than the threshold for other organs including lungs.[45] However, the model of blast injury used in this study is very similar to CCI model, which our group has been using for a number of years in rat TBI studies. The morphologic pattern of brain tissue injury in that model closely resembled the damage observed after CCI.[45]

A significant hippocampal accumulation of GFAP, and CNPase, established markers of activated glia, has been detected after blast (Figs. 4, B and 5, B). GFAP has only recently gained attention as a TBI biomarker when GFAP blood level was shown to be a good predictor of patient's mortality with sensitivity between 70% and 84% depending on the time it was measured after injury.[46,47] The roles for glia activation and GFAP as astrocyte marker after CCI in rats have been frequently reported.[48,49] However, GFAP levels in blood and CSF during experimental TBI have not been studied and its biomarker utility has not been validated, particularly in BBI models. Our data clearly demonstrate a rapid increase in serum GFAP within 24 hours after blast followed by a decline thereafter with a gradual accumulation in CSF (Fig. 6).

Similar to GFAP, NSE was substantially increased in serum at 24 hours and 48 hours after blast, whereas the CSF NSE concentrations showed a tendency to increase, but it was not statistically significant (Fig. 7). NSE initially held promise as a brain injury biomarker because it was originally thought to be strictly neuronal.[23] The sensitivity and specificity of serum NSE after pediatric TBI determined by receiver operating characteristic curves were found to be 71% and 64%, respectively.[14] After multiple trauma, elevated NSE levels have been observed but systemic NSE increased by similar degrees, with and without TBI, limiting its ability to discriminate brain injury magnitude.[50] In addition, NSE has a long half-life, >20 hours in serum that may account for its limitation as a TBI biomarker.[51]

UCH-L1 has attracted attention as a crucial enzyme linked to Parkinson's disease and memory and is selectively expressed in neurons at high levels.[52–55] Experimental evidence suggests that UCH-L1 plays a critical role in removal of excessive, oxidized, or misfolded proteins both during normal and neuropathological conditions. The release of UCH-L1 has been shown in lumbar CSF samples from 19 surgical cases of aortic aneurysm repair and 7 involving cardiopulmonary bypass with deep hypothermic circulatory arrest.[53] Recently, it has been shown by our group that the UCH-L1 is a potential biomarker for TBI in CCI models in rats.[56] We developed, validated, and used SW ELISA assay for quantitative detection of UCH-L1 in biofluids including plasma/serum with a high sensitivity of the assay of 10 pg/mL. Using the UCH-L1 SW ELISA, we showed a strong correlation between UCH-L1 levels in human CSF and outcome after severe TBI in patients.[57] Here, in an experimental study, we demonstrate a rapid and significant release and accumulation of UCH-L1 in blood at 24 hours after blast exposure compared with naïve and shams animal followed by a gradual decline (Fig. 8). The CSF levels of UCH-L1, although not statistically significant, were slightly elevated and persistent for a longer period of time after blast (Fig. 8, A). These data suggest an increase of extensity of neuronal ubiquitination that may contribute to neurodegeneration as long consequences of blast exposure.

Taken together, a characteristic time course of GFAP, NSE, and UCH-L1 indicates a blood-brain barrier disruption after severe blast exposure triggering the pathologic events in the brain that lead to hemorrhages, gliosis, and glia/neuronal interactions and may lead to neuronal degeneration.

In summary, we developed a comprehensive and reproducible model of blast exposure and injury in rats. The data suggest that mechanisms underlying blast brain injuries, particularly mild and moderate, appear to be distinct from those imposed by mechanical impact and may be triggered by systemic, cerebrovascular, and neuroglia responses as consecutive but overlapping events.

ACKNOWLEDGMENTS

We thank Dr. Zhiqun Zhang, Ms. Qiushi Tang, Ms. Olena Glushakova, and Ms. Olga Tchigrinova for their ex-

cellent technical assistance and Mr. Archie Svetlov for his help in preparation of the manuscript for publication.

REFERENCES

1. Cramer F, Paster S, Stephenson C. Cerebral injuries due to explosion waves, cerebral blast concussion; a pathologic, clinical and electroencephalographic study. *Arch Neurol Psychiatry.* 1949;61:1–20.
2. Murthy JM, Chopra JS, Gulati DR. Subdural hematoma in an adult following a blast injury. Case report. *J Neurosurg.* 1979;50:260–261.
3. Stuhmiller JH, Ho KH, Vander Vorst MJ, Dodd KT, Fitzpatrick T, Mayorga M. A model of blast overpressure injury to the lung. *J Biomech.* 1996;29:227–234.
4. Savic J, Tatic V, Ignjatovic D, et al. [Pathophysiologic reactions in sheep to blast waves from detonation of aerosol explosives]. *Vojnosanit Pregl.* 1991;48:499–506 [in Serbian].
5. Jaffin JH, McKinney L, Kinney RC, et al. A laboratory model for studying blast overpressure injury. *J Trauma.* 1987;27:349–356.
6. Guy RJ, Kirkman E, Watkins PE, Cooper GJ. Physiologic responses to primary blast. *J Trauma.* 1998;45:983–987.
7. Cernak I, Wang Z, Jiang J, Bian X, Savic J. Cognitive deficits following blast injury-induced neurotrauma: possible involvement of nitric oxide. *Brain Inj.* 2001;15:593–612.
8. Chavko M, Adeeb S, Ahlers ST, McCarron RM. Attenuation of pulmonary inflammation after exposure to blast overpressure by N-acetylcysteine amide. *Shock.* 2009;32:325–331.
9. Saljo A, Bao F, Haglid KG, Hansson HA. Blast exposure causes redistribution of phosphorylated neurofilament subunits in neurons of the adult rat brain. *J Neurotrauma.* 2000;17:719–726.
10. Svetlov SI, Larner SF, Kirk DR, Atkinson J, Hayes RL, Wang KK. Biomarkers of blast-induced neurotrauma: profiling molecular and cellular mechanisms of blast brain injury. *J Neurotrauma.* 2009;26:913–921.
11. Bazarian JJ, Zemlan FP, Mookerjee S, Stigbrand T. Serum S-100B and cleaved-tau are poor predictors of long-term outcome after mild traumatic brain injury. *Brain Inj.* 2006;20:759–765.
12. Piazza O, Storti MP, Cotena S, et al. S100B is not a reliable prognostic index in paediatric TBI. *Pediatr Neurosurg.* 2007;43:258–264.
13. Berger RP, Beers SR, Richichi R, Wiesman D, Adelson PD. Serum biomarker concentrations and outcome after pediatric traumatic brain injury. *J Neurotrauma.* 2007;24:1793–1801.
14. Berger RP, Adelson PD, Pierce MC, Dulani T, Cassidy LD, Kochanek PM. Serum neuron-specific enolase, S100B, and myelin basic protein concentrations after inflicted and noninflicted traumatic brain injury in children. *J Neurosurg.* 2005;103:61–68.
15. de Olmos JS, Beltramino CA, de Olmos de Lorenzo S. Use of an amino-cupric-silver technique for the detection of early and semiacute neuronal degeneration caused by neurotoxicants, hypoxia, and physical trauma. *Neurotoxicol Teratol.* 1994;16:545–561.
16. Switzer RC III. Application of silver degeneration stains for neurotoxicity testing. *Toxicol Pathol.* 2000;28:70–83.
17. Ringger NC, O'Steen BE, Brabham JG, et al. A novel marker for traumatic brain injury: CSF alpha II-spectrin breakdown product levels. *J Neurotrauma.* 2004;21:1443–1456.
18. Cooper PW. *Explosives Engineering.* New York, NY: Wiley-VCH; 1996.
19. Elsayed NM. Toxicology of blast overpressure. *Toxicology.* 1997;121:1–15.
20. Stuhmiller JH. Biological response to blast overpressure: a summary of modeling. *Toxicology.* 1997;121:91–103.
21. Doran JF, Jackson P, Kynoch PA, Thompson RJ. Isolation of PGP 9.5, a new human neurone-specific protein detected by high-resolution two-dimensional electrophoresis. *J Neurochem.* 1983;40:1542–1547.
22. Chiaretti A, Barone G, Riccardi R, et al. NGF, DCX, and NSE upregulation correlates with severity and outcome of head trauma in children. *Neurology.* 2009;72:609–616.
23. Vinores SA, Herman MM, Rubinstein LJ, Marangos PJ. Electron microscopic localization of neuron-specific enolase in rat and mouse brain. *J Histochem Cytochem.* 1984;32:1295–1302.
24. Taber KH, Warden DL, Hurley RA. Blast-related traumatic brain injury: what is known? *J Neuropsychiatry Clin Neurosci.* 2006;18:141–145.
25. Kirk DR, Faure JM, Gutierrez M, et al. Generation and analysis of blast waves from a compressed air-driven shock tube. *J Appl Mech.* In press.
26. Mayorga MA. The pathology of primary blast overpressure injury. *Toxicology.* 1997;121:17–28.
27. Cernak I, Radosevic P, Malicevic Z, Savic J. Experimental magnesium depletion in adult rabbits caused by blast overpressure. *Magnes Res.* 1995;8:249–259.
28. Cernak I, Savic VJ, Lazarov A, Joksimovic M, Markovic S. Neuroendocrine responses following graded traumatic brain injury in male adults. *Brain Inj.* 1999;13:1005–1015.
29. Elsayed NM, Gorbunov NV. Interplay between high energy impulse noise (blast) and antioxidants in the lung. *Toxicology.* 2003;189:63–74.
30. Gorbunov NV, Elsayed NM, Kisin ER, Kozlov AV, Kagan VE. Air blast-induced pulmonary oxidative stress: interplay among hemoglobin, antioxidants, and lipid peroxidation. *Am J Physiol.* 1997;272:L320–L334.
31. Chavko M, Prusaczyk WK, McCarron RM. Lung injury and recovery after exposure to blast overpressure. *J Trauma.* 2006;61:933–942.
32. Elsayed NM, Gorbunov NV. Pulmonary biochemical and histological alterations after repeated low-level blast overpressure exposures. *Toxicol Sci.* 2007;95:289–296.
33. Elsayed NM, Gorbunov NV, Kagan VE. A proposed biochemical mechanism involving hemoglobin for blast overpressure-induced injury. *Toxicology.* 1997;121:81–90.
34. Januszkiewicz AJ, Mundie TG, Dodd KT. Maximal exercise performance-impairing effects of simulated blast overpressure in sheep. *Toxicology.* 1997;121:51–63.
35. Cernak I, Ignjatovic D, Andelic G, Savic J. [Metabolic changes as part of the general response of the body to the effect of blast waves]. *Vojnosanit Pregl.* 1991;48:515–522 [in Serbian].
36. Cernak I, Savic J, Mrsulja B, Duricic B. [Pathogenesis of pulmonary edema caused by blast waves]. *Vojnosanit Pregl.* 1991;48:507–514 [in Serbian].
37. Stuhmiller JH. *Blast Injury Thresholds. JAYCOR Technical Report on Contract DAMD17–89-C-9150*. San Diego: Department of the Army; 1990.
38. Tenkova TI, Goldberg MP. A modified silver technique (de Olmos stain) for assessment of neuronal and axonal degeneration. *Methods Mol Biol.* 2007;399:31–39.
39. Wang KK, Ottens AK, Liu MC, et al. Proteomic identification of biomarkers of traumatic brain injury. *Expert Rev Proteomics.* 2005;2:603–614.
40. Ottens AK, Kobeissy FH, Golden EC, et al. Neuroproteomics in neurotrauma. *Mass Spectrom Rev.* 2006;25:380–408.
41. Pineda JA, Wang KK, Hayes RL. Biomarkers of proteolytic damage following traumatic brain injury. *Brain Pathol.* 2004;14:202–209.
42. Pike BR, Flint J, Dutta S, Johnson E, Wang KK, Hayes RL. Accumulation of non-erythroid alpha II-spectrin and calpain-cleaved alpha II-spectrin breakdown products in cerebrospinal fluid after traumatic brain injury in rats. *J Neurochem.* 2001;78:1297–1306.
43. Pike BR, Zhao X, Newcomb JK, Posmantur RM, Wang KK, Hayes RL. Regional calpain and caspase-3 proteolysis of alpha-spectrin after traumatic brain injury. *Neuroreport.* 1998;9:2437–2442.
44. Beer R, Franz G, Srinivasan A, et al. Temporal profile and cell subtype distribution of activated caspase-3 following experimental traumatic brain injury. *J Neurochem.* 2000;75:1264–1273.
45. Kato K, Fujimura M, Nakagawa A, et al. Pressure-dependent effect of shock waves on rat brain: induction of neuronal apoptosis mediated by a caspase-dependent pathway. *J Neurosurg.* 2007;106:667–676.
46. Nylen K, Ost M, Csajbok LZ, et al. Increased serum-GFAP in patients with severe traumatic brain injury is related to outcome. *J Neurol Sci.* 2006;240:85–91.
47. Pelinka LE, Kroepfl A, Leixnering M, et al. GFAP versus S100B in serum after traumatic brain injury: relationship to brain damage and outcome. *J Neurotrauma.* 2004;21:1553–1561.
48. Urrea C, Castellanos DA, Sagen J, Tsoulfas P, Bramlett HM, Dietrich WD. Widespread cellular proliferation and focal neurogenesis after

traumatic brain injury in the rat. *Restor Neurol Neurosci.* 2007;25: 65–76.
49. Johnson EA, Svetlov SI, Pike BR, et al. Cell-specific upregulation of survivin after experimental traumatic brain injury in rats. *J Neurotrauma.* 2004;21:1183–1195.
50. Pelinka LE, Hertz H, Mauritz W, et al. Nonspecific increase of systemic neuron-specific enolase after trauma: clinical and experimental findings. *Shock.* 2005;24:119–123.
51. Ingebrigtsen T, Romner B. Biochemical serum markers for brain damage: a short review with emphasis on clinical utility in mild head injury. *Restor Neurol Neurosci.* 2003;21:171–176.
52. Liu Z, Meray RK, Grammatopoulos TN, et al. Membrane-associated farnesylated UCH-L1 promotes {alpha}-synuclein neurotoxicity and is a therapeutic target for Parkinson's disease. *Proc Natl Acad Sci U S A.* 2009;106:4635–4640.
53. Siman R, Roberts VL, McNeil E, et al. Biomarker evidence for mild central nervous system injury after surgically-induced circulation arrest. *Brain Res.* 2008;1213:1–11.
54. Harada T, Harada C, Wang YL, et al. Role of ubiquitin carboxy terminal hydrolase-L1 in neural cell apoptosis induced by ischemic retinal injury in vivo. *Am J Pathol.* 2004;164:59–64.
55. Osaka H, Wang YL, Takada K, et al. Ubiquitin carboxy-terminal hydrolase L1 binds to and stabilizes monoubiquitin in neuron. *Hum Mol Genet.* 2003;12:1945–1958.
56. Kobeissy FH, Ottens AK, Zhang Z, et al. Novel differential neuroproteomics analysis of traumatic brain injury in rats. *Mol Cell Proteomics.* 2006;5:1887–1898.
57. Papa L, Akinyi L, Liu MC, et al. Ubiquitin C-terminal hydrolase is a novel biomarker in humans for severe traumatic brain injury. *Crit Care Med*. 2010;38:138–144.

JOURNAL OF NEUROTRAUMA 30:1881–1887 (November 15, 2013)

DOI: 10.1089/neu.2012.2758

Impact of Moderate Blast Exposures on Thrombin Biomarkers Assessed by Calibrated Automated Thrombography in Rats

Victor Prima,[1,2] Victor L. Serebruany,[3] Artem Svetlov,[1] Ronald L. Hayes,[1] and Stanislav I. Svetlov[1,2]

Abstract

Severe blast exposures are frequently complicated with fatal intracranial hemorrhages. However, many more sustain low level blasts without tissue damage detectable by brain imaging. To investigate effects of nonlethal blast on thrombin-related biomarkers, rats were subjected to two different types of head-directed blast: 1) moderate ''composite'' blast with strong head acceleration or 2) moderate primary blast, without head acceleration. Thrombin generation (TG) *ex vivo* after blast was studied by calibrated automated thrombography (CAT). In the same blood samples, we assessed maximal concentration of TG (TG_{max}), start time, peak time, mean time, and concentrations of protein markers for vascular/hemostatic dysfunctions: integrin α/β, soluble endothelial selectin (sE-selectin), soluble intercellular cell adhesion molecule-1 (sICAM-1), and matrix metalloproteinases (MMP)-2, MMP-8, and MMP-13. Blast remarkably affected all TG indices. In animals exposed to ''composite'' blast, TG_{max} peaked at 6 h ($\sim$4.5-fold vs. control), sustained at day 1 ($\sim$3.8-fold increase), and declined to a 2-fold increase over control at day 7 post-blast. After primary blast, TG_{max} also rose to $\sim$4.2-fold of control at 6 h, dropped to $\sim$1.7-fold of control at day 1, and then exhibited a slight secondary increase at 2-fold of control at day 7. Other TG indices did not differ significantly between two types of blast exposure. The changes were also observed in other microvascular/inflammatory/hemostatic biomarkers. Integrin α/β and sICAM-1 levels were elevated after both ''composite'' and primary blast at 6 h, 1 day, and 7 days. sE-selectin exhibited near normal levels after ''composite'' blast, but increased significantly at 7 days after primary blast; MMP-2, MMP-8, and MMP-13 slightly rose after ''composite'' blast and significantly increased ($\sim$2-4-fold) after primary blast. In summary, CAT may have a clinical diagnostic utility in combination with selected set of microvascular/inflammatory biomarkers in patients subjected to low/moderate level blast exposures.

Key words: animal studies; biomarkers; cerebral vascular disease; traumatic brain injury

Introduction

Blast-related traumatic brain injury (TBI) is the most common combat-related injury that ''has emerged as a leading injury among service members'' on the battlefield,[1] while the proportion of civilian casualties caused by explosives has increased as well.[2] TBI can lead to sustained neuro-somatic damage and neurodegeneration,[3] especially when repeated. As the over-pressurization wave propagates through the body, a blast generates primary damage at gas–fluid interfaces,[4] including pulmonary barotraumas, tympanic membrane ruptures with middle ear damage, abdominal hemorrhage and perforation, rupture of the eyeballs, and concussions.[5] Pulmonary barotraumas, together with TBI, are the most common fatal primary blast injuries, including free radical-associated injuries such as thrombosis, lipoxygenation, and disseminated intravascular coagulation. TBI-related coagulopathies substantially increase the risk of death and disability both in civilian[6] and military[7] settings. Current research suggests that blast injury and/or hemorrhage leads to hypotensive and hypoxemic secondary injury and impairs cerebral vascular compensatory responses.[8] Therefore, the effects of mild blast injury on the critical components of hemostasis are of high importance for the development of novel TBI diagnostics and therapeutics, and warrant more in-depth investigation.

Thrombin, or activated factor II, is a protease in the bloodstream that plays a key role in the modulation of hemostasis in general, but specifically in the activation of the coagulation cascade. Thrombin is produced by enzymatic cleavage of prothrombin by activated factor X, and is required to convert soluble protein fibrinogen into insoluble fibrin, promoting formation of a clot.[9,10] In addition,

[1]Banyan Laboratories, Inc., Alachua, Florida.
[2]Departments of Medicine and Urology, University of Florida, Gainesville, Florida.
[3]Heart Drug Research LLC, Towson, Maryland.

thrombin is believed to affect other biological activities in various cell types, including endothelial cells[11] and platelets.[12] Being a potent vasoconstrictor and mitogen, thrombin is recognized as a contributor to both acute and prolonged vasospasm, playing an important role in the pathogenesis of stroke by promoting cerebral ischemia, and/or enhancing risks for intracranial hemorrhage.[13] Several studies identified thrombin as an important contributor to the pathological developments following various injury types.[14,15]

Therefore, assessing thrombin activity represents an attractive, and potentially clinically useful, diagnostic tool for blast-related injury triage.

However, considering fast cleavage and aggressive binding patterns, measurement of thrombin activity is challenging. The most reliable among presently available tests is serial assessment of thrombin in plasma as a function of time, by comparing the fluorescent signal from a thrombin-generating sample using the calibrated automated thrombography (CAT) method, developed by Hemker and colleagues.[16,17] Applying the CAT system, we determined the blast wave-induced effects on multiple indices of thrombin generation (TG) potential and compared them with concomitant changes of several other markers of coagulation/inflammation vessel wall crosstalk. Using these proteins as a supplementary biomarkers panel for TBI diagnostics can validate and support otherwise injury type-nonspecific CAT data.

Methods

Blast generator design and setup

The compressed air-driven shock tube, capable of generating a wide range of controlled blast waves, has been described in detail previously.[18] The tube consists of two sections: high-pressure (driver) and low-pressure (driven) separated by a diaphragm. Peak overpressure (OP), composition, and duration of the generated high pressure shockwaves are determined by the shock tube configuration, including thickness, type of diaphragm material, driver/driven length ratio, and the initial driver pressure at the moment of diaphragm rupture. In the presented series of experiments, we employed different spatial setups as will be described subsequently. The blast pressure data were acquired using PCB Piezoelectric blast pressure transducers and LabView 8.2 software. A National Instruments 1.25 M samples/sec data acquisition card was used to acquire data from multiple channels. The rat head images during the blast event were captured at 40,000 frames/sec using a high speed video camera (Phantom V310, Vision Research, Wayne, NJ).

Animal exposure to a controlled blast wave

Modeling of the primary blast and the ''composite'' OP load was achieved by variable positioning of the target versus the blast generator. All rats were anesthetized with isoflurane inhalations, described previously in detail. After reaching a deep plane of anesthesia, they were placed into a holder exposing only their heads (body-armored setup) at a distance 5 cm below the exit nozzle of the shock tube. Rats were positioned either directly on the shock tube axis ($n=5$) to expose them to the ''composite'' blast including the compressed air jet (Fig.1 A, B) or at the 45 degree angle to it ($n=6$) for exposure only to the primary blast wave (Fig.1 D, E). Animals were then subjected to a single blast with a mean peak OP of 230–380 kPa at the target. The exact static and dynamic overpressure values depending upon the angle and distance of rat head from the nozzle of shock tube were established during the prior calibration tests. The control group of animals ($n=4$) underwent the same treatment (anesthesia, handling, recovery), except they were not exposed to a blast.

Blood collection

At the required time points following blast exposure, animals were euthanized according to guidelines approved by the Institutional Animal Care and Use Committee (IACUC) of the University of Florida. With the animal under isoflurane anesthesia, blood was withdrawn directly from the heart with an 18 gauge needle, and processed to obtain plasma and serum. One half of collected blood aliquot was drawn into 0.5 mL Capiject EDTA (K2) tubes (Terumo, Elkton, MD) at room temperature. The Capiject tube was gently inverted three to five times to ensure complete mixing of the anticoagulant. Platelet poor plasma (PPP) was centrifuged at 6000*g* for 15 min at room temperature, and frozen at -80°C until analysis. Another half of the blood aliquot was drawn into Multivette 600 tubes with clotting activator (Sarstedt, Nümbrecht, Germany) and was allowed to clot at room temperature for 40 min. Serum was separated by centrifugation at 10,000*g* for 5 min and frozen at -80°C until analysis. All samples were labeled with a coded number and analyzed by blinded technicians.

Antibody-based assays

Custom Biotin Label-based (L-series) RatAntibody arrays (Ray Biotech, Norcross, GA) were used to assess relative levels of integrin α/β, soluble endothelial selectin (sE-selectin), and matrix metalloproteinases (MMP)-2, MMP-8 and MMP-13 in rat serum following blast exposure. Commercially available Sandwich ELISA kits for soluble intercellular adhesion molecule-1 (soluble intercellular cell adhesion molecule-1 [sICAM-1]; CUSABIO Biotech) were used according to the manufacturer's instructions.

CAT reagents

Fluobuffer containing 20 mM HEPES and 60 mg/mL bovine serum albumin (Sigma, St. Louis, MO) were prepared *ex tempore* on the day of the experiment. Working buffer consisted of 140 mM NaCl, 20 mM HEPES, and 5 mg/mL human serum albumin. The fluorogenic substrate Z-Gly-Gly-Arg-amino-methyl-coumarin (Bachem, Bubendorf, Switzerland) was solubilized in pure dimethylsulfoxide (DMSO, Sigma, St. Louis, MO). The PPP reagent with a content of 5 pM tissue factor, and the thrombin calibrator (Thrombinoscope BV, Maastricht, Netherlands), was provided by Diagnostica Stago (Parsipanny, NJ).

CAT

Measurement of TG potential was performed using the CAT system. The validation details of the method are described elsewhere.[16,17,19] Briefly, for each experiment, a fresh mixture of fluobuffer and CaCl2 solution was prepared and incubated for 5 min at 37°C. After 5 min, 75 μL of the Fluo-DMSO-solution were added, mixed and incubated for a further 5 min. The resulting clear solution was referred to as FluCa. PPP reagent was solubilized with 2 mL deionized water. Twenty microliters of this trigger solution were put into each sample well of a 96 well round-bottom microtiter plate made of polypropylene (Nunc, Roskilde, Denmark). After reconstitution with 1 mL sterile water, the thrombin calibrator was used in each experiment to compare the simultaneously measured thrombin activity in the sample with that from a known and stable concentration in the calibrator well. Finally, 80 μL of plasma were put into each well. The 96 well plate was then placed in the fluorometer (Fluoroskan Ascent, Thermolabsystems OY, Helsinki, Finland) with an excitation filter at 390 nm and an emission filter at 460 nm. The automated dispensing of 20 μL FluCa indicated the onset of measurement of thrombin indices. Each well was measured every 20 sec for the duration of 40 min. Each experiment was performed fourfold. We used Analysis Software from Diagnostica Stago, Inc. (Parsippany, NJ) to assess four indices, namely TG_{max}

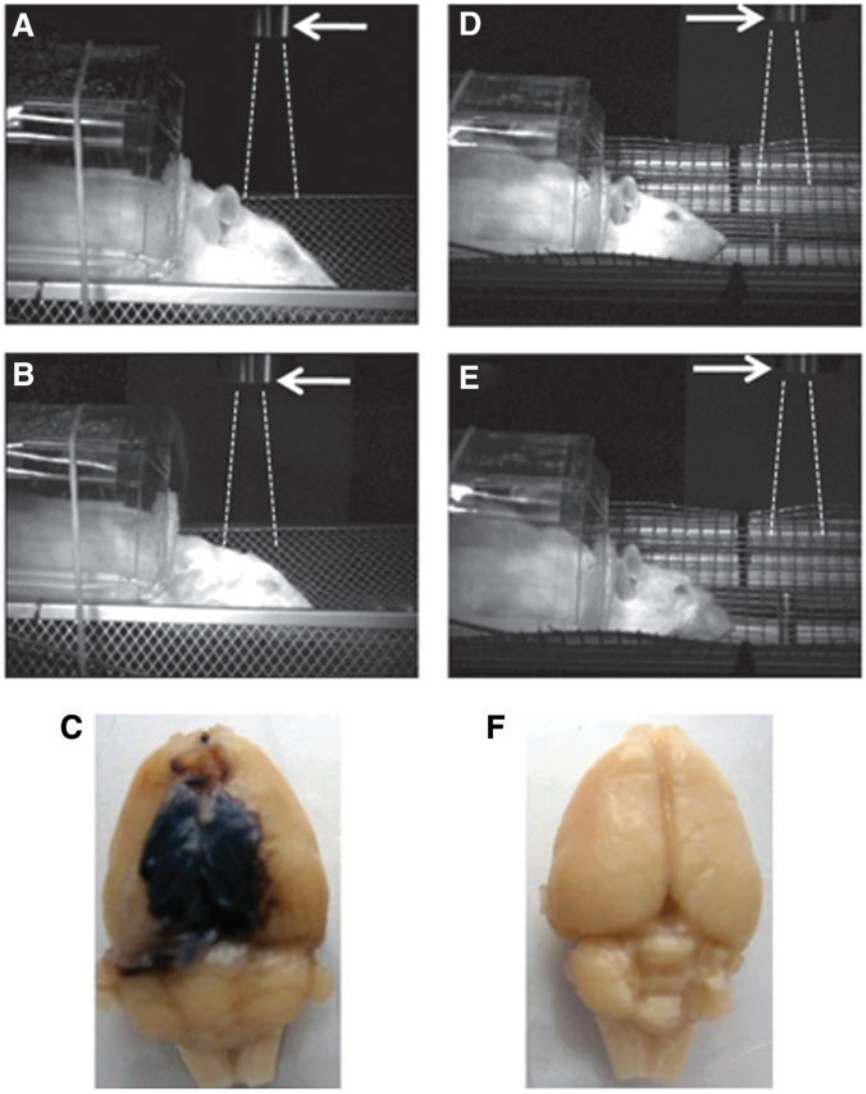

FIG. 1. Rat models of brain injury with ''composite'' or primary blast overpressure. High speed video images recorded before **(A, D)** and after **(B, E)** blast wave passage illustrate rat head movement on ''composite'' on-axis **(A, B)** versus primary off-axis **(D, E)** blast wave load for 10 msec. Arrows indicate the shock tube exit. Dashed lines depict trajectory of compressed air jet. Brain pathomorphology after head-directed exposure to blast wave: anesthetized rats were subjected to a ''composite'' **(C)** or a primary **(F)** blast overpressure load as described in the Methods section. Forty-eight hours after exposures brains were perfused *in situ*, removed, and recorded. Gross pathology: typical focal intracranial hematomas observed following ''composite'' overpressure load of 230–380 kPa. Color images are available online at www.liebertpub.com/neu

(max concentration of TG), start time (t-start) peak time (t-peak), and mean time (t-mean).

Statistical analysis

The Mann–Whitney *U* test was used to analyze nonparametric data. Normally distributed data were expressed as mean ± SD, and skewed data as median (range). All *p* values were two sided, with the significance level set at 0.05. Statistical analyses were performed using GraphPad Prism (GraphPad Software, La Jolla, CA).

Results

Blast-induced gross pathology

The high speed video recordings shown in Figure 1 present different biomechanics of target movement on the load of the ''composite'' or primary blast. Significant head acceleration and deformation after ''composite'' blast exposure (Fig. 1 A, B) were accompanied by typical focal and massive intracranial hematomas and brain swelling. The hemorrhages and hematomas developed within hours after impact and appeared visibly through the undamaged skull at 24–48 h after blast exposure (data not shown). The size of hematomas varied significantly in different rats and formed a capsule at 5 days post-blast, as shown in one of the most damaged rat brains after *in situ* perfusion (Fig. 1 C). The intracranial blood accumulation partially resolved at day 14 in a majority of rats observed (data not shown). On the other hand, primary blast exposure in the described model did not lead to noticeable hematomas.

Thrombin biomarkers

The combined data on TG potential at different time points and blast setups are presented in the Table 1.

Table 1. Indices of Thrombin Activity after Exposure to a Primary/Composite Blast Wave Load

	CAT parameter	*Baseline*	*6 h post-blast*	*1 day post-blast*	*7 days post-blast*
Primary blast	TG_{max} (nM)	121.0 ± 38.0	513.0 ± 44.0*	212.0 ± 68.0*	255.0 ± 49.0*
	t (peak) (min)	4.8 ± 0.19	8.0 ± 0.24*	7.0 ± 0.12*	5.0 ± 0.11*
	t (start) (min)	1.1 ± 0.07	1.0 ± 0.08*	1.0 ± 0.09*	1.0 ± 0.07*
	t (mean) (min)	6.4 ± 0.17	5.4 ± 0.18*	4.5 ± 0.15*	4.0 ± 0.13*
	CAT parameter	*Baseline*	*6 h post-blast*	*1 day post-blast*	*7 days post-blast*
Composite blast	TG_{max} (nM)	120.1 ± 7.2	540.0 ± 26.1*	450.0 ± 23.3*	250.0 ± 11.1*
	t (peak) (min)	5.0 ± 0.14	8.0 ± 0.13*	7.0 ± 0.13*	5.0 ± 0.10
	t (start) (min)	1.2 ± 0.08	1.0 ± 0.07*	1.0 ± 0.06*	1.0 ± 0.06*
	t (mean) (min)	6.4 ± 0.12	5.5 ± 0.13*	4.5 ± 0.11*	4.0 ± 0.10*

*p value < 0.05 versus naïve samples.
CAT, calibrated automated thrombography.

All indices of TG were remarkably affected in all blast-exposed rats compared with naïve animals. However, in ''composite'' blast-exposed animals, TG_{max} peaked at 6 h (~4.5-fold vs. control), sustained at 1 day (~3.8-fold increase), and declined to a 2-fold increase over control levels at day 7 post-blast. In rats subjected to primary blast, TG_{max} also rose to ~4.2-fold of control values at 6 h, dropped to ~1.7-fold of control levels at 1 day post-blast, and then exhibited a secondary increase to 2-fold of control values at day 7 post-blast (Fig. 2A).

Other TG indices did not differ significantly between two types of blast exposure. After either ''composite'' or primary blast loads, the t-peak times significantly increased compared with control values, whereas corresponding t-mean values decreased at both blast setups. The representative overlapped TG tracings after a primary blast wave load are illustrated in Figure 2 B.

The cumulative analysis of the data suggests strong time-dependent stimulation of overall TG potential by blast exposure.

Blast-induced expression induction of hemostasis-related proteins

Integrin α/β levels in serum were raised at both blast setups, indicating that overpressure wave load is triggering microcirculatory disorders whether it produces head hyperacceleration or not (Fig. 3A). After blast, the integrin α/β levels stayed elevated at both assayed time points: 1 day and 7 days. Soluble E-selectin displayed stable serum levels after ''composite'' blast, but increased significantly at 7 days after primary blast (Fig. 3 B). Soluble ICAM-1 levels were elevated in serum at both blast setups from 6 h to 7 days post-blast, most significantly (approximately fourfold of control) at 6 h after ''composite'' and 7 days after primary blast (Fig. 3 C). MMP-2, MMP-8, and MMP-13 displayed similar post-blast responses: slight elevation of relative serum concentrations after ''composite'' blast and significant increase (~2-4-fold) after primary blast (Fig. 3 D–F).

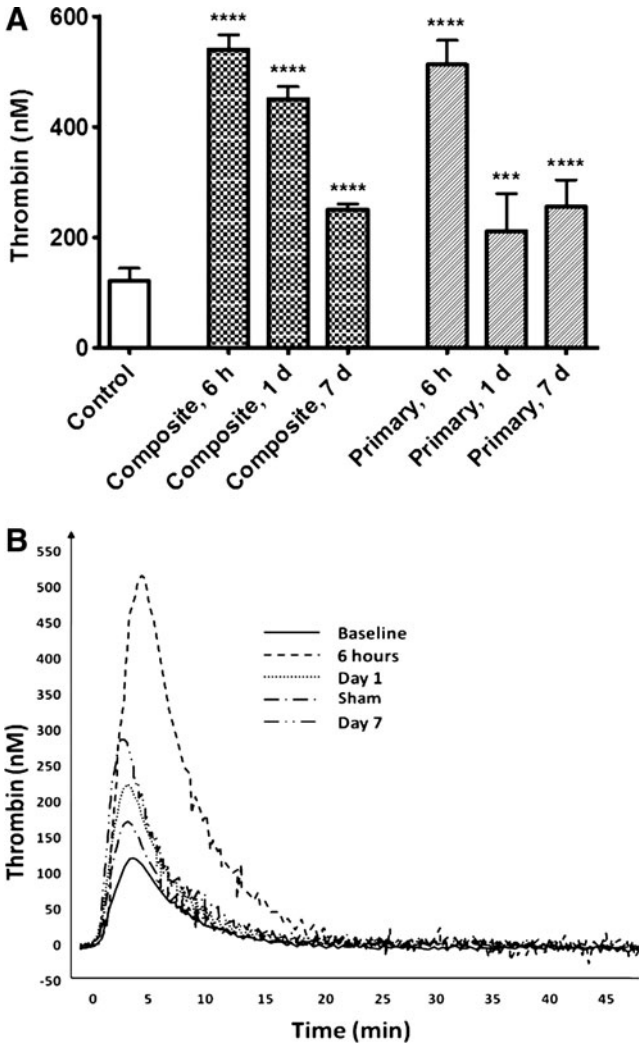

FIG. 2. Plasma levels of thrombin after blast. Thrombin generation potential was assessed in rat plasma by calibrated automated thrombography (CAT) technology **(A)**. Representative thrombography tracings after primary blast exposure **(B)**. Please see Methods section for details. Blood was collected from overpressure (OP)-exposed rats at different time-points and shock tube set-ups. Data shown are mean ± SEM of four independent experiments. ***$p < 0.001$; ****$p < 0.0001$ versus control samples.

Discussion

Our previous studies[18,20] suggested that blast wave composition should be taken into account in the explosive blast modeling with compressed gas-driven shock tubes. Here we explored the impact on hemostasis of two different types of blast: 1) moderate composite (head on-axis) blast with strong head acceleration, and 2) moderate primary off-axis blast load on the frontal part of rat skull without head acceleration. There have been multiple studies[20–23]

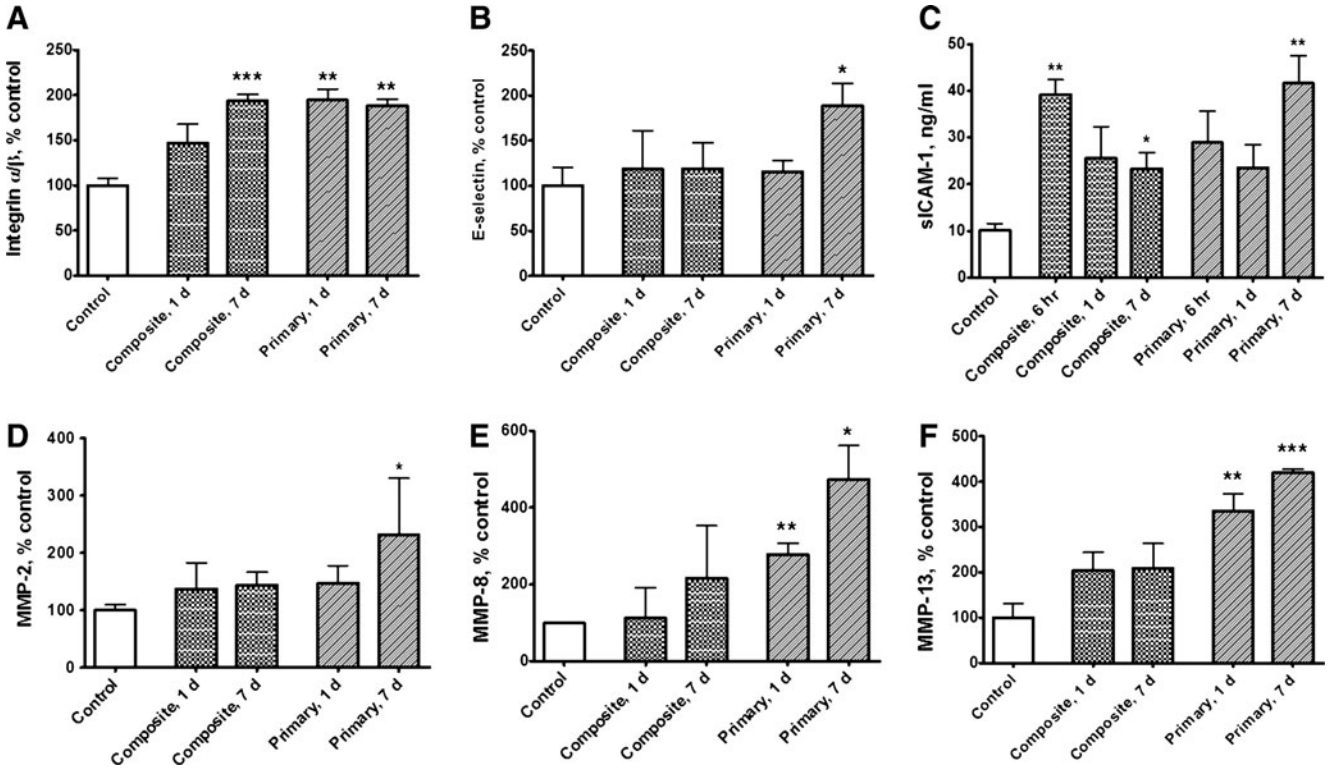

FIG. 3. Serum levels of hemostasis-related proteins after blast. Concentrations of integrin α/β **(A)**, soluble endothelial selectin (E-selectin) **(B)**, soluble intercellular cell adhesion molecule-1 (ICAM-1) **(C)** and matrix metalloproteinases (MMP)-2 **(D)**, MMP-8 **(E)**, and MMP-13 **(F)** were assessed in rat serum by antibody arrays and ELISA. Please see Methods section for details. Blood was collected from overpressure (OP)-exposed rats at different shock tube setups. Data shown are mean ± SEM of four to six independent experiments. $^{*}p < 0.05$; $^{**}p < 0.005$; $^{***}p < 0.001$ vs. control samples.

showing that angular and linear head accelerations (''bobblehead effect'') have much more severe impact than primary blast wave passing through the brain tissue. Moreover, some studies suggest that angular accelerations generate more powerful pressures in the brain than do linear accelerations.[24,25] Also, because of the presence of compressed air jet in the ''composite'' blast wave, the target experienced much higher OP impact resulting in intracranial hematomas (the typical post-blast gross pathology represented in Fig. 1 C).

In mammals, hemostasis is achieved through primary platelet activation-aggregation and secondary coagulation cascade. TBI induces loss of equilibrium in tightly regulated hemostatic systems, which can lead to either hypercoagulable states with microthrombosis and ischemia, or hypocoagulable states with possible progression of hemorrhagic legions.[26] In our studies, only the animal's head was exposed to blast waves, because of a rigid protective shield covering the rest of the body. Nevertheless, hemostasis-related indices were strongly affected in the peripheral blood. TG, the key process in the secondary hemostasis, was strongly affected by blast exposure. Usually thrombin levels are difficult to measure, and TG is commonly assessed indirectly through either enzyme-inhibitor complexes or prothrombin cleavage fragments. In our studies, we employed a novel method, CAT, which has been used recently for analysis of hemostasis in stroke patients.[27] As the data presented in Table 1 and further illustrated by Figure 2 show, all indices of TG were remarkably affected in all blast-exposed rats compared with control animals. An early more than fivefold spike of TG gradually decreased over 7 days post-blast, but still significantly exceeded the control values, suggesting it as a potential candidate for a clinical biomarker.

Following the blast, we observed coincident changes in the other important coagulation and inflammation factors in the hemostasis cascade, which exhibited trends in agreement with TG upregulation. However, contrary to the initial expectations, serum levels of the biomarkers studied after ''composite'' blast with strong head acceleration did not in general exceed corresponding levels after primary blast. In this respect, coagulation/inflammation biomarker data oppose our blast-induced gross pathology findings (Fig. 1A–C), and the existing hypothesis that head acceleration-deceleration resulting from blast forces exerted on the skull (''bobblehead effect'') would be the prevailing cause of persistent brain injury.[23] As shown in Figure 3, serum integrin α/β concentrations were raised after either primary or composite blast exposures and remained significantly elevated up to 7 days post-blast. It is known that the integrins, a large family of cell surface receptors, play pivotal roles in platelet adhesion and aggregation, white cell/endothelium interactions, and platelet-mediated thrombin generation.[28] Our findings are in line with the available data, which indicate that vascular injury is a stimulus for expression of α/β integrins by vascular cells.[29] Concomitant rise of thrombin and integrin α/β reflects important interplay between thrombin and β3-integrins in hemostasis. Thrombin, by binding to G protein coupled, protease-activated receptors, is a potent activator of integrins. Conversely, outside-in signaling through integrins amplifies events initiated by thrombin, and is necessary for full platelet spreading, platelet aggregation, and the formation of a stable platelet thrombus.[30]

As was shown in animal models of TBI, an influx of peripheral blood cells through disrupted blood-brain barrier (BBB) begins within hours after injury.[31] Multiple TBI-related animal studies[32,33] and clinical data[34,35] in agreement with our findings (Fig. 3 B, C) also demonstrate significant elevation in serum of inflammatory cell adhesion molecules, such as sICAM-1 and sE-selectin, which bind to circulating leukocytes and facilitate their migration into the injured brain regions. Endothelial pro-inflammatory processes are potently induced by thrombin.[36–38] Adverse effects of inflammatory response to injury are reflected by highly significant relationship between serum sICAM-1 and poor neurological outcome.[35,39]

Another group of molecules deeply involved in the neuroinflammation processes, MMPs, are known to be rapidly upregulated in patients with TBI,[40] and contribute to BBB breakdown[41] by degrading tight-junction proteins.[42] The consequent increase in blood vessel permeability[43,44] facilitates the development of edema. Our observations that MMP-2, MMP-8, and MMP-13 increase following primary blast wave exposure (Fig. 3 D–F) support the current vision of the diverse mechanisms of MMPs' involvement in brain injury either directly through degradation of brain matrix-substrates or indirectly through interaction with other bioactive molecules,[45] including thrombin[46,47] and integrin.[48] At this point, we do not have sufficient explanation as to why MMPs' levels after primary blast significantly exceed their levels after ''composite'' blast with strong head acceleration. If confirmed by independent studies, this effect may have a special advantage for the detection of mild blast-induced vascular abnormalities in the absence of the ''boblehead effect'' accompanied by severe hematomas.

Only recently has the development of compressed gas-driven blast wave generators with controlled OP enabled quantitative assessment of closed head blast TBI *in vivo*.[18,23,49,50] Analysis of the details of blast wave interaction with the target in the animal models have set it apart both from the civilian accidental TBI cases and from the penetrating brain injuries.[20] Notably, blast-induced closed head injuries are rarely as gruesome as their open counterparts, even though they can be just as damaging. Because these injuries neither puncture the dura mater nor necessarily breach the skull or scalp, they tend to be very hard to detect in the field or even in the hospital, as conventional imaging techniques such as MRI, functional MRI (fMRI), and CT can only detect gross internal deformities. Especially difficult is the objective assessment of mild blast trauma severity when the apparent trauma signs are benign or hidden.[1,3] As discussed previously,[51,52] vasospasm and rapidly developing diffuse cerebral edema leading to intracranial hypertension have been identified among the unique hallmarks of blast-induced closed head injuries encountered in military and civilian settings, which underlines the need for adequate diagnostic tools for hemodynamic and hemostatic abnormalities. Because thrombin, a central molecule in coagulation, is also involved in inflammation,[53] it positions TG among potential biomarkers for predicting neurological outcome after blast-induced TBI. Further human studies would be required to evaluate its clinical applications. Assessing TG potential, in combination with a carefully selected panel of blood biomarkers related to the cerebral hemostasis disruption, may be an attractive and reliable diagnostic tool for mild blast-related injury triage.

Acknowledgments

The authors thank Danny Johnson for his expert technical assistance. This work was supported by grants W81XWH-8-1-0376 and W81XWH-07-01-0701 from the Department of Defense.

Author Disclosure Statement

No competing financial interests exist.

References

1. Kanof, M. (2008). VA HEALTH CARE: Mild Traumatic Brain Injury Screening and Evaluation Implemented for OEF/OIF Veterans, but Challenges Remain. Washington DC: U.S. Government Printing Office.
2. Coupland, R.M., and Samnegaard, H.O. (1999). Effect of type and transfer of conventional weapons on civilian injuries: retrospective analysis of prospective data from Red Cross hospitals. BMJ 319, 410–412.
3. Chen, Y., and Huang, W. (2011). Non-impact, blast-induced mild TBI and PTSD: concepts and caveats. Brain Inj. 25, 641–650.
4. Guy, R.J., Glover, M.A., and Cripps, N.P. (1998). The pathophysiology of primary blast injury and its implications for treatment. Part I: The thorax. J. R. Nav. Med. Serv. 84, 79–86.
5. Wightman, J.M., and Gladish, S.L. (2001). Explosions and blast injuries. Ann. Emerg. Med. 37, 664–678.
6. Harhangi, B.S., Kompanje, E.J., Leebeek, F.W., and Maas, A.I. (2008). Coagulation disorders after traumatic brain injury. Acta Neurochir. (Wien) 150, 165–175.
7. Cap, A.P., and Spinella, P.C. (2011). Severity of head injury is associated with increased risk of coagulopathy in combat casualties. J. Trauma 71, S78–81.
8. DeWitt, D.S., and Prough, D.S. (2009). Blast-induced brain injury and posttraumatic hypotension and hypoxemia. J. Neurotrauma 26, 877–887.
9. Bode, W. (2006). Structure and interaction modes of thrombin. Blood Cells Mol. Dis. 36, 122–130.
10. Wolberg, A.S. (2007). Thrombin generation and fibrin clot structure. Blood Rev. 21, 131–142.
11. Lockard, M.M., Witkowski, S., Jenkins, N.T., Spangenburg, E.E., Obisesan, T.O., and Hagberg, J.M. (2010). Thrombin and exercise similarly influence expression of cell cycle genes in cultured putative endothelial progenitor cells. J. Appl. Physiol. 108, 1682–1690.
12. Sossdorf, M., Konig, V., Gummert, J., Marx, G., and Losche, W. (2008). Correlations between platelet-derived microvesicles and thrombin generation in patients with coronary artery disease. Platelets 19, 476–477.
13. Kang, D.W., Yoo, S.H., Chun, S., Kwon, K.Y., Kwon, S.U., Koh, J.Y., and Kim, J.S. (2009). Inflammatory and hemostatic biomarkers associated with early recurrent ischemic lesions in acute ischemic stroke. Stroke 40, 1653–1658.
14. Groves, H.M., Kinlough–Rathbone, R.L., Richardson, M., Jorgensen, L., Moore, S., and Mustard, J.F. (1982). Thrombin generation and fibrin formation following injury to rabbit neointima. Studies of vessel wall reactivity and platelet survival. Lab. Invest. 46, 605–612.
15. Walters, T.K., Gorog, D.A., and Wood, R.F. (1994). Thrombin generation following arterial injury is a critical initiating event in the pathogenesis of the proliferative stages of the atherosclerotic process. J. Vasc. Res. 31, 173–177.
16. Hemker, H.C., Giesen, P., Al Dieri, R., Regnault, V., de Smedt, E., Wagenvoord, R., Lecompte, T., and Beguin, S. (2003). Calibrated automated thrombin generation measurement in clotting plasma. Pathophysiol. Haemost. Thromb. 33, 4–15.
17. Hemker, H.C., Giesen, P., AlDieri, R., Regnault, V., de Smed, E., Wagenvoord, R., Lecompte, T., and Beguin, S. (2002). The calibrated automated thrombogram (CAT): a universal routine test for hyper- and hypocoagulability. Pathophysiol. Haemost. Thromb. 32, 249–253.
18. Svetlov, S.I., Prima, V., Kirk, D.R., Gutierrez, H., Curley, K.C., Hayes, R. L., and Wang, K. K. (2010). Morphologic and biochemical characterization of brain injury in a model of controlled blast overpressure exposure. J. Trauma 69, 795–804.
19. Luddington, R., and Baglin, T. (2004). Clinical measurement of thrombin generation by calibrated automated thrombography requires contact factor inhibition. J. Thromb. Haemost. 2, 1954–1959.
20. Svetlov, S.I., Prima, V., Glushakova, O., Svetlov, A., Kirk, D.R., Gutierrez, H., Serebruany, V.L., Curley, K.C., Wang, K.K., and Hayes, R.L. (2012). Neuro-glial and systemic mechanisms of pathological responses in rat models of primary blast overpressure compared to ''composite'' blast. Front. Neurol. 3, 15.
21. Risling, M., Plantman, S., Angeria, M., Rostami, E., Bellander, B.M., Kirkegaard, M., Arborelius, U., and Davidsson, J. (2011). Mechanisms

of blast induced brain injuries, experimental studies in rats. Neuroimage 54, Suppl. 1, S89–97.
22. Fijalkowski, R.J., Stemper, B.D., Pintar, F.A., Yoganandan, N., Crowe, M.J., and Gennarelli, T.A. (2007). New rat model for diffuse brain injury using coronal plane angular acceleration. J Neurotrauma 24, 1387–1398.
23. Goldstein, L.E., Fisher, A.M., Tagge, C.A., Zhang, X.L., Velisek, L., Sullivan, J.A., Upreti, C., Kracht, J.M., Ericsson, M., Wojnarowicz, M.W., Goletiani, C.J., Maglakelidze, G.M., Casey, N., Moncaster, J.A., Minaeva, O., Moir, R.D., Nowinski, C.J., Stern, R.A., Cantu, R.C., Geiling, J., Blusztajn, J.K., Wolozin, B.L., Ikezu, T., Stein, T.D., Budson, A.E., Kowall, N.W., Chargin, D., Sharon, A., Saman, S., Hall, G.F., Moss, W.C., Cleveland, R.O., Tanzi, R.E., Stanton, P.K., and McKee, A.C. (2012). Chronic traumatic encephalopathy in blast-exposed military veterans and a blast neurotrauma mouse model. Sci. Transl. Med. 4, 134–160.
24. Zhang, J., Yoganandan, N., Pintar, F.A., and Gennarelli, T.A. (2006). Role of translational and rotational accelerations on brain strain in lateral head impact. Biomed Sci Instrum 42, 501–506.
25. Krave, U., Hojer, S., and Hansson, H.A. (2005). Transient, powerful pressures are generated in the brain by a rotational acceleration impulse to the head. Eur J Neurosci 21, 2876–2882.
26. Laroche, M., Kutcher, M.E., Huang, M.C., Cohen, M.J., and Manley, G.T. (2012). Coagulopathy following traumatic brain injury. Neurosurgery 70, 1334–1345.
27. Serebruany, V., Sani, Y., Lynch, D., Schevchuck, A., Svetlov, S., Fong, A., Thevathasan, L., and Hanley, D. (2012). Effects of dabigatran in vitro on thrombin biomarkers by calibrated automated thrombography in patients after ischemic stroke. J. Thromb. Thrombolysis 33, 22–27.
28. Ni, H., and Freedman, J. (2003). Platelets in hemostasis and thrombosis: role of integrins and their ligands. Transfus. Apher. Sci. 28, 257–264.
29. Stouffer, G.A., Hu, Z., Sajid, M., Li, H., Jin, G., Nakada, M.T., Hanson, S.R., and Runge, M.S. (1998). Beta3 integrins are upregulated after vascular injury and modulate thrombospondin- and thrombin-induced proliferation of cultured smooth muscle cells. Circulation 97, 907–915.
30. Stouffer, G.A., and Smyth, S.S. (2003). Effects of thrombin on interactions between beta3-integrins and extracellular matrix in platelets and vascular cells. Arterioscler. Thromb. Vasc. Biol. 23, 1971–1978.
31. Ghajar, J. (2000). Traumatic brain injury. Lancet 356, 923–929.
32. Chen, G., Shi, J., Hu, Z., and Hang, C. (2008). Inhibitory effect on cerebral inflammatory response following traumatic brain injury in rats: a potential neuroprotective mechanism of N-acetylcysteine. Mediators Inflamm 2008, 716458.
33. Balabanov, R., Goldman, H., Murphy, S., Pellizon, G., Owen, C., Rafols, J., and Dore–Duffy, P. (2001). Endothelial cell activation following moderate traumatic brain injury. Neurol. Res. 23, 175–182.
34. Yilmaz, G., and Granger, D.N. (2008). Cell adhesion molecules and ischemic stroke. Neurol. Res. 30, 783–793.
35. Wang, H.C., Lin, W.C., Lin, Y.J., Rau, C.S., Lee, T.H., Chang, W.N., Tsai, N.W., Cheng, B.C., Kung, C.T., and Lu, C.H. (2011). The association between serum adhesion molecules and outcome in acute spontaneous intracerebral hemorrhage. Crit. Care 15, R284.
36. Miho, N., Ishida, T., Kuwaba, N., Ishida, M., Shimote–Abe, K., Tabuchi, K., Oshima, T., Yoshizumi, M., and Chayama, K. (2005). Role of the JNK pathway in thrombin-induced ICAM-1 expression in endothelial cells. Cardiovasc. Res. 68, 289–298.
37. Kaplanski, G., Marin, V., Fabrigoule, M., Boulay, V., Benoliel, A.M., Bongrand, P., Kaplanski, S. & Farnarier, C. (1998). Thrombin-activated human endothelial cells support monocyte adhesion in vitro following expression of intercellular adhesion molecule-1 (ICAM-1; CD54) and vascular cell adhesion molecule-1 (VCAM-1; CD106). Blood 92, 1259–1267.
38. Alabanza, L.M., and Bynoe, M.S. (2012). Thrombin induces an inflammatory phenotype in a human brain endothelial cell line. J. Neuroimmunol. 245, 48–55.
39. McKeating, E.G., Andrews, P.J., and Mascia, L. (1998). The relationship of soluble adhesion molecule concentrations in systemic and jugular venous serum to injury severity and outcome after traumatic brain injury. Anesth. Analg. 86, 759–765.
40. Vilalta, A., Sahuquillo, J., Rosell, A., Poca, M.A., Riveiro, M., and Montaner, J. (2008). Moderate and severe traumatic brain injury induce early overexpression of systemic and brain gelatinases. Intensive Care Med. 34, 1384–1392.
41. Petty, M.A., and Lo, E.H. (2002). Junctional complexes of the blood–brain barrier: permeability changes in neuroinflammation. Prog. Neurobiol. 68, 311–323.
42. Yang, Y., Estrada, E.Y., Thompson, J.F., Liu, W., and Rosenberg, G.A. (2007). Matrix metalloproteinase-mediated disruption of tight junction proteins in cerebral vessels is reversed by synthetic matrix metalloproteinase inhibitor in focal ischemia in rat. J. Cereb. Blood Flow Metab. 27, 697–709.
43. Harkness, K.A., Adamson, P., Sussman, J.D., Davies–Jones, G.A., Greenwood, J., and Woodroofe, M.N. (2000). Dexamethasone regulation of matrix metalloproteinase expression in CNS vascular endothelium. Brain 123, 698–709.
44. Suehiro, E., Fujisawa, H., Akimura, T., Ishihara, H., Kajiwara, K., Kato, S., Fujii, M., Yamashita, S., Maekawa, T., and Suzuki, M. (2004). Increased matrix metalloproteinase-9 in blood in association with activation of interleukin-6 after traumatic brain injury: influence of hypothermic therapy. J Neurotrauma 21, 1706–1711.
45. Morancho, A., Rosell, A., Garcia–Bonilla, L., and Montaner, J. (2010). Metalloproteinase and stroke infarct size: role for anti-inflammatory treatment? Ann. N. Y. Acad. Sci. 1207, 123–133.
46. Orbe, J., Rodriguez, J.A., Calvayrac, O., Rodriguez–Calvo, R., Rodriguez, C., Roncal, C., Martinez de Lizarrondo, S., Barrenetxe, J., Reverter, J.C., Martinez–Gonzalez, J., and Paramo, J.A. (2009). Matrix metalloproteinase-10 is upregulated by thrombin in endothelial cells and increased in patients with enhanced thrombin generation. Arterioscler. Thromb. Vasc. Biol. 29, 2109–2116.
47. Galis, Z.S., Kranzhofer, R., Fenton, J.W., 2nd, and Libby, P. (1997). Thrombin promotes activation of matrix metalloproteinase-2 produced by cultured vascular smooth muscle cells. Arterioscler. Thromb. Vasc. Biol. 17, 483–489.
48. Brooks, P.C., Stromblad, S., Sanders, L.C., von Schalscha, T.L., Aimes, R.T., Stetler–Stevenson, W.G., Quigley, J.P., and Cheresh, D.A. (1996). Localization of matrix metalloproteinase MMP-2 to the surface of invasive cells by interaction with integrin alpha v beta 3. Cell 85, 683–693.
49. Cernak, I. (2005). Animal models of head trauma. NeuroRx 2, 410–422.
50. Long, J.B., Bentley, T.L., Wessner, K.A., Cerone, C., Sweeney, S., and Bauman, R.A. (2009). Blast overpressure in rats: recreating a battlefield injury in the laboratory. J. Neurotrauma 26, 827–840.
51. Ling, G., Bandak, F., Armonda, R., Grant, G., and Ecklund, J. (2009). Explosive blast neurotrauma. J. Neurotrauma 26, 815–825.
52. Bauman, R.A., Ling, G., Tong, L., Januszkiewicz, A., Agoston, D., Delanerolle, N., Kim, Y., Ritzel, D., Bell, R., Ecklund, J., Armonda, R., Bandak, F., and Parks, S. (2009). An introductory characterization of a combat-casualty-care relevant swine model of closed head injury resulting from exposure to explosive blast. J. Neurotrauma 26, 841–860.
53. van Hinsbergh, V.W. (2012). Endothelium–role in regulation of coagulation and inflammation. Semin. Immunopathol. 34, 93–106.

Address correspondence to:
Stanislav I. Svetlov, MD
Banyan Laboratories, Inc.
12085 Research Drive
Alachua, FL 32615

E-mail: ssvetlov@banyanbio.com

or

Victor Prima, PhD
University of Florida
Gainesville, FL 32610

E-mail: vprima@ufl.edu

frontiers in
NEUROLOGY

ORIGINAL RESEARCH ARTICLE
published: 09 February 2012
doi: 10.3389/fneur.2012.00015

Neuro-glial and systemic mechanisms of pathological responses in rat models of primary blast overpressure compared to "composite" blast

Stanislav I. Svetlov[1,2]*, Victor Prima[1]*, Olena Glushakova[1], Artem Svetlov[1], Daniel R. Kirk[3], Hector Gutierrez[3], Victor L. Serebruany[4], Kenneth C. Curley[5], Kevin K. W. Wang[6] and Ronald L. Hayes[1]

[1] *Banyan Laboratories, Inc, Alachua, FL, USA*
[2] *Department of Medicine, University of Florida, Gainesville, FL, USA*
[3] *Department of Mechanical and Aerospace Engineering, Florida Institute of Technology, Melbourne, FL, USA*
[4] *Heart Drug Research LLC, Towson, MD, USA*
[5] *United States Army Medical Research and Materiel Command, Fort Detrick, MD, USA*
[6] *Department of Psychiatry, University of Florida, Gainesville, FL, USA*

Edited by:
Ibolja Cernak, Johns Hopkins University, USA

Reviewed by:
Jeffrey J. Bazarian, University of Rochester, USA
Eng Lo, Harvard University, USA

****Correspondence:***
Stanislav I. Svetlov and Victor Prima, Banyan Laboratories, Inc., 12085 Research Drive, Alachua, FL 32615, USA.
e-mail: ssvetlov@banyanbio.com; vprima@banyanbio.com

A number of experimental models of blast brain injury have been implemented in rodents and larger animals. However, the variety of blast sources and the complexity of blast wave biophysics have made data on injury mechanisms and biomarkers difficult to analyze and compare. Recently, we showed the importance of rat position toward blast generated by an external shock tube. In this study, we further characterized blast producing moderate traumatic brain injury and defined "composite" blast and primary blast exposure set-ups. Schlieren optics visualized interaction between the head and a shock wave generated by external shock tube, revealing strong head acceleration upon positioning the rat on-axis with the shock tube (composite blast), but negligible skull movement upon peak overpressure exposure off-axis (primary blast). Brain injury signatures of a primary blast hitting the frontal head were assessed and compared to damage produced by composite blast. Low to negligible levels of neurodegeneration were found following primary blast compared to composite blast by silver staining. However, persistent gliosis in hippocampus and accumulation of GFAP/CNPase in circulation was detected after both primary and composite blast. Also, markers of vascular/endothelial inflammation integrin alpha/beta, soluble intercellular adhesion molecule-1, and L-selectin along with neurotrophic factor nerve growth factor-beta were increased in serum within 6 h post-blasts and persisted for 7 days thereafter. In contrast, systemic IL-1, IL-10, fractalkine, neuroendocrine peptide Orexin A, and VEGF receptor Neuropilin-2 (NRP-2) were raised predominantly after primary blast exposure. In conclusion, biomarkers of major pathological pathways were elevated at all blast set-ups. The most significant and persistent changes in neuro-glial markers were found after composite blast, while primary blast instigated prominent systemic cytokine/chemokine, Orexin A, and Neuropilin-2 release, particularly when primary blast impacted rats with unprotected body.

Keywords: blast, brain injury, biomarkers, rat models, neuro-glia damage, systemic responses

INTRODUCTION

The nature of twenty-first century warfare has led to a significant increase in human exposure to blast overpressure (OP) impulses, which result in a complex of neuro-somatic disorders, including traumatic brain injury (TBI). Blast-related casualties outnumber conventional injuries during the last several years in Iraq and Afghanistan, while blast itself is being termed "the fourth weapon of mass destruction" (Born, 2005). Moreover, for every blast-related fatality, many more soldiers suffer multiple, low level non-lethal blast exposures. This often leads to mild traumatic brain injury (mTBI), which is rarely recognized in a timely manner and has become a signature injury of the Iraq and Afghanistan conflicts (Warden, 2006; Jones et al., 2007; Terrio et al., 2009). Symptoms of mild or moderate blast brain injury often do not manifest themselves until sometime after the injury has occurred (Cernak et al., 1999, 2011; Yilmaz and Pekdemir, 2007; Cernak and Noble-Haeusslein, 2010) and go undiagnosed and untreated because emergency medical attention is directed toward more visible injuries, such as penetrating flesh wounds (Belanger et al., 2005; Nelson et al., 2006; Wolf et al., 2009). However, even mild and moderate brain injuries can produce significant deficits and, particularly when repeated, can lead to sustained neuro-somatic damage and neurodegeneration (Cernak and Noble-Haeusslein, 2010). Thus, identifying pathogenic mechanisms and biochemical markers of blast brain injury in relevant experimental models is vital to the development of diagnostics for mTBI through severe TBI.

However, because of the design inconsistency of blast/shock generators used in the different studies, incomplete understanding of blast wave biophysics associated with real explosives vs. those produced by air or gas-driven shock tubes, and the details of wave interaction with model animals, disparities between laboratory models and data on brain injury mechanisms and putative biomarkers have been difficult to analyze and compare (Jaffin et al., 1987; Elsayed, 1997; Guy et al., 1998b; Chavko et al., 2009; Gyorgy et al., 2011, see Bass et al., 2012 for review). Moreover, pathogenic pathways and molecular signatures of neural responses and injurious effects of blast exposures remain elusive. Recently, we developed and employed a model of "composite" blast exposure with controlled parameters of blast wave impact and brain injury in rats (Svetlov et al., 2010). Our studies demonstrated the importance of positional orientation of the head and whole body of rats toward a blast wave generated from an external shock tube (Svetlov et al., 2011). Data from several laboratories including our studies (Svetlov et al., 2010, 2011) suggest that the mechanisms underlying blast-induced injuries, particularly mild/moderate, appear to be distinct from those imposed by mechanical impact or acceleration, and may involve the prominent systemic response (please see Cernak, 2010 for review).

The main objective of this study was to compare the effects of moderate peak overpressure exposure (primary blast) with brain injury produced by a severe/moderate blast accompanied by strong head acceleration (composite blast). The high speed imaging using Schlieren optic demonstrated blast wave interaction with the animal's head/body and revealed a negligible degree of acceleration at a position "off-axis" with the shock tube (primary blast wave exposure) compared to the "on-axis" experimental setup, which was accompanied by strong head/cervical acceleration generated by peak OP + venting gas (composite blast, or primary blast wave plus gas jetting phenomena). The specific dynamics of systemic, vascular inflammatory, and neuro-glial injury signatures, including neuron-specific enolase (NSE)/ubiquitin C-terminal hydrolase L1 (UCH-L1), GFAP, and CNPase biomarkers in serum, were established and characterized. For major pathway signatures and biomarkers, the detected levels raised at all the set-ups studied. However, the most significant and persistent changes in neuro-glial markers were found after composite blast, while primary blast instigated prominent systemic/vascular reactions, particularly when the whole animal body was subjected to blast wave.

MATERIALS AND METHODS

HARDWARE DESIGN AND SETUP

The compressed air-driven shock tube capable of generating a wide range of controlled blast waves was described in details previously (Svetlov et al., 2010). The tube consists of two sections: high pressure (driver) and low-pressure (driven) separated by a diaphragm. Peak overpressure, composition, and duration of the generated high pressure shockwaves are determined by the shock tube configuration including thickness, type of diaphragm material, driver/driven ratio, and the initial driver pressure at the moment of diaphragm rupture. In the presented series of experiments to explore the effects of different components of the blast/shock waves on the targeted animal brain we employed different spatial set-ups as described below. The blast pressure data was acquired using PCB piezoelectric blast pressure transducers and LabView 8.2 software. A National Instruments 1.25 M samples/s data acquisition card was used to acquire data from multiple channels. The rat head images during the blast event were captured at 40,000 frames/s using a high speed video camera (Phantom V310, Vision Research, Wayne, NJ, USA) and mirror-based Schlieren optics.

ANIMAL EXPOSURE TO A CONTROLLED BLAST WAVE

All experimental procedures in rats, including post-blast euthanasia, tissue, and blood collection were performed under guidelines and upon approval by the IACUC of the University of Florida and the ACURO office of the Department of Defense. Modeling of the primary blast and the "composite" overpressure load was achieved by variable positioning of the target vs. blast generator. All rats were anesthetized with isoflurane inhalations described previously in detail. After reaching a deep plane of anesthesia, they were placed into a holder exposing either only their head (body-armored setup) or whole body at the distance 5 cm below the exit nozzle of the shock tube. Rats were positioned either directly on the shock tube axis or at the 45° angle to it to expose them correspondingly to the "composite" blast including the compressed air jet or only to the primary blast wave (**Figure 1D**). Animals were then subjected to a single blast with a mean peak overpressure at the target of 230–380 kPa (**Figures 1A,B**). The exact static and dynamic overpressure values depending on the angle and distance of rat head from the nozzle of shock tube were established during the prior calibration tests (**Figure 1C**). The control group of animals underwent the same treatment (anesthesia, handling, recovery) except they were not exposed to blast.

BLOOD AND TISSUES COLLECTION

At the required time points following blast exposure, animals were euthanized, blood was withdrawn directly from the heart under isoflurane anesthesia and brain tissue samples were collected, snap-frozen in liquid nitrogen and stored at −70°C until further analysis. Immunohistochemical analysis. At 1 and 7 days after TBI (primary, head-only blast) animals were euthanized with lethal dose of pentobarbital, transcardially perfused with 4% paraformaldehyde and whole brains were removed, processed, and embedded in paraffin. Immunohistochemistry analysis was performed on paraffin-embedded 6 μm brain sections. Slides were de-paraffinized, incubated for 10 min at 95°C in Trilogy solution (Cell Marque, Rocklin, CA, USA) for antigen retrieval, blocked for endogenous peroxides, and incubated with primary antibodies for GFAP (Cell Signaling Technology, Danvers, MA, USA) or CNPase (Abcam, Cambridge, MA, USA) overnight at 4°C followed by treatments with secondary antibodies. The staining was visualized with 3,3′-diaminobenzidine (DAB; Dako, Carpinteria, CA, USA) for brown color development. Sections were counterstained with Hematoxylin (Dako). Negative controls were performed by treatment with species-matched secondary antibodies only (not shown). The slides were scanned and examined using Aperio ScanScope GL system with either 5× or 20× objective and ScanScope software.

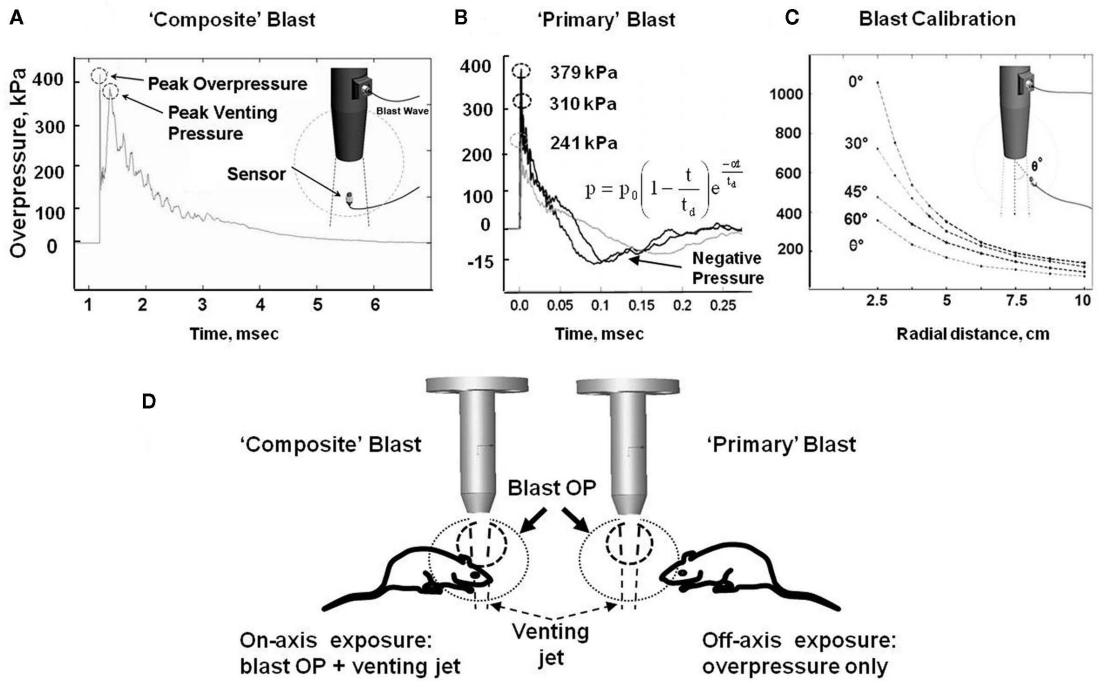

FIGURE 1 | Schematic presentation of blast exposure modeling in rats. (A) Overpressure recording on shock tube axis at 5 cm from the nozzle. **(B)** Overpressure recording with external "pencil" PCB at 5 cm and 45° from shock tube nozzle at three different diaphragm configurations. **(C)** Calibration of pressure on rat head depending on the angle and distance from the nozzle of shock tube. **(D)** Different shock tube set-ups to model "primary" and "composite" blast. Inset formula in **(B)** an empirical expression for the pressure decay with time at a fixed distance is characterized by a decay parameter α Kinney (1985).

SILVER STAINING ASSESSMENT OF NEURODEGENERATION IN RAT BRAIN

Neuroinjury and neurodegeneration was examined in the perfused and fixed brains using silver staining histochemical procedures according to Neuroscience Associates (Knoxville, TN, USA) utilizing the de Olmos Amino Cupric Silver Stain as previously described in detail (Svetlov et al., 2010). In addition, silver staining Kit from FD NeuroTechnologies (Ellicott City, MD, USA) was used where indicated. Rats were subjected to (i) "composite" head-directed severe blast exposure (358 kPa/10 ms total) on-axis (body protected); (ii) primary blast-off-axis exposure to peak overpressure only (233 kPa/113 μs total); and (iii) controlled cortical impact (CCI) of 2.0 mm depth performed as described previously (Liu et al., 2010).

WESTERN BLOT ANALYSIS OF BRAIN TISSUES

For Western blot analyses tissue samples were prepared, separated by SDS-polyacrylamide gel electrophoresis and electro-blotted onto polyvinylidene difluoride membranes as described previously in detail (Svetlov et al., 2010). After overnight incubation with primary antibodies for CNPase or Neuropilin-2 (Cell Signaling Technology, Danvers, MA, USA) proteins were incubated with conjugated secondary antibodies and detected by either colorimetric or chemiluminescent (ECL) detection system. Actin was used as a loading control and bands of interest were normalized for actin expression. Semi-quantitative assessment of protein levels by western blot densitometry was conducted using NIH ImageJ image processing program.

Protein ELISA assays. Commercially available Sandwich ELISA (SW ELISA) kits for GFAP (BioVendor, Candler, NC, USA), NSE (Life Sci. Advanced Tech., St. Petersburg, FL, USA), β-NGF; Abnova, Walnut, CA, USA), Orexin A (Uscn Life Sci., Wuhan, P. R. China), L-selectin (CUSABIO Biotech, Wuhan, P. R. China) and soluble intercellular adhesion molecule-1 (sICAM-1; CUSABIO Biotech) were used according to the manufacturer's instructions. UCH-L1 in CSF and plasma was quantitatively detected using proprietary SW ELISA (Banyan Biomarkers, Inc.) and recombinant UCH-L1 as standard.

ANTIBODY ARRAY ASSAYS

Custom Biotin Label-based (L-series) Rat Antibody array (RayBiotech, Norcross, GA, USA) was used to assess relative levels of Interleukin-1, Interleukin-10, Neuropilin-2, Fractalkine, and Integrin α/β in rat serum following blast exposure.

STATISTICS

Statistical analyses were performed using GraphPad Prism 5 software. Values are means ± SEM. Data were evaluated by two-tailed unpaired *t*-test with or without Welch corrections where indicated.

RESULTS

RAT MODELS OF BLAST EXPOSURE USING EXTERNAL SHOCK TUBE: PRIMARY BLAST LOAD VS. "COMPOSITE" BLAST EXPOSURE

Our shock tube was designed and built to model a freely expanding blast wave as generated by a typical explosion. Both static and

dynamic (total) pressures were measured as functions of angle and radial distance from shock tube exit using piezoelectric blast pressure transducers positioned at the target (**Figure 1C**). The pressure transducers registered three distinct events: (i) peak OP, (ii) gas venting jet-on-axis only, and (iii) negative pressure phase-off-axis only (**Figures 1A,B**). The exhaust of venting gas apparently distorted propagation of the blast wave and no negative phase was registered when dynamic pressure was measured on-axis of shock tube (**Figure 1A**), while a distinct and substantial negative phase (15–20 kPa) was detected off-axis (**Figure 1B**). Peak OP, positive phase duration, and impulse appear to be the key parameters that correlate to injury and likelihood of fatality in animals and humans, for various orientations of the specimen relative to the blast wave. A schematic of a shock tube nozzle and the alternative rat locations relative to the shock tube axis, blast OP wave, and gas venting cone is shown in **Figure 1D**. Shock tubes produce a "venting gas jet" immediately after the blast wave forms, substantially contaminating the blast wave in the direction of the shock tube axis (**Figure 1D**). In a composite blast setup, venting gas jet lasts the longest (up to ∼3–5 ms), albeit lower in magnitude than peak overpressure, represents the bulk of blast impulse, and possibly produces the most devastating impact. Schlieren optics (**Figure 2A**) demonstrated a strong downward head acceleration following the passage of peak overpressure which lasts 50–100 μs. However, cranial deformation was more severe during the gas venting phase, lasting up to 5 ms. This effect was eliminated by placing rats off-axis from the venting jet in a way that the main effect acting on the specimen is the peak overpressure event. The high speed recording coupled with Schlieren optical system visualized interaction of the blast wave with the animal head/body and revealed a negligible degree of acceleration at rat positioning "off-axis" toward shock tube (primary blast; **Figure 2B**). The pressure on the surface of rats was calibrated depending on the distance and angle from the nozzle of shock tube (**Figure 1C**).

NEURAL INJURY AND GLIOSIS IN RAT BRAIN AFTER DIFFERENT BLAST EXPOSURES ASSESSED BY SILVER STAINING AND IMMUNOHISTOCHEMISTRY

As can be seen in **Figure 3**, composite blast (on-axis) produces silver accumulation at the seventh day post-blast (**Figures 3A,D**), particularly in the hippocampus (indicated by arrows). CCI also results in positive staining in ipsilateral cortex and hippocampus (**Figures 3C,F**). In contrast, there was a rare occurrence of silver accumulation observed in the cortex or hippocampus after exposure to primary blast (**Figures 3B,E**; indicated by arrowheads).

Time-dependent expression of GFAP and CNPase characteristic for astrocytes and oligodendrocytes, respectively was studied by IHC after moderate composite on-axis blast (358 kPa/∼10 ms) with strong head acceleration or moderate primary off-axis blast (234 kPa/113.8 μs positive phase) with minor head acceleration (**Figure 4**). These data suggest that both primary and "composite" blasts strongly induce astrogliosis (GFAP, **Figure 4**: upper panel) and oligodendrocytosis (CNPase, **Figure 4**: lower panel) in rat hippocampus evident as early as 1 day and lasting up to 7 days post-blast.

SERUM LEVELS OF BIOMARKERS OF NEURO-GIAL INJURY FOLLOWING BLAST EXPOSURE

To asses if markers of neuronal injury are released into circulation, we assayed serum levels of NSE and UCH-L1 after different blast exposures (**Figure 5**). As shown in **Figure 5A**, remarkable accumulation of NSE in serum occurred within 6 h following exposure to either "composite" or primary blast, and persisted up to 7 days post-blast. Average serum UCH-L1 level was also elevated during 1–7 days after "primary" blast (**Figure 5B**), though its difference from controls was statistically significant only at 1 day post-blast.

Glia cell-specific up-regulation of GFAP and CNPase in brain after either "composite" or primary blast was accompanied by a significant serum accumulation of GFAP and CNPase biomarkers measured by SW ELISA for GFAP (**Figure 6A**) and semi-quantitative western blot densitometry for serum CNPase (**Figure 6B**). These biomarkers persisted in blood up to 7 days post-blast at both blast set-ups employed.

SYSTEMIC, VASCULAR INFLAMMATORY, NEUROENDOCRINE AND GROWTH FACTOR RESPONSES FOLLOWING DIFFERENT BLAST EXPOSURES

Based on our previous global and targeted proteomic data, the following molecular components and injury biomarkers were assessed in rat serum. Systemic/vascular responses: interleukin-1 and interleukin-10 (IL-1, IL-10), adipo-chemokine Fractalkine/CX3CL1, Integrin α/β, a complement receptor composed of CD11c/CD18, sICAM-1, and L-, E-selectin.

CYTOKINE/CHEMOKINE LEVELS AFTER BLAST EXPOSURES

We hypothesized that systemic responses and neuroinflammmation together with impaired vascular reaction in the brain, result in enhancement of endothelial permeability/leakage, infiltration of macrophages from circulation and activation of brain-resident microglia cells. As can be seen in **Figures 7A,B**, both pro-inflammatory (IL-1) and counteracting anti-inflammatory molecules (IL-10) accumulate in circulation at 24 h after open body exposure to frontal (off-axis) blast. These results are in agreement with data obtained using non-blast TBI models (Dietrich et al., 2004; Maegele et al., 2007). Moreover, CX3CL1 chemokine Fractalkine was also significantly elevated after primary blast further suggesting a systemic component in response to blast (**Figure 7C**) consistent with reports on the level of this chemokine in patients with TBI and in mouse model of closed head injury (Rancan et al., 2004; Ralay Ranaivo et al., 2011). While immune cell-derived IL-1, IL-10, and fractalkine were significantly increased predominantly after primary blast exposure, integrin alpha/beta levels were elevated at all set-ups indicating that blast is triggering microcirculatory disorders whether it produces head hyperacceleration or not.

SERUM ACCUMULATION OF SICAM-1 AND L-SELECTIN CONNECTING VASCULAR INFLAMMATORY AND TISSUE DAMAGE

Soluble intercellular adhesion molecule, E-selectin and L-selectin are adhesion molecules which reflect the activation of the vascular component of inflammation and interaction of circulatory cells with the endothelial component of blood–brain-barrier (BBB; Nottet, 1999; Whalen et al., 1999, 2000). sICAM levels in serum

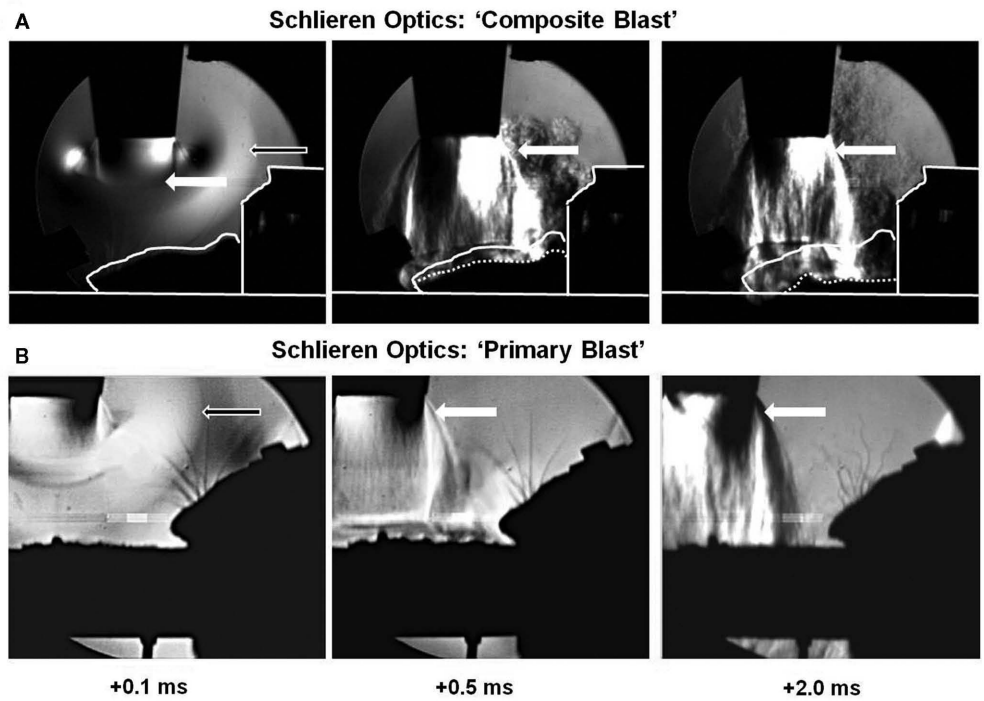

FIGURE 2 | Visualization of blast wave interaction with head on-axis ("composite" blast) and off-axis (primary blast) using Schlieren optics. High speed recording with Schlieren optics: **(A)** "composite blast"; **(B)** "primary blast." Black arrows indicate formation, traveling, and interaction of blast wave with rat head (accomplished within ∼0.1 ms). White arrows show gas venting jet hitting rat head after blast wave passed through (persists for milliseconds). The solid contour line in **(A)** outlines the shape of animal head at time point 0; the dotted line-current shape. Please see Section "Materials and Methods" for details.

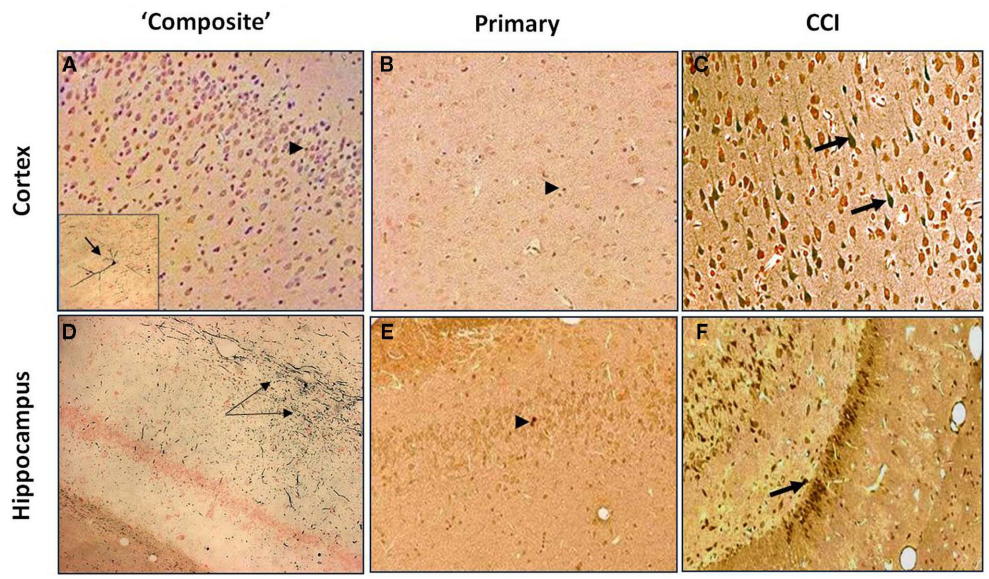

FIGURE 3 | Silver Staining of coronal brain sections following primary or "composite" blast exposure. Corresponding tissue staining 7 days after "composite blast," primary blast, and CCI is shown in **(A–C)** for cortex, and in **(D–F)** for hippocampus. Arrowheads indicate occasional silver accumulation in the cells of non-neuronal origin. Arrows indicate diffuse silver accumulation in neurons. **Figure 3A** inset: a very rare accumulation of silver in a cortical neuron. Please see Section "Materials and Methods" for details.

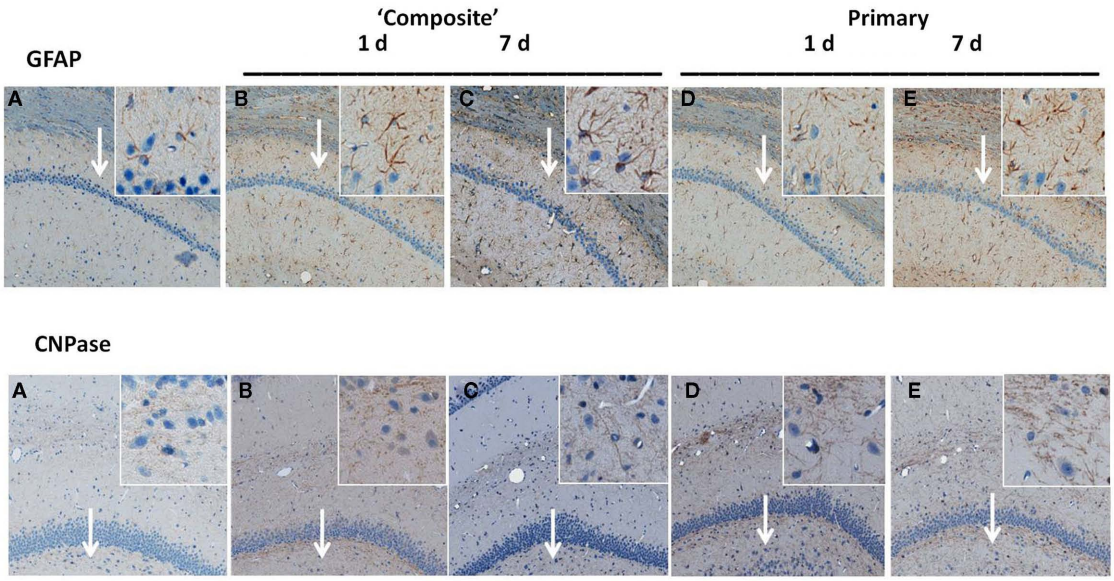

FIGURE 4 | Immunohistochemical analysis of astrocyte and oligodendrocyte markers in hippocampus after blast. Time-dependent GFAP and CNPase expression was studied by IHC on paraffin-embedded 6 μm brain sections after blast exposure at different set-ups. **(A)** Naive; **(B)** "composite" blast, 1 day; **(C)** "composite," 7 days; **(D)** "primary," 1 day; and **(E)** "primary," 7 days. Magnifications 5× and 20× (insets) are shown. Arrows indicate inset locations for CA1 region (GFAP) and DG region (CNPase) in hippocampus. Please see Section "Materials and Methods" for details.

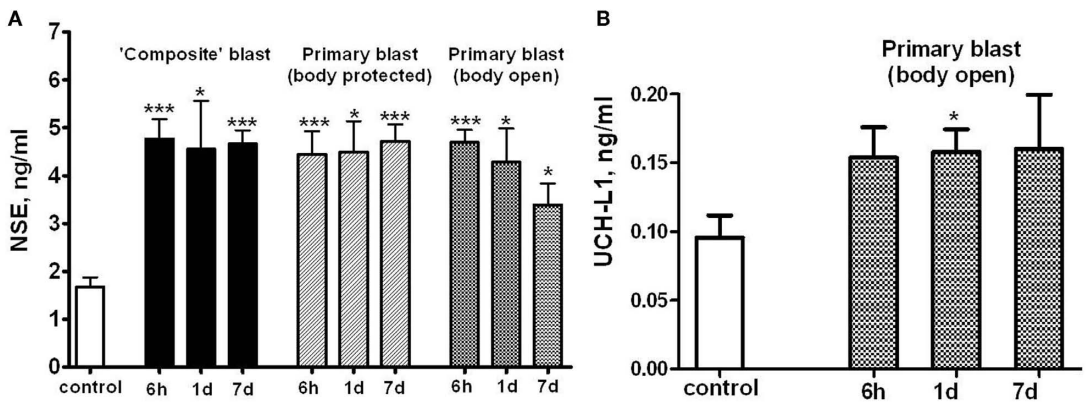

FIGURE 5 | Blast-induced accumulation of NSE and UCHL-1 in rat serum. Blood was collected from overpressure-exposed rats at different shock tube set-ups and assayed by NSE **(A)** and UCHL1 **(B)** SW ELISA Kits. Unpaired *t*-test was used to analyze statistical significance of values. Data shown are mean ± SEM of at least three independent experiments. $*p < 0.05$; $**p < 0.01$; $***p < 0.005$ vs. naïve. Please see Section "Materials and Methods" for details.

raised nearly fourfold within 6 h post-blast, followed by a decline to lower, but still significantly higher than control levels, values at day 7 after exposure to both composite and primary blast (**Figure 8A**). In contrast, serum L-selectin content increased remarkably at 1 and 7 days, but not 6 h following blast (**Figure 8B**). Thus, the prominent activation of the L-selectin component of blast responses occurs when peak overpressure interacts with the frontal part of the head without significant acceleration, reflecting a somewhat delayed involvement of leukocytes compared with earlier (6 h) vascular endothelial activation indicated by sICAM-1 and, to some extent, serum integrin alpha/beta increases.

NEUROENDOCRINE, NEUROTROPHIC, AND GROWTH FACTOR RESPONSES AFTER BLAST EXPOSURE

Orexin A is a neuropeptide secreted by the hypothalamus, which promotes food intake, wakefulness, and metabolic activity/energy consumption. As seen in **Figure 9**, a nearly threefold increase in serum Orexin A occurs 1 and 7 days after primary blast with open body, but not after composite blast, at least within the 7 day interval.

Using a targeted approach, we identified additional components of neurotrophic response to blast exposure – nerve growth factor beta (NGF-beta) and Neuropilin-2 (NRP-2). NGF-beta has

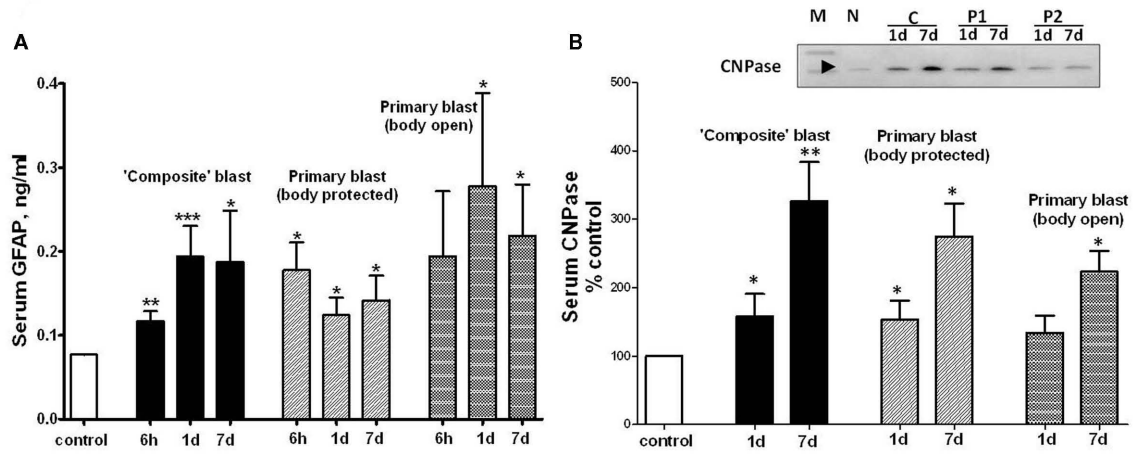

FIGURE 6 | GFAP and CNPase levels in blood after different blast exposures. Blood was collected after OP exposure at different shock tube set-ups. **(A)** Serum GFAP detection by SW ELISA; **(B)** semi-quantitative serum CNPase detection by western blot densitometry. Inset: representative western blot. (N, naïve; C, "composite"; P1, primary/head; P2, primary/body). *t*-Test with Welch correction was done. Data shown are mean ± SEM of at least three independent experiments. $*p < 0.05$; $**p < 0.01$; $***p < 0.005$ vs. naïve. Please see Section "Materials and Methods" for details.

been suggested to play a neurotrophic role in several neurodegenerative diseases (Li et al., 2007; Syed et al., 2007; Calissano et al., 2010). Neuropilin-2 is a receptor for VEGF and semaphorins, a large family of secreted and transmembrane signaling proteins that regulate axonal guidance in the developing CNS (Cloutier et al., 2002; Bannerman et al., 2008; Roffers-Agarwal and Gammill, 2009). Serum levels of NGF-beta were assessed using SW ELISA and NRP-2 by antibody array (Ray Biotech) and semi-quantitative western blot after blast exposure at different set-ups (**Figure 10**). Generally, exposures to composite and primary blast resulted in a significant increase of NGF-beta in serum 1 and 7 day after challenge, however the magnitude of increase was much higher after primary blast hit open body compared to composite blast exposure (**Figure 10A**). Likewise, high levels of NRP-2 were found in circulation at 1 and 7 day in rats exposed to primary blast with unprotected body, as compared to composite blast together with NRP-2 up-regulation in hippocampus at all blast set-ups. These data suggest that predominantly primary blast activates neuroregeneration and that NRP-2 may be involved in this process. In addition, these results indicate that NGF-beta and NRP-2 may have neuroprotective functions and be involved in adaptive responses/neurorepair after blast-induced TBI.

DISCUSSION

Over the last several decades, a number of experimental animal models to study blast wave effects have been implemented, including rodents and larger animals, such as sheep (Savic et al., 1991; Stuhmiller et al., 1996). Shock tubes have been used as the fundamental research tool for the last several decades (Jaffin et al., 1987; Elsayed, 1997; Guy et al., 1998a,b). There is still concern whether a blast waves generated by shock tubes using compressed gas accurately reflect real explosive blast. In our study, dynamic pressure measured by a PCB "pencil" sensor indicated that shock tubes produce a "venting gas jet" immediately after blast wave formation (see the shoulder at **Figure 1A**), substantially contaminating the blast wave in the direction of shock tube axis (**Figure 1A**). In addition, the exhaust "venting gas" apparently masked the negative phase of the shock wave, which was present when the dynamic pressure was recorded at an angle to the shock tube nozzle (**Figure 1B**). Schlieren optics techniques clearly defined the areas of pressure, either peak OP or venting gas jet (**Figure 2**).

This pattern is characteristic of "external" shock tube models where the target/animal is placed outside rather than within the tube. Placing animals within the tube also can produce confounding effects when the animal is very large relative to the tube diameter or when the animal is suspended and or shielded inappropriately. The shape of the blast wave and the development of constructive or destructive secondary waves as the primary wave exits the tube can be affected by the size and shape of the exit as well. This can be visualized with Schlieren optics. By placing rats off-axis from the shock tube nozzle, we eliminated the venting gas in a way that the main effect acting on the rat is the peak overpressure event and negative phase of the blast wave. Thus, we examined the pathological impact of two different types of blast with precisely controlled magnitude, duration, and impulse at the surface of the rat, different orientations of the head to the blast wave, and open or armored body: (i) primary blast/peak overpressure only with rats located off-axis with the shock tube and (ii) composite blast with rats located on-axis, accompanied by linear and, to a lesser extent, rotational head hyperacceleration (**Figure 2**). It should be noted that any blast produced in the laboratory models only a particular component of a complex blast that might be experienced on the battlefield. The detonation of real explosives in the field does not produce the "venting gas," but can result in significant bulk flow of air and debris. This makes the separation of the effects of primary and particularly tertiary blast (the target being displaced by the blast) difficult to separate in most existing testing regimes. Although the blast generated in our on-axis model is a single blast event, the type of blast load observed resembles the complex effect produced by multiple blasts, such as in a confined

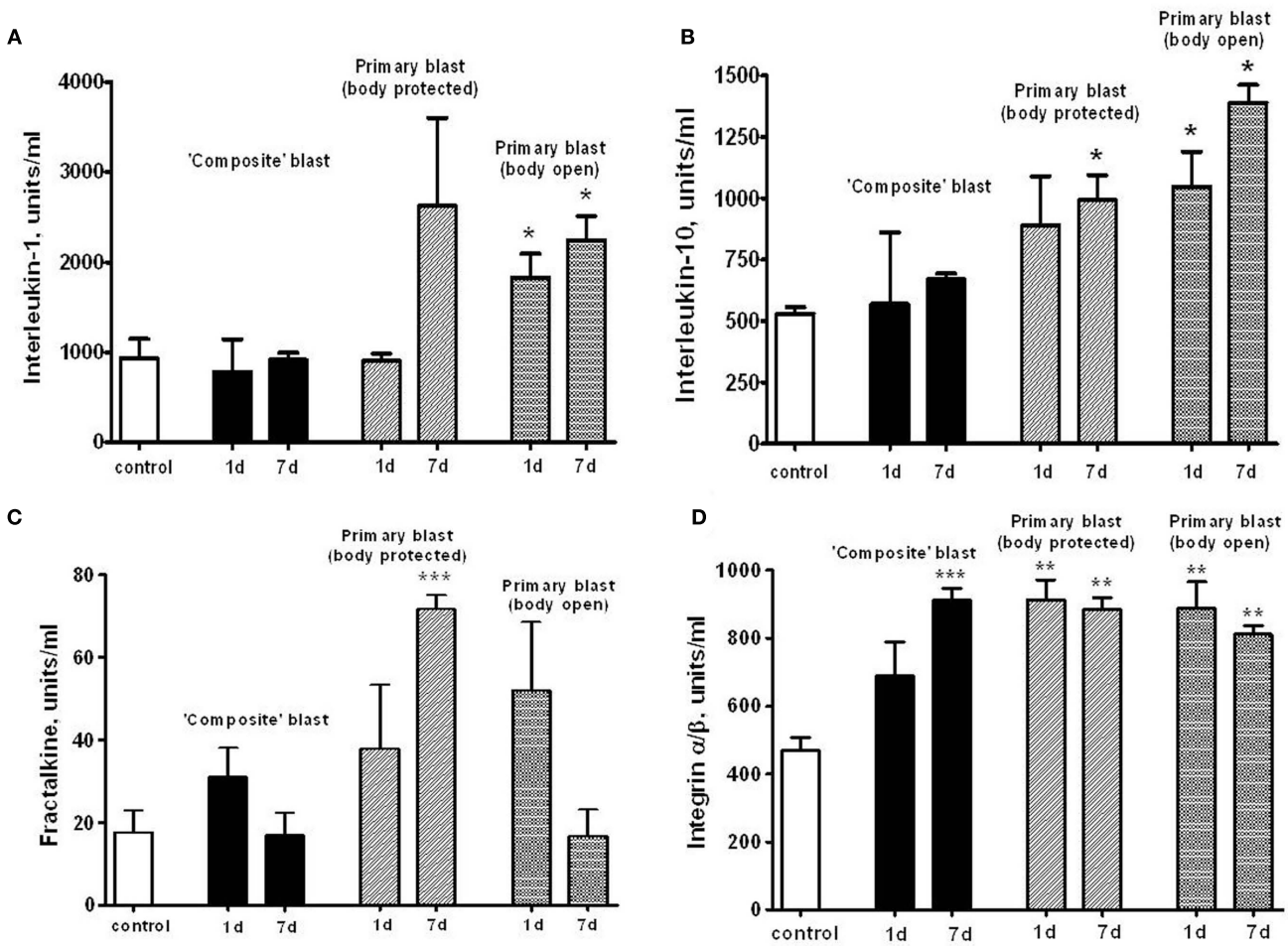

FIGURE 7 | Serum levels of interleukins, fractalkine, and integrin α/β after blast. Concentrations of interleukin-1 **(A)**, interleukin-10 **(B)**, fractalkine **(C),** and integrin α/β **(D)** were assessed in rat serum by RayBiotech antibody arrays. Please see Section "Materials and Methods" for details. Blood was collected from OP-exposed rats at different shock tube set-ups. Unpaired *t*-test was used to analyze statistical significance of values. Data shown are mean ± SEM of at least three independent experiments. $*p < 0.05$; $**p < 0.01$; $***p < 0.005$.

space where the blast waves reverberate and overlap, hence the effect of displaced air mass flow on the resultant wave structure and magnitude can be important.

There was a substantial difference in the effects of composite vs. primary blast on neurodegenerative processes in the cortex and, particularly, hippocampus at 7 day post-blast (**Figure 3**). Silver accumulation in the cortex after composite blast was modest, with a very rare finding of "classical type" neurodegeneration (**Figure 3A**, inset). On the other hand, the hippocampus significantly accumulated silver in fiber-like structures after composite blast (**Figure 3D**), while very occasional silver staining was observed in both cortex and hippocampus after primary blast (**Figures 3B,E**). As expected and in accordance with data reported previously, CCI evoked a distinct cellular neurodegeneration in both cortical and hippocampal tissue (**Figures 3C,F**). The most common types of closed head impact TBI are diffuse axonal injury, contusion, and subdural hemorrhage as an overall result of rotational acceleration (Vander Vorst et al., 2007). Diffuse axonal injuries are very common following closed head injuries. They result when shearing, stretching, and/or angular forces pull on axons and small vessels. Impaired axonal transport leads to focal axonal swelling and, after several hours, may result in axonal disconnection (Hurley et al., 2004). The typical locations are the corticomedullary (gray matter-white matter) junction, internal capsule, deep gray matter, upper brainstem, and corpus callosum. Multifocal axonal degeneration, as evidenced by amino cupric silver staining is characteristic also for shock wave insult as was shown in a study with head-only exposed rats inside a shock tube (Garman et al., 2011). Our recent (Svetlov et al., 2010) and present studies clearly demonstrate the presence of neural degeneration in deeper structures of the brain, specifically hippocampus after composite blast producing linear and rotational head acceleration, which is lacking or negligible following primary blast.

Exposure to a single moderate blast, both composite and primary, led to prominent gliosis in the hippocampus, evidenced by expression of GFAP and CNPase (**Figure 4**). Markers of activated

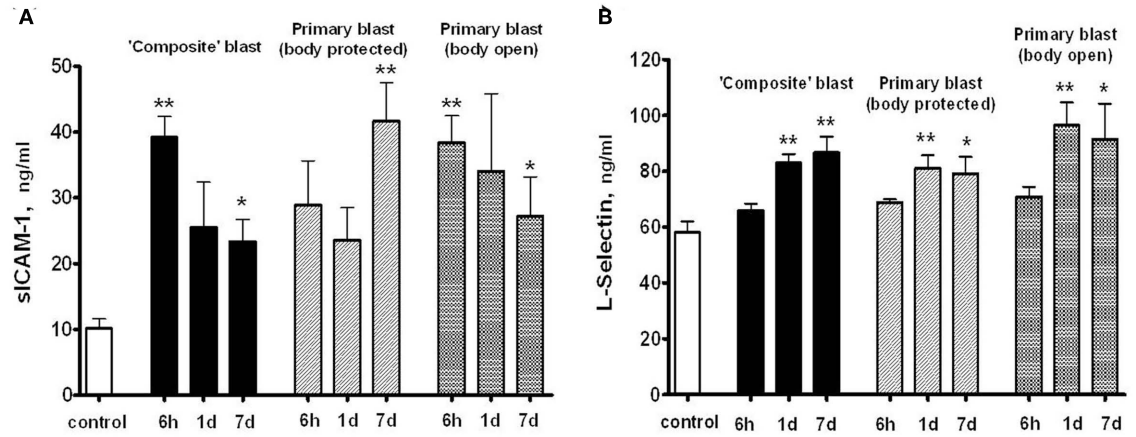

FIGURE 8 | Soluble intercellular adhesion molecule -1 (A) and L-selectin (B) concentrations in rat serum following blast exposure. Blood was collected after blast at different shock tube set-ups and assayed by SW ELISA. Unpaired *t*-test was done to analyze statistical significance of values. Data shown are mean ± SEM of at least three independent experiments. $*p < 0.05$; $**p < 0.01$; $***p < 0.005$ vs. naïve. Please see Section "Materials and Methods" for details.

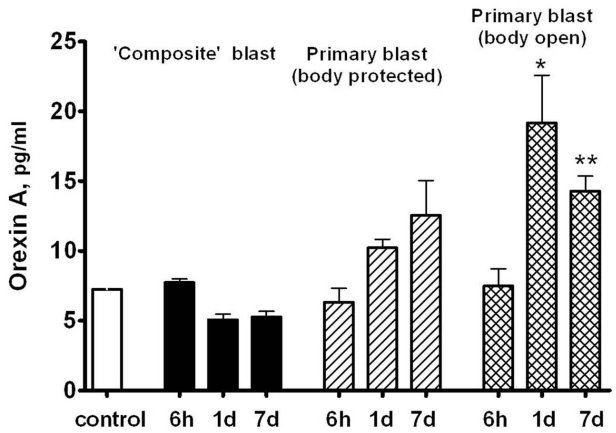

FIGURE 9 | Orexin A content in rat serum after blast. Blood was collected from overpressure-exposed rats at different shock tube set-ups and assayed by SW ELISA. Unpaired *t*-test was done to analyze statistical significance of values. Data shown are mean ± SEM of at least three independent experiments. $*p < 0.05$; $**p < 0.01$; $***p < 0.005$ vs. naïve. Please see Section "Materials and Methods" for details.

astrocytes GFAP and oligodendrocytes CNPase were strongly up-regulated in CA1 and DG regions of hippocampus, respectively, at 1 day and sustained up to 7 days post-blast. These findings are in strict accordance with many previous reports, including from our group, supporting the notion that gliosis represents a common and rapid response to brain insult regardless of the nature-mechanical or blast-induced exposure (Urrea et al., 2007; Svetlov et al., 2010; Kwon et al., 2011).

NSE was significantly elevated in serum within 6 h after both composite and primary blast (**Figure 5A**), and the increased levels generally persisted up to 7 days, although was not statistically significant upon open body primary blast exposure. In these experiments, we used NSE SW ELISA Kit from Life Sciences Advanced Technologies designed to detect specifically rat NSE. However, several reports indicate that NSE may not be highly specific for the CNS and is present in platelets and red blood cells (see Svetlov et al., 2009 for review). In previous studies, we reported a slight UCH-L1 increase after "composite" blast, followed by a rapid decline (Svetlov et al., 2010). The UCH-L1 SW ELISA used in early experiments had low specificity and sensitivity for rat samples, thus many serum substances interfered and masked the UCH-L1 content. In this study, an improved version of the UCH-L1 assay was employed, still not particularly specific for rats (data not shown). Increases in serum UCH-L1 were statistically significant only at day 1 after a single primary blast exposure ($n = 4$), although an elevation trend could be detected (**Figure 5B**). In contrast, a rat-specific GFAP SW ELISA has been generated and employed in these studies. Serum GFAP increase was prominent within 6 h after composite and primary blast with body protected (**Figure 6A**), and elevated levels persisted up to 7 days post-blast, consistent with up-regulation in hippocampus. The CNPase content assessed by semi-quantitative western blot was raised at day 1 after blast exposure (except primary blast with open body) and further substantially increased at 7 day post-blast (**Figure 6B**). It remains to be examined whether CNPase up-regulation reflects a long-term disorder of myelination following blast exposure and whether CNPase can be a biomarker of chronic injury.

We postulated that impaired vascular reactions, systemic responses, and neuroinflammmation, result in enhancement of endothelial permeability/leakage, recruitment of immune/inflammatory cells from circulation, and activation of brain-resident glial cells. This paradigm is in line with the previous hypothesis set forth by Cernak (2010) and is further supported by present data.

As can be seen in **Figures 7A,B**, both pro-inflammatory (IL-1) and counteracting anti-inflammatory molecules (IL-10) accumulate in circulation at 1 and 7 days post-blast, predominantly after

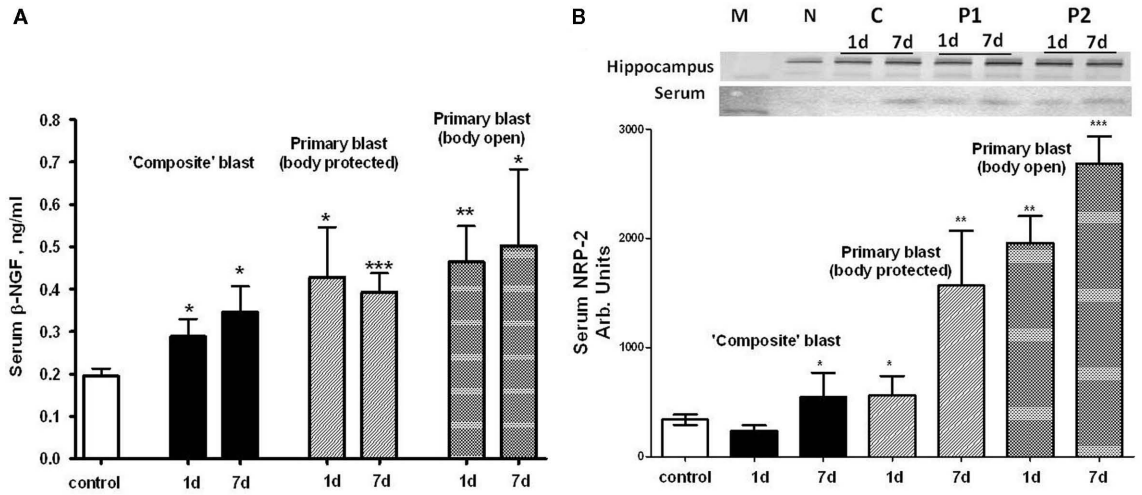

FIGURE 10 | Blast-induced accumulation of β-NGF and Neuropilin-2 in rat serum. (A) Serum β-NGF after different types of blast (SW ELISA); **(B)** serum Neuropilin-2 detection by antibody arrays. Inset: representative western blots for hippocampus and serum. (N, naïve; C, "composite"; P1, primary/head; P2, primary/body). *t*-Test with Welch correction was done. Data shown are mean ± SEM of at least three independent experiments. $*p < 0.05$; $**p < 0.01$; $***p < 0.005$ vs. naïve. Please see Section "Materials and Methods" for details.

primary blast exposure with open body (**Figures 7A,B**). These results are in agreement with data obtained using non-blast TBI models (Dietrich et al., 2004; Maegele et al., 2007). Moreover, CX3CL1 chemokine Fractalkine was also significantly elevated after primary blast (mostly with protected body), further suggesting a systemic component in response to blast (**Figure 7C**), consistent with reports on the level of this chemokine in patients with TBI and in mouse model of closed head injury (Rancan et al., 2004; Ralay Ranaivo et al., 2011). Most intriguing is that serum IL-1, IL-10, and Fractalkine did not rise significantly after composite blast at 1 and 7 days post-blast. In contrast, integrin alpha/beta, a complement receptor composed of CD11c/CD18, was increased substantially at all set-ups (**Figure 7D**), further supporting the important roles for a microcirculatory component of neuroinflammation in brain injury shown in rat models of fluid percussion injury (Utagawa et al., 2008).

L-selectin and ICAM-1 are adhesion molecules which characterize the activation of a vascular component of inflammation and interaction of circulatory cells with the endothelial component of the (BBB; Nottet, 1999; Whalen et al., 1999, 2000). As can be seen in **Figure 8**, prominent activation of the L-selectin after blast occurs when peak overpressure interacts with the frontal part of head without significant acceleration, reflecting a somewhat delayed involvement of leukocytes compared with earlier (6 h) vascular endothelial activation reflected by sICAM-1 and, to some extent, serum integrin alpha/beta increases. Thus, the sustained activation of vascular components of blast responses occurs when peak overpressure interacts with the frontal part of the head without significant acceleration: "flowing blast inside the brain" (blast off-axis open body).

Orexin A, a neuroendocrine component of rat response to blast exposure, exhibited the most prominent pattern of difference between composite and primary blast (**Figure 9**). Serum Orexin A levels raised gradually within 1–7 days after primary blast and were significantly elevated in rats subjected to blast with open body. Although at present the precise mechanisms are not clear, this suggests that several systemic factors affected by primary blast wave in the whole body other than brain structures directly or indirectly stimulate hypothalamic release of Orexin A as well as interleukins/chemokines in circulation. We speculate that the presence of a distinct negative phase in primary blast wave is capable of producing cavitation-induced secondary microblasts. This could partially explain the different pattern in systemic/vascular responses to primary vs. composite blast exposure which lacks the negative phase. Further in-depth studies are needed to explore this hypothesis and elucidate potential roles for blast cavitation in damage, particularly at the interface of gas, liquid, and tissue.

Beta-NGF has been suggested to play a neurotrophic role in several neurodegenerative diseases (Li et al., 2007; Syed et al., 2007; Calissano et al., 2010). Our data indicate that NGF may also have neuroprotective functions and be involved in adaptive responses/neurorepair after blast-induced TBI. Exposure of whole body to primary overpressure blast instigated a rapid and sustained accumulation of beta-NGF in serum. Neuropilin-2 is the receptor for VEGF and semaphorins, a large family of secreted and transmembrane signaling proteins that regulate axonal guidance in the developing CNS (Cloutier et al., 2002; Bannerman et al., 2008; Roffers-Agarwal and Gammill, 2009). Our present data (**Figure 10B**) suggest that predominantly primary blast activates neuroregeneration and that NRP-2 may be involved in this process.

In conclusion, the specific dynamics of systemic, vascular inflammatory, neuroendocrine, growth factor, and neuroglial biomarkers in serum were established and characterized. For major pathway signatures and biomarkers, the detected levels raised at all the set-ups studied. However, the most

significant and persistent changes in neuro-glial injury markers were found after composite blast, while primary blast instigated the most prominent systemic/vascular, neuroendocrine, and growth factor responses, particularly when the rat was subjected to frontal, head-directed, open body exposure. We suggest that the mechanisms underlying primary blast brain injuries, particularly mild and moderate, are different from blast accompanied by head acceleration and may be triggered by systemic, cerebrovascular, and neuro-glia responses as overlapping events.

ACKNOWLEDGMENTS

The authors wish to thank Mr. Danny Johnson for his excellent technical assistance. This work was supported by grants W81XWH-8-1-0376 and W81XWH-07-01-0701 from Department of Defense. The research was conducted in the absence of any commercial or financial relationships that could be construed as a potential conflict of interest. The views and opinions expressed in this manuscript are those of the author(s) and do not reflect official policy or position of the Department of Defense or the U.S. Government.

REFERENCES

Bannerman, P., Ara, J., Hahn, A., Hong, L., McCauley, E., Friesen, K., and Pleasure, D. (2008). Peripheral nerve regeneration is delayed in neuropilin 2-deficient mice. *J. Neurosci. Res.* 86, 3163–3169.

Bass, C. R., Panzer, M. B., Rafaels, K. A., Wood, G., Shridharani, J., and Capehart, B. (2012). Brain injuries from blast. *Ann. Biomed. Eng.* 40, 185–202.

Belanger, H. G., Scott, S. G., Scholten, J., Curtiss, G., and Vanderploeg, R. D. (2005). Utility of mechanism-of-injury-based assessment and treatment: Blast Injury Program case illustration. *J. Rehabil. Res. Dev.* 42, 403–412.

Born, C. T. (2005). Blast trauma: the fourth weapon of mass destruction. *Scand. J. Surg.* 94, 279–285.

Calissano, P., and Matrone, C., Amadoro, G. (2010). Nerve growth factor as a paradigm of neurotrophins related to Alzheimer's disease. *Dev. Neurobiol.* 70, 372–383.

Cernak, I. (2010). The importance of systemic response in the pathobiology of blast-induced neurotrauma. *Front. Neurol.* 1:151. doi:10.3389/fneur.2010.00151

Cernak, I., Merkle, A. C., Koliatsos, V. E., Bilik, J. M., Luong, Q. T., Mahota, T. M., Xu, L., Slack, N., Windle, D., and Ahmed, F. A. (2011). The pathobiology of blast injuries and blast-induced neurotrauma as identified using a new experimental model of injury in mice. *Neurobiol. Dis.* 41, 538–551.

Cernak, I., and Noble-Haeusslein, L. J. (2010). Traumatic brain injury: an overview of pathobiology with emphasis on military populations. *J. Cereb. Blood Flow Metab.* 30, 255–266.

Cernak, I., Savic, J., Ignjatovic, D., and Jevtic, M. (1999). Blast injury from explosive munitions. *J. Trauma.* 47, 96–103; discussion 103–104.

Chavko, M., Adeeb, S., Ahlers, S. T., and McCarron, R. M. (2009). Attenuation of pulmonary inflammation after exposure to blast overpressure by N-acetylcysteine amide. *Shock* 32, 325–331.

Cloutier, J. F., Giger, R. J., Koentges, G., Dulac, C., Kolodkin, A. L., and Ginty, D. D. (2002). Neuropilin-2 mediates axonal fasciculation, zonal segregation, but not axonal convergence, of primary accessory olfactory neurons. *Neuron* 33, 877–892.

Dietrich, W. D., Chatzipanteli, K., Vitarbo, E., Wada, K., and Kinoshita, K. (2004). The role of inflammatory processes in the pathophysiology and treatment of brain and spinal cord trauma. *Acta Neurochir. Suppl.* 89, 69–74.

Elsayed, N. M. (1997). Toxicology of blast overpressure. *Toxicology* 121, 1–15.

Garman, R. H., Jenkins, L. W., Switzer, R. C., Bauman, R. A., Tong, L. C., Swauger, P. W., Parks, S. A., Ritzel, D. V., Dixon, C. E., Clark, R. S. B., Bayir, H., Kagan, V., Jackson, E. K., and Kochanek, P. M. (2011). Blast exposure in rats with body shielding is characterized primarily by diffuse axonal injury. *J. Neurotrauma* 28, 947–959.

Guy, R. J., Glover, M. A., and Cripps, N. P. (1998a). The pathophysiology of primary blast injury and its implications for treatment. Part I: the thorax. *J. R. Nav. Med. Serv.* 84, 79–86.

Guy, R. J., Kirkman, E., Watkins, P. E., and Cooper, G. J. (1998b). Physiologic responses to primary blast. *J. Trauma.* 45, 983–987.

Gyorgy, A., Ling, G., Wingo, D., Walker, J., Tong, L., Parks, S., Januszkiewicz, A., Baumann, R., and Agoston, D. V. (2011). Time-dependent changes in serum biomarker levels after blast traumatic brain injury. *J. Neurotrauma* 28, 1121–1126.

Hurley, R. A., McGowan, J. C., Arfanakis, K., Taber, K. H. (2004). Traumatic axonal injury: novel insights into evolution and identification. *J. Neuropsychiatry Clin. Neurosci.* 16, 1–7.

Jaffin, J. H., McKinney, L., Kinney, R. C., Cunningham, J. A., Moritz, D. M., Kraimer, J. M., Graeber, G. M., Moe, J. B., Salander, J. M., and Harmon, J. W. (1987). A laboratory model for studying blast overpressure injury. *J. Trauma.* 27, 349–356.

Jones, E., Fear, N. T., and Wessely, S. (2007). Shell shock and mild traumatic brain injury: a historical review. *Am. J. Psychiatry* 164, 1641–1645.

Kinney, G. F. (1985). *Explosive Shocks in Air*. New York: Spinger-Verlag.

Kwon, S. K., Kovesdi, E., Gyorgy, A. B., Wingo, D., Kamnaksh, A., Walker, J., Long, J. B., and Agoston, D. V. (2011). Stress and traumatic brain injury: a behavioral, proteomics, and histological study. *Front. Neurol.* 2:12. doi:10.3389/fneur.2011.00012

Li, Y., Zhang, S. F., Zou, S. E., Xia, X., Bao, L. (2007). Accumulation of nerve growth factor and its receptors in the uterus and dorsal root ganglia in a mouse model of adenomyosis. *Reprod. Biol. Endocrinol.* 9, 30.

Liu, M. C., Akinyi, L., Scharf, D., Mo, J., Larner, S. F., Muller, U., Oli, M. W., Zheng, W., Kobeissy, F., Papa, L., Lu, X. C., Dave, J. R., Tortella, F. C., Hayes, R. L., and Wang, K. K. (2010). Ubiquitin C-terminal hydrolase-L1 as a biomarker for ischemic and traumatic brain injury in rats. *Eur. J. Neurosci.* 31, 722–732.

Maegele, M., Sauerland, S., Bouillon, B., Schafer, U., Trubel, H., Riess, P., and Neugebauer, E. A. (2007). Differential immunoresponses following experimental traumatic brain injury, bone fracture and "two-hit"-combined neurotrauma. *Inflamm. Res.* 56, 318–323.

Nelson, T. J., Wall, D. B., Stedje-Larsen, E. T., Clark, R. T., Chambers, L. W., and Bohman, H. R. (2006). Predictors of mortality in close proximity blast injuries during Operation Iraqi Freedom. *J. Am. Coll. Surg.* 202, 418–422.

Nottet, H. S. (1999). Interactions between macrophages and brain microvascular endothelial cells: role in pathogenesis of HIV-1 infection and blood – brain barrier function. *J. Neurovirol.* 5, 659–669.

Ralay Ranaivo, H., Zunich, S., Choi, N., Hodge, J., Wainwright, M. (2011). Mild stretch-induced injury increases susceptibility to interleukin-1beta-induced release of matrix metalloproteinase-9 from astrocytes. *J Neurotrauma.* 28, 1757–1766.

Rancan, M., Bye, N., Otto, V. I., Trentz, O., Kossmann, T., Frentzel, S., and Morganti-Kossmann, M. C. (2004). The chemokine fractalkine in patients with severe traumatic brain injury and a mouse model of closed head injury. *J. Cereb. Blood Flow Metab.* 24, 1110–1118.

Roffers-Agarwal, J., and Gammill, L. S. (2009). Neuropilin receptors guide distinct phases of sensory and motor neuronal segmentation. *Development* 136, 1879–1888.

Savic, J., Tatic, V., Ignjatovic, D., Mrda, V., Erdeljan, D., Cernak, I., Vujnov, S., Simovic, M., Andelic, G., and Duknic, M. (1991). Pathophysiologic reactions in sheep to blast waves from detonation of aerosol explosives. *Vojnosanit. Pregl.* 48, 499–506.

Stuhmiller, J. H., Ho, K. H., Vander Vorst, M. J., Dodd, K. T., Fitzpatrick, T., and Mayorga, M. (1996). A model of blast overpressure injury to the lung. *J. Biomech.* 29, 227–234.

Svetlov, S. I, Prima, V., Kirk, D. R., Gutierrez, H., Curley, K. C., Hayes, R. L., and Wang, K. K. W. (2011). "Neuro-glial and systemic mechanisms of pathological responses to primary blast overpressure (OP) compared to "composite" blast accompanied by head acceleration in rats," in Proceeding of NATO conference 'A Survey of Blast Injury across the Full Landscape of Military Science http://www.rto.nato.int/

Svetlov, S. I., Larner, S. F., Kirk, D. R., Atkinson, J., Hayes, R. L., and Wang, K. K. (2009). Biomarkers of blast-induced neurotrauma: profiling molecular and cellular mechanisms of blast brain injury. *J. Neurotrauma* 26, 913–921.

Svetlov, S. I., Prima, V., Kirk, D. R., Gutierrez, H., Curley, K. C., Hayes,

R. L., and Wang, K. K. (2010). Morphologic and biochemical characterization of brain injury in a model of controlled blast overpressure exposure. *J. Trauma.* 69, 795–804.

Syed, Z., Dudbridge, F., and Kent, L. (2007). An investigation of the neurotrophic factor genes GDNF, NGF, and NT3 in susceptibility to ADHD. *Am. J. Med. Genet. B Neuropsychiatr. Genet.* 144B, 375–378.

Terrio, H., Brenner, L. A., Ivins, B. J., Cho, J. M., Helmick, K., Schwab, K., Scally, K., Bretthauer, R., Warden, D. (2009). Traumatic brain injury screening: preliminary findings in a US Army Brigade Combat Team. *J. Head Trauma Rehabil.* 24, 14–23.

Urrea, C., Castellanos, D. A., Sagen, J., Tsoulfas, P., Bramlett, H. M., and Dietrich, W. D. (2007). Widespread cellular proliferation and focal neurogenesis after traumatic brain injury in the rat. *Restor. Neurol. Neurosci.* 25, 65–76.

Utagawa, A., Bramlett, H. M., Daniels, L., Lotocki, G., Dekaban, G. A., Weaver, L. C., and Dietrich, W. D., (2008). Transient blockage of the CD11d/CD18 integrin reduces contusion volume and macrophage infiltration after traumatic brain injury in rats. *Brain Res.* 1207, 155–163.

Vander Vorst, M., Ono, K., Chan, P., and Stuhmiller, J. (2007). Correlates to traumatic brain injury in nonhuman primates. *J. Trauma* 62, 199–206.

Warden, D. (2006). Military TBI during the Iraq and Afghanistan wars. *J. Head Trauma Rehabil.* 21, 398–402.

Whalen, M. J., Carlos, T. M., Dixon, C. E., Robichaud, P., Clark, R. S., Marion, D. W., and Kochanek, P. M. (2000). Reduced brain edema after traumatic brain injury in mice deficient in P-selectin and intercellular adhesion molecule-1. *J. Leukoc. Biol.* 67, 160–168.

Whalen, M. J., Carlos, T. M., Kochanek, P. M., Clark, R. S., Heineman, S., Schiding, J. K., Franicola, D., Memarzadeh, F., Lo, W., Marion, D. W., and Dekosky, S. T. (1999). Neutrophils do not mediate blood-brain barrier permeability early after controlled cortical impact in rats. *J. Neurotrauma* 16, 583–594.

Wolf, S. J., Bebarta, V. S., Bonnett, C. J., Pons, P. T., and Cantrill, S. V. (2009). Blast injuries. *Lancet* 374, 405–415.

Yilmaz, S., and Pekdemir, M. (2007). An unusual primary blast injury Traumatic brain injury due to primary blast injury. *Am. J. Emerg. Med.* 25, 97–98.

Conflict of Interest Statement: The authors declare that the research was conducted in the absence of any commercial or financial relationships that could be construed as a potential conflict of interest.

Received: 02 December 2011; accepted: 24 January 2012; published online: 09 February 2012.

Citation: Svetlov SI, Prima V, Glushakova O, Svetlov A, Kirk DR, Gutierrez H, Serebruany VL, Curley KC, Wang KKW and Hayes RL (2012) Neuro-glial and systemic mechanisms of pathological responses in rat models of primary blast overpressure compared to "composite" blast. Front. Neur. ***3****:15. doi: 10.3389/fneur.2012.00015*

This article was submitted to Frontiers in Neurotrauma, a specialty of Frontiers in Neurology.

Neuroscience Letters 544 (2013) 62–67

Contents lists available at SciVerse ScienceDirect

Neuroscience Letters

journal homepage: www.elsevier.com/locate/neulet

Overpressure blast-wave induced brain injury elevates oxidative stress in the hypothalamus and catecholamine biosynthesis in the rat adrenal medulla

Nihal Tümer[a,c,*], Stanislav Svetlov[b], Melissa Whidden[h], Nataliya Kirichenko[a,c], Victor Prima[b], Benedek Erdos[d], Alexandra Sherman[b], Firas Kobeissy[b,e], Robert Yezierski[g], Philip J. Scarpace[c], Charles Vierck[f], Kevin K.W. Wang[e,f]

[a] Geriatric Research, Education and Clinical Center, Department of Veterans Affairs Medical Center, Gainesville, FL 32608, United States
[b] Banyan Biomarkers Inc., Alachua, FL 32615, United States
[c] Department of Pharmacology and Therapeutics, University of Florida, Gainesville, FL 32610, United States
[d] Department of Physiology, University of Florida, Gainesville, FL 32610, United States
[e] Department of Psychiatry, University of Florida, Gainesville, FL 32610, United States
[f] Department of Neuroscience, University of Florida, Gainesville, FL 32610, United States
[g] Department of Orthodontics, University of Florida, Gainesville, FL 32610, United States
[h] Department of Kinesiology, West Chester University, West Chester, PA 19383, United States

HIGHLIGHTS

- A single OBI was performed in rats to assess the activation of hypothalamic sympatho-adrenal-medullary axis.
- Adrenal medullary catecholamine synthetic enzymes and NPY protein expression as well as plasma NE were elevated.
- NADPH oxidase activity was increased in the hypothalamus.
- TH protein was elevated in the NTS.

ARTICLE INFO

Article history:
Received 6 February 2013
Received in revised form 13 March 2013
Accepted 18 March 2013

Keywords:
Brain injury
Blast injury
Autonomic dysfunction
Hypothalamus
Adrenal medulla
Nucleus tractus solitarius

ABSTRACT

Explosive overpressure brain injury (OBI) impacts the lives of both military and civilian population. We hypothesize that a single exposure to OBI results in increased hypothalamic expression of oxidative stress and activation of the sympatho-adrenal medullary axis. Since a key component of blast-induced organ injury is the primary overpressure wave, we assessed selective biochemical markers of autonomic function and oxidative stress in male Sprague Dawley rats subjected to head-directed overpressure insult. Rats were subjected to single head-directed OBI with a 358 kPa peak overpressure at the target. Control rats were exposed to just noise signal being placed at ~2 m distance from the shock tube nozzle. Sympathetic nervous system activation of the adrenal medullae (AM) was evaluated at 6 h following blast injury by assessing the expression of catecholamine biosynthesizing enzymes, tyrosine hydroxylase (TH), dopamine-β hydroxylase (DβH), neuropeptide Y (NPY) along with plasma norepinephrine (NE). TH, DβH and NPY expression increased 20%, 25%, and 91% respectively, following OBI ($P < 0.05$). Plasma NE was also significantly elevated by 23% ($P < 0.05$) following OBI. OBI significantly elevated TH (49%, $P < 0.05$) in the nucleus tractus solitarius (NTS) of the brain stem while AT1 receptor expression and NADPH oxidase activity, a marker of oxidative stress, was elevated in the hypothalamus following OBI. Collectively, the increased levels of TH, DβH and NPY expression in the rat AM, elevated TH in NTS along with increased plasma NE suggest that single OBI exposure results in increased sympathoexcitation. The mechanism may involve the elevated AT1 receptor expression and NADPH oxidase levels in the hypothalamus. Taken together, such effects may be important factors contributing to pathology of brain injury and autonomic dysfunction associated with the clinical profile of patients following OBI.

Published by Elsevier Ireland Ltd.

* Corresponding author at: Department of Pharmacology and Therapeutics, University of Florida, PO Box 100267, Gainesville, FL 32610, United States.
Tel.: +1 352 374 6114; fax: +1 352 374 6142.
E-mail address: ntumer@ufl.edu (N. Tümer).

0304-3940/$ – see front matter. Published by Elsevier Ireland Ltd.
http://dx.doi.org/10.1016/j.neulet.2013.03.042

1. Introduction

Blast-related traumatic brain injury (TBI) poses a significant concern for military personnel engaged or veterans previously deployed in war zones [3]. The pathophysiology of blast exposure is complex and uniquely different than typical civilian traumatic brain injury as a result of physical trauma or impact to the head. Blast exposure in military situations has various components including: (a) blast overpressure wave-induced injury; (b) secondary injury caused by debris fragments; (c) tertiary injury due to the acceleration or deceleration of the body or body parts due to blast wind or surrounding object; (d) toxic gas, flash burns or intense heat induced bodily injury; and (e) blast noise [3]. Because blast overpressure wave is a primary component of blast-induced organ injury, we previously described an overpressure brain injury (OBI) procedure in rodents using a shock-tube device that can be used as a model for the blast overpressure wave experienced by military personnel [26]. The major effects of OBI have been generally attributed to its external physical impact on the organs, causing internal mechanical damage. The resulting pathophysiological effects include elevated heart rate, blood pressure, respiratory rate, and body temperature [10], as well as cognitive impairment and post-traumatic stress disorder related traits [28].

One recognized pathophysiological consequence of blunt-force-mediated TBI is disruption of autonomic function, resulting in augmented sympathoactivation, but the precise nature of this disruption is not completely understood. Sympathoactivation contributes to systemic stress and cardiovascular complications [3,10]. It is known that TBI is associated with activation of the hypothalamic-pituitary-adrenal (HPA) axis [9]. Another critical participant in the stress response is the hypothalamic sympatho-adrenal-medullary axis [17]. Whether TBI also activates this axis is unknown. Blast induced TBI increases reactive oxygen species (ROS), such as superoxide radicals and nitric oxide [6,29]. In addition, we previously demonstrated that AT1 receptor expression and NADPH oxidase activity in hypothalamus contribute to the activation of the hypothalamic mediated sympathetic outflow [7,8]. Collectively, these data suggest that OBI may stimulate hypothalamic AT1 receptors and NADPH oxidase leading to increased ROS with subsequent activation of the sympatho-adrenal-medullary system.

The nucleus tractus solitarius (NTS) is another brain nucleus that participates in the stimulation of sympatho-adrenal-medullary system following stress [13,17]. The NTS serves as the primary autonomic center that receives viscerosensory inputs from the spinal cord, and cranial nerves project to the NTS through the sensory trigeminal tract. Noradrenergic neurons within the A2 cell group of the NTS, in turn project to the hypothalamus [17].

The sympatho-adrenal-medullary axis leads to marked activation of the AM and sympathetic ganglia characterized by elevated activity of the catecholamine biosynthesizing enzymes such as TH and DβH, resulting in a rise in circulating epinephrine and NE [23]. TH is the rate-limiting step in catecholamine biosynthesis as it catalyzes the hydroxylation of tyrosine to dopamine [20], while DβH catalyzes the conversion of dopamine to NE. In addition to catecholamines, neuropeptide Y (NPY) is synthesized in the AM and is co-released with epinephrine and NE [12,27]. The aforementioned factors, TH, DβH, and NPY are considered the biomarkers of sympathetic nervous system (SNS) activity.

The present study tests the hypothesis that a single exposure to OBI results in increased hypothalamic expression of oxidative stress and activation of the sympatho-adrenal medullary axis. To this end, we measured NADPH oxidase activity and AT1 mRNA expression in the hypothalamus, TH protein expression in the NTS, TH, DβH, and NPY protein expression in the AM as well as plasma NE following a mild-moderate blast overpressure wave.

2. Materials and methods

2.1. Animals

Three month old (250–300 g) male Sprague-Dawley (Harlan Laboratories, Indianapolis, IN) rats were randomly assigned to one of two experimental groups: (1) control ($n = 4$) and (2) brain injury (TBI) induced by blast overpressure wave ($n = 4$). Animals were maintained on a 12:12 h light–dark cycle and provided food and water ad libitum for 2 weeks prior to the experimental protocol. Experiments were conducted according to the Guiding Principles in the Care and Use of Laboratory Animals, and procedures were approved by the local Institutional Animal Care and Use Committee.

2.2. Experimental protocol

Animals in the TBI group were exposed to a single head-directed overpressure blast injury (OBI). A compressed air-driven shock tube was used to expose the TBI rats to a supra-atmospheric wave of air pressure [26]. The tube was separated into two sections: high-pressure (driver) and low-pressure (driven) separated by a metal diaphragm. In these experiments 0.05 mm thick stainless steel diaphragms were used to generate the high pressure shockwaves. The diaphragms were scored with two diagonal and perpendicular lines thus the diaphragms will break away along the score lines without any shrapnel generated. The ratio of driver versus driven section lengths was equal to 15. The driver section was initialized to a pressure of 5170 kPa and maintained at ambient conditions. The diaphragm rupture was initiated by an internal cutter that led to the sudden exposure of a low pressure gas to a gas at a significantly higher pressure resulting in the formation of a shock wave. The blast pressure data were acquired using PCB piezoelectric blast pressure transducers and LabView 8.2 software. A National Instruments 500,000 samples/s data acquisition card was used to acquire data from multiple channels.

Under isoflurane anesthesia rats were placed into a dense Polyethylene holder exposing only their head (body-armored setup) from the exit nozzle of the shock tube with the head positioned directly under the exit nozzle at distance of 5 cm, as described previously [26]. Rats were subjected to a blast wave with a mean peak overpressure of 358 kPa, and a positive pressure phase duration of approximately 10 ms. The noise control animals were positioned 2 m from the exit nozzle thus preventing the rats from experiencing the pressure wave during the diaphragm rupture. The noise duration is about 10 ms with a peak noise level at 100–105 dB. In addition, a control group of naïve animals were included for some western blot analyses.

During the recovery period, the rats are awake and able to walk normally without vocalization of pain. Based on our observation and previous study the above overpressure exposure produces a mild to moderate brain injury. Rats show significant and punctate neurodegeneration as evidenced by increased silver staining in subcortical regions, hippocampus and subthalamic nuclei [26]. Using neurodegeneration cupric silver staining, we observed significant diffused neuronal injury in caudal diencephalon as well as subthalamicus [25].

2.3. Tissue preparation

Six hours following exposure, animals were over-anesthetized with pentobarbital (120 mg/kg ip) and the AM, hypothalamus, and

NTS rapidly removed, immediately frozen in liquid nitrogen and stored at −80 °C until subsequent analyses. Prior to homogenization, AM were decapsulated and the medullae were separated from the cortex.

2.4. NADPH oxidase activity

NADPH oxidase activity was measured with a lucigenin-enhanced chemiluminescence assay using hypothalamus homogenates. Tissue samples were incubated at 37 °C in a spectrophotometer. Relative light units were obtained for 30 min in the presence of NADH (500 μm) and lucigenin (230 μM), and background-corrected values were normalized to protein content determined by DC Bradford.

2.5. Reverse transcriptase-PCR

AT1 mRNA expression was identified in the hypothalamus by using relative quantitative reverse transcriptase-PCR through the use of Quantum RNA 18s Internal Standards kit (Ambion, Austin, TX). PCR was performed by multiplexing AT_1 primers (sense, 5′-CAGCTTGGTGGTGATTGTC; antisense, 5′-GCCATCGGTATTCCATAGC) and 18S primers. The optimum ratio of 18S primer to competimer was 1:9. PCR was performed at 94 °C denaturation for 120 s, 55 °C annealing temperature for 60 s and 72 °C elongation temperature for 120 s for 27 cycles.

2.6. Western blot analysis

AM or NTS were homogenized and assayed for protein levels of the catecholamine biosynthetic enzymes, TH and DβH, along with NPY as previously described [31] using antibodies directed to TH (Pel Freez Biologicals, Rogers, AR), DβH (Novus Biologicals, Littleton, CO), and NPY (Santa Cruz Biotechnology, Santa Cruz, CA). An equal amount of protein for each AM homogenate (1.5 μg protein for TH, 10 μg for DβH and 35 μg for NPY) or NTS homogenates (4 μg protein for TH) was applied to the gels.

2.7. ELISA measurements of norepinephrine

Blood samples were taken via cardiac puncture at the time of sacrifice and centrifuged at room temperature in serum-separating tubes containing 1 mM EDTA and 4 mM sodium metabisulfite. The samples were stored at −80 °C until further analysis by an enzyme-linked immunosorbent assay (ELISA) kit (Rocky Mountain Diagnostics, Inc., Colorado Springs, CO), following the instructions of the manufacturer.

2.8. Statistics

Data are presented as means ± SE. Comparisons between groups for each dependent variable were made by Student's *t*-tests (two-tailed). Significance was established at $P < 0.05$.

3. Results

3.1. Blast injury elevates oxidative stress in the hypothalamus

Changes in the level of oxidative stress in the hypothalamus 6 h following OBI was analyzed by evaluating levels of NADPH oxidase activity. NADPH oxidase activity was significantly increased by 36% following blast injury ($P < 0.05$) (Fig. 1, Top). One known activator of NADPH oxidase activity is the renin–angiotensin II system, thus, we also examined AT1 receptor expression in the hypothalamus. AT1 mRNA expression was significantly elevated following OBI ($P < 0.05$) (Fig. 1, Bottom).

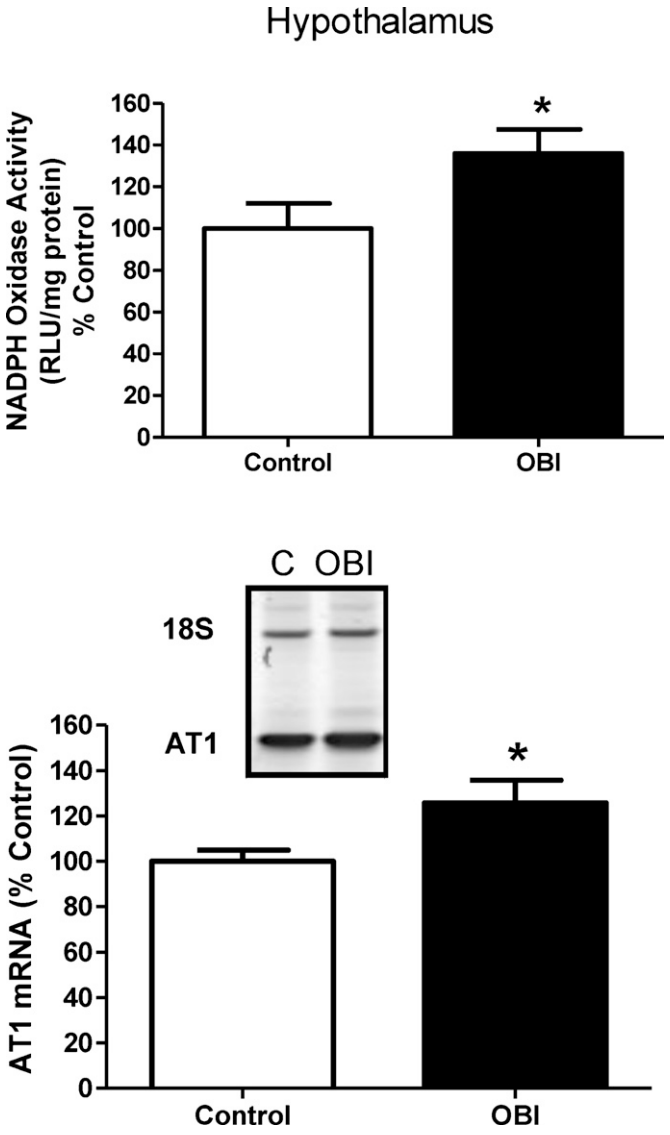

Fig. 1. Effect of OBI on hypothalamic NADPH oxidase activity expressed as relative light units (RLU)/mg protein (Top) and hypothalamic AT1 receptor mRNA expression (Bottom). Values expressed as percentage of control and represent mean ± SE of 4 rats/group. *$P = 0.043$ (Top) and $P = 0.031$ (Bottom) versus corresponding control.

3.2. Blast injury increases tyrosine hydroxylase expression in the nucleus tractus solitarius

We examined TH protein expression following OBI in the NTS. The NTS of the brain stem is one of the most important brain regions involved in neurochemical modulation of stress, cardiovascular control and of central autonomic pathways [5]. Following OBI there was a significant elevation in TH protein expression by 49% compared with control ($P < 0.05$) (Fig. 2, Top).

3.3. Blast injury increases plasma norepinephrine

To determine if the increase in biosynthetic enzyme levels translated to elevated plasma NE levels, plasma NE was assessed following blast injury. Plasma NE was increased by 23% at 6 h post blast injury (Fig. 2, Bottom).

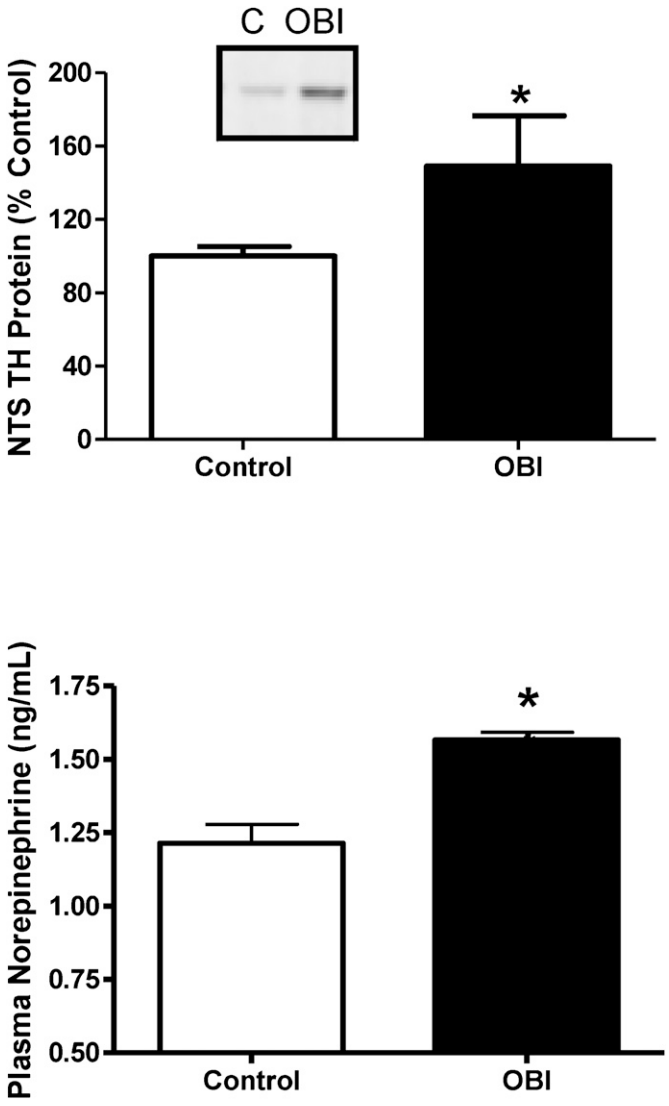

Fig. 2. Effect of OBI on NTS protein level of TH expressed as percentage of control (Top) and plasma norepinephrine (Bottom). Values represent mean ± SE of 4 rats/group. *$P = 0.048$ (top) and $P = 0.002$ (bottom) versus corresponding control.

3.4. Blast injury increases catecholamine biosynthetic enzymes and NPY expression in the adrenal medullae

Sympathetic nervous system activation of the AM was evaluated after blast injury by assessing the expression of catecholamine biosynthesizing enzymes, TH and DβH, along with NPY. Following OBI, TH and DβH expression increased by 20% and 25%, respectively ($P < 0.05$) (Table 1). NPY is synthesized and co-released with catecholamines in the AM and NPY expression correlates with catecholamine biosynthesis. Interestingly, NPY expression was significantly elevated by 91% ($P < 0.01$) following OBI compared with age-matched noise controls (Table 1). We also assessed TH, DβH and NPY expression in the AM of naïve animals; there was no significant difference between the noise control and naïve rats (data not shown).

Table 1
Catecholamine biosynthetic enzymes and NPY protein in the adrenal medulla of control and overpressure blast injury animals.

Protein	Control ($n = 4$)	OBI ($n = 4$)
TH	100 ± 2%	120 ± 7%*
DβH	100 ± 4%	125 ± 9%*
NPY	100 ± 9%	191 ± 20%*

Values are mean ± SE of 4 rats/group expressed as percentage of control. The level of the averaged control for each protein is arbitrarily set to 100 with SE adjusted proportionally with remaining groups normalized to the level in control. TH, tyrosine hydroxylase; DβH, dopamine β-hydroxylase; NPY, neuropeptide Y.

* Significantly increased versus Control; $P = 0.022$ (TH), $P = 0.031$ (DβH), $P = 0.006$ (NPY).

4. Discussion

Overpressure wave exposure with 358 kPa peak pressure used in the present study "on-axis" exposure induces head acceleration and mild to moderate brain injury. The results provide evidence that OBI increases NADPH oxidase activity and AT1 mRNA in the hypothalamus with a parallel increase in TH protein levels in the NTS of the brain stem just 6 h post injury. Moreover, the primary finding is that OBI is associated with increased levels of TH, DβH and NPY protein expression in the AM along with elevated plasma NE level in adult Sprague-Dawley rats.

These data suggest that OBI activates the sympatho-adrenal-medullary axis resulting in elevated adrenal medullary catecholamine synthetic enzymes and NPY protein expression as well as elevated plasma NE. Moreover, the magnitude of the increase in catecholamine biosynthetic enzymes in the present study (20–25%) is similar to that observed in AM and for urinary catecholamines in rats during adaptation to repeated immobilization stress [16], indicating that OBI is a potent stress inducer. It is well known that TH protein increases with the enhanced synthesis and release of catecholamines [30]. Moreover, our demonstration of elevated plasma NE confirms sympathetic activation. In addition, NPY protein level is one biomarker of SNS activity, and there is evidence of a role for NPY in the autocrine regulation of TH expression. NPY expression often increases concomitantly with TH expression. For example, we have demonstrated that carbachol, a mixed nicotinic-muscarinic agonist, stimulates both TH and NPY mRNA expression [27]. NPY may be a part of the homeostatic mechanisms that are involved in the adaptation to stress [11]. Collectively, the present data strongly suggest that post blast injury results in sympathoexcitation.

The effects of brain injury on central and peripheral alterations in the catecholaminergic system have been reported. Within 2 weeks of brain injury, TH protein levels and activity as well as dopamine and NE levels were increased in rat cortical tissue. The increase was transient, and by day 28, TH levels normalized [14]. Others reported a slightly different time course, with cortical TH levels increased at 28 days following post-injury, but with no increase prior to this time point [32], and an acute decrease in dopamine concentrations in the injured cortex at 1 h post-injury, which persisted for up to 2 weeks [19]. Striatal concentrations of dopamine were increased only at 6 h following injury. Hypothalamic concentrations of dopamine and NE increased significantly beginning at 1 h post-injury and persisted up to 24 h for dopamine and 1 week for NE. These investigators speculated that acute alterations occur in regional concentrations of brain catecholamines following brain trauma, which may persist for prolonged periods after brain injury. In humans, elevated plasma NE was reported during the first 3 days of trauma [4]. In another study, elevated plasma NE was detected by day 14, and increased CSF NE levels were decreased at day 6 post-injury [18]. Clearly, NE availability depends on the severity and time after TBI. Adrenoreceptors are also modulated following brain injury. For example, α1a adrenoreceptor mRNA, but not α1b or α1d adrenoreceptor mRNA, is increased in frontal cortex at 2 weeks after TBI [24]. These results indicate that there are markedly conflicting findings as to the functional effects that alter NE availability and influence post-injury cerebral function and cell loss.

We have previously shown that elevated hypothalamic NADPH activity increases blood pressure, indicative of elevated sympathetic activity [7]. Thus, increases in oxidative stress in the CNS may be one mechanism by which blast injury leads to sympathetic hyperactivity and hypertension. NADPH oxidase catalyzes the one electron reduction of oxygen into superoxide using either NADPH or NADH as the electron donor. In the present study, NADPH oxidase activity is significantly elevated just 6 h post OBI. This is similar to a report by Ansari et al. [2], who found significant time-dependent changes in antioxidants as early as 3 h post trauma and paralleled increases in oxidants in hippocampus. In addition, Readnower et al. [21] also reported that 3 h following blast injury 4-hydroxynoneal (4-HNE) and 3-tyrosine (3-NT) were significantly elevated in the hippocampus indicating an increase in oxidative stress.

The renin–angiotensin system (RAS), specifically angiotensin II (ANG II) has also been recognized as participating in various stress-induced responses, including an increase in sympathetic activity and stress-related cardiovascular disorders [22]. Thus ANG II and its receptors contribute to the development of various sympathetic and neuroendocrine responses during stress exposure. In the present report, AT1 expression was significantly elevated following OBI, suggesting the renin angiotensin II system may be involved in the blast injury mediated sympathoactivation. Because stimulation of renin angiotensin II system increases oxidative stress via AT1 receptor stimulation [15], this may provide the mechanism that links OBI and the increase in oxidative stress as well as the downstream sympathoexcitation and cardiovascular dysfunction.

Furthermore, TH protein expression was found to be elevated in the NTS of the brain stem. The NTS is involved in the central autonomic pathway [1]. The exact consequences of elevated TH in the NTS on sympathoexcitation in our experiments are unclear. Neuronal cell bodies which synthesize noradrenaline and adrenaline are found in cell groups within the NTS, including the A2 noradrenergic and C2 adrenergic neurons [5]. These neurons project to the hypothalamus [17] and participate in the modulation of cardiovascular, neuroendocrine, behavioral and metabolic responses to stress [5]. The elevated TH levels in the NTS in the present study may play a role in the sympathetic hyperactivity that is observed following OBI. The elevated oxidative stress in the hypothalamus along with the increased TH protein in the NTS either sequentially or collectively may partially mediate the sympathoexcitation leading to the augmented catecholamine biosynthetic enzymes in the AM.

In summary, our data demonstrate increased TH, DβH and NPY protein expression in the AM as well as elevated plasma NE suggesting that OBI results in increased sympathoexcitation. The mechanism may involve central activation of the sympathoadrenal-medullary axis through increases in AT1 receptors and NADPH oxidase levels in the hypothalamus and elevated TH protein in the NTS. In addition, this data provides evidence for elevated central oxidative stress following OBI. Such effects may contribute to OBI induced autonomic dysfunction. Further studies are needed to explore the detailed mechanisms to determine the effect of overpressure blast-wave on sympathoactivation and to enhance the understanding the pathophysiology of autonomic dysfunction.

Disclosures

None.

Acknowledgements

This work was supported by the Medical Research Service of the Department of Veterans Affairs, Banyan Biomarkers Inc., McKnight Brain Institute, University of Florida, and National Institute of Aging T32 AG000196.

References

[1] M.C. Andresen, D.L. Kunze, Nucleus tractus solitarius – gateway to neural circulatory control, Annu. Rev. Physiol. 56 (1994) 93–116.
[2] M.A. Ansari, K.N. Roberts, S.W. Scheff, Oxidative stress and modification of synaptic proteins in hippocampus after traumatic brain injury, Free Radic. Biol. Med. 45 (2008) 443–452.
[3] I. Cernak, The importance of systemic response in the pathobiology of blast-induced neurotrauma, Front. Neurol. 1 (2010) 1–9.
[4] G.L. Clifton, C.S. Robertson, K. Kyper, A.A. Taylor, R.D. Dhekne, R.G. Grossman, Cardiovascular response to severe head injury, J. Neurosurg. 59 (1983) 447–454.
[5] D.L. Daubert, M. McCowan, B. Erdos, D.A. Scheuer, Nucleus of the solitary tract catecholaminergic neurons modulate the cardiovascular response to psychological stress in rats, J. Physiol. 19 (2012) 4881–4895.
[6] D.S. DeWitt, D.S. Prough, Blast-induced brain injury and posttraumatic hypotension and hypoxemia, J. Neurotrauma 6 (2009) 877–887.
[7] B. Erdos, C.S. Broxson, M.A. King, P.J. Scarpace, N. Tümer, Acute pressor effect of central angiotensin II is mediated by NAD(P)H-oxidase-dependent production of superoxide in the hypothalamic cardiovascular regulatory nuclei, J. Hypertens. 24 (2006) 109–116.
[8] B. Erdos, N. Kirichenko, M. Whidden, B. Basgut, M. Woods, I. Cudykier, R. Tawil, P.J. Scarpace, N. Tümer, Effect of age on high-fat diet-induced hypertension, Am. J. Physiol. Heart Circ. Physiol. 301 (2011) 164–172.
[9] G.S. Griesbach, D.A. Hovda, D.L. Tio, A.N. Taylor, Heightening of the stress response during the first weeks after a mild traumatic brain injury, Neuroscience 178 (2011) 147–158.
[10] H.E. Hinson, K.N. Sheth, Manifestation of the hyperadrenergic state after acute brain injury, Curr. Opin. Crit. Care 18 (2012) 139–145.
[11] B. Hiremagalur, R. Kvetnansky, B. Nankova, J. Fleischer, R. Geertman, K. Fukuhara, E. Viskupic, E.L. Sabban, Stress elicits trans-synaptic activation of adrenal neuropeptide Y gene expression, Mol. Brain Res. 27 (1994) 138–144.
[12] M. Hong, S. Li, A. Fournier, S. St-Pierre, G. Pelletier, Role of neuropeptide Y in the regulation of tyrosine hydroxylase gene expression in rat adrenal glands, J. Neuroendocrinol. 61 (1995) 85–88.
[13] W. Janig, Organization of the sympathetic nervous system: peripheral and central aspects, in: A. del Rey, G.P. Chrousos, H.O. Besedovsky (Eds.), Neuroimmune Biology, The HPA Axis Book, Elsevier B.V., 2007, pp. 55–85.
[14] N. Kobori, G.L. Clifton, P.K. Dash, Enhanced catecholamine synthesis in the prefrontal cortex after traumatic brain injury: implications for prefrontal dysfunction, J. Neurotrauma 23 (2006) 1094–1102.
[15] N. Koumallos, G. Nteliopoulos, A. Paschalis, I. Dimarakis, N. Yonan, Therapeutic interventions to renin–angiotensin–aldosterone system, and vascular redox state, Recent Pat. Cardiovasc. Drug Discov. 6 (2011) 115–122.
[16] R. Kvetnansky, L. Mikulaj, Adrenal and urinary catecholamines in rats during adaptation to repeated immobilization stress, Endocrinology 87 (1970) 738–743.
[17] R. Kvetnansky, E.L. Sabban, M. Palkovits, Catecholaminergic systems in stress: structural and molecular genetic approaches, Physiol. Rev. 89 (2009) 535–606.
[18] A.E. Mautes, M. Müller, F. Cortbus, K. Schwerdtfeger, B. Maier, M. Holanda, A. Nacimiento, I. Marzi, W.I. Steudel, and Homburg Traumatic Injury Group (HOTBIG), Alterations of norepinephrine levels in plasma and CSF of patients after traumatic brain injury in relation to disruption of the blood-brain barrier, Acta Neurochir. (Wien) 143 (2001) 51–57.
[19] T.K. McIntosh, T. Yu, T.A. Gennarelli, Alterations in regional brain catecholamine concentrations after experimental brain injury in the rat, J. Neurochem. 63 (1994) 1426–1433.
[20] T. Nagatsu, M. Levitt, S. Udenfriend, Tyrosine hydroxylase: the initial step in norepinephrine biosynthesis, J. Biol. Chem. 238 (1964) 2910–2917.
[21] R.D. Readnower, M. Chavko, S. Adeeb, M.D. Conroy, J.R. Pauly, R.M. McCarron, P.G. Sullivan, Increase in blood–brain barrier permeability oxidative stress, and activated microglia in a rat model of blast-induced traumatic brain injury, J. Neurosci. Res. 88 (2010) 3530–3539.
[22] J.M. Saavedra, E. Sánchez-Lemus, J. Benicky, Blockade of brain angiotensin II AT1 receptors ameliorates stress, anxiety, brain inflammation and ischemia: therapeutic implications, Psychoneuroendocrinology 36 (2011) 1–18.
[23] E.L. Sabban, R. Kvetnansky, Stress-triggered activation of gene expression in catecholaminergic systems: dynamics of transcriptional events, Trends Neurosci. 24 (2001) 91–98.
[24] S.M. Southwick, J.H. Krystal, C.A. Morgan, D. Johnson, L.M. Nagy, A. Nicolaou, G.R. Heninger, D.S. Charney, Abnormal noradrenergic function in posttraumatic stress disorder, Arch. Gen. Psychiatry 50 (1993) 266–274.
[25] S.I. Svetlov, V. Prima, D.R. Kirk, H. Gutierrez, K.C. Curley, R.L. Hayes, K.K.W. Wang, Morphologic and biochemical characterization of brain injury in a model of controlled blast overpressure exposure, J. Trauma 69 (2010) 795–804.
[26] S.I. Svetlov, V. Prima, D.R. Kirk, H. Gutierrez, K.C. Curley, R.L. Hayes, K.K.W. Wang, Neuro-glial and systemic mechanisms of pathological responses to primary blast overpressure (OP) compared to 'composite' blast accompanied by head acceleration in rats, NATO Research and Technology Organization RTO-MP-HFM-207 (2011) 37-1–37-10.

[27] N. Tümer, C.S. Broxson, J.S. LaRochelle, P.J. Scarpace, Induction of tyrosine hydroxylase and NPY by carbachol: modulation with age, J. Gerontol. A: Biol. Sci. Med. Sci. 54 (1999) B418–B423.
[28] P.J. Vandevord, R. Bolander, V.S. Sajja, K. Hay, C.A. Bir, Mild neurotrauma indicates a range-specific pressure response to low level shock wave exposure, Ann. Biomed. Eng. 40 (2012) 227–236.
[29] M. Vuceljić, G. Zunić, P. Romić, M. Jevtić, Relation between both oxidative and metabolic-osmotic cell damages and initial injury severity in bombing casualties, Vojnosanit Pregl. 63 (2006) 545–551.
[30] N. Weiner, Regulation of epinephrine biosynthesis, Annu. Rev. Pharmacol. Toxicol. 10 (1970) 273–290.
[31] M.A. Whidden, N. Kirichenko, Z. Halici, B. Erdos, T.C. Foster, N. Tümer, Lifelong caloric restriction prevents age-induced oxidative stress in the sympathoadrenal system of Fischer 344 × Brown Norway rats, Biochem. Biophys. Res. Commun. 408 (2011) 454–458.
[32] H.Q. Yan, A.E. Kline, X. Ma, E.L. Hooghe-Peters, D.W. Marion, C.E. Dixon, Tyrosine hydroxylase, but not dopamine beta-hydroxylase, is increased in rat frontal cortex after traumatic brain injury, Neuroreport 12 (2001) 2323–2327.

frontiers in
NEUROLOGY

REVIEW ARTICLE
published: 21 November 2013
doi: 10.3389/fneur.2013.00186

Assessing neuro-systemic & behavioral components in the pathophysiology of blast-related brain injury

Firas Kobeissy [1,2 *†], ***Stefania Mondello*** [3 *†], ***Nihal Tümer*** [4,5], ***Hale Z. Toklu*** [4,5,6], ***Melissa A. Whidden*** [7], ***Nataliya Kirichenko*** [4,5], ***Zhiqun Zhang*** [1], ***Victor Prima*** [8], ***Walid Yassin*** [9], ***John Anagli*** [8], ***Namas Chandra*** [10], ***Stan Svetlov*** [8] ***and Kevin K. W. Wang*** [1 *]

[1] *Department of Psychiatry, Center of Neuroproteomics & Biomarker Research, University of Florida, Gainesville, FL, USA*
[2] *Department of Biochemistry and Molecular Genetics, American University of Beirut Medical Center, Beirut, Lebanon*
[3] *Department of Neurosciences, University of Messina, Messina, Italy*
[4] *Geriatric Research, Education and Clinical Center, Department of Veterans Affairs Medical Center, University of Florida, Gainesville, FL, USA*
[5] *Department of Pharmacology and Therapeutics, University of Florida, Gainesville, FL, USA*
[6] *Department of Pharmacology, Marmara University, Istanbul, Turkey*
[7] *Department of Kinesiology, West Chester University, West Chester, PA, USA*
[8] *Banyan Laboratory, Banyan Biomarkers, Inc., Alachua, FL, USA*
[9] *Department of Neuropsychiatry, Kyoto University, Kyoto, Japan*
[10] *Department of Biomedical Engineering, New Jersey Institute of Technology, Newark, NJ, USA*

Edited by:
Mårten Risling, Karolinska Institutet, Sweden

Reviewed by:
Karin A. Rafaels, Army Research Laboratory, USA
Denes V. Agoston, Uniformed Services University, USA

****Correspondence:***
Firas Kobeissy and Kevin K. W. Wang, Department of Psychiatry, University of Florida, 100 S Newell Drive Room L4-100, Gainesville, FL 32611, USA
e-mail: firasko@gmail.com, kwang@ufl.edu;
Stefania Mondello, Department of Neurosciences, University of Messina, Via Consolare Valeria, Messina 98125, Italy
e-mail: stm_mondello@hotmail.com

† Firas Kobeissy and Stefania Mondello have contributed equally to this work.

Among the U.S. military personnel, blast injury is among the leading causes of brain injury. During the past decade, it has become apparent that even blast injury as a form of mild traumatic brain injury (mTBI) may lead to multiple different adverse outcomes, such as neuropsychiatric symptoms and long-term cognitive disability. Blast injury is characterized by blast overpressure, blast duration, and blast impulse. While the blast injuries of a victim close to the explosion will be severe, majority of victims are usually at a distance leading to milder form described as mild blast TBI (mbTBI). A major feature of mbTBI is its complex manifestation occurring in concert at different organ levels involving systemic, cerebral, neuronal, and neuropsychiatric responses; some of which are shared with other forms of brain trauma such as acute brain injury and other neuropsychiatric disorders such as post-traumatic stress disorder. The pathophysiology of blast injury exposure involves complex cascades of chronic psychological stress, autonomic dysfunction, and neuro/systemic inflammation. These factors render blast injury as an arduous challenge in terms of diagnosis and treatment as well as identification of sensitive and specific biomarkers distinguishing mTBI from other non-TBI pathologies and from neuropsychiatric disorders with similar symptoms. This is due to the "distinct" *but shared* and partially identified biochemical pathways and neuro-histopathological changes that might be linked to behavioral deficits observed. Taken together, this article aims to provide an overview of the current status of the cellular and pathological mechanisms involved in blast overpressure injury and argues for the urgent need to identify potential biomarkers that can hint at the different mechanisms involved.

Keywords: biomarkers, blast injury, brain injury, neurotrauma, blast overpressure, mild TBI, PTSD, neuropsychiatry

INTRODUCTION

Traumatic Brain Injury (TBI) represents a major public health problem with an over 150,000 military personnel diagnosed with form of mild traumatic brain injury (mTBI), due to the exposure to blast resulting in a wide range of neurological and psychological symptoms (1, 2). Blast-related brain injuries can be provocatively described as "a silent epidemic of an invisible wound." Current Explosive mechanisms [improvised explosive devices (IEDs), landmines, and rocket-propelled grenades (RPGs)] are believed to account for 56–78% of Operation Enduring Freedom (OEF), Operation Iraqi Freedom (OIF), and Operation New Dawn (OND) related injuries (3, 4). This has led to labeling the blast-induced TBI (bTBI) as the signature brain injury for combat troops in today's military (5, 6).

Between 2000 and 2010, the Department of Defense (DoD) reported ∼200,000 head injuries as a consequence of combat-related incidents as well as events occurred in a non-deployed environment (civilian injuries) (7). However, even this number may be an underestimate due to the fact that the majority of blast-related mTBIs go misdiagnosed and untreated as a consequence of in-appropriate approaches of screening, invalidated diagnostic criteria or specific detectable abnormalities, and lack of diagnostic tools. Acute blunt penetrating injuries comprised 2.8% of this total, the rest were classified as mTBI (7).

Out of more than 8,000 cases of TBI reviewed by the Defense and Veterans Brain Injury Center, ∼50% were related to blast-related barotrauma (8). The clinical features observed in mTBI resulting from blast exposure vary, these include: headache, fatigue,

tinnitus, and irritability which have been highly recognized in recent conflicts. Blast overpressure (BOP) injury has been considered the main cause of both morbidity and mortality in neurotrauma (9, 10). Furthermore, blast TBI has been the center for military medical concern in the context of polytrauma, since blast-induced injury, due to its complex components (*primary*, *secondary*, *tertiary*, and *quaternary* injuries) is often accompanied by hemorrhagic blood loss, multiple fractures, burns, and systemic injury coupled with TBI (11–13).

The recognition of the high incidence and impact of bTBI; in addition, to the need for a more accurate diagnosis and effective therapeutic interventions, led to an impressive number of experimental and human blast injury studies aiming at investigating the complex interconnected pathways involved in the blast-induced neuropathological/behavioral changes.

This review will focus on three major questions: (i) What is the experimental and human evidence that blast is associated with progressive alterations in the brain and via what mechanism(s) they are mediated? (ii) What is the relation between blast-induced brain injury and the development of neuropsychological disorders such as post-traumatic stress disorder (PTSD)? (iii) What are the biochemical markers that can identify, track and predict the injury and symptoms observed in patients exposed to blast injury?

BIOMECHANICS OF BLAST INJURY

Blast overpressure-induced injury results from an explosion characterized by an abrupt release of energy in such a short period of time within a small volume creating a non-linear shock and pressure wave (14). The blast shock wave of the primary blast is solitary supersonic pressure wave (peak overpressure) characterized with a rapid (sub-milliseconds–milliseconds) increase in pressure followed by sharp fall in pressure, often to sub-atmospheric levels before returning to ambient pressure (15, 16). This is coupled with the "blast wind" (forced super-heated air flow) that gives rise to a very large volume of gas that may throw victim's body against other objects. Blast wind, along with the shock wave are the main components of the "blast wave" (17, 18). Blast waves comprise the shock front followed by the blast wind (19). Blast waves impinge on the head-brain complex while mechanical pressure pulses in the brain; the severity of the injury is dependent upon the magnitude and duration of the pressure cycle (20). The net loading at a material point in the brain comprised of a direct transmissive load and deflection-induced indirect loads. The pressure pulse in the brain is governed by the acoustic impedance mismatches between the head and the brain, and the flexural rigidity of the skull (20).

Blast can cause four different types of insults: (i) the *primary injury* resulting from the BOP waves due to the shock-wave overpressure or/and under pressure. This event is usually associated with contusion, edema, hemorrhage, and diffuse axonal injury (DAI) (11, 17, 21, 22). (ii) The *secondary injury* that is due to shrapnel or hard objects propelled at the body. (iii) The *tertiary insult* involves head translation/rotation coupled with acceleration/deceleration due to blunt impact arising from blast wind and finally (iv) the *quaternary insult* resulting from thermal burns or the probable use of toxic gases or chemicals.

Compared to previous past conflicts, the majority of war zone wounds have been attributed to secondary blast injury (shrapnel propelled by explosions), while tertiary and quaternary blast injuries were related to terrorist-linked acts involving structural collapse and the use of toxic material. Previous studies on primary injury (BOP) have traditionally focused on gas-containing hollow organs such as the lungs and gastrointestinal tract (14, 23).

In one study by Clemedson discussing blast injury, the term "blast injury" has been used to describe the biophysical and pathophysiological events post exposure to high explosion or the shock wave associated with it (24). The greatest interest was devoted to study the peak pressure, as well as the impulse relevant to pulmonary injuries produced (25–28). Interestingly, on the pathophysiology focused on the sudden alteration in the body ambient pressure, primarily in gas-air filled organs including the lungs, intestines, or in tissues with different specific weight such as the ear and intestines; this occurred at the interface between media with very large differences in density (16, 24, 29, 30).

Furthermore, BOP can induce a mild form of brain injury with significant neurological conditions involving cerebral edema, neuroinflammation, and vasospasm along with DAI and neuronal death. This neuronal injury phase is followed by a series of complex neuropsychiatric symptoms which may include memory loss and behavioral changes (5, 13, 31–33). As such, exposure to complex blast waves can be viewed as the inducer of multitude of injuries or even polytrauma involving several organ injuries interaction that exacerbates blast insult outcome (13). Finally, blast wave propagation to the brain parenchyma is another controversial mechanism which may involves both direct propagation through the skull or in an indirect propagation via blood vessels which has a direct implication on vascular disturbance (31, 34).

Blast wind passage to the skull causes acceleration/rotation to the brain comprising the direct injury. Indirect injury involves the compression of the abdomen and chest transferring kinetic energy to the body's biofluid. This rippling effect generates oscillating waves from blood to the brain distant from the contact point. In turn, this kinetic energy transfer will induce functional and morphological changes in brain structures which represent a distinct complex feature of blast-induced brain injury not present in other traditional brain injury models (21, 31, 35). The complex mechanism of blast injury involves consequences of primary blast effects on autonomous nervous system. Taken together, it should be comprehended that the mechanics of neurotrauma due to blast injuries are quite different from that of other types of injuries arising from motor vehicle accidents (blunt) or penetrating injuries (ballistics).

NEUROPATHOLOGICAL ALTERATION IN BLAST INJURY

Experimental studies of primary blast brain injuries (though limited) have shown evidence of altered cellular, molecular and biochemical processes, and behavioral outcomes. For instance, different studies have shown a heterogeneous profile of brain-associated cellular impairments including: elevation in β-amyloid precursor protein, altered expression of protooncogenes *c-Myc*, *c-Fos*, and *c-Jun* and impaired axonal transport along with oxidative stress with elevated nitric oxide generation (8, 33, 36–44). In addition, neuronal injury and glial activation (discussed later) coupled with elevation of biochemical markers such as, neuron specific enolase (NSE), ubiquitin C-terminal hydrolase 1 (UCH-L1), and

glial fibrillary acidic protein (GFAP) have been also reported. Other studies have shown evidence of axonopathy, edema, and hypertrophic astrogliosis with pronounced altered gene expression post-injury event (40, 44–46). However, there were a lot of ambiguity in the overpressure and duration utilized and the methods used to measure these parameters which were often unclear and not standardized (33, 43, 47).

Furthermore, such heterogeneous neural profile has been attributed to several factors including the suitable experimental model systems that can closely mimic "composite" primary, secondary, tertiary, and quaternary components of blast exposure, the lack of standardized blast wave instruments, different body localization and body armor, and the use of different animal species (31, 32, 41, 48) (see **Table 1**).

Several studies have been performed to assess neuropathological effect of BOP coupled with other comorbid factors (17, 29, 47–51). In these studies, several parameters were varied (different blast injury models, intensity, animal species used) or other modifications were included (protective vests, stressors, and animal localization).

One representative study is that of Kamnaksh et al. where they assessed different stressors and their contribution to blast injury. These stressors included transportation and blast sound with or without blast injury. Of interest, all groups exhibited increased anxiety, while injured and blast noise-exposed rats showed elevated corticosterone, interferon-c (IFN-c), and interleukin-6 (IL-6) in the amygdala and hippocampus. Injured animals showed elevated Iba1, GFAP, and apoptotic immunoreactivity (52). These data demonstrate that exposure to biological stressors can lead to behavioral changes and trigger specific neuropathological alteration even in the absence of detectable injury.

Pun et al. using a rat model, assessed the effects of a single sublethal blast over pressure (BOP) exposure (48.9–77.3 kPa) in an open-field set up. Histopathological analysis of inflicted brains revealed "darkened" and shrunken cortical neurons with narrowed vasculature at day 1 post-injury. Signs of recovery were demonstrated at days 4 and 7 post-blast exposure. Oligodendrocytes and astrocytes showed TUNEL-positivity in the white matter at day 1. Acute axonal damage was observed in the white matter as indicated by elevated amyloid precursor protein immunoreactivity with no sign of macrophages/microglia change. Major gene changes were observed at day 1 and 4 post-blast pointing toward signs of repair at day 4 and 7. These findings suggest that the BOP levels in the study resulted in mild cellular injury and white matter perturbations (47). In another study by Koliatsos et al. primary (BOP) wave effect of mild BOP (68, 103, and 183 kPag) was compared to secondary and tertiary effects. Using a shock tube generating shock waves, the effects of blast on parenchymatous organs including brain, were evaluated. The main injuries in non-brain organs included hemorrhages in the lung interstitium, hemorrhagic infarcts in liver, spleen, and kidney. Neuropathological changes and behavioral outcomes were evaluated at mild blast intensity showing signs of multifocal axonal injury in the cerebellum, the corticospinal system, and optic tract. These findings were accompanied with prolonged behavioral and motor abnormalities (deficits in social recognition, spatial memory, and in motor coordination). Interestingly, shielding of the torso ameliorated axonal injury and behavioral deficits (50).

In a different study, de Lanerolle et al. used a swine model to assess different scenarios of blast exposure including: simulated free field (blast tube), high-mobility multipurpose wheeled vehicle surrogate, and building 4-walled structure. Of interest, histological changes in the three blast scenarios showed minimal neuronal injury with fiber tract demyelination and intra-cranial hemorrhage. Neuropathological changes involving increased astrocyte activation coupled with proliferation and periventricular axonal injury detected were observed with β-amyloid precursor protein (53).

Long et al. assessed blast-induced physiological, neuropathological, and neurobehavioral changes coupled with Kevlar protective vest encasing the thorax and part of the abdomen using a compression-driven shock tube (at 126- and 147-kPa). Kevlar vest effect reduced air blast mortality and also ameliorated the widespread fiber degeneration in rat brains. BOP was shown to induce abnormal neurologic and neurobehavioral performance along with cardiovascular disruptions involving hemorrhagic hypotension with disruption in cardio-compensatory resilience (reduced peak shed blood volume, etc.) (10). Similarly, Rafaels et al. using a male ferrets with protected thorax and abdomen, evaluated intra-cranial hemorrhage and cardiorespiratory coupling at different ranges of blast exposures. Increasing severity of blast exposure demonstrated increasing apnea immediately after blast accompanied by hemorrhages in proximity to the brain stem (51).

In an interesting study, Garman et al. characterized the neuropathological changes produced by a single blast exposure in rats with body shielding using a helium-driven shock tube (exposure of 35 Psi with left side-head-only exposure) (54). Neuropathological analysis was conducted at various time points (24 h, 72 h, or 2 weeks post-blast). Multifocal axonal degeneration was present in all blast-exposed rats at all-time points coupled with diffused axonal injury in the cerebellar and brainstem white matter tracts. In addition, reactive microglial activation was also identified despite subtle GFAP, ED1, and Iba1 staining. Finally, increased blood–brain barrier (BBB) permeability was seen at 24 h. Findings from this study indicated axonal, dendritic, neuronal, and synaptic degeneration in the initial 2 weeks post exposure with body shielding. Over time, there was also evidence of progression of the axonal degenerative process characterized by increased axonal fragmentation similar to the process of DAI that follows TBI which is suggestive of a therapeutic window in the immediate post-blast period (54).

In conclusion, these different blast studies presented distinguished heterogeneous results (summarized in **Table 1**); and provided different insights into the associated neuropathological changes occurring post-blast exposure. These findings highlight the challenges encountered in modeling experimental blast injury and translating the findings into preclinical brain injury studies to be evaluated and verified clinically (discussed in different sections).

NEURONAL INJURY MECHANISMS

The exact mechanism by which BOP mediates neuronal injury has not been fully elucidated (47). The neuropathological changes

Table 1 | Recent major studies on experimental blast injury with different parameters assessed (behavioral, neuropathological, and biomarker changes).

Reference	Animal model/ device used-BOP intensity	Time point assessment post injury	Repeats of blast and time between exposure	Additional variables studied	Behavioral assessment (if available)	Neuro, systemic, and other organ-specific pathology/ biomarkers parameters
Abdul-Muneer et al. (102)	Rat/primary blast/shock tube/123 kPa	1/6/6/24/ 48 h/8 days	One or two (24 h between intervals)	None		Vascular damage, BBB leakage, neuroinflammation MMPs changes, AQP-4, oxidative stress (4HNE-3-NT), and edema; S100B and NSE (serum)
Ahmed et al. (136)	Rat/compressed air-driven shock tube/138 kPa	1, 3, 7, 14, 26, 36, and 42 days	Single or five (24 h between each blast)	Repeated vs. single blast comparison		Oxidative stress, vascular abnormalities, neuronal, and glial cell death
Arun et al. (137)	Mouse/A compressed air-driven shock tube/21 psi	6 or 24 h	Three blast (1.5 min)	Mice restrained in the prone position with a tautly-drawn net		Initial decrease and later increase GFAP and total tau proteins (liver, spleen, brain, and plasma)
Zou et al. (138)	Rat/5 kg TNT and PETN detonation: 3 m distance (high exposure, 480 kPa) and 2 m distance (low injury, 180 kPa)	24, 72 h and 2 weeks	Single	None		Retina injury: blast-dependent increase in VEGF, iNOS, eNOS, nNOS, AQP4, GFAP, elevated inflm cytokines, and chemokines
Prima et al. (139)	Rat/composite blast with head acceleration and Primary blast with no acceleration/ 230–380 kPa	6 h and 1 and 7 days	Single	Primary blast vs. composite' blast animals are body armored		Thrombin generation (TG) serum integrin α/β, sE-selectin, sICAM-1, and matrix metalloproteinases MMP-2, MMP-8, and MMP-13
Tumer et al. (104)	Rat/compressed air-driven shock tube ∼2 m distance/358 kPa for 10 ms/noise level noise level (100–105 dB)	6 h	Single	None		Increased oxidative stress; activation of the sympatho-adrenal medullary axis; (TH), dopamine-β hydroxylase (DβH), neuropeptide Y (NPY) plasma norepinephrine (NE); diffused neuronal injury
Genovese et al. (135)	SD-rat/shock tube airblast exposure 74.5 kPa	Every 7 days for 8 weeks	1/day for 3 days	None	Conditioned fear/PTSD	Neuronal pathology
Huber et al. (131)	Mouse/compressed gas-driven shock tube	24 and 30 days	Single	None		Elevation of multiple phospho-, cleaved-tau, and (MnSOD or SOD2) levels
Sajja et al. (140)	Rat/helium shock tube/117 kPa	7.5 ms	24, 48 h	Magic angle spinning 1H MRS analysis		Elevated *N*-acetyl aspartate, glutamate, and increased GFAP, Bcl-2, Bax, caspase-3, signs excitotoxicity (glutamate/creatine; hippocampal neuronal loss; mitochondrial distress

(Continued)

Table 1 | Continued

Reference	Animal model/ device used-BOP intensity	Time point assessment post injury	Repeats of blast and time between exposure	Additional variables studied	Behavioral assessment (if available)	Neuro, systemic, and other organ-specific pathology/ biomarkers parameters
Skotak et al. (141)	Rat/helium driven shock tube/(130, 190, 230, 250, and 290 kPa)	24 h	Single	Biomechanical loading assessed with pressure gauges (thorax, cranial space, and nose)		Diffuse blood-brain barrier breakdown in brain parenchyma; fatality; lung hemorrhage; no evident neuronal injury
Valiyaveettil et al. (34)	Mouse/blast over-pressure/20.6 psi	4, 24, and 72 h	Three times (1–30 min)	None		Platelet serotonin decreased at 4 h post blast; increase in the plasma serotonin levels. Increase in blood, plasma, and brain myeloperoxidase enzyme activity. Constriction of blood vessels of the brain
Takeuchi et al. (142)	Rats/laser-induced shock waves/0.5–1, 0.5 J/cm^2	14 days	Single	None		Decrease in the CB (cingulum bundle) axonal density
Turner et al. (143)	Rats/tabletop shock tube/31, 50, 72, and 90 psi	72 h	Single	Thorax and abdomen protection		Neural degeneration; increased glial activation (GFAP); extensive intracranial bleeding leading to death
Tweedie et al. (144)	Mouse/concussive head trauma (weight drop with metal protection)/ explosion shock wave pressure (7 m distance ∼2.5 psi–17.2 kPa)	7 days	Single	Comparison between mild TBI and blast injury	Altered cognitive and emotional behaviors (Y maze, novel object recognition passive avoidance/elevated plus maze cognition and anxiety	Altered hippocampal gene expression
Cho et al. (134)	Mouse/bast chamber (compression wave attached to a PVC tube)/94, 123, and 181 kPa	7, 14, 28 days and 3 months	Single	Body is protected with fiberglass screen mesh/hearing loss model		Decreased spiral ganglion neurons (SGNs) and afferent nerve synapses, loss of outer hair cells (OHCs), tinnitus, hearing loss
Yeoh et al. (103)	SD rat, rifle primary shock tube (145, 232, and 323 kPa)	5 min and 24, 48 h	Single	None		IgG assessment cardiovascular injury due to primary blast injury is distinct from a typical TBI
Cho et al. (134)	Male SD rat, shock tube 129.23 ± 3.01 kPa for 2.5 ms	4, 24, 48 h and 2 weeks post BOP	Single	None	Short term memory	Immunological assessment (TMF-γ, MCP-1) neuronal loss
Ahlers et al. (145)	Rat/pneumatically driven shock tube at 116.7, 74.5, and 36.6 kPa	6, 24 h and 1 week	Single or 12 blasts (24 h at 36.6 kPa)	Three body orientation (sideway, facing away vs. frontal)	Morris water maze task 116.7 kPa demonstrated transient alteration or loss of consciousness, 74.5 kPa demonstrated anterograde memory deficits	Subdural hemorrhage and cortical contusions

(Continued)

Table 1 | Continued

Reference	Animal model/ device used-BOP intensity	Time point assessment post injury	Repeats of blast and time between exposure	Additional variables studied	Behavioral assessment (if available)	Neuro, systemic, and other organ-specific pathology/ biomarkers parameters
Ahmed et al. (146)	Swine/blast overpressure/mild (24–37 psi) or moderate (40–52 psi)	6, 24, 72 h and 2 weeks	Single	None		CSF biomarkers (CK-BB NFH, GFAP, S100B, VEGF, Claudin 5, and NSE); neuronal and glial cell damage, altered vascular permeability, and inflammation
Balakathiresan et al. (123)	Rat/air-driven shock tube 120 kPa	3 and 24 h	Short interval (three times – 2 h), long interval (three times – 24 h each)	None		CSF and serum miRNAs (let-7i)
Hines-Beard et al. (147)	Mouse/primary ocular blast injury; pressurized air tank with paintball gun/23.6, 26.4, and 30.4 psi)	3,7, 14, and 28 days		Visual acuity deficit detected in 30 psi group eyes via optokinetics		Retinal damage was present in the eyes from the 30 psi group-corneal edema, corneal abrasions, at optic nerve avulsion
Bir et al. (148)	Rat/gas-driven shock tube, 90, 103, 117, 193, and 159 kPa	24, 48, and 72 h	Single	None		MRI analysis showed hippocampal reduction in the Cerebral Blood Flow
Kovesdi et al. (150)	Rat/shock tube/20.6 psi	8 and 45 days	Single	Minocycline (50 mg/kg i.p. NSAID); mitigate neurobehavioral changes/body protection	Impaired memory and increased anxiety. (open field, elevated plus maze, and Barnes maze) minocycline showed neuroprotection	Elevated brain and Serum: CRP, MCP-1, NFH, NSE, Tau, GFAP, MBP, S100B, CRP, MCP-1, TLR-9, Claudin 5, and AQP4
Li et al. (95)	Macaca fascicularis/120 kg of TNT/80 and 200 kPa	3 days and 1 month	Single and double (3 days interval at 80 kPa)	Monkey Cambridge neuropsychological test automated battery motor coordination and working memory		Increased (AQP-4) white matter degeneration, astrocyte hypertrophy; MRI revealed ultrastructural in Purkinje neurons in the cerebellum and hippocampal pyramidal neurons
Rafaels et al. (51)	Ferrets/8′ shock tube/variable peak overpressure (98–818 kPa range)	1–5 h	Direct recording	Head exposure/thorax and abdomen protection		Apnea; brain bleeding; fatality
Shridharani et al. (153)	Pigs/compressed-gas shock tube/variable (107–740 kPa range)	1.3–6.9 ms	Direct recording	Heads exposed/lungs and thorax protected (ballistic protective vests)		Apnea intracranial pressures indicates pressure attenuation by the skull up to a factor of 8.4
Sundaramurthy et al. (96)	Rat/Nebraska's shock tube/100, 150, 200, and 225 kPa)	NA	Single	Variable *Animal Placement Location* along the shock tube (i.e., inside, outside, and near the exit)		Surface and intracranial pressure elevation linearly with the incident peak overpressures

(Continued)

Table 1 | Continued

Reference	Animal model/ device used-BOP intensity	Time point assessment post injury	Repeats of blast and time between exposure	Additional variables studied	Behavioral assessment (if available)	Neuro, systemic, and other organ-specific pathology/ biomarkers parameters
Svetlov et al. (92)	Rat, external shock tube (230–380 kPa)	1 and 7 days post trauma	Single	Primary and composite blast		Persistent gliosis accumulation of GFAP/CNPase in circulation as well as IL-1/IL-10 fractalkine, orexin A, VEGF-R, NRP-2 increased after primary, and composite; integrin-α/β, ICAM-1, L-selectin, NGF-β increased after primary blast
Elder et al. (154)	Rat/air blast shock tube (WRAIR)/74.5	4.5 months	Three times (24 h)	Anxiety and fear; locomotor activity, MWM, rotarod, elevated zero arm, predator scent exposure; movement restricted with shielding; contextual and cued fear conditioning		Elevation in the amygdala of the protein stathmin 1 (proteomic changes)
Dalle Lucca et al. (155)	Rat/compressed air-driven shock tube/120 kPa	0.5, 3, 48, 72, 120, and 168 h	Two	None		Hemorrhage and edema in the brain cortex; elevated TNF-α, C3/C5b-9, and AQP-4; increased leukocyte infiltration
Arun et al. (22)	*In-vitro* 96 well plates-SH-SY5Y human neuroblastoma cells bTBI model/compressed air-driven shock tube (13.68, 18.03, and 21.05 psi)	24 h	Sing1e or three times (2 min intervals at 21.05 psi)	Plate orientation (horizontal vs. vertical)		Decreased ATP levels, increased LDH, and ROS; downregulation of CyPA protein
Chavko et al. (62)	Rat/air-driven shock tube/36 kPa point-pressure measurements of cerebral ventricles	∼2.94 ms	Single	Head orientation (head facing blast, right side exposed, head facing away)		Pressure wave propagation and head orientation dependence
Kuehn et al. (156)	Rat/cranium only blast injury apparatus/137.9–515 kPa	24 h and 7 and 10 days	Single	None	Accelerating rotarod; apnea	H&E staining subarachnoid hemorrhages; brain injury (caspase-3, and β-amyloid precursor protein (β-APP), IgG labeling, and Fluoro-Jade C); cardiac arrest; vasogenic edema
Cernak et al. (157)	Mouse/helium modular, multi-chamber shock tube/mild (183 kPa) moderate (213 kPa), severe (295 kPa)	1–5, 7, 10, 14, 21, and 30 days	Single	Supine vs. prone position)	Motor, cognitive, and behavioral) outcomes, assessed via : rotarod, anxiety learning, and memory via active avoidance procedure	Inflammation elevated in tissue CCL, osteopontin, MRP8, ED1, and GFAP at different time points

(Continued)

Table 1 | Continued

Reference	Animal model/ device used-BOP intensity	Time point assessment post injury	Repeats of blast and time between exposure	Additional variables studied	Behavioral assessment (if available)	Neuro, systemic, and other organ-specific pathology/ biomarkers parameters
Koliatsos et al. (50)	Mouse/helium multi chamber shock tube/high (25–45 psi), low (2.1 psi)	3, 5 days (biochem testing) and 7–14 (behavioral)	Single	Either Head or Torso Covered	Rotarod, Y maze open field social and spatial recognition memory and motor deficits	Axonal swellings (injury), APP, but degeneration staining 7–14 days after exposure
Kovesdi et al. (149)	Rat/compression-driven shock tube/20.6 psi	15, 44, 66 days (behavioral) and 66 days (biochemical)	Single	Enriched environment (EEN) contribution	Memory problems, increased anxiety, and depression; improved spatial memory in EEN	Axonal degeneration; elevation in IL-6, IFNγ VEGF, and tau protein levels; hippocampal GFAP and DCX
de Lanerolle et al. (53)	Swine/explosive blast levels in three scenarios: simulated free field (35 psi), high-mobility, vehicle (65 psi), and building setup (63 psi)	72 h and 2 weeks	Single	Blast varied settings: blast tube, high mobility; multipurpose wheeled vehicle, and four-sided structure		Little neuronal injury, fiber tract demyelination, or intracranial hemorrhage observed; increased astrocyte activation; bulbs positive for BAPP
Pun et al. (47)	Rat/120 kg of 2,4,6-trinitrotoluene (TNT)/48.9 kPa (7.1 psi) or 77.3 kPa (11.3 psi) at 24 or 40 m	1, 4, and 7 days	Single	Concrete block was placed between the animals and the explosive source at a distance of 1.5 m from the animals		Cortical neurons were "darkened" and shrunken with narrowed vasculature (day 1, not at 4–7 days); no Iba-1 change; TUNEL-positive cells in the white matter of the brain (day 1); an increase in APP in the white (acute axonal damage); genomics analysis showed signs of repair at day 4 and 7 post-blast
Reneer et al. (151)	Rat/multi-mode shock tube, the McMillan blast device (compressed air/ helium driven tube mode, or oxyhydrogen – RDX explosives mode/ 100, 150, and 200 kPa)	3 min post blast	Single	Two overpressure modes (air vs. explosives), Kevlar vest body protection		Rats exposed to compressed air-driven blasts had more pronounced vascular damage than those exposed to oxyhydrogen-driven blasts of the same peak overpressure
Risling et al. (152)	Rat/blast tube with pressure wave/130 and 260 kPa	2 h, 1, 3, 5 days, and 3 weeks		Three groups comparison – (1) fixed no head acceleration forces; (2) controlled penetration of a 2-mm thick needle; and (3) high-speed sagittal rotation angular acceleration		Diffuse axonal injury (DAI) in penetration and rotation models; genomics changes in the expression in a large number of gene families cell death, inflammation, and neurotransmitters in the hippocampus (acceleration and penetration injuries); downregulation of genes involved in neurogenesis and synaptic transmission

(Continued)

Table 1 | Continued

Reference	Animal model/ device used-BOP intensity	Time point assessment post injury	Repeats of blast and time between exposure	Additional variables studied	Behavioral assessment (if available)	Neuro, systemic, and other organ-specific pathology/ biomarkers parameters
Rubovitch et al. (93)	Mouse/open field explosives ∼500 g TNT detonation (1 m elevated)/5.5 and 2.5 psi	30 days		Mice in plastic net 4 or 7 m; MRI and DTI analysis	Significant decrease in cognitive and behavioral (Y maze; hippocampal function and spatial memory; novel object recognition task	Increased BBB permeability; 1 month post-blast; increase in fractional anisotropy (FA); no visible organ damage; and elevated MnSOD2
Connell et al. (158)	Female Guinea pig/2.5-cm strips of shock tubing/(23, 41, and 64 kPa	30 min		*Ex vivo* model of spinal cord white; shock tubing (explosive lining of 0.1 grain/foot composed of tetranitramine and aluminum)		Nervous tissue compression, and increased axonal permeability
Garman et al. (54)	Rat/helium-driven shock tube/35 psi (4 ms)	24, 72 h and 2 week		Head exposure with body armor		Increased blood–brain barrier permeability; elevated APP, GFAP, Iba1, ED1, and rat IgG.
Gyorgy et al. (122)	Pig/compression-driven shock tube/∼20, 20–40, and ∼40 psi	6, 24, 72 h and 2 week		None		Serum elevation of S100B, MBP, and NF-H, but not NSE
Readnower et al. (44)	Rat/air-driven shock tube/120 kPa	3, 24 h and 5 days	Single	None	BBB breakdown: At 3 and 24 h post exposure; increase in IgG staining in the cortex; brain oxidative stress: (4-HNE) and (3-NT) were significantly increased at 3 h post exposure and returned to control levels at 24 h post exposure; and microglia activation: at 5 days	
Cheng et al. (159)	Rat/electric detonator with the explosive equivalent of 400 mg TNT (100, −400 kPa) (distance of 5, 7.5, and 10 cm)	1, 2, 3, 5, and 7 days	Single	Head orientation(frontal, parietal, and occipital head exposure)	87% Rats developed apnea, limb seizure, poor appetite, and limpness	Diffuse subarachnoid hemorrhage and edema; cortical capillary damage; and tissue water and NSE
Cai et al. (160)	Rat/5 g compressed dynamite stick (75 cm from chest)	3, 6, 12 h and 1, 2, 3, 7 days	Single	Blast vs. burn-blast		Serum neutrophil elastase (NE); water lung content
Long et al. (10)	Rat/compression-driven shock tube/126 and 147 kPa	24 h	Single	Kevlar – protective vest (thorax – abdomen)	MWM testing beam walking and spatial navigation(disrupted neurologic neurobehavioral performance)	Heart rate, MAP, brain axonopathy, and widespread fiber degeneration
Säljö et al. (42)	Rat shock tube/10, 30, and 60 kPa (4 ms)	0.5, 3, 6, and 10 h and 1, 2, 3, 5, and 7 days	Single	Morris water maze: impaired cognitive function: 48 h post injury		Dose-dependent rise in intracranial pressure ICP in rats exposed to blast and an increasing time delay in elevation with decreasing intensity of exposure. the ICP returned to control levels after 7 days

(Continued)

Table 1 | Continued

Reference	Animal model/ device used-BOP intensity	Time point assessment post injury	Repeats of blast and time between exposure	Additional variables studied	Behavioral assessment (if available)	Neuro, systemic, and other organ-specific pathology/ biomarkers parameters
Säljö et al. (41)	Pig – Howitzer (9 and 30 kPa); Bazooka (42 kPa); automatic rifle (23 kPa) Rat/shock tube (8.7 kPa)	3 and 7 days	Three (exposure in air; 15 min intervals) two (exposure under water; 6–7 min)	Comparison of pressure time of different blast overpressure in: air, underwater, and localized blast		In pig study: small parenchymal and subarachnoid hemorrhages, predominately in the occipital lobe, cerebellum, and medulla oblongata; no observation in rat study
Cernak et al. (45)	Rat/large-scale BT-I shock tube/3389 kPa and small-scale BT-III shock tube (440 kPa)	3, 24 h and 5 days	Single	Protected head vs. whole body exposure	Deficits in active avoidance task	Swellings of neurons, glial reaction, and myelin debris in the hippocampus, laminal body and vacuoles formation (electron microscope)

B APP, B-amyloid precursor protein; GFAP, glial fibrillary acidic protein; AQP-4, aquaporin-4; MnSOD or SOD2, manganese superoxide-dismutase I; UCH-L1, ubiquitin C-terminal hydrolase; vWF, von Willebrand factor; NA, not applicable; NSE, neuronspecific enolase; Mwm, Morris water maze; CK-BB, brain-specific creatine kinase; MAP, mean arterial pressure; H&E, hematoxylin and eosin; 4-HNE, 4-hydroxynonenal; 3-NT, 3-nitrotyrosine; TNT, 2,4,6-trinitrotoluene; RDX, oxyhydrogen; ms, milliseconds; MMP8, matrix metalloproteinase 8; BOP, blast over pressure; NF-H, neurofilament-heavy chain.

evoked by BOP are different than those described following acute models of brain injury (i.e., acceleration–deceleration injury or direct impact) (10, 55–58) highlighting at the complex pathways involved. Elegant work with experimental data by Cernak et al. has shown that primary closed non-impact blast injury-induced neurotrauma involves the interaction of cerebral, local, and systemic responses (31, 32, 45, 48). These experimental data seem to highlight the fact that blood vessels vasculature (venous as well as arterial) may be acting as a conduit for blast energy transfer to the brain contributing to blast pressure-induced fiber degeneration.

In non-blast brain injury, the primary injury occurs as a consequence of mechanical force due to direct contusion of the brain against skull's rough interior or due to shearing and stretching forces against the brain tissue (31, 59). This may also involve vascular injury including subdural hematoma from ruptured blood, brain edema from elevated permeability of cerebral vasculature along with reduced blood flow due to intra-cranial pressure or infarction (59). Taken together, these complications represent the secondary and tertiary phases of blast injury.

Cernak et al. assessed the contribution of body-central nervous system (CNS) cross talk involved in blast-induced trauma related to the activation of autonomous nervous system and the neuroendocrine–immune system which contributes significantly to the mechanism of blast injury. Inflammation has been proposed to play an important role in the pathogenesis of long-term neurological deficits due to blast (31). Experiments using rigid body- or head-protection in animals subjected to blast showed that head protection failed to prevent inflammation in the brain while body protection was able to alleviate blast-induced brain functional impairments highlighting the role of body-CNS interaction (31).

Cernak et al. studies have demonstrated that blast exposure (mild-to-moderate) induces the activation of autonomous nervous system in rabbit exposed to BOP. Distinct pathological components in the brain including impaired energy metabolism, and increase in the sodium–potassium ATPase measured in the brainstem and erythrocyte membranes were coupled with edema formation (48, 60). In addition, to link systemic alteration and cerebral inflammation to long-term neurological deficits caused by blast, migration, and accumulation of polymorphonuclear leukocytes as key inflammatory markers of host response were assessed after helium-driven shock tube delivering mild blast injury (103 kPa). *In vivo* real time imaging of myeloperoxidase (MPO) inflammatory enzyme activity of activated phagocytes was conducted on three groups of rats: (1) whole-body blast; (2) blast with "body armor," (chest and abdomen) with the head exposed; or (3) blast with "helmet" as head protection (neck and skull) while the rest of the body exposed. One day post-blast exposure, MPO activity was observed in the gastrointestinal tract and the diaphragmal mediastinal parts of the lungs (61).

In the brain, this activity was observed at 7, 14, and 30 days post-blast injury. Of interest, MPO increase in the brain was independent of head protection at 14 and 30 days post-injury suggesting chronic inflammation and highlighting the role of systemic origin of the inflammatory activation mediating brain injury which highly reflects on the role of the vagal afferent neurons mediating gut–brain communication. Taken together, the results of this study clearly demonstrate the importance of the indirect, i.e., blast–body interaction as well as the decisive role of autonomous nervous–neuroendocrine–immune systems interaction in the pathogenesis of blast-induced brain trauma (31).

Similarly, Chavko et al. assessed the theory of the indirect effect of kinetic energy transfer via the blood vessels and the surrounding cerebrospinal fluid (CSF) to the CNS (62). In their work, they evaluated the contribution of direct versus indirect transfer and its correlation to the head orientation and the surface area exposed.

Brain biomechanical responses involving pressure inside the brains were assessed in rats exposed to low blast exposure (35 kPa) and positioned in three different orientations with respect to primary blast wave. These positions included: frontal exposure (i.e., head facing blast) right side exposed and head positioned away from blast. Frontal exposures showed higher traces of pressure amplitude and longer duration, suggestive of dynamic pressure transfer (62). On the other hand, the pressure wave inside the brain in the head facing away was similar to hydrodynamic pressure within the brain. It has become more evident that the primary pressure wave can induce functional, biochemical, and morphological alterations in different ways than those observed in other types of traumatic injuries (penetrating head injury).

MILD TBI AND NEUROPSYCHIATRIC IMPAIRMENTS IN BLAST INJURY AND PTSD COMORBIDITY

Another significant aspect of blast injury is psychological health which is highly affected. Many injured troops returning from war zones are afflicted with blast-induced BI experiencing post concussive symptoms (PCS), characterized by memory and cognitive disruption, irritability, anxiety, and fatigue (63). Among these with mTBI, PCS can persist long after exposure leading to major functional impairments (64). Unlike casualties suffered from moderate to severe TBI patients diagnosed with mTBI present with no apparent structural injury and are conscious with typical symptoms including headache, confusion, dizziness, memory impairment, and behavioral changes.

The nomenclature of mTBI has been a challenge for both civilian and military settings as described by Rosenfeld et al. (65). mTBI, according to the DoD, involves head trauma with loss of consciousness for <30 min or exhibiting post-traumatic amnesia for <24 h (66). Patients with mTBI have a Glasgow coma score of 13–15 usually experiencing poor unspecific diagnostic symptoms involving headaches, cognitive dysfunction, etc. independent whether mTBI is blast related or not. It is of high interest to deliver accurate diagnosis for such condition due to the overlapping symptoms mistaken with neuropsychiatric disorders. This in contrary to the moderate and severe blast-related TBI which have 9–12 and 3–8 Glasgow coma score respectively and require special treatment as they exhibit intra-cranial hemorrhage and brain edema (2, 67, 68). Patients with blast-related severe TBI are characterized with delayed vasospasm, and pseudoaneurysm formation requiring early intervention (2, 67). Severe blast-related TBI cases are usually due to the primary and secondary (penetrating injury) phases of blast and would require strict clinical guidelines that are similar to those in non-blast-related severe TBI cases (65).

Mild traumatic brain injury is the most frequent form of brain trauma among deployed military populations (69). It has been shown that repeated exposure to multiple low levels of blast injury account for the majority of mTBIs cases. These victims remain conscious and often are redeployed without proper diagnosis and treatment while they undergo severe mental stress (70, 71). The heterogeneous presentation of BOB injuries among mTBI patients depends on several factors (similar to what is observed in experimental blast injury studies) including: device composition, environment (e.g., presence of intervening protective barriers), distance from blast, and the use of protective shields, etc. (11, 72).

Primary blast component of blast injury is among the main contributors in developing neuropsychiatric impairments associated with the primary phase profile (30, 73). There had been an urgent quest to for future research examining the impact of blast concussion (particularly recurrent concussion) on neuropsychological performance. Neuropsychological evaluation of cognitive status post-blast exposure can be challenging for a variety of reasons. In particular, clinicians may have difficulty assessing: true concussion severity due to limited knowledge of the blast events which may be reflective of self-report months or years post the event(s) occurrence. In addition, the lack of several features of the blast environment may complicate the accuracy of the "blast self-report" involving distance from the blast, concussion severity which these are often unavailable from primary records (74). Thus, the lack of reliable information pertaining to injury characteristics makes it challenging to determine the course of cognitive recovery and rehabilitation. Usually, concussion severity is usually determined based on current PCS on screening instruments which are not necessarily specific to concussion and can be shared with depression or PTSD or even these PCS may be reflective of PTSD itself as elegantly discussed by Nelson et al. (74). Of interest, Hoge et al. reported that more than 40% of soldiers who experienced symptoms associated with mTBI (loss of consciousness) met the criteria for PTSD (1). This same study suggested that increased rates of health problems reported by soldiers exposed to mTBI are mediated mainly via neuropsychiatric disorders such as PTSD or depression, rather than mTBI (1).

Post-traumatic stress disorder, a psychiatric condition that arises after exposure to a life threatening experience such as conditions experienced in combat war zone with or without blast exposure as a form of mTBI (75). This, by itself, poses a challenge in the clinical diagnosis in veterans who are exposed to mTBI since the symptoms may overlap between these conditions exacerbated by other comorbid conditions such as drug abuse or other neuropsychiatric complications (75, 76). A Rand Corporation study indicated that ∼20% of returning service personnel (∼300,000) have had a TBI and that there was substantial overlap of TBI with the occurrence of PTSD (77).

Psychological stress resulting from exposure to blast wave leads to an altered psychological health status which contribute significantly to the development of PTSD (52, 70). However, a major recurring question arises-due to the similarity of blast injury clinical symptoms and those of PTSD, is how do we clinically differentiate between these two conditions and other neuropsychiatric conditions?

Post-traumatic stress disorder is deemed an effect of psychological and emotional determinants/trauma (i.e., event associated with threat of harm or loss of life to which the individual responds with extreme fear or horror), while mild bTBI is a result of destructive biomechanical forces acting on the brain (78). There is substantial overlap in symptom profile associated with these two conditions (1). For instance, impaired concentration, increased irritability, insomnia, and lack of interest are among the symptoms shared in the diagnosis for mTBI and PTSD (79). Additionally, blast TBI is a well-documented risk factor for the development of PTSD (80–82). The association between the two conditions is further supported by structural and functional neuroimaging studies

showing similar abnormalities in patients with blast-related mTBI as well as in those with PTSD (83–86).Such overlap and link determines and contributes to several ambiguities emphasizing the urgent need for finding reliable objective test to make an accurate diagnosis and to improve the understanding of the nature of the interaction and pathophysiology of PTSD and mild bTBI.

Clinical evaluation of a blast-exposed personnel can be challenging as symptoms may range from neurologic problems, psychiatric, or emotional difficulties which may be attributed to blast or due to other psychiatric disorder where in several instances the occurrence of TBI and PTSD may be suggested (81, 87). For neurological assessment in TBI, similar criterion-based methodology to that in PTSD has been used rendering a specific diagnosis to either condition or even to those with both conditions (PTSD or TBI-exposed) uncertain (87–89). Thus, in many cases, clinical diagnosis may result in high rate of inaccurate PTSD diagnosis in persons exposed to TBI (87).

Based on the above, it is of high interest that an accurate detailed knowledge of blast injury biophysics and injury threshold may assist clinicians in better diagnosis (87). This includes expanded neuropsychological studies of blast injury (both experimental and clinical) to identify accurate, specific and sensitive anatomic, pathophysiologic, and behavioral responses to blast injury as discussed by Bass et al. (87). This is complicated by the complex nature of blast injury involving several combinations of primary or other phases of blast injury (secondary, tertiary, and/or quaternary blast).

ANIMAL MODELS OF BLAST INJURY

Over the last several decades, a number of experimental animal models have been implemented to study the mechanisms of blast wave impact which included rats, mice, ferrets, rabbits, and larger animals involving sheep and swine (33, 90–97). These experimental models exhibited heterogeneous outcomes and even contradictory findings which have been attributed to several factors. A summary of the recent and major blast injury studies (2001, 2009–2013) is summarized in **Table 1**. In addition, there is a lack in the reproducibility of blast injury models and a need to develop blast injury generators that precisely control blast injury parameters similar to other well-defined acute brain injury models such as (controlled cortical impact (CCI) and the fluid percussion (FP) which have been well characterized with predictable neurological, histological, physiological, and behavioral outcomes. Thus, the need of establishing well characterized reproducible models (animal and blast framework) is vital to identify relevant pathogenic pathways involved that can assist in the development of effective diagnostic, prognostic blast specific-biomarkers (panel of biomarkers) (98). Several blast injury instrumentations are available which include: compressed gas-driven shock tubes which are driven by air, helium, or nitrogen gas which may result in unrealistic duration of the overpressure wave leading to an inappropriate scaling between species (humans and animal models; **Table 1**) (99).

CHALLENGES IN ANIMAL MODELS OF BLAST INJURY

There are limited available basic and translational studies relevant to the mechanisms of primary blast-induced brain injury. A better understanding of injury mechanisms is required for the development of protection and treatment options and biomarker identification for prognosis.

Several animal models have been proposed at translating intracranial biophysics and pathophysiology experienced in human blast exposure (87). These models have a number of limitations including: neuronal tissue biomechanical properties, anatomical differences as well as physiological differences (87). In addition, other factors that are challenging for proper scaling between experimental and human blast injury are associated with neuroanatomy and physiology involving: size of different brain structures, neural mass (brain size, head, body, position, and architecture), as well as body fluid composition (thickness, volume, and components) (87). Other key factors that need to be considered are the potential for exposure scaling, consistency in experimental protocols, frequency of exposure, and overpressure levels, which should be mimicking real life exposure or at least translate equally to human exposure (**Figure 1**). Other external factors include: distance from the blast, the use of protective shields and the presence or absence of noise stressors, etc. (12) (**Figure 1**). In real life situation, soldiers are often deployed several times and exposed to numerous psychological stressors such as blast noise with or without blast injury (87). Such conditions can induce adverse physiological changes leading to post-traumatic symptoms without sustaining any prior physical injury (discussed previously). Taken together, these challenging factors contribute to the difficulty of truly modeling blast injury in animals resulting in an in-appropriate neuropathological and neurobehavioral assessment.

BLOOD–BRAIN BARRIER AND SECONDARY INJURY IN BLAST OVERPRESSURE

Traumatic brain injury leads to progressive pathophysiological changes resulting in a reduction in cerebral blood flow and a decrease in tissue oxygen levels leading to ischemia, BBB disruption with brain edema (100). Death of resident cells of the CNS has traditionally been accepted to take place in two phases: an early necrotic and an on-going long-term apoptotic phase. Secondary brain injury develops in minutes to months following the original insult, progressively contributing to the worsened neurological impairment. This complex phenomenon is defined by the activation of various neurochemical cascades and the systemic physiological responses which manifest following the traumatic event (101).

At the cellular level, the biphasic nature of secondary injury is mediated by numerous disturbed pathways which include: (a) excitotoxicity caused by an excess of the neurotransmitter glutamate; (b) free radical generation by mitochondrial dysfunction, causing damage to proteins and phospholipid membranes of neurons and glia; and (c) the neuroinflammatory response which takes place due to both CNS and systemic immunoactivation. Thus, diffuse brain injury mediated immune responses, BBB alterations, and neuroinflammation seem to play an important role in the pathology of BOP. The increase in BBB permeability was shown to recover by the third day after the blast exposure (44, 102). Following blast injury, loosening of the vasculature and perivascular unit is mediated by the activation of matrix metalloproteinases and

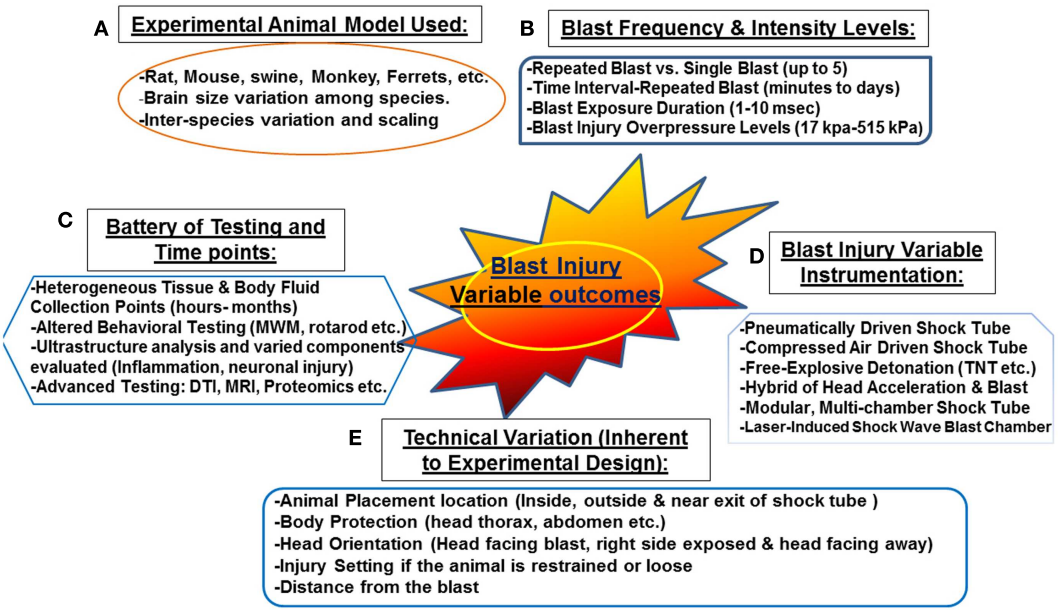

FIGURE 1 | Challenges associated with "experimental blast injury" modeling real life blast exposure. Several factors contribute to the heterogeneous behavioral, neuropathological, and systemic profile observed in the several experimental blast injury models. Even with models using the same injury parameters (animal model, blast shock tube, and intensity levels, etc.); reproducing the same results is rather challenging (refer to **Table 1**). These challenging variables are summarized in the following: **(A)** various animal models and interspecies variation, **(B)** blast injury frequency and intensity levels ranging from single blast up to five blast with some overpressure intensities reaching 515 kPa **(C)** the heterogeneous selection of biochemical/behavioral testing conducted and the several time points selected (hours to few months) **(D)** the non-standardized blast and not well characterized blast injury instrumentation **(E)** technical variation inherent to experimental design related to animal setting, body armor, head protection, and the distance from the blast. These factors contribute to the variable outcome observed in published work in blast injury field.

water channel aquaporin-4, promoting edema, enhanced leakiness of the BBB, and progression of neuroinflammation and neuronal degeneration (102). Although many studies demonstrate a similar pathophysiologic progression as the conventional TBI, a recent study reported that cerebrovascular injury due to primary blast is distinct from it; suggesting that BBB disruption in blast injury was an acute one, not resulting from a delayed inflammation as it is in the conventional ones (103).

Recent work from our laboratory has shown that blast injury leads to oxidative stress and autonomic dysfunction (104). Generation of free radicals and hypoxia leads to the failure of the Na^+, K^+-ATPase, a membrane-bound enzyme required for cellular transport. Dysfunction of this pump is a common feature in CNS pathologies related to ischemic conditions and TBI. The activity of Na^+, K^+-ATPase pump is very sensitive to free radical reactions and lipid peroxidation. Reductions in this activity can indicate membrane damage indirectly. Thus, Na^+, K^+-ATPase is clearly down regulated under low O_2 conditions which in turn triggers brain edema, enhances the loosening of tight junctions and causes BBB breakdown. MPO activity, an index for neutrophil infiltration, also increases as an evidence of inflammation (105). In summary, failure of pumps, cerebral edema, BBB permeability, neuroinflammation, and oxidative damage are among the major mechanisms that play important roles in the development of secondary brain injury following TBI.

TRAUMATIC BRAIN INJURY AND AUTONOMIC DYSFUNCTION

One deleterious consequence of brain injury is autonomic nervous system dysregulation and/or dysautonomia. Autonomic nervous system dysfunction has been documented after TBI but is not well understood. Ninety percent of TBI patients demonstrate signs of autonomic dysfunction during the first week after injury, with about one third of the patients developing longer lasting autonomic dysfunction. Autonomic dysregulation is characterized by distinct changes in cardiovascular hyperactivity, sleep function, and specific biomarkers of neural damage. System dysregulation might lead to a range of comorbidities such as hypertension, endothelial dysfunction, and end-organ perfusion abnormalities. Specifically, TBI disruption of autonomic function most often results in sustained sympatho-activation. This sympathetic hyperactivity after TBI remains poorly understood, although sympathetic hyperactivity likely contributes to the high morbidity and mortality associated with TBI. Sympathetic hyperactivity contributes to systemic stress, including neuroinflammation and oxidative stress in the autonomic nervous system. Eventually these disturbances lead to cardiovascular dysfunction (31, 32, 106) and sleep complications (107). Systemic stress is associated with activation of the hypothalamic-pituitary-adrenal (HPA) axis (108) and the hypothalamic sympatho-adrenal medullary axis (109). It is known that TBI activates the HPA, however little is known regarding the TBI-induced activation of the sympatho-adrenal

medullary axis, and there are limited therapeutic options to treat this sympatho-activation.

We recently demonstrated selective biochemical markers of autonomic function and oxidative stress in male Sprague Dawley rats subjected to head-directed overpressure insult (104). There were increased levels of tyrosine hydroxylase (TH), dopamine-β hydroxylase (DβH), Neuropeptide Y (NPY) along with plasma norepinephrine (NE). In addition, blast-induced injury significantly elevated TH in the nucleus tractus solitarius (NTS) of the brain stem while AT1 receptor expression and NADPH oxidase activity, a marker of oxidative stress, was elevated in the hypothalamus suggesting that single BOP exposure results in increased sympatho-excitation. The mechanism may involve the elevated AT1 receptor expression and NADPH oxidase levels in the hypothalamus. Taken together, such effects may be important factors contributing to pathology of brain injury and autonomic dysfunction associated with the clinical profile of patients following BOP exposure (104).

BLAST BRAIN INJURY AND OXIDATIVE STRESS

The primary effects of BOP have been generally attributed to its external physical impact on the body, causing internal mechanical damage. The pathophysiological effects on hollow organs have been extensively studied, but little attention has been given to the biochemical manifestations and molecular mechanism(s) of injury occurring in the brain after BOP exposure. Due to the biochemical nature of BOP compared to physical nature of TBI (impact or penetrating injury), subtle molecular changes such as free radical-mediated oxidative stress occur and contribute to the manifestation of BOP-induced brain injury (40, 44, 110). Previous studies have demonstrated that reactive oxygen species such as the superoxide radicals and nitric oxide can form peroxynitrite, a powerful oxidant that impairs cerebral vascular function following blast-induced brain injury (46, 111). Cernak et al. reported that bilateral vagotomy successfully mitigated bradycardia, hypotension, and apnea caused by blast; prevented extreme metabolic alterations and brain edema; but failed to eliminate oxidative stress in the brain due to blast (48). More recently, it was reported that the induction of oxidative and nitrosative damage leads to cerebrovascular inflammation in an animal model of mTBI induced by primary blast (102). Brain-specific oxidatively modified protein markers that are indicative of biochemical/proteomic and functional changes occurring post-BOP need to be considered. Insufficient published data are available to describe the long-term effects of TBI on central noradrenergic systems, particularly on neuroplastic adaptations within numerous targets of central noradrenergic projections. In addition, understanding the etiology of these changes may shed new light on the molecular mechanism(s) of injury, potentially offering new strategies for treatment.

BLAST INJURY BIOMARKERS IDENTIFICATION AND LIMITATIONS

The widespread recognition of the brain vulnerability to blast exposure and inadequate approaches to diagnose blast-related TBI led to design an mTBI Diagnostics Workshop (66) and the foundation of the Demographics and Clinical Assessment Working Group of the International and Interagency Initiative (112) to assess the current diagnostics technologies that can be used to detect brain injury following mTBI and BOP. One of the major recommendations was the use of biomarkers to supplement functional and imaging-based assessments for significant improvements in the diagnosis and characterization of the effects of blast exposure on brain and for distinguishing bTBI from other neuropsychiatric disorders including PTSD.

Current available imaging modalities, such as computed tomography (CT) and magnetic resonance imaging (MRI), primarily detect major structural changes in the brain (113); however, their utility has not been fully optimized following blast-related mTBI. More advanced neuroimaging techniques such as DTI, while have shown abnormalities post-blast-related TBI (114), have not been able to show consistent relationship to mild bTBI diagnosis (115). Additionally, there is no consensus on the ideal scan method or timing. Therefore, multiple studies have been conducted to identify ideal sensitive, inexpensive, non-invasive biochemical markers that can offer diagnostic and prognostic information, and reflect bTBI pathogenic mechanisms and pathology (116, 117).

To date, several biomarkers such as GFAP (118), UCH-L1 (119), and S-100ß(120) have been identified as potential excellent "candidates" of blast TBI. However, a limited number of studies did specifically evaluate biochemical brain damage markers in the setting of blast-induced brain injury (43, 121). In one study by Svetlov et al. they assessed temporal pattern of serum putative biomarkers that have been characterized in acute TBI including GFAP, NSE, and UCH-L1 in brain tissue, CSF, and blood. Serum biomarkers levels distinctively increased 24 h post-blast, followed by a decline thereafter, indicating a potential use to assess blast-induced brain damage acutely after injury (33). Supporting these observations, Gyorgy and colleagues, using reverse phase protein microarray (RPPM) technology to determine serum protein levels, showed a rise in S-100B, MBP, NF-H, and NSE protein levels in serum after injury in a large-animal model of bTBI. Remarkably, serum NF-H was reported to increase in an overpressure dose-dependent manner reflecting the extent of the damage caused by bTBI (122).

More recently, Balakathiresan et al. proposed microRNAs as novel serum diagnostic biomarkers of bTBI. They investigated microRNA signatures in CSF and serum of rats exposed to BOP injury. Specifically, microRNA let-7i was elevated in both CSF and serum post-blast wave exposure and was considered as an ideal candidate biomarker of brain injury (123). Importantly, microRNAs can be considered the third generation molecular signature after proteomics and genomics studies (123). Elevated concentrations of serum vascular endothelial growth factor, associated with neuroinflammation and vascular pathology in blast-related TBI have also been reported (124).

Studies investigating biomarkers of mTBI in humans continue to be limited as illustrated in one study by Ingebrigtsen and Romner (125). In their research paper, MEDLINE database was surveyed for biochemical serum markers specific to mild head injuries. Three serum markers including creatine kinase isoenzyme BB (CKBB), NSE, and S-100B were evaluated. Of these markers, S-100B protein was proposed as the most promising marker for mTBI while the other two lacked specificity, sensitivity, or injury correlation (125). In an another study by Blennow

et al. military personnel exposed to explosions or repeated firing of heavy weapons did not show any evidence of brain damage as assessed by CSF biomarkers. (126). Conversely, the New Zealand Breacher Study demonstrated a degree of brain perturbation as assessed by serum biomarker levels, neurocognitive performance, and self-reported symptoms in members of the New Zealand Defense Force exposed to repeated low-level blast (127). Taken the controversial results of these different studies, these findings, in fact, stimulate the need for further research to evaluate the usefulness of biochemical markers after repeated exposure of different blast levels.

Interestingly, recent experimental and human studies are suggesting a link between blast exposure and chronic traumatic encephalopathy (CTE), a tau protein-linked neurodegenerative disease (128–131). To date, no biofluid marker has been shown to assist with diagnosis of CTE. However, future studies to identify biomarkers tracking chronic processes and on-going degeneration and able to predict the development of neurodegenerative diseases of bTBI are of a critical need.

FUTURE RECOMMENDATIONS

For long, TBI has been considered one of the "signature injuries" of current conflicts in Iraq and Afghanistan which attracted concern from the DoD, Department of Veteran Affairs, and National Institutes of Health, encouraging combined efforts to understand brain injury pathophysiology and identify therapeutics and assess different approaches for rehabilitation platforms as well as deciphering novel blast specific biomarkers (7, 11). Better understanding of the biophysics of blast shock injury and its body propagation to the neural tissue may enhance the development body armor protection. Given the complexity of blast TBI pathobiology, the development of an objective, specific, and quantifiable panel of biomarkers is highly needed for the purpose of providing better monitoring of the real time injury mechanism and progression post-blast exposure (121, 122, 132, 133). An important consideration is that a panel combining different biomarkers be assembled that can establish the nature and severity of the head injury and reflect the contributing pathogenic mechanism(s) of the acute phase as well as the neurodegeneration and recovery (rehabilitative stages). Additionally, the integration of such bTBI diagnostic markers into routine clinical care will require a thorough validation and extensive standardization protocols coupled with well-defined recommendations for immunoassay and different measurement technologies.

A non-trivial and urgent issue in biomarker-panel design will be determining an appropriate instrument platform that is suited to measure these biomarker changes. At present, biomarkers are analyzed in clinical laboratories using closed, high throughput immunoassay analyzers allowing for high performance in terms of accuracy and precision which are suitable for major hospitals. Future recommendation is to focus research on the development of a miniaturized point-of-care (POC) system, which can be transported in the "field" (military and civilian) providing accurate measurements at a reasonable cost with short turnaround time (116).

REFERENCES

1. Hoge CW, Mcgurk D, Thomas JL, Cox AL, Engel CC, Castro CA. Mild traumatic brain injury in U.S. Soldiers returning from Iraq. *N Engl J Med* (2008) **358**:453–63. doi:10.1056/NEJMoa072972
2. Ling G, Bandak F, Armonda R, Grant G, Ecklund J. Explosive blast neurotrauma. *J Neurotrauma* (2009) **26**:815–25. doi:10.1089/neu.2007.0484
3. Owens BD, Kragh JF Jr, Wenke JC, Macaitis J, Wade CE, Holcomb JB. Combat wounds in operation Iraqi freedom and operation enduring freedom. *J Trauma* (2008) **64**:295–9. doi:10.1097/TA.0b013e318163b875
4. Sayer NA, Chiros CE, Sigford B, Scott S, Clothier B, Pickett T. Characteristics and rehabilitation outcomes among patients with blast and other injuries sustained during the global war on terror. *Arch Phys Med Rehabil* (2008) **89**:163–70. doi:10.1016/j.apmr.2007.05.025
5. Okie S. Reconstructing lives – a tale of two soldiers. *N Engl J Med* (2006) **355**:2609–15. doi:10.1056/NEJMp068235
6. Bhattacharjee Y. Neuroscience. Shell shock revisited: solving the puzzle of blast trauma. *Science* (2008) **319**:406–8. doi:10.1126/science.319.5862.406
7. DePalma RG, Cross GM, Beck LB, Chandler DW. Epidemiology of mTBI (mild traumatic brain injury) due to blast: history, DOD/VA data bases: challenges and opportunities. *Proceedings of the NATO RTO-MP-HFM-207 Symposium on A Survey of Blast Injury across the Full Landscape of Military Science.* Halifax (2011). p. 1–8.
8. Benzinger TL, Brody D, Cardin S, Curley KC, Mintun MA, Mun SK, et al. Blast-related brain injury: imaging for clinical and research applications: report of the 2008 St. Louis workshop. *J Neurotrauma* (2009) **26**:2127–44. doi:10.1089/neu.2009-0885
9. Shanker T. *Iraqi bombers thwart efforts to shield G.I.s.* The New York Times. (2007).
10. Long JB, Bentley TL, Wessner KA, Cerone C, Sweeney S, Bauman RA. Blast overpressure in rats: recreating a battlefield injury in the laboratory. *J Neurotrauma* (2009) **26**:827–40. doi:10.1089/neu.2008.0748
11. DePalma RG, Burris DG, Champion HR, Hodgson MJ. Blast injuries. *N Engl J Med* (2005) **352**:1335–42. doi:10.1056/NEJMra042083
12. Belanger HG, Proctor-Weber Z, Kretzmer T, Kim M, French LM, Vanderploeg RD. Symptom complaints following reports of blast versus non-blast mild TBI: does mechanism of injury matter? *Clin Neuropsychol* (2011) **25**:702–15. doi:10.1080/13854046.2011.566892
13. Schultz BA, Cifu DX, Mcnamee S, Nichols M, Carne W. Assessment and treatment of common persistent sequelae following blast induced mild traumatic brain injury. *NeuroRehabilitation* (2011) **28**:309–20. doi:10.3233/NRE-2011-0659
14. Moore DF, Jaffee MS. Military traumatic brain injury and blast. *NeuroRehabilitation* (2010) **26**:179–81. doi:10.3233/NRE-2010-0553
15. Brode H. Blast wave from a spherical charge. *Phys Fluids* (1959) **2**:217–29. doi:10.1063/1.1705911
16. Elsayed NM. Toxicology of blast overpressure. *Toxicology* (1997) **121**:1–15. doi:10.1016/S0300-483X(97)03651-2
17. Kirkman E, Watts S, Cooper G. Blast injury research models. *Philos Trans R Soc Lond B Biol Sci* (2011) **366**:144–59. doi:10.1098/rstb.2010.0240
18. Lemonick DM. Bombings and blast injuries: a primer for physicians. *Am J Clin Med* (2011) **8**:134–40.
19. Chandra N, Ganpule S, Kleinschmit NN, Feng R, Holmberg AD, Sundaramurthy A, et al. Evolution of blast wave profiles in simulated air blasts: experiment and computational modeling. *Shock Waves* (2012) **22**:403–15. doi:10.1007/s00193-012-0399-2
20. Selvan V, Ganpule S, Kleinschmit N, Chandra N. Blast wave loading pathways in heterogeneous material systems-experimental and numerical approaches. *J Biomech Eng* (2013) **135**:61002–14. doi:10.1115/1.4024132
21. Warden DL, French LM, Shupenko L, Fargus J, Riedy G, Erickson ME, et al. Case report of a soldier with primary blast brain injury. *Neuroimage* (2009) **47**(Suppl 2):T152–3. doi:10.1016/j.neuroimage.2009.01.060
22. Arun P, Spadaro J, John J, Gharavi RB, Bentley TB, Nambiar MP. Studies on blast traumatic brain injury using in-vitro model with shock tube. *Neuroreport* (2011) **22**:379–84. doi:10.1097/WNR.0b013e328346b138
23. Baker AJ, Topolovec-Vranic J, Michalak A, Pollmann-Mudryj MA, Ouchterlony D, Cheung B, et al. Controlled blast exposure during forced explosive entry training and mild traumatic brain injury. *J Trauma* (2011) **71**:S472–7. doi:10.1097/TA.0b013e318232e7da

24. Clemedson CJ. Blast injury. *Physiol Rev* (1956) **36**:336–54.
25. Clemedson CJ, Pettersson H. Genesis of respiratory and circulatory changes in blast injury. *Am J Physiol* (1953) **174**:316–20.
26. Clemedson CJ. Correlation between respiratory phase and extent of lung damage in air blast injury. *J Appl Physiol* (1954) **7**:38–42.
27. Celander H, Clemedson CJ, Ericsson UA, Hultman HI. A study on the relation between the duration of a shock wave and the severity of the blast injury produced by it. *Acta Physiol Scand* (1955) **33**:14–8. doi:10.1111/j.1748-1716.1955.tb01189.x
28. Clemedson CJ, Hartelius H, Holmberg G. The effect of high explosive blast on the cerebral vascular permeability. *Acta Pathol Microbiol Scand* (1957) **40**:89–95.
29. Mayorga MA. The pathology of primary blast overpressure injury. *Toxicology* (1997) **121**:17–28. doi:10.1016/S0300-483X(97)03652-4
30. Guy RJ, Glover MA, Cripps NP. Primary blast injury: pathophysiology and implications for treatment. Part III: injury to the central nervous system and the limbs. *J R Nav Med Serv* (2000) **86**:27–31.
31. Cernak I. The importance of systemic response in the pathobiology of blast-induced neurotrauma. *Front Neurol* (2010) **1**:151. doi:10.3389/fneur.2010.00151
32. Cernak I, Noble-Haeusslein LJ. Traumatic brain injury: an overview of pathobiology with emphasis on military populations. *J Cereb Blood Flow Metab* (2010) **30**:255–66. doi:10.1038/jcbfm.2009.203
33. Svetlov SI, Prima V, Kirk DR, Gutierrez H, Curley KC, Hayes RL, et al. Morphologic and biochemical characterization of brain injury in a model of controlled blast overpressure exposure. *J Trauma* (2010) **69**:795–804. doi:10.1097/TA.0b013e3181bbd885
34. Valiyaveettil M, Alamneh Y, Wang Y, Arun P, Oguntayo S, Wei Y, et al. Contribution of systemic factors in the pathophysiology of repeated blast-induced neurotrauma. *Neurosci Lett* (2013) **539**:1–6. doi:10.1016/j.neulet.2013.01.028
35. Cernak I, Savic J, Ignjatovic D, Jevtic M. Blast injury from explosive munitions. *J Trauma* (1999) **47**:96–103. doi:10.1097/00005373-199907000-00021 discussion 103-104,
36. Saljo A, Bao F, Haglid KG, Hansson HA. Blast exposure causes redistribution of phosphorylated neurofilament subunits in neurons of the adult rat brain. *J Neurotrauma* (2000) **17**:719–26. doi:10.1089/089771500415454
37. Saljo A, Bao F, Hamberger A, Haglid KG, Hansson HA. Exposure to short-lasting impulse noise causes microglial and astroglial cell activation in the adult rat brain. *Pathophysiology* (2001) **8**:105–11. doi:10.1016/S0928-4680(01)00067-0
38. Saljo A, Bao F, Jingshan S, Hamberger A, Hansson HA, Haglid KG. Exposure to short-lasting impulse noise causes neuronal c-Jun expression and induction of apoptosis in the adult rat brain. *J Neurotrauma* (2002) **19**:985–91. doi:10.1089/089771502753594945
39. Saljo A, Huang YL, Hansson HA. Impulse noise transiently increased the permeability of nerve and glial cell membranes, an effect accentuated by a recent brain injury. *J Neurotrauma* (2003) **20**:787–94. doi:10.1089/089771503767870014
40. Ansari MA, Roberts KN, Scheff SW. Oxidative stress and modification of synaptic proteins in hippocampus after traumatic brain injury. *Free Radic Biol Med* (2008) **45**:443–52. doi:10.1016/j.freeradbiomed.2008.04.038
41. Saljo A, Arrhen F, Bolouri H, Mayorga M, Hamberger A. Neuropathology and pressure in the pig brain resulting from low-impulse noise exposure. *J Neurotrauma* (2008) **25**:1397–406. doi:10.1089/neu.2008.0602
42. Saljo A, Bolouri H, Mayorga M, Svensson B, Hamberger A. Low-level blast raises intracranial pressure and impairs cognitive function in rats: prophylaxis with processed cereal feed. *J Neurotrauma* (2009) **27**:383–9. doi:10.1089/neu.2009.1053
43. Svetlov SI, Larner SF, Kirk DR, Atkinson J, Hayes RL, Wang KK. Biomarkers of blast-induced neurotrauma: profiling molecular and cellular mechanisms of blast brain injury. *J Neurotrauma* (2009) **26**:913–21. doi:10.1089/neu.2008.0609
44. Readnower RD, Chavko M, Adeeb S, Conroy MD, Pauly JR, McCarron RM, et al. Increase in blood-brain barrier permeability, oxidative stress, and activated microglia in a rat model of blast-induced traumatic brain injury. *J Neurosci Res* (2010) **88**:3530–9. doi:10.1002/jnr.22510
45. Cernak I, Wang Z, Jiang J, Bian X, Savic J. Ultrastructural and functional characteristics of blast injury-induced neurotrauma. *J Trauma* (2001) **50**:695–706. doi:10.1097/00005373-200104000-00017
46. DeWitt DS, Prough DS. Blast-induced brain injury and posttraumatic hypotension and hypoxemia. *J Neurotrauma* (2009) **26**:877–87. doi:10.1089/neu.2007.0439
47. Pun PB, Kan EM, Salim A, Li Z, Ng KC, Moochhala SM, et al. Low level primary blast injury in rodent brain. *Front Neurol* (2011) **2**:19. doi:10.3389/fneur.2011.00019
48. Cernak I, Savic J, Malicevic Z, Zunic G, Radosevic P, Ivanovic I, et al. Involvement of the central nervous system in the general response to pulmonary blast injury. *J Trauma* (1996) **40**:S100–4. doi:10.1097/00005373-199603001-00023
49. Davenport ND, Lim KO, Armstrong MT, Sponheim SR. Diffuse and spatially variable white matter disruptions are associated with blast-related mild traumatic brain injury. *Neuroimage* (2011) **59**:2017–24. doi:10.1016/j.neuroimage.2011.10.050
50. Koliatsos VE, Cernak I, Xu L, Song Y, Savonenko A, Crain BJ, et al. A mouse model of blast injury to brain: initial pathological, neuropathological, and behavioral characterization. *J Neuropathol Exp Neurol* (2011) **70**:399–416. doi:10.1097/NEN.0b013e3182189f06
51. Rafaels KA, Bass CR, Panzer MB, Salzar RS, Woods WA, Feldman SH, et al. Brain injury risk from primary blast. *J Trauma Acute Care Surg* (2012) **73**:895–901. doi:10.1097/TA.0b013e31825a760e
52. Kamnaksh A, Kovesdi E, Kwon SK, Wingo D, Ahmed F, Grunberg NE, et al. Factors affecting blast traumatic brain injury. *J Neurotrauma* (2011) **28**:2145–53. doi:10.1089/neu.2011.1983
53. de Lanerolle NC, Bandak F, Kang D, Li AY, Du F, Swauger P, et al. Characteristics of an explosive blast-induced brain injury in an experimental model. *J Neuropathol Exp Neurol* (2011) **70**:1046–57. doi:10.1097/NEN.0b013e318235bef2
54. Garman RH, Jenkins LW, Switzer RC III, Bauman RA, Tong LC, Swauger PV, et al. Blast exposure in rats with body shielding is characterized primarily by diffuse axonal injury. *J Neurotrauma* (2011) **28**:947–59. doi:10.1089/neu.2010.1540
55. Lighthall JW. Controlled cortical impact: a new experimental brain injury model. *J Neurotrauma* (1988) **5**:1–15. doi:10.1089/neu.1988.5.1
56. McIntosh TK, Vink R, Noble L, Yamakami I, Fernyak S, Soares H, et al. Traumatic brain injury in the rat: characterization of a lateral fluid-percussion model. *Neuroscience* (1989) **28**:233–44. doi:10.1016/0306-4522(89)90247-9
57. Dixon CE, Clifton GL, Lighthall JW, Yaghmai AA, Hayes RL. A controlled cortical impact model of traumatic brain injury in the rat. *J Neurosci Methods* (1991) **39**:253–62. doi:10.1016/0165-0270(91)90104-8
58. Hall ED, Bryant YD, Cho W, Sullivan PG. Evolution of post-traumatic neurodegeneration after controlled cortical impact traumatic brain injury in mice and rats as assessed by the de Olmos silver and fluorojade staining methods. *J Neurotrauma* (2008) **25**:235–47. doi:10.1089/neu.2007.0383
59. Greve MW, Zink BJ. Pathophysiology of traumatic brain injury. *Mt Sinai J Med* (2009) **76**:97–104. doi:10.1002/msj.20104
60. Cernak I, Radosevic P, Malicevic Z, Savic J. Experimental magnesium depletion in adult rabbits caused by blast overpressure. *Magnes Res* (1995) **8**:249–59.
61. Cernak I, Merkle AC, Koliatsos VE, Bilik JM, Luong QT, Mahota TM, et al. The pathobiology of blast injuries and blast-induced neurotrauma as identified using a new experimental model of injury in mice. *Neurobiol Dis* (2010) **41**:538–51. doi:10.1016/j.nbd.2010.10.025
62. Chavko M, Watanabe T, Adeeb S, Lankasky J, Ahlers ST, McCarron RM. Relationship between orientation to a blast and pressure wave propagation inside the rat brain. *J Neurosci Methods* (2011) **195**:61–6. doi:10.1016/j.jneumeth.2010.11.019
63. Okie S. Traumatic brain injury in the war zone. *N Engl J Med* (2005) **352**:2043–7. doi:10.1056/NEJMp058102
64. Carroll LJ, Cassidy JD, Peloso PM, Borg J, Von Holst H, Holm L, et al. Prognosis for mild traumatic brain injury: results of the WHO collaborating centre task force on mild traumatic brain injury. *J Rehabil Med* (2004) **43**:84–105. doi:10.1080/16501960410023859
65. Rosenfeld JV, Mcfarlane AC, Bragge P, Armonda RA, Grimes JB, Ling GS. Blast-related traumatic brain injury. *Lancet Neurol* (2013) **12**:882–93. doi:10.1016/S1474-4422(13)70161-3

66. Marion DW, Curley KC, Schwab K, Hicks RR, mTBI Diagnostics Workgroup. Proceedings of the military mTBI diagnostics workshop, St. Pete Beach, August 2010. *J Neurotrauma* (2011) **28**:517–26. doi:10.1089/neu.2010.1638
67. Armonda RA, Bell RS, Vo AH, Ling G, Degraba TJ, Crandall B, et al. Wartime traumatic cerebral vasospasm: recent review of combat casualties. *Neurosurgery* (2006) **59**:1215–25. doi:10.1227/01.NEU.0000249190.46033.94 discussion 1225,
68. Management of patients with severe head trauma: joint theater trauma system clinical practice guideline. (2012). Available from: http://www.usaisr.amedd.army.mil/assets/cpgs/Mgmt_of_Patients_with_%20Severe_Head_Trauma_7_Mar_12.pdf
69. Vanderploeg RD, Belanger HG, Horner RD, Spehar AM, Powell-Cope G, Luther SL, et al. Health outcomes associated with military deployment: mild traumatic brain injury, blast, trauma, and combat associations in the Florida national guard. *Arch Phys Med Rehabil* (2012) **93**:1887–95. doi:10.1016/j.apmr.2012.05.024
70. Trudeau DL, Anderson J, Hansen LM, Shagalov DN, Schmoller J, Nugent S, et al. Findings of mild traumatic brain injury in combat veterans with PTSD and a history of blast concussion. *J Neuropsychiatry Clin Neurosci* (1998) **10**:308–13.
71. Santiago PN, Wilk JE, Milliken CS, Castro CA, Engel CC, Hoge CW. Screening for alcohol misuse and alcohol-related behaviors among combat veterans. *Psychiatr Serv* (2010) **61**:575–81. doi:10.1176/appi.ps.61.6.575
72. Taber KH, Warden DL, Hurley RA. Blast-related traumatic brain injury: what is known? *J Neuropsychiatry Clin Neurosci* (2006) **18**:141–5. doi:10.1176/appi.neuropsych.18.2.141
73. Kocsis JD, Tessler A. Pathology of blast-related brain injury. *J Rehabil Res Dev* (2009) **46**:667–72. doi:10.1682/JRRD.2008.08.0100
74. Nelson NW, Hoelzle JB, Mcguire KA, Ferrier-Auerbach AG, Charlesworth MJ, Sponheim SR. Neuropsychological evaluation of blast-related concussion: illustrating the challenges and complexities through OEF/OIF case studies. *Brain Inj* (2011) **25**:511–25. doi:10.3109/02699052.2011.558040
75. Zatzick DF, Rivara FP, Jurkovich GJ, Hoge CW, Wang J, Fan MY, et al. Multisite investigation of traumatic brain injuries, posttraumatic stress disorder, and self-reported health and cognitive impairments. *Arch Gen Psychiatry* (2010) **67**:1291–300. doi:10.1001/archgenpsychiatry.2010.158
76. Seal KH, Cohen G, Waldrop A, Cohen BE, Maguen S, Ren L. Substance use disorders in Iraq and Afghanistan veterans in VA healthcare, 2001-2010: implications for screening, diagnosis and treatment. *Drug Alcohol Depend* (2011) **116**:93–101. doi:10.1016/j.drugalcdep.2010.11.027
77. Tanielian E, Jayco LH. *Invisible Wounds of War: Psychological and Cognitive Injuries, Their Consequences, and Services to Assist Recovery*. Los Angeles: Rand Corporation (2008).
78. Stein MB, McAllister TW. Exploring the convergence of posttraumatic stress disorder and mild traumatic brain injury. *Am J Psychiatry* (2009) **166**:768–76. doi:10.1176/appi.ajp.2009.08101604
79. APA. *Diagnostic and Statistical Manual of Mental Disorders*. 4th ed. Washington, DC: American Psychiatric Association (2000).
80. Vasterling JJ, Verfaellie M, Sullivan KD. Mild traumatic brain injury and posttraumatic stress disorder in returning veterans: perspectives from cognitive neuroscience. *Clin Psychol Rev* (2009) **29**:674–84. doi:10.1016/j.cpr.2009.08.004
81. Rosenfeld JV, Ford NL. Bomb blast, mild traumatic brain injury and psychiatric morbidity: a review. *Injury* (2010) **41**:437–43. doi:10.1016/j.injury.2009.11.018
82. Bryant R. Post-traumatic stress disorder vs traumatic brain injury. *Dialogues Clin Neurosci* (2011) **13**:251–62.
83. Di Stefano G, Bachevalier J, Levin HS, Song JX, Scheibel RS, Fletcher JM. Volume of focal brain lesions and hippocampal formation in relation to memory function after closed head injury in children. *J Neurol Neurosurg Psychiatry* (2000) **69**:210–6. doi:10.1136/jnnp.69.2.210
84. Geuze E, Vermetten E, Bremner JD. MR-based in vivo hippocampal volumetrics: 2. Findings in neuropsychiatric disorders. *Mol Psychiatry* (2005) **10**:160–84. doi:10.1038/sj.mp.4001580
85. Francati V, Vermetten E, Bremner JD. Functional neuroimaging studies in posttraumatic stress disorder: review of current methods and findings. *Depress Anxiety* (2007) **24**:202–18. doi:10.1002/da.20208
86. Scheibel RS, Newsome MR, Troyanskaya M, Lin X, Steinberg JL, Radaideh M, et al. Altered brain activation in military personnel with one or more traumatic brain injuries following blast. *J Int Neuropsychol Soc* (2012) **18**:89–100. doi:10.1017/S1355617711001433
87. Bass CR, Panzer MB, Rafaels KA, Wood G, Shridharani J, Capehart B. Brain injuries from blast. *Ann Biomed Eng* (2011) **40**:185–202. doi:10.1007/s10439-011-0424-0
88. First MB, Frances A, Pincus HA. *DSM-IV Handbook of Differential Diagnosis*. Washington, DC: American Psychiatric Press (1995).
89. Bombardier CH, Fann JR, Temkin N, Esselman PC, Pelzer E, Keough M, et al. Posttraumatic stress disorder symptoms during the first six months after traumatic brain injury. *J Neuropsychiatry Clin Neurosci* (2006) **18**:501–8. doi:10.1176/appi.neuropsych.18.4.501
90. Irwin RJ, Lerner MR, Bealer JF, Lightfoot SA, Brackett DJ, Tuggle DW. Global primary blast injury: a rat model. *J Okla State Med Assoc* (1998) **91**:387–92.
91. Garner JP, Watts S, Parry C, Bird J, Kirkman E. Development of a large animal model for investigating resuscitation after blast and hemorrhage. *World J Surg* (2009) **33**:2194–202. doi:10.1007/s00268-009-0105-4
92. Svetlov SI, Prima V, Glushakova O, Svetlov A, Kirk DR, Gutierrez H, et al. Neuro-glial and systemic mechanisms of pathological responses in rat models of primary blast overpressure compared to "composite" blast. *Front Neurol* (2012) **3**:15. doi:10.3389/fneur.2012.00015
93. Rubovitch V, Ten-Bosch M, Zohar O, Harrison CR, Tempel-Brami C, Stein E, et al. A mouse model of blast-induced mild traumatic brain injury. *Exp Neurol* (2011) **232**:280–9. doi:10.1016/j.expneurol.2011.09.018
94. Lei T, Xie L, Tu W, Chen Y, Tan Y. Development of a finite element model for blast injuries to the pig mandible and a preliminary biomechanical analysis. *J Trauma Acute Care Surg* (2012) **73**:902–7. doi:10.1097/TA.0b013e3182515cb1
95. Li J, Topaz M, Xun W, Li W, Wang X, Liu H, et al. New swine model of infected soft tissue blast injury. *J Trauma Acute Care Surg* (2012) **73**:908–13. doi:10.1097/TA.0b013e318253b592
96. Sundaramurthy A, Alai A, Ganpule S, Holmberg A, Plougonven E, Chandra N. Blast-induced biomechanical loading of the rat: an experimental and anatomically accurate computational blast injury model. *J Neurotrauma* (2012) **29**:2352–64. doi:10.1089/neu.2012.2413
97. Yarnell AM, Shaughness MC, Barry ES, Ahlers ST, McCarron RM, Grunberg NE. Blast traumatic brain injury in the rat using a blast overpressure model. *Curr Protoc Neurosci* (2013). Chapter 9, Unit 9.41. doi:10.1002/0471142301.ns0941s62
98. Kochanek PM, Bauman RA, Long JB, Dixon CR, Jenkins LW. A critical problem begging for new insight and new therapies. *J Neurotrauma* (2009) **26**:813–4. doi:10.1089/neu.2008.0893
99. Pervin F, Chen WW. Effect of inter-species, gender, and breeding on the mechanical behavior of brain tissue. *Neuroimage* (2011) **54**(Suppl 1):S98–102. doi:10.1016/j.neuroimage.2010.03.077
100. Unterberg AW, Stover J, Kress B, Kiening KL. Edema and brain trauma. *Neuroscience* (2004) **129**:1021–9. doi:10.1016/j.neuroscience.2004.06.046
101. Morganti-Kossmann MC, Satgunaseelan L, Bye N, Kossmann T. Modulation of immune response by head injury. *Injury* (2007) **38**:1392–400. doi:10.1016/j.injury.2007.10.005
102. Abdul-Muneer PM, Schuetz H, Wang F, Skotak M, Jones J, Gorantla S, et al. Induction of oxidative and nitrosative damage leads to cerebrovascular inflammation in an animal model of mild traumatic brain injury induced by primary blast. *Free Radic Biol Med* (2013) **60**:282–91. doi:10.1016/j.freeradbiomed.2013.02.029
103. Yeoh S, Bell ED, Monson KL. Distribution of blood-brain barrier disruption in primary blast injury. *Ann Biomed Eng* (2013) **41**(10):2206–14. doi:10.1007/s10439-013-0805-7
104. Tumer N, Svetlov S, Whidden M, Kirichenko N, Prima V, Erdos B, et al. Overpressure blast-wave induced brain injury elevates oxidative stress in the hypothalamus and catecholamine biosynthesis in the rat adrenal medulla. *Neurosci Lett* (2013) **544**:62–7. doi:10.1016/j.neulet.2013.03.042
105. Biber N, Toklu HZ, Solakoglu S, Gultomruk M, Hakan T, Berkman Z, et al. Cysteinyl-leukotriene receptor antagonist montelukast decreases blood-brain barrier permeability but does not prevent oedema formation in traumatic brain injury. *Brain Inj* (2009) **23**:577–84. doi:10.1080/02699050902926317
106. Hinson HE, Sheth KN. Manifestations of the hyperadrenergic state after acute brain injury. *Curr Opin Crit Care* (2012) **18**:139–45. doi:10.1097/MCC.0b013e3283513290
107. Viola-Saltzman M, Watson NF. Traumatic brain injury and sleep disorders. *Neurol Clin* (2012) **30**:1299–312. doi:10.1016/j.ncl.2012.08.008
108. Griesbach GS. Exercise after traumatic brain injury: is it a double-edged sword? *PM R* (2011) **3**:S64–72. doi:10.1016/j.pmrj.2011.02.008

109. Kvetnansky R, Sabban EL, Palkovits M. Catecholaminergic systems in stress: structural and molecular genetic approaches. *Physiol Rev* (2009) **89**:535–606. doi:10.1152/physrev.00042.2006
110. Kochanek PM, Dixon CE, Shellington DK, Shin SS, Bayir H, Jackson E, et al. Screening of biochemical and molecular mechanisms of secondary injury and repair in the brain after experimental blast-induced traumatic brain injury in rats. *J Neurotrauma* (2012) **30**(11):920–37. doi:10.1089/neu.2013.2862
111. Vuceljic M, Zunic G, Romic P, Jevtic M. Relation between both oxidative and metabolic-osmotic cell damages and initial injury severity in bombing casualties. *Vojnosanit Pregl* (2006) **63**:545–51. doi:10.2298/VSP0606545V
112. Menon DK, Schwab K, Wright DW, Maas AI, Demographics and Clinical Assessment Working Group of the International and Interagency Initiative toward Common Data Elements for Research on Traumatic Brain Injury and Psychological Health. Position statement: definition of traumatic brain injury. *Arch Phys Med Rehabil* (2010) **91**:1637–40. doi:10.1016/j.apmr.2010.05.017
113. Bazarian JJ, Blyth B, Cimpello L. Bench to bedside: evidence for brain injury after concussion – looking beyond the computed tomography scan. *Acad Emerg Med* (2006) **13**:199–214. doi:10.1197/j.aem.2005.07.031
114. Mac Donald CL, Johnson AM, Cooper D, Nelson EC, Werner NJ, Shimony JS, et al. Detection of blast-related traumatic brain injury in U.S. military personnel. *N Engl J Med* (2011) **364**:2091–100. doi:10.1056/NEJMoa1008069
115. Levin HS, Wilde E, Troyanskaya M, Petersen NJ, Scheibel R, Newsome M, et al. Diffusion tensor imaging of mild to moderate blast-related traumatic brain injury and its sequelae. *J Neurotrauma* (2010) **27**:683–94. doi:10.1089/neu.2009.1073
116. Mondello S, Muller U, Jeromin A, Streeter J, Hayes RL, Wang KK. Blood-based diagnostics of traumatic brain injuries. *Expert Rev Mol Diagn* (2011) **11**:65–78. doi:10.1586/erm.10.104
117. Mondello S, Schmid K, Berger RP, Kobeissy F, Italiano D, Jeromin A, et al. The challenge of mild traumatic brain injury: role of biochemical markers in diagnosis of brain damage. *Med Res Rev* (2013). doi:10.1002/med.21295
118. Papa L, Lewis LM, Falk JL, Zhang Z, Silvestri S, Giordano P, et al. Elevated levels of serum glial fibrillary acidic protein breakdown products in mild and moderate traumatic brain injury are associated with intracranial lesions and neurosurgical intervention. *Ann Emerg Med* (2012) **59**:471–83. doi:10.1016/j.annemergmed.2011.08.021
119. Papa L, Lewis LM, Silvestri S, Falk JL, Giordano P, Brophy GM, et al. Serum levels of ubiquitin C-terminal hydrolase distinguish mild traumatic brain injury from trauma controls and are elevated in mild and moderate traumatic brain injury patients with intracranial lesions and neurosurgical intervention. *J Trauma Acute Care Surg* (2012) **72**:1335–44. doi:10.1097/TA.0b013e3182491e3d
120. Unden J, Romner B. Can low serum levels of S100B predict normal CT findings after minor head injury in adults? an evidence-based review and meta-analysis. *J Head Trauma Rehabil* (2010) **25**:228–40. doi:10.1097/HTR.0b013e3181e57e22
121. Agoston DV, Gyorgy A, Eidelman O, Pollard HB. Proteomic biomarkers for blast neurotrauma: targeting cerebral edema, inflammation, and neuronal death cascades. *J Neurotrauma* (2009) **26**:901–11. doi:10.1089/neu.2008.0724
122. Gyorgy A, Ling G, Wingo D, Walker J, Tong L, Parks S, et al. Time-dependent changes in serum biomarker levels after blast traumatic brain injury. *J Neurotrauma* (2011) **28**:1121–6. doi:10.1089/neu.2010.1561
123. Balakathiresan N, Bhomia M, Chandran R, Chavko M, McCarron RM, Maheshwari RK. MicroRNA let-7i is a promising serum biomarker for blast-induced traumatic brain injury. *J Neurotrauma* (2012) **29**:1379–87. doi:10.1089/neu.2011.2146
124. Agoston DV, Elsayed M. Serum-based protein biomarkers in blast-induced traumatic brain injury spectrum disorder. *Front Neurol* (2012) **3**:107. doi:10.3389/fneur.2012.00107
125. Ingebrigtsen T, Romner B. Biochemical serum markers for brain damage: a short review with emphasis on clinical utility in mild head injury. *Restor Neurol Neurosci* (2003) **21**:171–6.
126. Blennow K, Jonsson M, Andreasen N, Rosengren L, Wallin A, Hellstrom PA, et al. No neurochemical evidence of brain injury after blast overpressure by repeated explosions or firing heavy weapons. *Acta Neurol Scand* (2011) **123**:245–51. doi:10.1111/j.1600-0404.2010.01408.x
127. Tate CM, Wang KK, Eonta S, Zhang Y, Carr W, Tortella FC, et al. Serum brain biomarker level, neurocognitive performance, and self-reported symptom changes in soldiers repeatedly exposed to low-level blast: a breacher pilot study. *J Neurotrauma* (2013) **30**(19):1620–30. doi:10.1089/neu.2012.2683
128. Omalu B, Hammers JL, Bailes J, Hamilton RL, Kamboh MI, Webster G, et al. Chronic traumatic encephalopathy in an Iraqi war veteran with posttraumatic stress disorder who committed suicide. *Neurosurg Focus* (2011) **31**:E3. doi:10.3171/2011.9.FOCUS11178
129. Goldstein LE, Fisher AM, Tagge CA, Zhang XL, Velisek L, Sullivan JA, et al. Chronic traumatic encephalopathy in blast-exposed military veterans and a blast neurotrauma mouse model. *Sci Transl Med* (2012) **4**:134ra60. doi:10.1126/scitranslmed.3003716
130. Miller G. Neuropathology. Blast injuries linked to neurodegeneration in veterans. *Science* (2012) **336**:790–1. doi:10.1126/science.336.6083.790
131. Huber BR, Meabon JS, Martin TJ, Mourad PD, Bennett R, Kraemer BC, et al. Blast exposure causes early and persistent aberrant phospho- and cleaved-tau expression in a murine model of mild blast-induced traumatic brain injury. *J Alzheimers Dis* (2013) **37**(2):309–23. doi:10.3233/JAD-130182
132. Berger RP. The use of serum biomarkers to predict outcome after traumatic brain injury in adults and children. *J Head Trauma Rehabil* (2006) **21**:315–33. doi:10.1097/00001199-200607000-00004
133. Beers SR, Berger RP, Adelson PD. Neurocognitive outcome and serum biomarkers in inflicted versus non-inflicted traumatic brain injury in young children. *J Neurotrauma* (2007) **24**:97–105. doi:10.1089/neu.2006.0055
134. Cho HJ, Sajja VS, Vandevord PJ, Lee YW. Blast induces oxidative stress, inflammation, neuronal loss and subsequent short-term memory impairment in rats. *Neuroscience* (2013) **253C**:9–20. doi:10.1016/j.neuroscience.2013.08.037
135. Genovese RF, Simmons LP, Ahlers ST, Maudlin-Jeronimo E, Dave JR, Boutte AM. Effects of mild TBI from repeated blast overpressure on the expression and extinction of conditioned fear in rats. *Neuroscience* (2013) **254C**:120–9. doi:10.1016/j.neuroscience.2013.09.021
136. Ahmed FA, Kamnaksh A, Kovesdi E, Long JB, Agoston DV. Long-term consequences of single and multiple mild blast exposure on select physiological parameters and blood-based biomarkers. *Electrophoresis* (2013) **34**:2229–33. doi:10.1002/elps.201300077
137. Arun P, Abu-Taleb R, Oguntayo S, Tanaka M, Wang Y, Valiyaveettil M, et al. Distinct patterns of expression of traumatic brain injury biomarkers after blast exposure: role of compromised cell membrane integrity. *Neurosci Lett* (2013) **552**:87–91. doi:10.1016/j.neulet.2013.07.047
138. Zou YY, Kan EM, Lu J, Ng KC, Tan MH, Yao L, et al. Primary blast injury-induced lesions in the retina of adult rats. *J Neuroinflammation* (2013) **10**:79. doi:10.1186/1742-2094-10-79
139. Prima V, Serebruany V, Svetlov A, Hayes RL, Svetlov S. Impact of moderate blast exposures on thrombin biomarkers assessed by Calibrated Automated Thrombography (CAT) in rats. *J Neurotrauma* (2013) **30**(22):1881–7. doi:10.1089/neu.2012.2758
140. Sajja VS, Galloway M, Ghoddoussi F, Kepsel A, Vandevord P. Effects of blast-induced neurotrauma on the nucleus accumbens. *J Neurosci Res* (2013) **91**:593–601. doi:10.1002/jnr.23179
141. Skotak M, Wang F, Alai A, Holmberg A, Harris S, Switzer RC, et al. Rat injury model under controlled field-relevant primary blast conditions: acute response to a wide range of peak overpressures. *J Neurotrauma* (2013) **30**:1147–60. doi:10.1089/neu.2012.2652
142. Takeuchi S, Nawashiro H, Sato S, Kawauchi S, Nagatani K, Kobayashi H, et al. A better mild traumatic brain injury model in the rat. *Acta Neurochir Suppl* (2013) **118**:99–101. doi:10.1007/978-3-7091-1434-6_17
143. Turner RC, Naser ZJ, Logsdon AF, Dipasquale KH, Jackson GJ, Robson MJ, et al. Modeling clinically relevant blast parameters based on scaling principles produces functional & histological deficits in rats. *Exp Neurol* (2013) **248**:520–9. doi:10.1016/j.expneurol.2013.07.008
144. Tweedie D, Rachmany L, Rubovitch V, Zhang Y, Becker KG, Perez E, et al. Changes in mouse cognition and hippocampal gene expression observed in a mild physical- and blast-traumatic brain injury. *Neurobiol Dis* (2013) **54**:1–11. doi:10.1016/j.nbd.2013.02.006
145. Ahlers ST, Vasserman-Stokes E, Shaughness MC, Hall AA, Shear DA, Chavko M, et al. Assessment of the effects of acute and repeated exposure to blast overpressure in rodents: toward a greater understanding of blast and the potential ramifications for injury in humans exposed to blast. *Front Neurol* (2012) **3**:32. doi:10.3389/fneur.2012.00032

146. Ahmed F, Gyorgy A, Kamnaksh A, Ling G, Tong L, Parks S, et al. Time-dependent changes of protein biomarker levels in the cerebrospinal fluid after blast traumatic brain injury. *Electrophoresis* (2012) **33**:3705–11. doi:10.1002/elps.201200299
147. Hines-Beard J, Marchetta J, Gordon S, Chaum E, Geisert EE, Rex TS. A mouse model of ocular blast injury that induces closed globe anterior and posterior pole damage. *Exp Eye Res* (2012) **99**:63–70. doi:10.1016/j.exer.2012.03.013
148. Bir C, Vandevord P, Shen Y, Raza W, Haacke EM. Effects of variable blast pressures on blood flow and oxygen saturation in rat brain as evidenced using MRI. *Magn Reson Imaging* (2012) **30**:527–34. doi:10.1016/j.mri.2011.12.003
149. Kovesdi E, Gyorgy AB, Kwon SK, Wingo DL, Kamnaksh A, Long JB, et al. The effect of enriched environment on the outcome of traumatic brain injury; a behavioral, proteomics, and histological study. *Front Neurosci* (2011) **5**:42. doi:10.3389/fnins.2011.00042
150. Kovesdi E, Kamnaksh A, Wingo D, Ahmed F, Grunberg NE, Long JB, et al. Acute minocycline treatment mitigates the symptoms of mild blast-induced traumatic brain injury. *Front Neurol* (2012) **3**:111. doi:10.3389/fneur.2012.00111
151. Reneer DV, Hisel RD, Hoffman JM, Kryscio RJ, Lusk BT, Geddes JW. A multi-mode shock tube for investigation of blast-induced traumatic brain injury. *J Neurotrauma* (2011) **28**:95–104. doi:10.1089/neu.2010.1513
152. Risling M, Plantman S, Angeria M, Rostami E, Bellander BM, Kirkegaard M, et al. Mechanisms of blast induced brain injuries, experimental studies in rats. *Neuroimage* (2011) **54**(Suppl 1):S89–97. doi:10.1016/j.neuroimage.2010.05.031
153. Shridharani JK, Wood GW, Panzer MB, Capehart BP, Nyein MK, Radovitzky RA, et al. Porcine head response to blast. *Front Neurol* (2012) **3**:70. doi:10.3389/fneur.2012.00070
154. Elder GA, Dorr NP, De Gasperi R, Gama Sosa MA, Shaughness MC, Maudlin-Jeronimo E, et al. Blast exposure induces post-traumatic stress disorder-related traits in a rat model of mild traumatic brain injury. *J Neurotrauma* (2012) **29**:2564–75. doi:10.1089/neu.2012.2510
155. Dalle Lucca JJ, Chavko M, Dubick MA, Adeeb S, Falabella MJ, Slack JL, et al. Blast-induced moderate neurotrauma (BINT) elicits early complement activation and tumor necrosis factor alpha (TNFalpha) release in a rat brain. *J Neurol Sci* (2012) **318**:146–54. doi:10.1016/j.jns.2012.02.002
156. Kuehn R, Simard PF, Driscoll I, Keledjian K, Ivanova S, Tosun C, et al. Rodent model of direct cranial blast injury. *J Neurotrauma* (2011) **28**:2155–69. doi:10.1089/neu.2010.1532
157. Cernak I, Merkle AC, Koliatsos VE, Bilik JM, Luong QT, Mahota TM, et al. The pathobiology of blast injuries and blast-induced neurotrauma as identified using a new experimental model of injury in mice. *Neurobiol Dis* (2011) **41**:538–51. doi:10.1016/j.nbd.2010.10.025
158. Connell S, Gao J, Chen J, Shi R. Novel model to investigate blast injury in the central nervous system. *J Neurotrauma* (2011) **28**:1229–36. doi:10.1089/neu.2011.1832
159. Cheng J, Gu J, Ma Y, Yang T, Kuang Y, Li B, et al. Development of a rat model for studying blast-induced traumatic brain injury. *J Neurol Sci* (2010) **294**:23–8. doi:10.1016/j.jns.2010.04.010
160. Cai JH, Chai JK, Shen CA, Yin HN, Zhou XF, Lu W, et al. Early changes in serum neutrophil elastase in rats with burn, blast injury or combined burn-blast injury and its significance. *Zhonghua Yi Xue Za Zhi* (2010) **90**:1707–10.

Conflict of Interest Statement: Drs. Prima and Svetlov are employees and receive salaries from Banyan Biomarkers, Inc. The other co-authors declare that the research was conducted in the absence of any commercial or financial relationships that could be construed as a potential conflict of interest.

Received: 31 October 2012; accepted: 02 November 2013; published online: 21 November 2013.
*Citation: Kobeissy F, Mondello S, Tümer N, Toklu HZ, Whidden MA, Kirichenko N, Zhang Z, Prima V, Yassin W, Anagli J, Chandra N, Svetlov S and Wang KKW (2013) Assessing neuro-systemic & behavioral components in the pathophysiology of blast-related brain injury. Front. Neurol. **4**:186. doi: 10.3389/fneur.2013.00186*
This article was submitted to Neurotrauma, a section of the journal Frontiers in Neurology.

Respiratory Physiology & Neurobiology 204 (2014) 112–119

Contents lists available at ScienceDirect

Respiratory Physiology & Neurobiology

journal homepage: www.elsevier.com/locate/resphysiol

Respiratory responses following blast-induced traumatic brain injury in rats☆

Sherry Adams[a], Jillian A. Condrey[a], Hsiu-Wen Tsai[a], Stanislav I. Svetlov[b,c], Paul W. Davenport[a,*]

[a] Department of Physiological Sciences, University of Florida, Gainesville, FL, USA
[b] Banyan Biomarkers, 13400 Progress Blvd, Alachua, FL, USA
[c] Departments of Medicine and Psychiatry, University of Florida, 1600 SW Archer Road, Box 100274, Gainesville, FL, USA

ARTICLE INFO

Article history:
Accepted 21 August 2014
Available online 19 September 2014

Keywords:
Overpressurization blast
Traumatic brain injury
Respiration
Electromyographic recording

ABSTRACT

Blast overpressure (OB) injury in rodents has been employed for modeling the traumatic brain injury (TBI) induced by an improvised explosive device (IED) in military service personnel. IED's can cause respiratory arrest if directed at the thorax due to the fluid–tissue interface of the lungs but it is unclear what respiratory changes occur in a head-directed OB injury. The diaphragm is the primary muscle of inspiration and electromyographic (EMG) recordings from this muscle are used for recording breathing in anesthetized and conscious rats. The breathing pattern of the rodents will be recorded during the OB injury. Our results indicate that a dorsal directed closed-head OB injury results in a neurally mediated apnea followed by respiratory timing changes.

1. Introduction

Traumatic brain injury (TBI) affects 1.7 million people annually in the United States (Faul et al., 2010). The CDC reports that TBI rates are higher for males than females in every age group. Soldiers in combat are most susceptible to sustain a TBI as a result of an overpressure blast (OB) wave from an improvised explosive device (IED). Overpressure wave causes damage to air-filled organs and air-fluid interfaces due to the interaction between the stress wave and shear wave (Guy et al., 1998a). Blast directed and localized to the dorsal surface of the head between bregma and lambda induces closed-head TBI if the pressure force is of sufficient magnitude. Closed-head OB injuries send shearing and stressing forces throughout the brain including the brainstem resulting in observational disruptions in breathing. TBI with body protection is known to result in observational apneic periods in rodent models (Cheng et al., 2010; Dixon et al., 1987; Guy et al., 1998b; Kuehn et al., 2011). These apneas may result from neuronal disruption in the brainstem respiratory control center, transmission of the pressure force vector throughout the body via the cerebrospinal fluid and circulatory system or other unknown reasons. The OB TBI disruption of breathing is, however, not well understood, especially during OBI exposure, hence our primary goal is to determine the respiratory rhythm pattern during an OB TBI isolated to the head.

1.1. OB TBI

The OB wave is experimentally produced by a shock tube driven by compressed air. An OB wave directed at the skull of a rodent results in an OB TBI if the pressure is of sufficient magnitude. OB waves directed at the dorsal skull of a rat between bregma and lambda may cause apnea based on anecdotal evidence. The OB shock tube can generate a controlled pressure wave which can be replicated under experimental conditions. A shock tube was designed, constructed and tested by the Florida Institute of Technology at Banyan Biomarkers (see their Fig. 1a) (Svetlov et al., 2010). There are two sections of the shock tube separated by a metal diaphragm. The two sections include the gas at high pressure (driver) and the gas at low pressure (driven) separated by a diaphragm. At a predetermined threshold level, the diaphragm ruptures which generates a shock wave propagating through the low-pressure section (driven) to the end of the shock tube. The peak and duration of the overpressure blast is determined by the driver/driven ratio, thickness and type of diaphragm material. Stainless steel diaphragms 0.05-mm thick with driver/driven ratio of 15–1 was used to produce the shock wave. An internal cutter was used to initialize the rupture of the diaphragm so the low-pressure

☆ This paper is part of a special issue entitled "Non-homeostatic control of respiration", guest-edited Dr. Eugene Nalivaiko and Dr. Paul Davenport.

* Corresponding author. Tel.: +1 352 294 4025; fax: +1 352 392 5145.
E-mail address: pdavenpo@ufl.edu (P.W. Davenport).

http://dx.doi.org/10.1016/j.resp.2014.08.015
1569-9048/

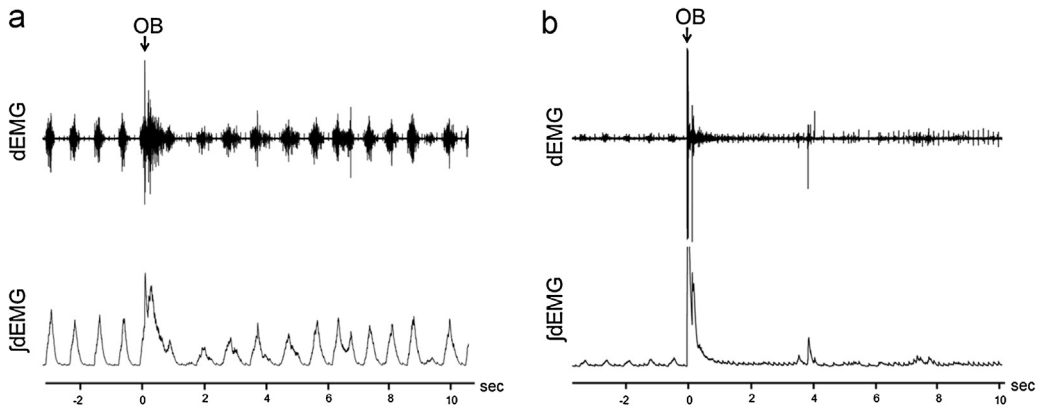

Fig. 1. Recordings of raw (top trace) and $\int$dEMG (bottom) for OB-1 animals. (a) dEMG in an OB-1, Group 1 animal, Psi = 69.9. (b) dEMG in an OB-1, Group 2 animal, Psi = 90.3.

air mixes with the high-pressure gas resulting in a shock wave. The blast pressure waveform (Svetlov et al., 2010) has a peak overpressure and gas venting phase, believed to cause the most damage due to the prolonged time spent in this phase. The blast wave is 10 ms at variable Psi levels measured at the shock tube. The blast pressure data was acquired from piezoelectric blast pressure transducers.

When the animal is positioned directly under the shock tube nozzle, it is known as a composite blast. Composite blast exposure (directed at the skull) can result in diffuse brain injury and neurodegeneration in the rostral and caudal diencaphalon and mesencephalon (Svetlov et al., 2010). OB injury can also result in intracranial hematomas as well as brain swelling (Svetlov et al., 2010). Upon autopsy of the animals (5/27) that succumbed to blast injury, hematomas were found on the dorsal aspect of the brain between bregma and lambda along with evidence of a disruption of vascular supply within the circle of Willis. The kinectic force of the OB on the superficial and interior portion of the brain is evident when mortality occurred (Svetlov et al., 2010).

The OB blast injury is reproducible and causes significant damage throughout the brain as evidenced by gross inspection and histology (Svetlov et al., 2010). Observational disruptions in breathing have been seen in multiple rodent models during both closed and open head injuries (Cheng et al., 2010; Dixon et al., 1987; Guy et al., 1998b; Kuehn et al., 2011). However, breathing pattern immediately before, during and immediately after OB TBI remains unknown. Specifically, it is unknown if inspiratory motor drive ceases (apnea) during and after OB exposure. It is also unknown if there is a relationship between the magnitude of the OB and apnea. Further, the effect of repeated OB on apnea is unknown.

1.2. TBI and respiration

Respiration is controlled both consciously and autonomically via the brainstem respiratory network. The respiratory control network receives afferent and efferent input and this information is processed to maintain homeostasis. Autonomic brainstem respiratory function is controlled by the pons and medulla. The pons and medulla have a network of respiratory neurons that generate the respiratory motor pattern. Inspiratory and expiratory neurons send axons to the inspiratory and expiratory motor units to provide the neuromuscular drive and breathing pattern. A disruption in this region can result in an absence of breathing (apnea) or an altered breathing pattern evidenced by gasping, sighs or irregularities in the breathing pattern. Apnea is defined as an absence in diaphragmatic muscle activity for a minimum of two respiratory cycles. Observational apneic periods have been seen in humans and animals during TBI. Changes in breathing patterns including apnea, partial recovery of respiration, followed by slow and deep respiration were observed in rodents during a skull-directed detonator blast (Cheng et al., 2010).

Apnea followed by a period of irregular breathing is believed to result from OB injury of sufficient magnitude but specific respiratory motor activity has not been recorded during OB exposure. It is likely that the respiratory control network is disrupted at the medullary level by the intracranial high pressure wave. Disruption within the respiratory network is hypothesized to result in an apneic period and the apneic duration may be a function of the magnitude of the pressure wave. It is also likely that the initial OB injury would cause this respiratory neural network to become hypersensitive to a second smaller magnitude OB, resulting in a longer apneic period. The present study will directly record diaphragm EMG (dEMG) during an OB to determine duration of the apneic period and subsequent irregular breathing pattern following the OB.

We hypothesized that blast-induced TBI: (1) will induce an apneic period during and immediately following blast exposure induced acute TBI directly related to the magnitude of the OB pressure wave; (2) will induce post-apnea irregular breathing pattern that is directly related to the magnitude of the OB pressure wave; (3) will induce apnea at lower pressures and longer durations with repeated OB injury (2 weeks after the first OB); and (4) will induce irregular breathing pattern directly related to magnitude of the second OB pressure wave with repeated OB injury (2 weeks after the first OB). To test these hypotheses, dEMG recordings were obtained in chronically instrumented rats immediately before, during and immediately after the dorsal head OB exposure.

2. Materials and methods

2.1. Animals

These experiments were performed on male Sprague-Dawley rats weighing 250–300 g. The animals were housed in the University of Florida animal care facility. They were exposed to a 12-h light/12-h dark cycle with food and water ad libitum. The experimental protocol was reviewed and approved by the Institutional Animal Care and Use Committee of the University of Florida.

2.2. Surgical procedure

Animals were anesthetized using isoflurane. The abdominal wall was incised and costal borders retracted to expose the diaphragm muscle. dEMG electrodes (stainless steel, Teflon-coated wire AS631, Cooner Wire, Chatsworth, CA, USA) were introduced into the diaphragm at the intercostal border on the right side and advanced through the diaphragm muscle and glued securely into

place with sterile VetBond. The wires were connected to a multi-wire harness and the connector was externalized at the dorsal surface between the scapulae. The abdominal cavity was sutured and animals recovered 5–7 days.

2.3. Chronic EMG recording methods

The dEMG signals were recorded from the diaphragm by attaching the external harness connector to a pre-amplifier which was led into an amplifier (gain: 100×) and band-pass filtered (100–1000 Hz). The signal was digitized using PowerLab and LabChart 7 Pro (ADInstruments).

The instrumented (dEMG electrodes) animals were randomized after the surgical recovery period into two experimental groups for the first OB exposure (OB-1); (Group 1) 68.6–73.1 Psi ($n = 7$) and (Group 2) 82.9–102.6 Psi ($n = 15$). On the day of the OB-1 procedure, the animals were anesthetized with isoflurane. The externalized electrode harness was connected to the pre-amplifier to record dEMG activity. The anesthetized animals were placed onto a flexible mesh surface with the dorsal surface of head positioned underneath the air nozzle. Body was protected with a plexiglass shield placed over the entire body leaving only the head exposed (Svetlov et al., 2010). dEMG activity was recorded for 5 min prior to OB exposure. Then a 10-ms duration OB (onset marked on the recording) was performed while dEMG was recorded continuously. The Psi was measured using piezoelectric blast pressure transducers. Post-OB-1, the dEMG activity was recorded for 3–5 min. The animals were then removed from anesthesia and returned to their cages. The second OB (OB-2) was presented 14 days Post-OB-1. Instrumented (dEMG electrodes) animals were randomized into two OB-2 experimental groups; (Group 3) 66.5–71.5 Psi ($n = 6$) and (Group 4) 86.7–94.0 ($n = 5$). The OB-2 procedure was performed the same as the OB-1 procedure (see above).

2.4. Data analysis

LabChart 7 Pro (ADInstruments) was used for analysis of the digitized dEMG activity. All data were analyzed off-line. The raw dEMG signal was integrated ($\int$dEMG) with a 50 ms time constant, moving time average. The OB zero time point was defined as the onset time of delivery of the overpressurization blast identified from the dEMG (Fig. 1). The apnea period was the time from OB delivery with breathing cessation (no diaphragm EMG activity) until dEMG inspiratory efforts returned. Apnea was defined as cessation of dEMG activity for a time greater than a minimum of two pre-OB respiratory cycles. The irregular breathing period was the time from initial return of inspiratory efforts until the frequency returned to less than ±1SD of the pre-OB respiratory cycle timing pattern. The inspiratory time (Ti) was determined from the onset of dEMG activity to the peak of the $\int$dEMG activity, expiratory time (Te) from the $\int$dEMG activity peak to the onset of the subsequent dEMG, total breath time (Ttot) was the sum of Ti and Te.

2.5. Statistical analysis

All respiratory parameters were represented as mean ± SD. Comparisons of apnea and respiratory modulations in Ti, Te, and Ttot between experimental groups were analyzed with one-way ANOVA and Tukey's post hoc analysis. Linear regression analysis of

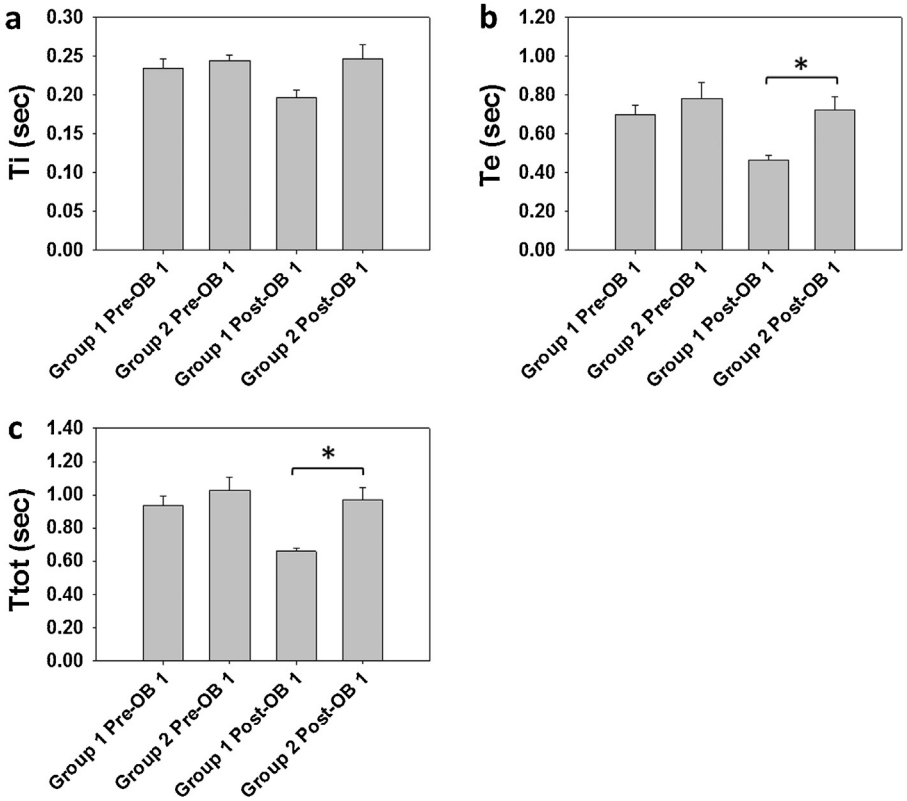

Fig. 2. Group mean respiratory phase timing in OB-1 animals. (a) Ti: Group 1 Ti 0.23 ± 0.03 was not significantly different than Group 2 Ti 0.24 ± 0.03 Pre-OB-1 breath times ($p = 0.450$). Group 1 Ti 0.20 ± 0.03 was not significantly different than Group 2 Ti 0.25 ± 0.06 Post-OB-1 breath times ($p = 0.053$). (b) Te: Group 1 Te 0.70 ± 0.13 was not significantly different than Group 2 Te 0.78 ± 0.31 Pre-OB-1 breath times ($p = 0.751$). Group 1 Te 0.46 ± 0.06 was significantly different than Group 2 Te 0.72 ± 0.24 Post-OB-1 breath times ($p = 0.012$). (c) Ttot: Group 1 Ttot 0.94 ± 0.16 was not significantly different than Group 2 Ttot 1.03 ± 0.30 Pre-OB-1 breath times ($p = 0.698$). Group 1 Ttot 0.66 ± 0.05 was significantly different than Group 2 Ttot 0.97 ± 0.26 Post-OB-1 breath times ($p = 0.005$).

Psi and apnea duration (s) with Shapiro–Wilk normality test was performed. Statistical significance was $p \leq 0.05$.

3. Results

A total of 27 animals were tested in this study. The OB-1 caused a 19% death rate (5/27) resulting in 22 animals analyzed after the initial OB injury: Group 1, $n = 7$; Group 2, $n = 15$. Of the OB-1 surviving animals, 12 were exposed to OB-2 with one animal death (1/12) resulting in 11 animals analyzed after the second OB injury: Group 3, $n = 6$; Group 4, $n = 5$. There were no differences in Psi for the animals that did not survive OB-1 (mean Psi = 83.2 ± 10.2) and OB-2 (Psi = 78.5).

3.1. Diaphragmatic EMG recordings

3.1.1. OB-1 group comparisons

Fig. 1a illustrates the raw and ∫dEMG breathing pattern obtained from the diaphragm EMG (dEMG) recording for a Group 1 (69.9 Psi) animal. Fig. 1b illustrates the raw and ∫dEMG breathing pattern obtained from the diaphragm EMG (dEMG) recording for a Group 2 (90.3 Psi) animal.

Fig. 2a illustrates the group mean ∫dEMG Ti breath phase times were: Pre-OB-1 Group 1 0.23 ± 0.03 and Group 2 0.24 ± 0.03; Post-OB-1 Group 1 0.20 ± 0.03 and Group 2 0.25 ± 0.06. There were no significance differences seen between either Pre-OB-1 Group 1 and Group 2 Ti ($p = 0.450$) and Post-OB-1 Group 1 and Group 2 Ti ($p = 0.053$).

Fig. 2b illustrates the group mean ∫dEMG Te breath phase times were: Pre-OB-1 Group 1 0.70 ± 0.13 and Group 2 0.78 ± 0.31; Post-OB-1 Group 1 0.46 ± 0.06 and Group 2 0.72 ± 0.24. There was no significance difference between Group 1 and Group 2 Te Pre-OB-1 ($p = 0.751$). There was a significance difference between Group 1 and Group 2 Te Post-OB-1 ($p = 0.012$).

Fig. 2c illustrates the group mean ∫dEMG Ttot breath phase times were: Pre-OB-1 Group 1 0.94 ± 0.16 and Group 2 1.03 ± 0.30; Post-OB-1 Group 1 0.66 ± 0.05 and Group 2 0.97 ± 0.26. There was no significance difference between Pre-OB-1 Group 1 and Group 2 Ttot ($p = 0.698$). There was a significance difference between Post-OB-1 Group 1 and Group 2 Ttot ($p = 0.005$).

3.1.2. OB-2 group comparisons

Fig. 3a illustrates the group mean ∫dEMG Ti breath phase times were: Pre-OB-2 Group 3 0.24 ± 0.05 and Group 4 0.22 ± 0.06; Post-OB-2 Group 3 (66.5–71.5 Psi) 0.19 ± 0.05 and Group 4 (86.7–94.0 Psi) 0.22 ± 0.08. There were no significance differences seen between either Pre-OB-2 Group 3 and Group 4 Ti ($p = 0.591$) and Post-OB-2 Group 3 and Group 4 Ti ($p = 0.544$).

Fig. 3b illustrates the group mean ∫dEMG Te breath phase times were: Pre-OB-2 Group 3 0.92 ± 0.10 and Group 4 0.77 ± 0.19; Post-OB-2 Group 3 0.53 ± 0.06 and Group 4 0.92 ± 0.42. There were no significance differences between Group 3 and Group 4 Te Pre-OB-2 ($p = 0.124$) and Post-OB-2 ($p = 0.126$).

Fig. 3c illustrates the group mean ∫dEMG Ttot breath phase times were: Pre-OB-2 Group 3 1.16 ± 0.14 and Group 4 0.99 ± 0.24; Post-OB-2 Group 3 0.72 ± 0.05 and Group 4 1.14 ± 0.39. There was no significance difference between Pre-OB-2 Group 3 and Group 4

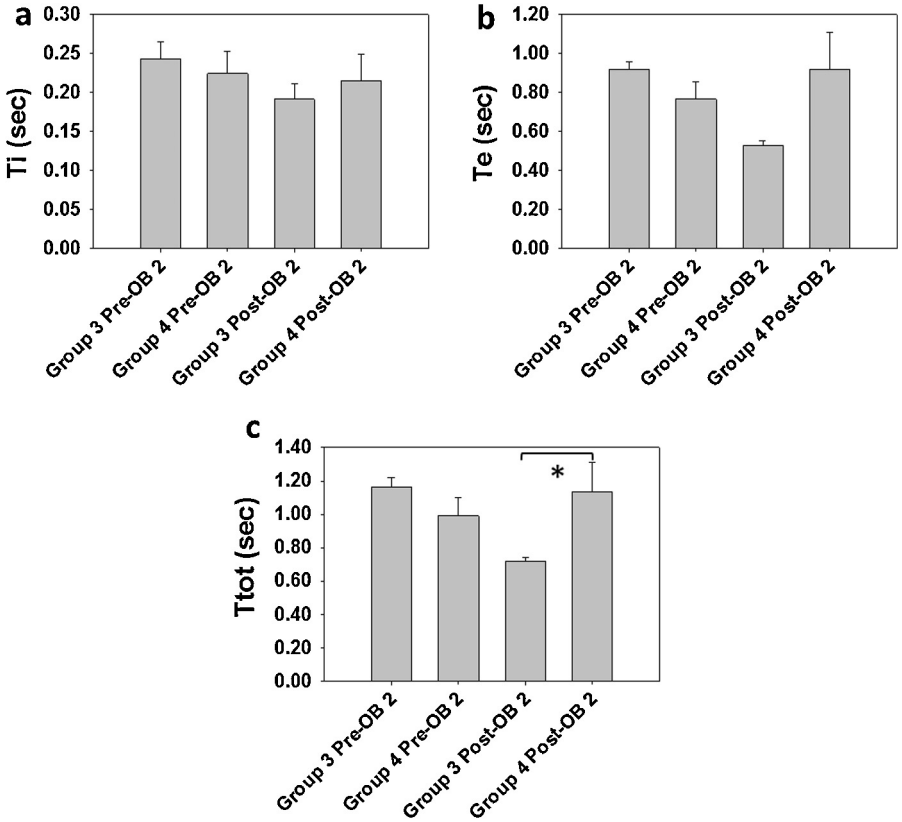

Fig. 3. Group mean respiratory phase timing in OB-2 animals. (a) Ti: Group 3 Ti 0.24 ± 0.05 was not significantly different than Group 4 Ti 0.22 ± 0.06 Pre-OB-2 breath times ($p = 0.591$). Group 3 Ti 0.19 ± 0.05 was not significantly different than Group 4 Ti 0.22 ± 0.08 Post-OB-2 breath times ($p = 0.544$). (b) Te: Group 3 Te 0.92 ± 0.10 was not significantly different than Group 4 Te 0.77 ± 0.19 Pre-OB-2 breath times ($p = 0.124$). Group 3 Te 0.53 ± 0.06 was not significantly different than Group 4 Te 0.92 ± 0.42 Post-OB-2 breath times ($p = 0.126$). (c) Ttot: Group 3 Ttot 1.16 ± 0.14 was not significantly different than Group 4 Ttot 0.99 ± 0.24 Pre-OB-2 breath times ($p = 0.175$). Group 3 Ttot 0.72 ± 0.05 was significantly different than Group 4 Ttot 1.14 ± 0.39 Post-OB-2 breath times ($p = 0.030$).

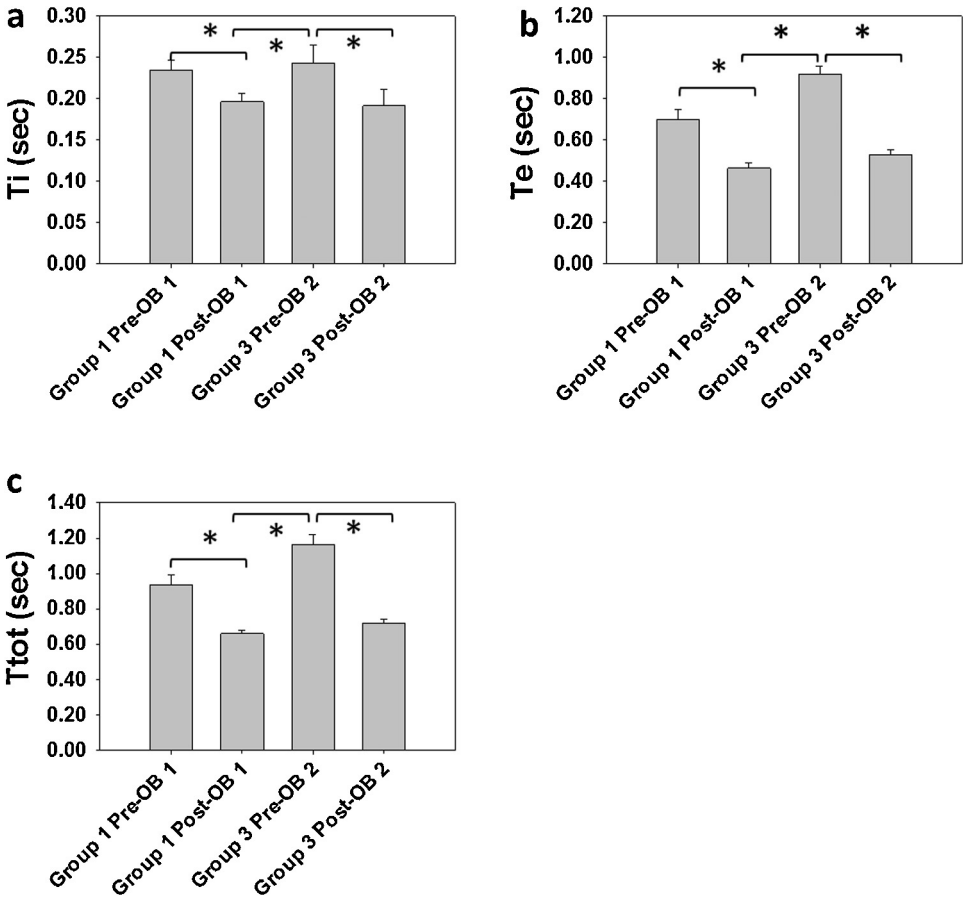

Fig. 4. Group 1 and Group 3 animals mean respiratory phase timing for OB-1 and OB-2. (a) Ti: Group 1 and Group 3 Ti phase times were: Pre-OB-1 0.23 ± 0.03; Post-OB-1 0.20 ± 0.03, Pre-OB-2 0.24 ± 0.05 and Post-OB-2 0.19 ± 0.05. There were significance differences between treatment groups ($p < 0.001$). (b) Te: Group 1 and Group 3 Te phase times were: Pre-OB-1 0.70 ± 0.13; Post-OB-1 0.46 ± 0.06, Pre-OB-2 0.92 ± 0.10 and Post-OB-2 0.53 ± 0.06. There were significance differences between treatment groups ($p < 0.001$). (c) Ttot: Group 1 and Group 3 Ttot phase times were: Pre-OB-1 0.94 ± 0.16; Post-OB-1 0.66 ± 0.05, Pre-OB-2 1.16 ± 0.14 and Post-OB-2 0.72 ± 0.05. There were significance differences between treatment groups ($p < 0.001$).

Ttot ($p = 0.175$). There was a significance difference between Post-OB-2 Group 3 and Group 4 Ttot ($p = 0.030$).

3.1.3. OB-1 and OB-2 comparisons

Fig. 4a illustrates the group mean ∫dEMG Ti breath phase times for Group 1 (OB-1) and Group 3 (OB-2) were: Pre-OB-1 0.23 ± 0.03; Post-OB-1 0.20 ± 0.03, Pre-OB-2 0.24 ± 0.05 and Post-OB-2 0.19 ± 0.05. There were significance differences between treatment groups ($p < 0.001$). Fig. 4b illustrates Te breath phase times for Group 1 (OB-1) and Group 3 (OB-2) were: Pre-OB-1 0.70 ± 0.13, Post-OB-1 0.46 ± 0.06, Pre-OB-2 0.92 ± 0.10 and Post-OB-2 0.53 ± 0.06. There were significance differences between treatment groups ($p < 0.001$). Fig. 4c illustrates the group mean Ttot breath phase for Group 1 (OB-1) and Group 3 (OB-2) were: Pre-OB-1 0.94 ± 0.16, Post-OB-1 0.66 ± 0.05, Pre-OB-2 1.16 ± 0.14 and Post-OB-2 0.72 ± 0.05. There was significance difference between treatment groups ($p < 0.001$).

Fig. 5a illustrates the group mean ∫dEMG Ti breath phase times for Group 2 (OB-1) and Group 4 (OB-2) were: Pre-OB-1 0.24 ± 0.03, Post-OB-1 0.25 ± 0.06, Pre-OB-2 0.22 ± 0.06 and Post-OB-2 0.22 ± 0.08. There were no significance differences between treatment groups ($p = 0.427$). Fig. 5b illustrates the group mean Te breath phase for Group 2 (OB-1) and Group 4 (OB-2) were: Pre-OB-1 0.78 ± 0.31, Post-OB-1 0.72 ± 0.24, Pre-OB-2 0.77 ± 0.19 and Post-OB-2 0.92 ± 0.42. There were no significance differences between treatment groups ($p = 0.426$). Fig. 5c illustrates the group mean Ttot breath phase for Group 2 (OB-1) and Group 4 (OB-2) were: Pre-OB-1 1.03 ± 0.30, Post-OB-1 0.97 ± 0.26, Pre-OB-2 0.99 ± 0.24 and Post-OB-2 1.14 ± 0.39. There were no significance differences between treatment groups ($p = 0.559$).

3.2. Apnea as a function of Psi

3.2.1. OB-1 group comparisons

Fig. 6a shows a scatter plot of the apneic duration and the Psi for OB-1. Group 1 animals ($n = 7$) with Psi = 70.29 ± 1.37, had shorter apneic duration (2.25 ± 1.48 s). The Group 1 animals had a significant relationship between Psi and apnea duration ($p < 0.001$, $R^2 = 0.893$). The Group 2 animals ($n = 15$) with Psi = 89.24 ± 4.82, had longer apneic durations (4.29 ± 3.83 s). The Group 2 animals had a significant relationship between Psi and apnea duration ($p = 0.012$, $R^2 = 0.370$). Apneic duration of the combined results for Group 1 and Group 2 were significantly correlated with Psi ($p = 0.016$, $R^2 = 0.233$).

3.2.2. OB-2 group comparisons

Fig. 6b shows a scatter plot of the apneic duration and the Psi for OB-2. Group 3 animals ($n = 6$) with Psi = 69.47 ± 2.28 had longer apneic durations (5.46 ± 4.05 s). The Group 3 animals had no significance between pressure Psi and apnea duration ($p = 0.613$, $R^2 = 0.000$). The Group 4 animals ($n = 5$) with Psi = 89.42 ± 3.07 had shorter apneic durations (3.84 ± 3.94 s). The Group 4 animals had no significance between Psi and apnea duration ($p = 0.114$, $R^2 = 0.492$). The apneic durations were not significantly correlated with Psi in

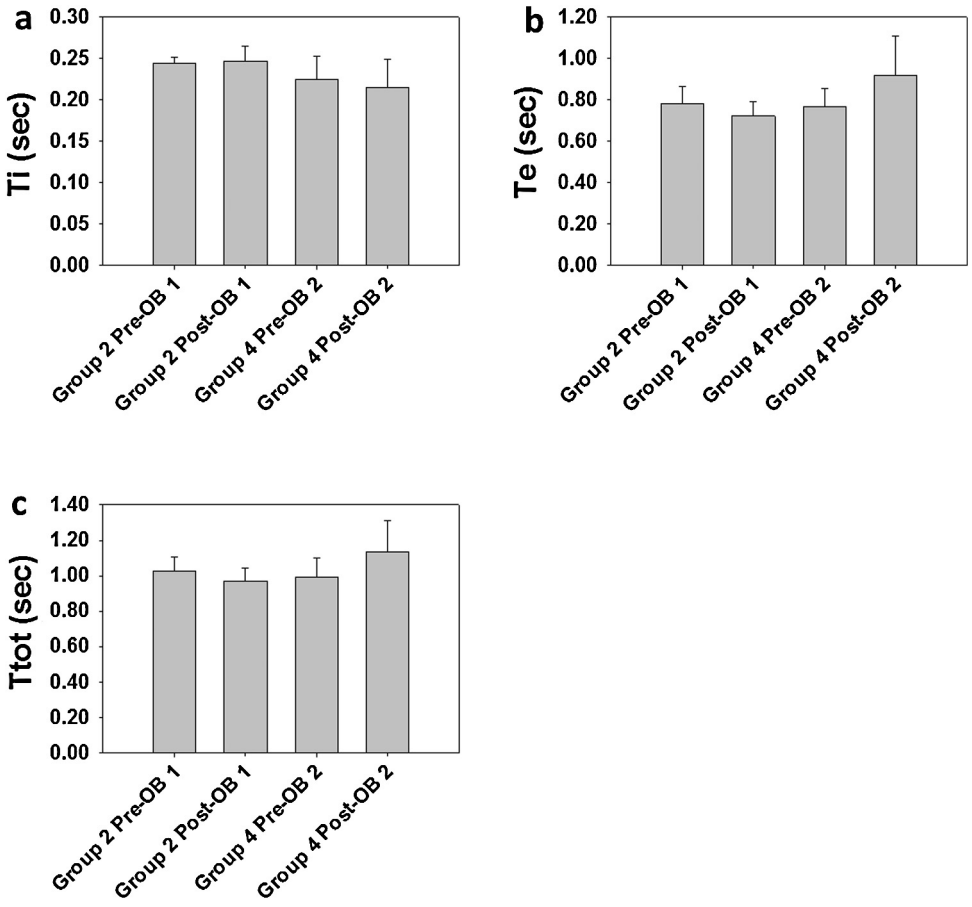

Fig. 5. Group 2 and Group 4 animals mean respiratory phase timing for OB-1 and OB-2. (a) Ti: Group 2 and Group 4 Ti phase times were: Pre-OB-1 0.24 ± 0.03; Post-OB-1 0.25 ± 0.06, Pre-OB-2 0.22 ± 0.06 and Post-OB-2 0.22 ± 0.08. There were no significance differences between treatment groups ($p = 0.427$). (b) Te: Group 2 and Group 4 Te phase times were: Pre-OB-1 0.78 ± 0.31; Post-OB-1 0.72 ± 0.24, Pre-OB-2 0.77 ± 0.19 and Post-OB-2 0.92 ± 0.42. There were no significance differences between treatment groups ($p = 0.426$). (c) Ttot: Group 2 and Group 4 Ttot phase times were: Pre-OB-1 1.03 ± 0.30; Post-OB-1 0.97 ± 0.26, Pre-OB-2 0.99 ± 0.24 and Post-OB-2 1.14 ± 0.39. There were no significance differences between treatment groups ($p = 0.559$).

Group 3 and Group 4 ($p = 0.790$, $R^2 = 0.000$). The apneic durations were similar regardless of the Psi during second blast. This suggests that even a mild TBI has cumulative effects due to two blasts on the apneic period.

3.2.3. OB-1 and OB-2 comparisons

Fig. 6c shows a scatter plot of the apneic duration and Psi for OB-1 ($n = 22$) and OB-2 ($n = 11$). OB-1 resulted in a linear increase in apneic duration (3.61 ± 3.34 s) as a relationship of Psi (82.92 ± 9.98). OB-2 resulted in a more scattered apneic duration (4.73 ± 3.89 s) as a function of Psi (78.54 ± 10.72). There was not a significant relationship between Psi and apnea for all animals when OB-1 and OB-2 were combined ($p = 0.178$, $R^2 = 0.028$).

4. Discussion

To our knowledge, this is the first study to record from the diaphragm EMG during blast-induced TBI in rats. Our results indicate that a dorsal directed closed-head OB injury results in a neurally mediated apnea. The occurance and duration of the apnea is a function of the OB Psi and repeat injury. The Ti, Te and Ttot periods increased relative to Psi during the first OB. The results become more varied with the second OB with increases in apneic periods seen in the lower OB-2 pressure group (Psi ≤ 70) when comparing all animals that had multiple blasts. The second OB Ttot was affected by overpressure blast pressure in all animals. The apneic period and disruption in normal breathing pattern was evidenced by the dEMG recordings during and following OB in these animals. These changes are consistent with observational reports in previous studies (Cheng et al., 2010; Dixon et al., 1987; Guy et al., 1998b; Kuehn et al., 2011).

It is likely that these responses are multifactorial in nature. The OB injury is a global insult to the brain and each injury is likely to have varying kinectic energy projections throughout the brain based on the individual animal anatomy and potential variations in head orientation. Although we took measures to orient the animal head the same with each OB, the head was not in a stereotaxic apparatus resulting in potential variations in the angle of the head under the blast tube.

It is difficult to identify the exact neuronal pathways that were affected by the OB. Previous studies have suggested that the brainstem is likely affected resulting in the initial apneic period followed by irregular breathing (Cheng et al., 2010; Dixon et al., 1987; Guy et al., 1998b; Kuehn et al., 2011). Therefore, it is likely this disruption is at least in part at the medullary level and one possibility may be that the respiratory neural network neurons are affected by the mechanical pressure wave. This disruption is a function of the magnitude of the pressure with smaller pressures resulting in lesser apneic periods as well as more stable breathing pattern (Ti, Te and Ttot).

Behavior and cognitive performance has been the topic of multiple TBI studies on mice using fluid percussion (DeRoss et al., 2002), impactor tip (Longhi et al., 2005) and weight-drop

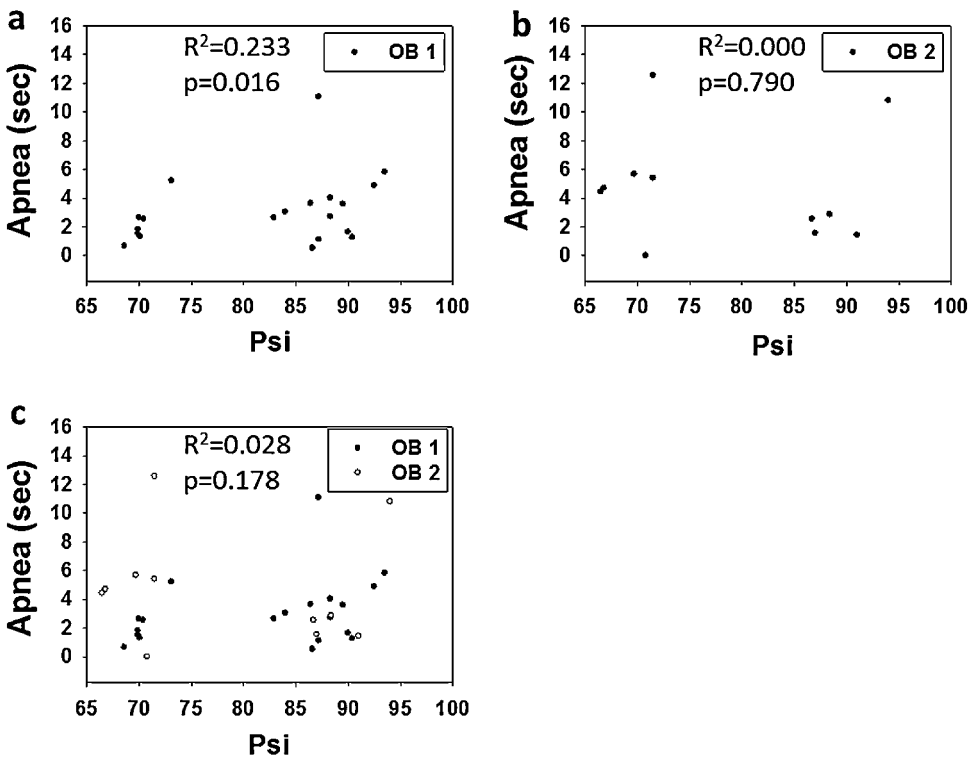

Fig. 6. Relationship between apnea duration and OB Psi. (a) Effect of Psi Group 1 (70.29 ± 1.37 Psi) and Group 2 (89.24 ± 4.82) on OB-1 (n = 22) apneic periods (2.25 ± 1.48) and (4.29 ± 3.83) respectively. There was a significant linear relationship (p = 0.016, R^2 = 0.233). (b) Effect of Psi of Group 1 (69.47 ± 2.28 Psi) and Group 2 (89.42 ± 3.07 Psi) on OB-2 (n = 11) apneic periods (5.46 ± 4.05) and (3.84 ± 3.94) respectively. There was no significance between Psi and apnea (p = 0.790, R^2 = 0.000). (c) There was not a significant (p = 0.178, R^2 = 0.028) relationship between Psi and apnea duration for all animals when OB-1 and OB-2 are combined.

(Creeley et al., 2004; DeFord et al., 2002). The TBIs in these studies were induced either every day or every other day for a week which is different from the present study. Two injuries within 7 days of each other was reported to increase damage to hippocampal neurons in the area of CA1 (Jenkins et al., 1989). Neuronal damage was found in the cortex and hypothalamus following single and repetitive concussive brain injury (Longhi et al., 2005). The multiple injury weight-drop model, however, did not report axonal injury in the brainstem (DeFord et al., 2002). Although no brainstem neuronal loss was reported with immunohistochemistry in the weight-drop model, a disruption in the neuronal network is feasible with the OB model that generates kinectic forces throughout the brain.

A mouse model using an impactor tip found that 15 animals had a brief observational apneic period 3–19 s with first injury and 9 animals had apneic periods of 6–21 s after second injury (Laurer et al., 2001). It is interesting to note that with multiple OB, the OB-2 lower pressures (Psi ≤ 70) compared to the higher OB-1 pressures (Psi ≥ 80) resulted in greater difference in apneic periods in the OB-2 condition. This may be a result of greater sensitivity due to less damage in the neuronal populations in the lower OB pressure group. A repeated (three days after initial injury) head injury mouse model using an impactor tip found neurodegeneration in the ipsilateral cortex with less damage seen in the hypothalamus, hippocampus and thalamus (Longhi et al., 2005). Although there was less injury seen in the hypothalamus and thalamus, this was a relatively mild injury and not a global insult. With silver staining, evidence of diencephalon damage was found in a composite OB injury (Svetlov et al., 2010) which could likely result in respiratory disturbances. Our OB injury model provides a global brain impact with repeat OBs most likely resulting in greater neurodegeneration especially in the lower OB pressure animals.

Although we are unable in the present study to determine the respiratory neural network neurons in the brainstem that are affected with the OB injury model, the length of the apneic period and duration of the respiratory cycle is increased following the OB-2 and appears to be more affected at low OB pressures. Although there were fewer deaths caused by the OB-2, perturbations in breathing still occur. This is important when considering the appropriate recovery time before individuals exposed to closed-head injury can return to service due to the cumulative effects of TBI.

Future experiments are needed to include different blast orientation and pressures to determine the affect of Psi magnitude on the apneic period and breathing cycle. A frontal injury may result in different neuromotor effects that is a function of the vector of kinectic energy transferred to the brainstem and respiratory neural control network. It would also be important to determine the OB pressure threshold for dorsal OB injury that results in apnea and alterations in the breathing pattern.

Grants

Training support to SLA was provied by NIH R01HL109025.

Disclosures

No real or potential conflict of interest exists for any of the authors in this study.

Acknowledgements

The authors express gratitude to Victor Prima for assistance with the OB injury and Lauren Donnangelo for assistance with animal care.

References

Cheng, J., Gu, J., Ma, Y., Yang, T., Kuang, Y., Li, B., Kang, J., 2010. Development of a rat model for studying blast-induced traumatic brain injury. J. Neurol. Sci. 294, 23–28.

Creeley, C.E., Wozniak, D.F., Bayly, P.V., Olney, J.W., Lewis, L.M., 2004. Multiple episodes of mild traumatic brain injury result in impaired cognitive performance in mice. Acad. Emerg. Med. 11, 809–819.

DeFord, S.M., Wilson, M.S., Rice, A.C., Clausen, T., Rice, L.K., Barabnova, A., Bullock, R., Hamm, R.J., 2002. Repeated mild brain injuries result in cognitive impairment in B6C3F1 mice. J. Neurotrauma 19, 427–438.

DeRoss, A.L., Adams, J.E., Vane, D.W., Russell, S.J., Terella, A.M., Wald, S.L., 2002. Multiple head injuries in rats: effects on behavior. J. Trauma 52, 708–714.

Dixon, C.E., Lyeth, B.G., Povlishock, J.T., Findling, R.L., Hamm, R.J., Marmarou, A., Young, H.F., Hayes, R.L., 1987. A fluid percussion model of experimental brain injury in the rat. J. Neurosurg. 67, 110–119.

Faul, M.X.L., Wald, M.M., Coronado, V.G., 2010. Traumatic Brain Injury in the United States: Emergency Department Visits, Hospitalizations, Deaths. Atlanta (GA): Centers for Disease Control and Prevention. National Center for Injury Prevention and Control.

Guy, R.J., Glover, M.A., Cripps, N.P., 1998a. The pathophysiology of primary blast injury and its implications for treatment. Part I: the thorax. J. R. Nav. Med. Serv. 84, 79–86.

Guy, R.J., Kirkman, E., Watkins, P.E., Cooper, G.J., 1998b. Physiologic responses to primary blast. J. Trauma 45, 983–987.

Jenkins, L.W., Moszynski, K., Lyeth, B.G., Lewelt, W., DeWitt, D.S., Allen, A., Dixon, C.E., Povlishock, J.T., Majewski, T.J., Clifton, G.L., et al., 1989. Increased vulnerability of the mildly traumatized rat brain to cerebral ischemia: the use of controlled secondary ischemia as a research tool to identify common or different mechanisms contributing to mechanical and ischemic brain injury. Brain Res. 477, 211–224.

Kuehn, R., Simard, P.F., Driscoll, I., Keledjian, K., Ivanova, S., Tosun, C., Williams, A., Bochicchio, G., Gerzanich, V., Simard, J.M., 2011. Rodent model of direct cranial blast injury. J. Neurotrauma 28, 2155–2169.

Laurer, H.L., Bareyre, F.M., Lee, V.M., Trojanowski, J.Q., Longhi, L., Hoover, R., Saatman, K.E., Raghupathi, R., Hoshino, S., Grady, M.S., McIntosh, T.K., 2001. Mild head injury increasing the brain's vulnerability to a second concussive impact. J. Neurosurg. 95, 859–870.

Longhi, L., Saatman, K.E., Fujimoto, S., Raghupathi, R., Meaney, D.F., Davis, J., McMillan, B.S.A., Conte, V., Laurer, H.L., Stein, S., Stocchetti, N., McIntosh, T.K., 2005. Temporal window of vulnerability to repetitive experimental concussive brain injury. Neurosurgery 56, 364–374, discussion 364–374.

Svetlov, S.I., Prima, V., Kirk, D.R., Gutierrez, H., Curley, K.C., Hayes, R.L., Wang, K.K., 2010. Morphologic and biochemical characterization of brain injury in a model of controlled blast overpressure exposure. J. Trauma 69, 795–804.